

JANUARY, 2014

Ph.D. in Mechanical Engineering

MEHMET VEYSEL ÇAKIR

UNIVERSITY OF GAZİANTEP  
GRADUATE SCHOOL OF  
NATURAL & APPLIED SCIENCES

EVALUATION OF MULTI-STAGE ELECTRO  
DISCHARGE MACHINING (EDM) PARAMETERS

Ph.D. THESIS  
IN  
MECHANICAL ENGINEERING

BY  
MEHMET VEYSEL ÇAKIR

JANUARY 2014

**Evaluation of Multi-Stage Electro Discharge Machining  
(EDM) Parameters**

**Ph.D. Thesis**

**In**

**Mechanical Engineering**

**University of Gaziantep**

**Supervisor**

**Prof. Dr. Ömer Eyerciođlu**

**By**

**Mehmet Veysel ÇAKIR**

**January 2014**

©2014 [Mehmet Veysel ÇAKIR].

REPUBLIC OF TURKEY  
UNIVERSITY OF GAZİANTEP  
GRADUATE SCHOOL OF NATURAL & APPLIED SCIENCES  
NAME OF THE DEPARTMENT

Name of the thesis: Evaluation of Multi-Stage Electro Discharge Machining (EDM)  
Parameters

Name of the student: Mehmet Veysel ÇAKIR

Exam date: 20.01.2014

Approval of the Graduate School of Natural and Applied Sciences

Assoc. Prof. Dr. Metin BEDİR

Director

I certify that this thesis satisfies all the requirements as a thesis for the degree of  
Doctor of Philosophy.

Prof. Dr. Sait SOYLEMEZ

Head of Department

This is to certify that we have read this thesis and that in our consensus opinion it is  
fully adequate, in scope and quality, as a thesis for the degree of Doctor of  
Philosophy.

Prof. Dr. Ömer EYERCİOĞLU

Supervisor

Examining Committee Members (Title and Name-surname)

Signature

1. Prof. Dr. İ. Hüseyin FİLİZ (Chairman)
2. Prof. Dr. M. Cengiz KAYACAN
3. Prof. Dr. M. Kemal APALAK
4. Prof. Dr. Ömer EYERCİOĞLU
5. Assoc. Prof. Dr. Abdulkadir ÇEVİK

.....  
.....  
.....  
.....  
.....  
.....

**I hereby declare that all information in this document has been obtained and presented in accordance with academic rules and ethical conduct. I also declare that, as required by these rules and conduct, I have fully cited and referenced all material and results that are not original to this work.**

Mehmet Veysel ÇAKIR

Signature

## ABSTRACT

### EVALUATION OF MULTI-STAGE ELECTRO DISCHARGE MACHINING (EDM) PARAMETERS

ÇAKIR, Mehmet Veysel

Ph.D. in Mechanical Eng.

Supervisor(s): Prof. Dr. Ömer EYERCİOĞLU

December 2013

126 page

Electrical discharge machining (EDM) is a well-established machining process for manufacturing geometrically complex and/or hard parts that are extremely difficult-to-machine by conventional machining processes. However, the process is a complex task due to the nonlinearities of the process parameters. In a whole EDM process, multi-stage machining is generally carried out from rough to finish for minimizing the machining time. In this thesis, the effects of the most important electrical parameters such as discharge current ( $I$ ), pulse on time ( $T_{on}$ ) and pulse off time ( $T_{off}$ ) to material removal rate (MRR), electrode wear ratio (EWR), surface roughness ( $R_a$ ) and average white layer thickness (AWLT) were experimentally investigated for different machining stages. The experimental data was modelled using artificial intelligence techniques and the alternative EDM parameter sets were generated by the help of these models. A multistage strategy and a computer program were developed to determine the required number of stages for minimum machining time. The resulting average white layer thickness of the previous stage was taken as a criterion to determine the machining depth. The machining depth and the corresponding parameters set in each stage according to the desired surface quality, volume and area of the workpiece can be defined by using the alternative EDM parameter sets which were generated by the models. The developed multi-stage EDM strategy and the computer program were experimentally verified.

**Key Words:** Multi-stage EDM, artificial intelligence, MRR, surface quality

## ÖZ

### ÇOK-KADEMELİ ELEKTRO EROZYONLA İŞLEME PARAMETRELERİNİN ARAŞTIRILMASI

ÇAKIR, Mehmet Veysel

Doktora Tezi, Makine Müh. Bölümü

Tez Yöneticisi: Prof. Dr. Ömer EYERCİOĞLU

Aralık 2013

126 sayfa

Elektro erozyonla işleme yöntemi, geleneksel imalat yöntemleri ile işlenmesi oldukça zor veya mümkün olmayan, karmaşık şekilli ve/veya sert parçaları işlemek için geliştirilmiş bir imalat seçeneğidir. Ancak, işleme parametrelerinin lineer olmadığından, EDM işlemi oldukça karmaşıktır. Komple bir EDM işlemi, işleme süresini kısaltmak amacıyla, genellikle kaba işlemeden bitirme işlemine, çok-kademeli olarak gerçekleştirilir. Bu tezde, en önemli elektriksel parametreler olan; deşarj akımı ( $I$ ), darbe süresi ( $T_{on}$ ), ve bekleme süresinin ( $T_{off}$ ), EDM performans parametreleri olan; malzeme kaldırma oranı (MRR), elektrot aşınma oranı (EWR), yüzey pürüzlülüğü ( $R_a$ ) ve ortalama beyaz katman kalınlığına (AWLT) etkileri, farklı işleme kademeleri için deneysel olarak irdelenmiştir. Deneysel sonuçlardan elde edilen veriler, yapay zekâ teknikleri kullanılarak modellenmiş ve bu modeller yardımıyla alternatif EDM parametre setleri oluşturulmuştur. Minimum işleme süresi için gereken kademe sayısını belirlemek için, çok-kademeli bir EDM stratejisi ve bilgisayar programı geliştirilmiştir. Bir önceki kademe de oluşan ortalama beyaz katman kalınlığı, işleme derinliğini belirlemede kriter olarak alınmıştır. Modellerden elde edilen alternatif parametre setleri kullanılarak, istenilen yüzey kalitesi, işlenecek malzeme hacmi ve iş parçası yüzey alanına göre; kademe sayısı, işleme derinliği ve her kademedeki parametre setleri belirlenebilmektedir. Geliştirilen çok-kademeli EDM stratejisi ve bilgisayar programı deneysel olarak doğrulanmıştır.

**Anahtar Kelimeler:** Çok-kademeli EDM, yapay zeka, MRR, yüzey kalitesi

*Rahmetli Babama .....*



## ACKNOWLEDGEMENTS

Firstly, I am very grateful to my supervisor Prof. Dr. Ömer EYERCİOĞLU for his guidance and support from the beginning to the end of this study. It has been an honour to be his student as well.

I also forward my sincere thanks to in my thesis committee members: Prof. Dr. İ. Hüseyin FİLİZ, Prof. Dr. M. Cengiz KAYACAN, Prof. Dr. M. Kemal APALAK and Assoc. Prof. Dr. Abdulkadir ÇEVİK for their input and valuable comments.

I also thank for assisting me in each stage of my studies, Expert Mr. Kürşad GÖV for his valuable comments and real camaraderie.

I also thank to instructor Hasan GÜLER for his help on programming of Multi-stage EDM program.

I extend my sincere thanks to all my friends and colleagues for the continuous motivation and support and prays.

My endless love and loyalty to my mother (Emine), my brothers, my sisters, my son (Furkan) and my daughters (Emine and Kevser) whom I will forever be indebted to for their ever-extending love, support, trust, and willingness to endure with me the challenges of my endeavours.

Finally, Special thanks to my wife, for her continuous encouragement, patience and real love.

## TABLE OF CONTENTS

ABSTRACT .....	v
ÖZ .....	vi
ACKNOWLEDGEMENTS .....	viii
TABLE OF CONTENTS .....	ix
LIST OF TABLES .....	xii
LIST OF FIGURES .....	xv
CHAPTER 1 .....	1
1 INTRODUCTION .....	1
CHAPTER 2 .....	4
2 LITERATURE SURVEY .....	4
2.1 Introduction .....	4
2.2 Literature of Multi-Stage EDM .....	5
2.3 Summary of Literature Survey .....	7
CHAPTER 3 .....	9
3 BASIS OF EDM .....	9
3.1 Introduction .....	9
3.2 Types of EDM .....	9
3.3 Ram EDM Machine Components .....	11
3.3.1 Power Supply Unit (Spark Generator) .....	11
3.3.2 Servo System .....	13
3.3.3 Dielectric Circuit Unit .....	13
3.3.4 Mechanical Structure .....	13
3.4 Removal Mechanism of EDM .....	13
3.5 Main EDM Process Parameters and Performance Measures .....	16
3.5.1 Gap Voltage .....	16
3.5.2 Peak or Discharge Current .....	16
3.5.3 Pulse on-time ( $T_{on}$ ) .....	17
3.5.4 Pulse off-time ( $T_{off}$ ): .....	17
3.5.5 Polarity .....	18
3.5.6 Duty Cycle: .....	19
3.5.7 Spark (Pulse) frequency: .....	19

3.5.8	Electrode Materials: .....	20
3.5.9	Dielectric Fluids .....	21
CHAPTER 4	.....	23
4	EXPERIMENTAL STUDY.....	23
4.1	Introduction .....	23
4.2	Machine Specification and Input Parameters .....	23
4.3	Workpiece Material .....	24
4.4	Electrode Material .....	25
4.5	Polarity .....	26
4.6	Dielectric .....	26
4.7	Design of Experiment.....	26
4.8	Experimental Procedure .....	30
4.9	Measurements of Output Parameters.....	30
4.9.1	Measurement of Material Removal Rate .....	31
4.9.2	Electrode Wear Ratio (EWR).....	31
4.9.3	Surface Quality.....	31
4.10	Results and Discussion of Experimental Studies.....	36
4.10.1	Influences of Process Parameters on MRR.....	36
4.10.2	Influences of Process Parameters on EWR.....	39
4.10.3	Influences of Process Parameters on Surface Roughness .....	40
4.10.4	Influences of Process Parameters on White Layer Thickness .....	42
4.11	Conclusions based on the Experimental Study.....	44
CHAPTER 5	.....	45
5	MODELING OF EDM PARAMETERS.....	45
5.1	Introduction .....	45
5.2	Fundamentals of Artificial Intelligence.....	45
5.2.1	Overview of Genetic Programming (GP) Models .....	46
5.2.2	Overview of Artificial Neural Networks (ANNs) Models.....	46
5.2.3	Overview of Adaptive Neuro-Fuzzy Inference System (ANFIS) Models	
	48	
5.3	Development of Models .....	49
5.3.1	Development of Genetic Programming (GP) Models.....	51
5.3.2	Development of Artificial Neural Networks (ANNs) Models.....	56

5.3.3	Development of ANFIS Models .....	58
5.3.4	Comparisons of MRR and EWR parameters modelling study .....	59
5.4	Modelling of $R_a$ and AWLT Parameters .....	62
5.5	Discussions and Conclusions of Modelling Studies.....	65
CHAPTER 6	.....	72
6	MULTI-STAGE EDM STRATEGY AND PROGRAMMING .....	72
6.1	Introduction .....	72
6.2	Development of A Multi-Stage Strategy.....	72
6.2.1	An illustrative example of Multi-Stage strategy .....	78
6.3	Procedure of Multi-Stage Machining Strategy.....	87
6.4	Multi-Stage Algorithm .....	88
6.5	Program Description.....	93
6.6	Case Studies .....	94
6.6.1	Case Study 1.....	94
6.6.2	Case Study 2.....	103
6.6.3	Case Study 3.....	106
6.6.4	Case Study 4.....	108
6.7	Verification Study .....	111
6.8	Summary of the Results of the Case Studies.....	115
CHAPTER 7	.....	116
7	CONCLUSIONS AND FUTURE WORKS.....	116
7.1	Conclusions .....	116
7.2	Future Works .....	118
8	REFERENCES.....	120
APPENDICES	.....	127
APPENDIX A. RESULTS OF EXPERIMENTAL STUDIES	.....	128
APPENDIX B. TABLES OF CASE STUDY 1	.....	132
Curriculum Vitae.....		154

## LIST OF TABLES

<b>Table 3.1.</b> Electrode polarities for different workpiece materials (Metals handbook, 1989) .....	18
<b>Table 4.1.</b> Variable and invariable parameters' levels .....	24
<b>Table 4.2</b> Chemical composition of workpiece material (1.2344) .....	24
<b>Table 4.3.</b> Electrode material specifications .....	25
<b>Table 4.4</b> Set of recommended electrical parameters.....	27
<b>Table 4.5</b> A contrast of machined area to current strength for copper and steel.....	27
<b>Table 4.6</b> Taguchi first group L <sub>25</sub> for finishing .....	28
<b>Table 4.7</b> Taguchi second group L <sub>25</sub> (OA) for roughing.....	29
<b>Table 4.8</b> EDM parameters and levels for first group L <sub>25</sub> for finishing .....	29
<b>Table 4.9</b> EDM parameters and levels for second group L <sub>25</sub> for roughing .....	29
<b>Table 4.10</b> Measuring Parameters .....	33
<b>Table 5.1</b> Training data.....	50
<b>Table 5.2</b> Testing data .....	51
<b>Table 5.3</b> Input and output parameters of GEP models.....	52
<b>Table 5.4</b> GEP model parameters .....	52
<b>Table 5.5</b> Function set's list.....	52
<b>Table 5.6</b> Results obtained from GEP models .....	53
<b>Table 5.7</b> Best statistical results obtained from GEP formulation .....	56
<b>Table 5.8</b> ANN model's specifications .....	56
<b>Table 5.9</b> Statistical values of the best results of ANN modelling for training data.	58
<b>Table 5.10</b> Statistical values of the best results of ANN modelling for testing data.	58
<b>Table 5.11</b> Statistical values of the best results of ANFIS modelling for training data .....	59
<b>Table 5.12</b> Statistical values of the best results of ANFIS modelling for testing data .....	59
<b>Table 5.13</b> ANFIS architecture and training parameters for MRR and EWR.....	59
<b>Table 5.14</b> Statistical values of MRR modelling for training and testing sets .....	60
<b>Table 5.15</b> Statistical values of EWR modelling for training and testing sets.....	61
<b>Table 5.16</b> ANFIS architecture and training parameters for Ra and AWLT .....	62
<b>Table 5.17</b> Statistical values of $R_a$ modelling for training and testing sets .....	63
<b>Table 5.18</b> Statistical values of AWLT modelling for training and testing sets .....	64
<b>Table 5.19</b> Training values of material removal rate (MRR) (mm <sup>3</sup> /min) .....	66
<b>Table 5.20</b> Training values of electrode wear ratio (EWR) (%) .....	67

<b>Table 5.21</b>	Training values of surface roughness ( $R_a$ ) ( $\mu\text{m}$ ) .....	68
<b>Table 5.22</b>	Training values of average white layer thickness (AWLT) ( $\mu\text{m}$ ) .....	69
<b>Table 5.23</b>	Testing values of material removal rate (MRR) ( $\text{mm}^3/\text{min}$ ) .....	70
<b>Table 5.24</b>	Training values of electrode wear ratio (EWR) (%) .....	70
<b>Table 5.25</b>	Testing values of surface roughness ( $R_a$ ) ( $\mu\text{m}$ ) .....	71
<b>Table 5.26</b>	Testing values of average white layer thickness (AWLT) ( $\mu\text{m}$ ) .....	71
<b>Table 6.1</b>	Classification of EDM stages (Su et al., 2004) .....	74
<b>Table 6.2</b>	Specifications of the example.....	78
<b>Table 6.3</b>	Levels of electrical parameters of the EDM machine .....	78
<b>Table 6.4</b>	Different choice for $R_a = 2.7 \mu\text{m}$ .....	79
<b>Table 6.5</b>	A contrast of machined area to current .....	79
<b>Table 6.6</b>	Set of process parameters for $I = 50$ amp.....	80
<b>Table 6.7</b>	Set of process parameters for $I = 44$ amp.....	83
<b>Table 6.8</b>	Process parameter set and machining time for each stages.....	83
<b>Table 6.9</b>	Some trials of two-stages machining .....	98
<b>Table 6.10</b>	Some trials of three-stages machining.....	98
<b>Table 6.11</b>	Some trials of four-stages machining.....	98
<b>Table 6.12</b>	Some trials of five-stages machining .....	99
<b>Table 6.13</b>	Parameter sets for optimum sub-stages for Case Study-1 .....	99
<b>Table 6.14</b>	Manual calculation results for Case Study-1.....	100
<b>Table 6.15</b>	Effects of machining set-up time.....	101
<b>Table 6.16</b>	Cutting thickness coefficient and machining time .....	101
<b>Table 6.17</b>	Changing machining times with $R_{af}$ .....	102
<b>Table 6.18</b>	Surface area and machining stage .....	104
<b>Table 6.19</b>	Surface area and machining stages (with setup time) .....	105
<b>Table 6.20</b>	The multi-stage program outputs for the spherical example.....	107
<b>Table 6.21</b>	Input data of a butt mould for case study 4 .....	109
<b>Table 6.22</b>	Outputs of the program for the butt mould.....	109
<b>Table 6.23</b>	Input data of the verification example.....	111
<b>Table 6.24</b>	The multi-stage program outputs .....	112
<b>Table 6.25</b>	Set of suitable parameters for the existing EDMachine .....	112
<b>Table 6.26</b>	The verification experiment results.....	113
<b>Table A. 1</b>	Experimental data for the first group $L_{25}$ .....	128
<b>Table A. 2</b>	Experimental data for the second group $L_{25}$ .....	129
<b>Table A. 3</b>	Experimental data for randomly input parameters .....	130

<b>Table B. 1</b> Alternatives of two-stages machining for Case Study 1.....	132
<b>Table B. 2</b> Alternatives of three-stages machining for Case Study 1.....	132
<b>Table B. 3</b> Alternatives of four-stages machining for Case Study 1 .....	134
<b>Table B. 4</b> Alternatives of five-stages machining for Case Study 1 .....	142

## LIST OF FIGURES

<b>Figure 3.1</b> Schematic view of ram EDM.....	9
<b>Figure 3.2</b> Schematic view of small-hole drilling EDM .....	10
<b>Figure 3.3</b> Schematic view of wire EDM.....	10
<b>Figure 3.4</b> Components of ram EDM (Ledvon, 2004).....	11
<b>Figure 3.5</b> R-C power-supply system for capacitor charge and discharge (Elman, 2001) .....	12
<b>Figure 3.6</b> Basic transistor sparking circuit (Elman, 2001).....	12
<b>Figure 3.7</b> Formation of spark between the electrode and workpiece (Elman, 2001) .....	14
<b>Figure 3.8</b> Formation of next spark (Elman, 2001).....	14
<b>Figure 3.9</b> View of a column of ionized dielectric (Elman, 2001).....	15
<b>Figure 3.10</b> Stages of EDM cycling a) Formation of vaporized cloud b) Suspended of vaporized cloud in the dielectric c) Solidification of cloud as form of EDM chip (debris) (Elman, 2001) .....	15
<b>Figure 3.11</b> Typical EDM pulse current train for controlled pulse generator.....	17
<b>Figure 3.12</b> Effect of discharge current on both removal rate and surface roughness .....	17
<b>Figure 3.13</b> Effect of pulse on-time on both MRR and surface roughness.....	18
<b>Figure 3.14</b> Illustration of $T_{on}$ , $T_{off}$ , pulse time and duty cycle.....	19
<b>Figure 3.15</b> Effect of frequency on surface finish (or crater size) .....	20
<b>Figure 3.16</b> Electrode Melting Points .....	20
<b>Figure 4.1</b> View of Furkan EDM machine.....	24
<b>Figure 4.2</b> View of Specimens .....	30
<b>Figure 4.3</b> Digital weighing machine (Radwag WTB 200) .....	31
<b>Figure 4.4</b> View of Mahr stylus instrument .....	33
<b>Figure 4.5</b> View of EDMed surface .....	34
<b>Figure 4.6</b> Transverse section of specimen .....	35
<b>Figure 4.7</b> Forcipol 2V grinder polisher.....	35
<b>Figure 4.8</b> View of Nikon Ma100 metallographic microscope.....	35
<b>Figure 4.9</b> The influences of both discharge current and pulse on-time (at $T_{off}=12$ $\mu$ s) on MRR at finishing stage .....	37
<b>Figure 4.10.</b> The influences of both discharge current and pulse on-time (at $T_{off}=50$ $\mu$ s) on MRR at roughing stage .....	37



<b>Figure 4.11</b> The influences of both discharge current and pulse off-time (at $T_{on}=100$ $\mu$ s) on MRR at roughing stage .....	38
<b>Figure 4.12</b> The influences of both discharge current and pulse on-time (at $T_{off}=6$ $\mu$ s) on EWR at finishing stage .....	39
<b>Figure 4.13</b> The influences of both discharge current and pulse on-time (at $T_{off}=25$ $\mu$ s) on EWR at roughing stage .....	39
<b>Figure 4.14</b> The influences of both discharge current and pulse off-time (at $T_{on}=100$ $\mu$ s) on EWR at roughing stage .....	40
<b>Figure 4.15</b> The influences of both discharge current and pulse on-time (at $T_{off}=6$ $\mu$ s) on $R_a$ at finishing stage .....	41
<b>Figure 4.16</b> The influences of both discharge current and pulse on-time (at $T_{off}=12$ $\mu$ s) on $R_a$ at roughing stage .....	41
<b>Figure 4.17</b> The influences of both discharge current and pulse off-time (at $T_{on}=100$ $\mu$ s) on $R_a$ at roughing stage .....	42
<b>Figure 4.18</b> The influences of both discharge current and pulse on-time (at $T_{off}=3$ $\mu$ s) on AWLT at finishing stage .....	43
<b>Figure 4.19</b> The influences of both discharge current and pulse on-time (at $T_{off}=12$ $\mu$ s) on AWLT at roughing stage .....	43
<b>Figure 4.20</b> The influences of both discharge current and pulse off-time (at $T_{on}=100$ $\mu$ s) on AWLT at roughing stage .....	44
<b>Figure 5.1</b> Main neuron model .....	46
<b>Figure 5.2</b> Three-layered feed forward neural network topology .....	48
<b>Figure 5.3</b> A typical ANFIS architecture (Jang, 1993). .....	49
<b>Figure 5.4</b> Expression tree for MRR .....	54
<b>Figure 5.5</b> Expression tree for EWR .....	55
<b>Figure 5.6</b> Comparisons of training and testing performances of all methods for MRR .....	60
<b>Figure 5.7</b> Comparisons of training and testing performance of all methods for EWR .....	61
<b>Figure 5.8</b> Training and testing performances of ANN and ANFIS methods for $R_a$ .....	63
<b>Figure 5.9</b> Training and testing performances of ANN and ANFIS methods for AWLT .....	64
<b>Figure 6.1</b> Views of white layer on various stage where a) $I=50$ A, $T_{on}=400\mu$ s, $T_{off}=100\mu$ s, $AWLT=111.1\mu$ m, $R_a=10.9\mu$ m b) $I=12$ A, $T_{on}=50\mu$ s, $T_{off}=3\mu$ s, $AWLT=22.3\mu$ m, $R_a=6.9\mu$ m c) $I=3$ A, $T_{on}=3\mu$ s, $T_{off}=3\mu$ s, $AWLT=6.7\mu$ m, $R_a=2.18\mu$ m .....	76
<b>Figure 6.2</b> A section view of rest material from previous machining stage .....	77
<b>Figure 6.3</b> View of two-stage machining .....	80
<b>Figure 6.4</b> View of three-stage machining for prismatic parts .....	84

<b>Figure 6.5</b> Main menu of program for rectangular shapes .....	93
<b>Figure 6.6</b> Main menu of program for circular shapes.....	93
<b>Figure 6.7</b> Main menu of program for complex shapes .....	94
<b>Figure 6.8</b> Entering input data into the program for rectangular part .....	95
<b>Figure 6.9</b> Output display from program for one-stage .....	95
<b>Figure 6.10</b> Output display from program for two-stage .....	95
<b>Figure 6.11</b> Output display from program for third-stage.....	96
<b>Figure 6.12</b> Output display from program for four-stage .....	96
<b>Figure 6.13</b> Output display from program for five-stage .....	96
<b>Figure 6.14</b> Display of minimum machining time tables for all trials .....	97
<b>Figure 6.15</b> Display of optimum machining time for each stage .....	97
<b>Figure 6.16</b> Effect of number of stages on machining time .....	100
<b>Figure 6.17</b> Effect of cutting thickness coefficient ( $k$ ) on machining time.....	102
<b>Figure 6.18</b> Relation between the machining time and $R_{af}$ .....	103
<b>Figure 6.19</b> View of three-stage machining for cylindrical shape .....	104
<b>Figure 6.20</b> The effects of surface area on the machining stages .....	106
<b>Figure 6.21</b> The solid model of spherical surface .....	107
<b>Figure 6.22</b> Solid model of the butt mould .....	109
<b>Figure 6.23</b> The solid model of the machining stock for 3-stage.....	110
<b>Figure 6.24</b> Photos of the white layers of the verification example (a ) rough , (b) middle and (c) finish stage .....	114

## **CHAPTER 1**

### **INTRODUCTION**

Machine parts used in the automobile, aerospace and medical industries are produced from very hard, high-strength and temperature-resistant materials and they have generally geometrically complex shapes. Therefore their manufacture them is quite difficult via traditional machining process, however Electrical Discharge Machining (EDM) is a mostly used process for manufacturing such parts.

EDM is an electro-thermal process in which material is removed rapidly and repeatedly by spark discharges across the gap between the workpiece and their tool both of them are immersed in a dielectric. The electrode and the workpiece must have electrical conductivity in order to generate the spark. No direct contact occurs between electrode and workpiece so no contact stress is caused with the processed material.

However, metal removal process in EDM has a nonlinear, randomness and time varying properties (Lee and Li, 2001). It is difficult to select process parameter set from experience or from the manufacturer tables to meet the specified machining performances. Therefore, a model is necessary that could automatically select an optimal process parameter set that results in corresponding machining performances equal to or at least nearest to that parameter specified. EDM process requires much skill or effort since it has a quite complex mechanism that is not clearly understood. Therefore, creating a model, that can positively predict the EDM performance by correlating the process parameter, is very difficult.

The application area of EDM process is limited due to its disadvantages such as lower productivity, a high specific energy consumption and longer processing time. To create a model that can predict the EDM performance by using input parameters is highly difficult because of the complexity of the process.

However, a quantitative relationship between the performance parameters and controllable input parameters is often needed in EDM.

In a complete EDM process, machining stages that usually include rough, middle and finish-stage are carried out sequentially. In order to obtain specified dimensional accuracy and surface quality, multi-stage process planning from rough to finish stages is necessary. The optimal machining parameters for each cutting operation can be obtained by seeking the minimum time under the constraints of surface roughness, white layer depth and the other constraints. Average surface roughness ( $R_a$ ), material removal rate (MRR) and electrode wear ratio (EWR) are the most important machining performance criteria often applied to evaluate the machining effects in each stage. Many process parameters that can be varied in the different machining stages of EDM process greatly affect the machining performances. For example, higher MRR and lower EWR are needed in the rough-cut without paying attention to  $R_a$ ; however, lower  $R_a$  is given much weight in the finish-cut. Consequently, it becomes important to select properly the process parameter set for different machining stages in order to promote efficiency and quality (Su et al., 2004).

The setting of machining parameters relies strongly on the experience of operators and machining-parameters tables provided by machine tool builders. It is difficult to utilize the optimal functions of an EDM machine owing to many adjustable machining parameters. Machining-parameter set from rough to finish stage helps EDM operator to make decisions of the stages of machining operations. This machining-parameter set is quite useful but that causes time-consuming. Moreover, this kind of machining decision is too conservative and does not lead to an optimal solution (Scott et al., 1991).

On the other hand, optimum number of machining stages from rough to finish cutting and set of process parameters of each stage have not been properly defined yet. Although many studies and results are available for single stage EDM, sufficient work is lacking in the area of multi-stage EDM process.

The objective of this study is to develop a parameter selection model for ram type EDM process by using multi-stage strategies. The strategy may allow the user to reduce costs by reducing the machining time and/or number of electrodes required to

complete the operation under the constraints of surface roughness and white layer thickness. For this purpose, a series of experiments were carried out and a parametric analysis was done to develop empirical models for performance variables using a suitable artificial intelligent tool (Artificial neural network, Genetic algorithm, ANFIS etc.). According to the developed strategy, EDM will be operated by automatically selecting the numbers and sequences of the stages and machining parameter set for each stage for minimum machining time and desired surface quality. For verification of the developed models, a number of case studies were performed in the multi-stage machining.

The thesis has been organized in seven chapters. Chapter 1 presents the area of research work to be undertaken has been identified, the objective and the work plan were discussed. Chapter 2 presents the literature survey of multistage EDM. The description of the EDM, the process and the performance parameters are given in Chapter 3. In Chapter 4, the experimental studies are explained and their results are discussed. Chapter 5 compares the ANN, ANFIS and GEP model in terms of the prediction performances of EDM outputs. In Chapter 6, the development of multi-stage strategy and a computer program have been presented. Four case studies and their results are shown. The conclusions drawn from the work and the proposed future plan are given in Chapter 7.

## CHAPTER 2

### LITERATURE SURVEY

#### 2.1 Introduction

Electrical discharge machining was firstly performed in 1943, by Russian scientists, Mr and Mrs. Lazarenko. (Lazarenko, 1943). They designed the first EDM machine, which was very useful to erode hard metals such as tungsten or tungsten carbide. They used controlled sparking as an erosion method. In the 1950's, by understanding the erosion phenomenon, industrial EDM machines were initially produced. These types of machines had a resistance-capacitance type of power supply. Owing to the lack of quality in electronic components, the performances of the machines were restricted at the time. (Germer and Haworth, 1949; Cobine and Burger, 1955; Zingerman, 1956). In the 1960's, EDM machines were significantly improved by the invention of the semiconductor. In the early 1970's, the electrodes could move more precisely with the numerical position control. Moreover, Computer numerically controlled system (CNC) raised up the EDM performance in middle 1970's. 1980's CNC EDM supplied radical advances in machining efficiency of EDM processes. Lastly, new methods for EDM process control arose in the 1990's by using soft computing techniques.

EDM is one of the profitable machining processes used for accurate and high precision geometry of the work piece. So, many studies have been reported about EDM by the authors since 1943. As far as EDM is concerned, mainly four kinds of research trends are carried out by the researches viz. modelling and optimizing the process variables, improving the output performances, monitoring (controlling) the process and new developments in EDM. Only a small number of works are particularly related with multi-stage EDM.

## 2.2 Literature of Multi-Stage EDM

Kishi et al. (1989) proposed a simple nonlinear model considering the amount of material removed at each stage as a function of the resulting surface finish for planetary EDM. Electrode wear ratio was taken as constant for each stage to make the strategy possible. Furthermore, dimensional tolerance cannot completely be provided owing to not considering electrode wear.

Imagana et al. (1989) analysed EDM process factors having effects to accuracy of final workpiece. The factors were positioning error of the electrode, thermally induced deviations, and tool wear. They suggested that to achieve dimensional accuracy, desired machining time, and final surface finish the parameters must be analysed rightly.

Niwa et al. (1995) studied the optimization of the machining time in rough and middle stages, in large moulds the strategy supplied a 50% improvements according to previous studies. However, they didn't deal with the elimination of white layer.

Optimization of the finish cutting process in WEDM was studied by Huang et al. (1999). The goal of the study was the minimization of the machining time where finishing surface quality and the recast layer depth were the limitations. They suggested an approach which contains the removal of heat affected zone and the recast layer with together. At the end of the experimental study, they concluded that better surface quality and exact dimension can be achieved by using their minimum machining time strategy.

Liao et al., (2001) used Genetic Algorithms (GA) to optimize no of stages, material removal rate, and tool wear at each stage. They made use of a back-propagation neural network to explain that relationship among material removal rate, surface finish, and electrode wear. Although the proposed strategy was valid to achieve finishing stage in terms of minimum machining time and surface quality, dimensional correctness of the final part was restricted for industrial application of the strategy.

Sanchez et al. (2002) evaluated the validity of various multi-stage planetary EDM strategies according to machining time and surface finish. They analysed various errors, especially related to thermally induced errors, which were arithmetically

replicated from experimental data gathered throughout the process. They reported that multi-stage planetary EDM was a good selection in order to minimize machining time and cost of electrode in finishing processes. Machining of  $R_t$  at each stage was taken as a strategy which gave the best results in terms of machining time but increased the final surface roughness values.

Su et al. (2004) presented a model to optimize EDM parameters at each stage from rough to finish. They utilized a neural network model to relate the EDM parameters and performances. The model was developed depended on the manufacturer classification tables. They were reveals that the machined area governs the strength of discharge current and was available to determine the low voltage discharge current in rough-cut. To find out optimum process parameters, genetic algorithms were adapted to neural network. Hence, the results showed that the GA-based neural network might be succeeded to create optimal process parameters from the rough to the finish stage. However, the machining stages are fixed as rough, middle and finish, respectively.

Zeng et al. (2005) and Lim et al (2007) showed that the sequencing of electrodes is critical in the EDM process since the roughing, semi-finishing and finishing electrodes cannot be distinguished visually. The physical difference between the electrodes is 50  $\mu\text{m}$  for each stage. The selection of electrodes is usually based on the availability of electrodes of the workshop supervisor's or operator's experiences. However, it is a potential source of mistake. They described an innovative low cost, easily adaptable shop-floor solution to eliminate manual intervention and potential errors.

Sanchez et al. (2006) described a method for the calculation of gap variation between two sequential stages that could be applied for both roughing and finishing processes. The surface roughness of each sequential stage was defined by experimental study for reliability of the method. Two strategies depended on the removal of  $R_t$  or the removal of  $R_t/3$  for each stage were applied. It was seen that the removal of  $R_t/3$  was not guaranteed for the sidewall surface roughness at each stage. However, the method based upon the whole removal of  $R_t$  was seen as the most suitable for assuring sidewall roughness and machining time.

Assarzadeh and Ghoreishi (2008) offered a new approach to optimize the parameters in EDM for accomplishing maximum MRR to suitable working restrictions on the



surface roughness ( $R_a$ ) and machining variables. In this study, the optimization procedure was applied out in each level of the machining stages, for example finishing stage ( $R_a \leq 2 \mu\text{m}$ ), middle stage ( $R_a \leq 4.5 \mu\text{m}$ ), and rough stage ( $R_a \leq 7 \mu\text{m}$ ), from which, the optimal machining parameter settings were obtained.

Sarkar et al. (2008) dealt with the features of trim cutting operation of wire electrical discharge machining of gamma-titanium aluminium in the work. Finally the trim cutting operation was optimized for a given machining condition by desirability function approach and Pareto optimization algorithm. It was observed that performance of the developed Pareto optimization algorithm was superior compared to desirability function approach.

Joshi and Pande (2011) reported an intelligent approach for process modelling and optimization of electric discharge machining (EDM). The developed ANN process model was used in conjunction with the evolutionary non-dominated sorting genetic algorithm (NSGA) to select optimal process parameters for roughing and finishing operations of EDM. The optimal ranges of process parameters for roughing and finishing operations were identified. During the present study the objective set for the optimization of roughing application was to maximize the MRR and minimize the tool wear ratio (TWR). For finishing operation of the EDM process, three objective criteria were thought, such as; low crater depth (surface roughness), low TWR and moderate MRR. The model is validated using the reported analytical and experimental results.

### **2.3 Summary of Literature Survey**

Literature survey can be summarised as follows;

- In order to obtain specified dimensional accuracy and surface quality, multi-stages process planning from rough to finish cutting is necessary.
- Machining of moulds and dies with electro erosion generally includes a number of machining stages from rough to finish, and various machining parameters are necessary for each stage.
- The purpose of the rough stage is to obtain maximum material removal rate, the surface quality cannot be considered as an important issue.

- The other next stages gradually increase the surface quality and dimensional accuracy.
- The machining parameters must be adjusted for different stages so as to minimize machining time and to provide the characterization of surface finish and dimensional tolerances. But, due to the many factors, an optimum technique may not be possible all the time.
- In general, researches are related to rough machining (optimizing material removal performance) or finishing (optimizing surface quality). However, there is a lack of knowledge about a complete EDM process (from rough to finish)
  - Three stages (rough, middle and finish) were applied to all EDM process. However, the limitations of machining stages were not properly defined or number and the sequence of stages were not optimized.
  - Optimum number of machining stages from rough to finish cutting and set of process parameters of each stage were not properly defined yet.

## CHAPTER 3

### BASIS OF EDM

#### 3.1 Introduction

In this chapter, types of Electrical Discharge Machines and their working principles are presented. Main components of ram-EDM machine and their functions are given. The removal mechanism of EDM process are explained. Main process parameters and the performance parameters of EDM are also mentioned.

#### 3.2 Types of EDM

There are three main types of EDM; ram EDM, fast-hole EDM and wire EDM. All EDM machines use sparks to remove electrically conductive material (Sommer and Sommer, 2005). However they use different electrode types, dielectric fluids. The operation technology and application field of them are different as well (Youssef and El-Hofy, 2008).

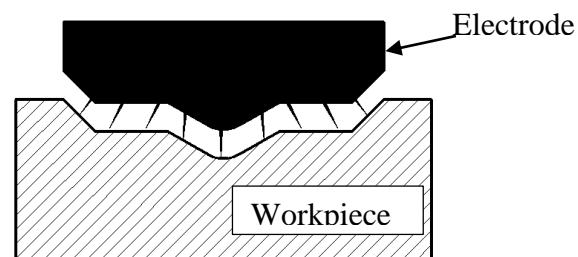


**Figure 3.1** Schematic view of ram EDM

Ram type EDM (Figure 3.1) machines are used to produce three dimensional shapes as mould cavities (Elman, 2001). The electrode and workpiece are submerged in a dielectric fluid, which is generally hydrocarbon oil. In order to machine desired shape, a formed electrode is used. End of the operation, opposite shape of the electrode produced in the workpiece. In ram EDM sparking occurs between the end surface and the corners of the electrode and workpiece.

Small-hole EDM drilling machines, as shown in Figure 3.2, use the similar principles as ram EDM (Sommer and Sommer, 2005). A constantly rotated hollow electrode and high pressurized pumping of dielectric fluid (deionized water) through the inner surface of electrode tube are the two separate features. The process is used to produce fuel injectors, venting holes of injection moulds, coolant holes of injection cutting tools, hardened punch ejector holes, wire-EDM starter holes, holes in turbine blades and other similar operations.

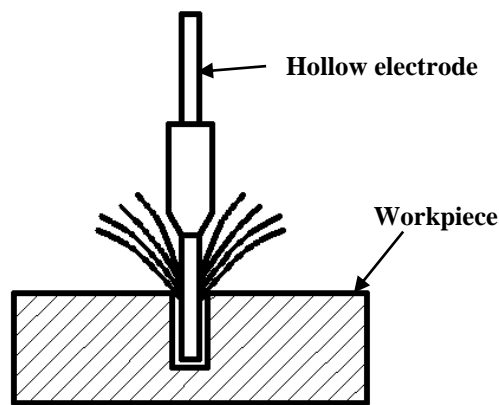


**Figure 3.2** Schematic view of small-hole drilling EDM

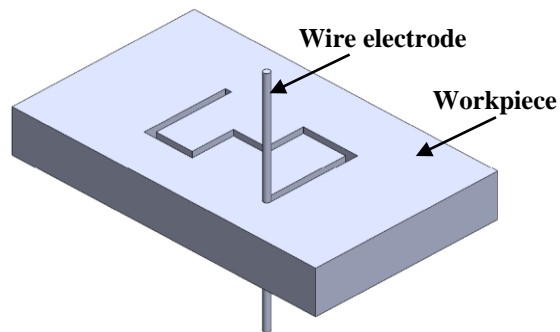


**Figure 3.3** Schematic view of wire EDM

Wire EDM is a special form of EDM which uses a continuously moving conductive wire electrode (Figure 3.3). Sparking takes place from the electrode wire-side surface to the workpiece. As the wire feeds from spool to spool, material removal occurs as a result of spark erosion on conductive work-piece along a computer-controlled (CNC) path by the relative motion of the machine's axis (El-Hofy, 2005). The wire is usually made of brass or copper, and is between 0.1 and 0.3 mm diameter. The dielectric fluid being used in wire EDM is deionized water that is only sprayed into the sparking area. Extrusion dies and blanking punches are very often machined by wire cutting, since cutting is always passing through the workpiece.

Since Ram type EDM is the subject of the thesis, the detailed knowledge about Ram EDM will be given following section.

### 3.3 Ram EDM Machine Components

Ram EDM is the main EDM process wherein a male electrode submerges into a workpiece to produce a female cavity. Ram EDM is commonly used in die and mould making industry to produce 3D complex shapes. A typical EDM sinker machine has mainly four components (Figure 3.4) as below;

- 1) Power supply unit (spark generator)
- 2) Servo mechanism (system )
- 3) Dielectric liquid system
- 4) Mechanical structure

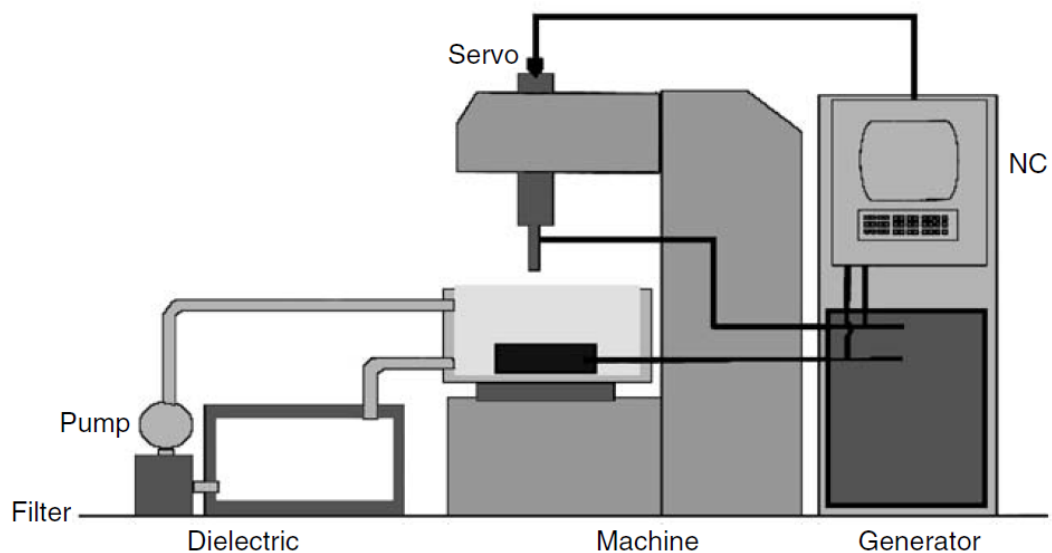


**Figure 3.4** Components of ram EDM (Ledvon, 2004)

#### 3.3.1 Power Supply Unit (Spark Generator)

Power supply unit, the main part of EDM machine, is used as the source of electrical pulses. This generator supplies enough voltage to start and keep on the discharge process, and essential control over the process parameters such as pulse, voltage, current, pulse on-time, and off time by means of a controllable semiconductor switching circuit. The power generators are grouped into two types according to the voltage transformation and the pulse controlling. These are the resistance-capacitance generator (RC circuit) and the pulse-type-power generator.

In the RC circuit (Figure 3.5), electricity flows from the DC-power source through the resistor and is then deposited in the capacitor. During off-time, the capacitor is charged to its electrical capacity, it discharges through the electrode, through the workpiece, and through the sparking gap in the form of a spark at on-time.

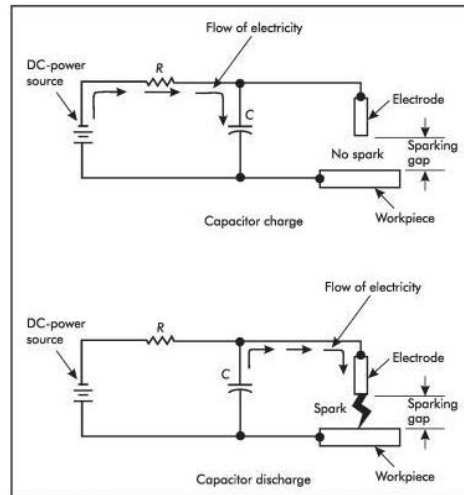


**Figure 3.5** R-C power-supply system for capacitor charge and discharge (Elman, 2001)

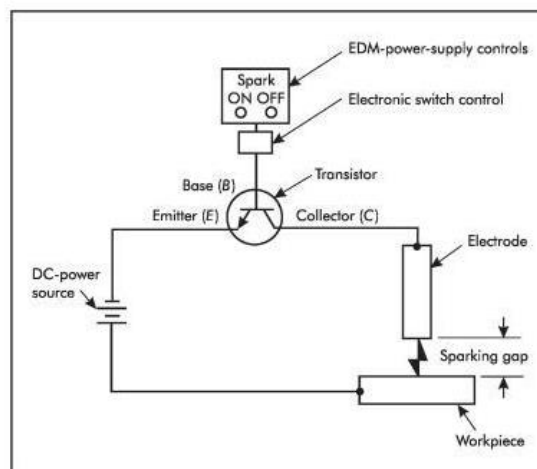


**Figure 3.6** Basic transistor sparking circuit (Elman, 2001)

In Pulse-Type-Power Generator (Figure 3.6), the transistor acts as an electronic switch that can be opened or closed by an electronic signal. When the transistor is closed, the electricity flows from the DC-power source to the electrode, across the sparking gap to the workpiece, and then returns to the DC power source, the time is called pulse on-time ( $T_{on}$ ). When the transistor is open, the flow of electricity stops, and that is known as pulse off-time ( $T_{off}$ ). Figure 3.6 illustrates a basic electrical diagram for a transistor sparking circuit.

### **3.3.2 Servo System**

In EDM, a spark jumps across a gap between the electrode and the workpiece. Both electrode and workpiece are eroded during the process, after a while, the changes in dimensions of the electrodes results increase in the gap. This causes to be increased the voltage required for the next sparking. However, the required voltage can increase to the levels that spark generator cannot supply. To overcome this problem, the gap distance must be reduced to initial level. A servo mechanism controls the down feed of the electrode to hold constant gap. It stops the electrode to touch the workpiece to overcome a short circuit which causes no cutting. The servo system takes its input signal from the variance between the designated reference voltage and the real voltage across the gap. This signal is amplified and the tool is advanced by hydraulic control.

### **3.3.3 Dielectric Circuit Unit**

During the off-time, eroded material particles (debris) must be removed from the inter electrode gap to prevent pollution and to improve the machining performance. The pressurized dielectric oil cools the medium and removes debris from the gap. The dielectric unit which is composed of a pump, filter, tank and gages, supplies the circulation. A filter system cleans the suspended particles from the dielectric oil. The chiller cools the dielectric oil to maintenance the machining accuracy.

### **3.3.4 Mechanical Structure**

A typical EDM sinker machine has similar construction to a vertical milling machine, with vertical tool feeding and horizontal worktable movements. The electrode attached to the sinking head (vertical slide) which is moved down and up by a servo system. The workpiece is clamped inside the tank which contains the dielectric fluid and its movements can be adjusted by numerical controls.

## **3.4 Removal Mechanism of EDM**

There is a distance between workpiece and electrode, which is required for sparking. When the electrode and the workpiece get near enough, the spark jump between the closest points of the electrode and the workpiece in EDM (Figure 3.7).

Due to the sparking, the workpiece material is eroded, so the closest point changes. This causes the next spark to occur at the next-closest points between the electrode and workpiece (Figure 3.8).

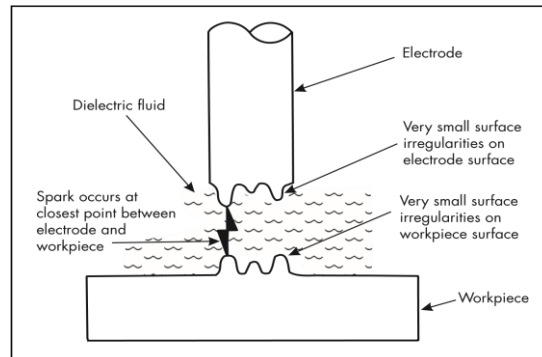


**Figure 3.7** Formation of spark between the electrode and workpiece (Elman, 2001)

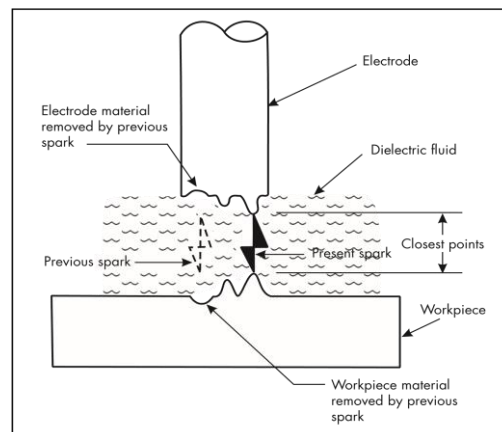


**Figure 3.8** Formation of next spark (Elman, 2001)

EDM is a thermal process; material is removed by heat. The spark between the electrode and workpiece causes the material to heat until about 8000-12000 °C. The heat also melts and vaporizes the material. While the heat does not affect the electrode and workpiece as a whole, it affects very limited area where each spark occurs.

The dielectric fluid rapidly cools the molten material and the electrode and workpiece surfaces. However, the spark heating can cause metallurgical changes on the workpiece surface. The sparking gap between the electrode and workpiece is surrounded with dielectric fluid. The dielectric fluid normally acts as an insulator. When the sufficient electrical voltage is applied, the fluid ionizes and the insulating feature of dielectric fluid breaks down at the closest points between the electrode and the workpiece. This occurs during controlled pulse on-time phase of the power supply.



This change of the dielectric fluid from an insulator to a conductor goes on for each spark. Figure 3.9 shows the EDM spark occurring within an ionized column of the dielectric fluid.

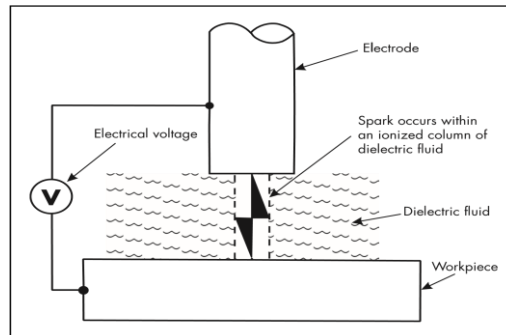


**Figure 3.9** View of a column of ionized dielectric (Elman, 2001)

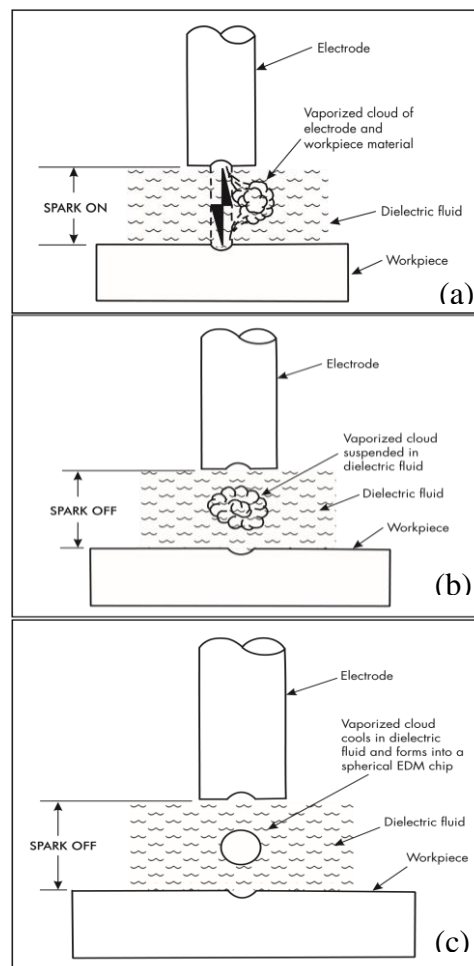


**Figure 3.10** Stages of EDM cycling a) Formation of vaporized cloud b) Suspended of vaporized cloud in the dielectric c) Solidification of cloud as form of EDM chip (debris) (Elman, 2001)

When the spark turn off, the fluid deionizes and backs to being an insulator. Each spark vaporizes a small amount of the electrode, workpiece material and also some of the

fluid. The vaporized material is located in the gap between the electrode and workpiece where it can be defined as a gas bubble. When the spark is turned off, the vaporized bubble solidifies. Each spark then creates an EDM chip or a very tiny hollow sphere of particles made up of the electrode and workpiece material.

Figure 3.10 shows the spark producing the vapour cloud, the cloud in suspension, and the vaporized cloud being cooled and forming into an EDM chip (debris). The debris must be removed from the sparking area for efficient machining. Removal of the debris is supplied by flowing dielectric fluid through the sparking gap.

### **3.5 Main EDM Process Parameters and Performance Measures**

There are a lot of process parameters affecting the EDM performances, especially the material removal rate, electrode wear ratio and surface quality. There are some different views to classify the parameters. Some researchers classify the parameters as two groups; electrical and non-electrical (Garg et al., 2010), the others classify the parameters as 5 categories; dielectric fluid, machine characteristic, tool, workpiece, and adjustable parameters which are discharge current, gap voltage, pulse on-time, pulse off-time, polarity, frequency, flushing. However the adjustable parameters are always considered as the most vital parameters (Wang and Yan, 2000; Singh et.al 1985; Tzeng and Chen, 2003).

#### **3.5.1 Gap Voltage**

Gap voltage or discharge voltage is supplied usually from a DC power source. This gap voltage is related to breakdown strength of the dielectric and regulates the thickness of the spark gap between the electrode and the workpiece as well. (Kansal et al., 2005). The gap increases by increasing voltage and this increase improves the flushing conditions and aids to stabilize the cut. Gap width is not measured directly, but can be inferred from the average gap voltage (Crookall and Heuvelman, 1971)

#### **3.5.2 Peak or Discharge Current**

There are two types of currents (Figure 3.11):

- Peak current: is the maximum current that can occur during the discharge.

- Average (discharge) current: is the average of the amperage in the spark gap measured over a complete cycle. It is calculated by multiplying peak current to duty cycle.

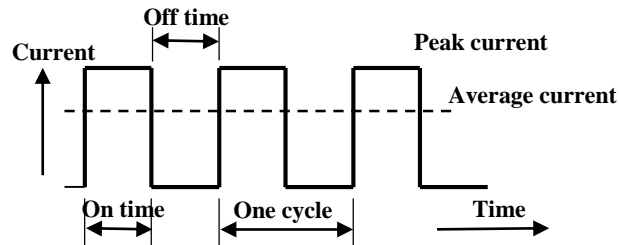


**Figure 3.11** Typical EDM pulse current train for controlled pulse generator

When discharge current rises up, each spark removes a larger crater from the workpiece. In this case, the amount of material removed on both electrode and workpiece increases, however; the surface finish produced gets worse (Figure 3.12).

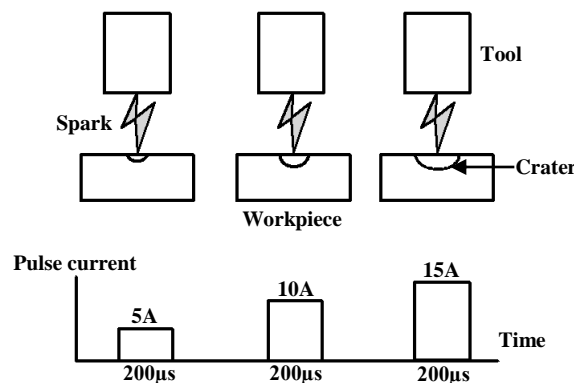


**Figure 3.12** Effect of discharge current on both removal rate and surface roughness

### 3.5.3 Pulse on-time ( $T_{on}$ )

Pulse duration is also known as pulse on-time measured in micro seconds ( $\mu\text{s}$ ). During  $T_{on}$ , the current flows from the electrode towards the work material. Longer  $T_{on}$  results in an increase in removal rate of debris from the machined area that also influences the wear of electrode. (Rao et al., 2008). Thus, the resulting craters will be wider and deeper; so the surface finish will be rougher. Clearly with shorter  $T_{on}$  the surface finish will be improved. (Figure 3.13)

### 3.5.4 Pulse off-time ( $T_{off}$ ):

Pulse off-time (pulse interval) is the time during which re-ionization of the dielectric take place. In pulse off-time, the melt material solidifies and is washed out of the spark

gap and no machining happens.  $T_{off}$  should be long enough to start the next cycle. Although MRR increases with decreasing  $T_{off}$ , but the dielectric fluid will not clean the molten material from the gap and not have enough time to be deionized.  $T_{off}$  must be longer than the deionized time to supply consistency of regular sparking. So this prohibits unpredictable cycling and movement of the servo-system, reducing the machining speed.

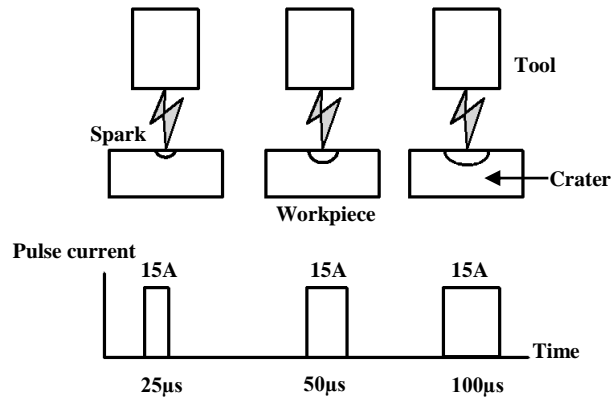


**Figure 3.13** Effect of pulse on-time on both MRR and surface roughness

### 3.5.5 Polarity

Polarity is the direction of the current movement between the electrode and workpiece. Polarity has the effects on machining speed, surface finish, electrode wear and stability of the EDM operation. Electrode polarity is based on both the workpiece and electrode materials. The change of polarity for the same electrode vitally affects the output performances. On the other side, wrong polarity selection can alter both speed and stability.

**Table 3.1.** Electrode polarities for different workpiece materials (Metals handbook, 1989)

Electrode material	Workpiece material				
	Steel	Tungsten Carbide	Copper	Aluminium	Ni-based alloys
Graphite	+, -	-	-	+	+, -
Copper	+	+, -	-	+	+
Cu-W	+, -	+, -	-	+	+
Steel	+, -	+	-	-	-
Brass	-	-		+	-

Table 3.1 shows the possible suggested electrode polarities for different workpieces and tool selections (Metals handbook, 1989). Generally, electrodes with positive polarity wear better, while electrodes with negative polarity cut faster. However, some

metals do not respond this way. Carbide, titanium, and copper are generally cut with negative polarity.

The polarity, pulse on-time, pulse off-time and the peak current are the basic machine settings. These parameters can also be expressed as duty cycle, pulse frequency and average current (Kumar et al., 2008).

### 3.5.6 Duty Cycle:

Duty cycle is the ratio of the pulse duration over the total cycle time, as shown below (Figure 3.14).

$$\text{Duty cycle} = \frac{T_{on}}{T_{on} + T_{off}} \quad 3.1$$

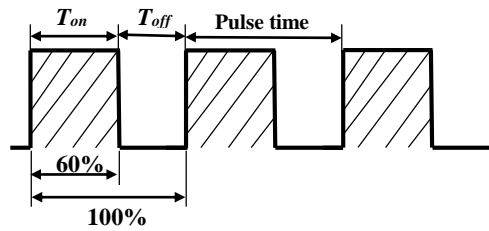


**Figure 3.14** Illustration of  $T_{on}$ ,  $T_{off}$ , pulse time and duty cycle

Since, the intensity of spark increases by resulting in higher MRR, MRR increases with increasing duty cycle at constant peak current and  $T_{on}$  (Rao et al., 2008). Average current is calculated based on the duty cycle and the peak current as;

$$I_a = I_p \times \text{duty cycle} \quad 3.2$$

where:  $I_a$ = average current,  $I_p$ = peak current

### 3.5.7 Spark (Pulse) frequency:

The number of cycles generated across sparking gap in one second is defined as pulse frequency. Pulse frequency is calculated by dividing 1000 by the total cycle time ( $T_{on}+T_{off}$ ) in microseconds.

$$\text{Pulse Frequency (kHz)} = \frac{1000}{\text{Total cycle time } (\mu s)} \quad 3.3$$

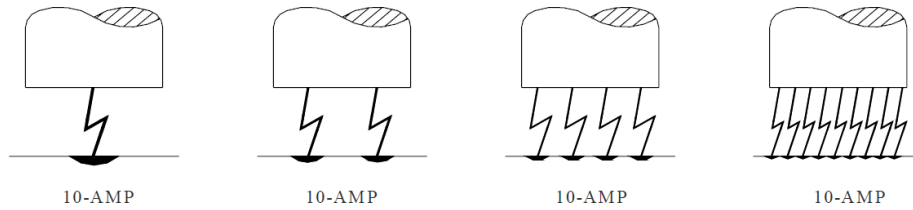


**Figure 3.15** Effect of frequency on surface finish (or crater size)

Since short  $T_{on}$  removes very little material and produces smaller craters (Figure 3.15), high spark frequencies are normally used for finishing operations where fine surface finish is desired. On the other side, low spark frequencies are used for roughing operations. Additionally, electrode wears much with high frequency.

### 3.5.8 Electrode Materials:

Electrode selection is important for ram EDM. Because, an electrode is necessary for transmission of the electrical charges so as to form desired shape in the workpiece. As some of electrode materials give efficient MRR and have large electrode wear; other electrode materials have slight wear and reduce MRR. In the selection of electrode, MRR, wear resistance, quality of surface finish, cost of electrode material must be taken into consideration (Pandey et al., 2010).

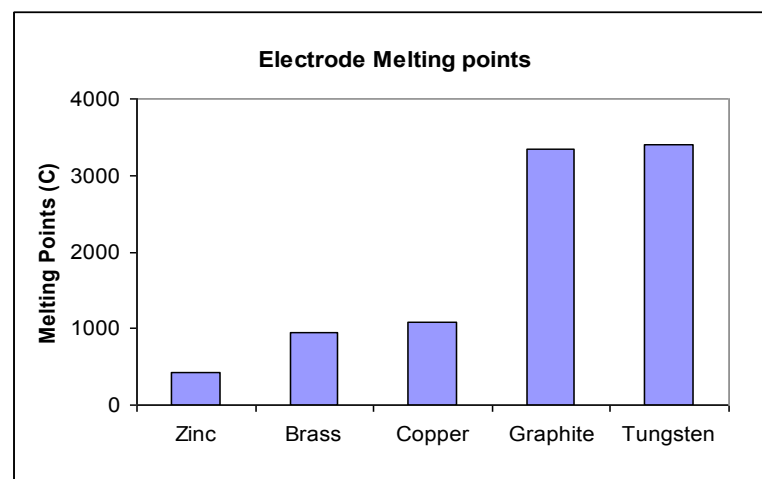


**Figure 3.16** Electrode Melting Points

Electrode materials are grouped as; metallic and graphite. Commonly used electrodes are brass, copper, tungsten, zinc, and graphite (Figure 3.16). In general, metallic electrodes are utilized for machining of low temperature alloys and graphite electrode are used for machining of high temperature alloys.

Graphite and Copper are the most commonly used electrode materials in EDM industry.

**Copper:** is widely used when smooth workpiece surface finishes are required. Because, it is suitable for usages in high frequency. Copper can be machined with traditional machining methods. But sometimes it can be difficult because copper tends to drag on the edge of the cutting tool and the grinding wheel. Copper has the ability to be coined and then to be a very good material for engraving electrodes. Copper is used in medical industry, due to its capability to be highly polished. Furthermore, during CNC cutting, the copper electrode can be sized by using a sizing plate and then it is able to be reused for finishing operation or used to produce another part.

**Graphite:** has different grain sizes. As coarse grain sized graphite electrodes are appropriate for roughing operation, small grain sized graphite is suitable for finishing operation. It supplies a high material removal rate and low electrode wear as compared to metallic electrodes. Since density of graphite is lesser than those of copper, it is the best material for large electrodes. It is easy to be machined by all the conventional machining processes. But, during the machining, being produced the fine dust can be mixed with the cutting fluid so it can cause the fluid to act like a lapping compound, which eventually reduces the exactness of the machine.

### 3.5.9 Dielectric Fluids

The dielectric fluid has three main roles:

- Flushing away the debris from the sparking gap
- Providing insulation between the electrode and the workpiece
- Cooling the sparking area that was heated by the discharging effect

The main requirements of the EDM dielectric fluids are high dielectric strength and quick recovery after breakdown, effective quenching and flushing ability (Wong et al., 1995). In ram EDM, the hydrocarbon compounds are generally used, in the form of refined oil (known as kerosene). Flushing of the dielectric has a significant role to keep machining stability and the accomplishment of close tolerance and high surface quality. Insufficient flushing can cause arcing, decreasing electrode life, and

decreasing MRR. (El-hofy, 2005). There are five types of flushing fluid system in EDM (Sommer, 2005);

1. Pressure flushing
  - a. Through electrode
  - b. Through workpiece
2. Suction flushing
3. Combined pressure and suction flushing
4. Jet flushing
5. Pulse flushing
  - a. Vertical flushing
  - b. Rotary flushing
  - c. Orbiting flushing



## CHAPTER 4

### EXPERIMENTAL STUDY

#### 4.1 Introduction

In this chapter, experimental studies are presented for understanding the EDM process. These experiments will supply helpful knowledge about the EDM such as influences of input parameters on output performances and practical data about different machining stages. These data are necessary to develop multi-stage strategy and they will be used to model output performances via a suitable artificial intelligent tool.

#### 4.2 Machine Specification and Input Parameters

The ram EDM machine (Furkan Model M50A) with servo head (constant gap) was used to perform the experiments (Figure 4.1). The machine allows you to set levels of current intensity and the current voltage and frequency at each level are automatically adjusted by the machine itself. In this study, discharge currents ( $I$ ), pulse on-time ( $T_{on}$ ), pulse off-time ( $T_{off}$ ) were taken as variable parameters, on the other hand, gap voltage, flushing pressure and polarity were taken as invariable parameters (see Table 4.1). Because, these parameters are the most effective electrical parameters which were reported by many researches (Mandal et al., 2007; Maji and Pratihari, 2010; Yilmaz et al., 2006). These are also mainly given parameters at technological tables of many EDM companies.



**Figure 4.1** View of Furkan EDM machine

**Table 4.1.** Variable and invariable parameters' levels

Variable parameters	Level Values
Discharge current, $I$ (A)	3,6,9,12,18,25,50
Pulse on-time, $T_{on}$ ( $\mu$ s)	3,6,12,25,50,100,200,400,800,1600
Pulse off-time, $T_{off}$ ( $\mu$ s)	3,6,12,25,50,100,200
Invariable parameters	
Dielectric	Kerosene
Gap voltage (volt)	60 V
Dielectric flushing pressure	0.1 MPa
Polarity of tool electrode	Positive

### 4.3 Workpiece Material

The hot work tool steel (DIN 1.2344, X40CrMoV5.1) was selected as workpiece material. The application area of the material in industry is very wide such as pressure casting dies, metal extrusion tools, forging dies, moulds, screws and hot-shear blades etc. The material has exclusive properties such as high hot-wear resistance, high hot tensile strength and toughness, good thermal conductivity and insusceptibility to hot cracking. In Table 4.2, the chemical composition of the material is given.

**Table 4.2** Chemical composition of workpiece material (1.2344)

%C	%Si	%Cr	%Mo	%V
0.40	1.05	5.2	1.40	1.00

#### 4.4 Electrode Material

Most EDM works can be done with copper electrode and also with graphite electrode. The result of work may be the same, but the cost to accomplish the work can be quite different. Both of the electrode materials have certain advantages and disadvantages for different applications (Haron et al, 2008; Amorim and Weingartener, 2007).

Normally, graphite is the mostly preferred material for EDM users in USA. However, copper is largely used in Europe or Asia. The electrode material selection will be based primarily on the tool size, the workpiece necessities, type of EDM machine and the methods of making the electrodes.

In this study commercial copper (Table 4.3) electrode was selected as electrode material owing to the following advantages (Amorim and Weingartener, 2007):

- It can produce very fine surface finishes, even without special polishing circuits due to its structural properties.
- It can be machined by traditional methods
- It has the ability to be coined and then to be a very good material for engraving electrodes.
- It is the best choice in medicine engineering field, because of its facility to be highly polished.
- It has good EDM wear and better conductivity.
- It performs better in “discharge-dressing”. The copper electrode can be sized automatically by using a sizing plates and then it can be reused for a next cut.

**Table 4.3.** Electrode material specifications

Material	Copper
Density (kg/m <sup>3</sup> )	8905
Melting point (°C)	1083
Electrical resistivity (μΩ cm)	8.9
Hardness (HB)	100

## 4.5 Polarity

Polarity refers to the direction of the current flow between the workpiece and electrode. While the usage of negative polarity is suitable for fast machining, positive polarity is suitable for electrode wear. Electrode polarity depends on both the workpiece and electrode materials. In this study, because of the fact that the workpiece is the steel and electrode material is copper, so polarity were selected positive according to recommendation of specialists (see Table 3.1).

## 4.6 Dielectric

Kerosene was selected as dielectric fluid because of its high flash point, good dielectric strength, transparent characteristics and low viscosity and specific gravity.

## 4.7 Design of Experiment

In order to see the effect of selected input parameters to machine performances at each cutting stages, a wide range of values of input parameters are taken. However, the following limitations have to be considered during the selection of the input values:

- $T_{on}$  has to be selected based on the used level of the discharge current, and also  $T_{off}$  has to be chosen based on the  $T_{on}$ .
- If machining speed is important and surface roughness is less important, high current and short  $T_{on}$  values must be selected. On the other side, if surface roughness is important, then low current values must be chosen.
- If  $T_{off}$  is selected less than  $T_{on}$ , electrode wear decreases and machining speed increases. However; if  $T_{off}$  is inadequately selected, next spark may not be occur and surface roughness increases and carbonization is carried out.
- Electrode-zoom value (front surface area of workpiece) limits the maximum value of the discharge current. Because, if high amperage is passed from the thin electrode (has a small front area), electrode will be worn excessively.

The appropriate parameter set ( $I$ ,  $T_{on}$  and  $T_{off}$ ) that is recommended by some EDM firms for both roughing and finishing stages are seen in Table 4.4.

**Table 4.4** Set of recommended electrical parameters

<i>I</i>	Roughing (no wear)		Finishing	
	<i>T<sub>on</sub></i>	<i>T<sub>off</sub></i>	<i>T<sub>on</sub></i>	<i>T<sub>off</sub></i>
3	50-100	6-25	3-12	3-9
6	100-200	12-50	3-12	3-9
9	100-400	12-100	6-25	6-12
12	100-400	12-100	6-25	6-12
18	200-800	24-200	6-25	6-12
25	400-800	50-200	6-25	6-12
50	800-1600	100-400	12-50	6-12

The data in Table 4.5, which was also offered by EDM firms, reveals that the machined area governs the strength of discharge current and is available to determine the low voltage discharge current in rough-cut.

**Table 4.5** A contrast of machined area to current strength for copper and steel

Classification	Machined Area (cm <sup>2</sup> )	Current (A)
Very small	0-0.25	1-6
Small	0.25-1	6-10
Middle	1-4	10-25
Large	4-16	25-50
Very large	>16	50-100

Normally, number of levels of discharge current, pulse on-time and pulse off-time are selected as 7, 10 and 7 respectively (see Table 4.1). However, due to the above mentioned limitations, some parameter set cannot be used. In order to use logical parameter set combination in experiments, design of experiments (Taguchi) method were used.

Design of experiments (DOE) is an approach used for decreasing the number of experiments to accomplish the optimum conditions (Armstrong, 2006). It is a statistical technique that made it possible to investigate not only the effect of any factor but also their interactions. Statistical approaches are significant in planning, conducting, analysing and interpreting data from engineering experiments.

The mostly used one of DOE techniques is the Taguchi approach. Using the Taguchi approach the experimental design and the results' analysis can be done with less effort and expenses. The Taguchi method uses a special design of orthogonal array to study

the entire parameter space with only a small number of experiments (Roy, 2001). An orthogonal array provides a balanced set of experimentation (Taguchi, 2000).

Here, the experiments were designed by using two  $L_{25}$  orthogonal arrays (OA) to examine both machining stages. The first set is appropriate for finishing stage and the other is appropriate for roughing stage. Both test groups have 3 factors ( $I, T_{on}, T_{off}$ ) and five levels (see Table 4.8 and 4.9). According to  $L_{25}$  experiment setups, suggested parameter sets are seen in Table 4.6 and 4.7.

**Table 4.6** Taguchi first group  $L_{25}$  for finishing

		Factor 1	Factor 2	Factor 3	Factor 1	Factor 2	Factor 3
Std	Run	A:A	B:B	C:C	$I$	$T_{on}$	$T_{off}$
9	1	2	4	5	6	50	50
25	2	5	5	4	25	100	25
13	3	3	3	5	12	25	50
24	4	5	4	3	25	50	12
8	5	2	3	4	6	25	25
14	6	3	4	1	12	50	3
15	7	3	5	2	12	100	6
12	8	3	2	4	12	12	25
22	9	5	2	1	25	12	3
10	10	2	5	1	6	100	3
2	11	1	2	2	3	12	6
7	12	2	2	3	6	12	12
6	13	2	1	2	6	6	6
11	14	3	1	3	12	6	12
23	15	5	3	2	25	25	6
5	16	1	5	5	3	100	50
20	17	4	5	3	18	100	12
19	18	4	4	2	18	50	6
4	19	1	4	4	3	50	25
3	20	1	3	3	3	25	12
16	21	4	1	4	18	6	25
17	22	4	2	5	18	12	50
21	23	5	1	5	25	6	50
1	24	1	1	1	3	6	3
18	25	4	3	1	18	25	3

**Table 4.7** Taguchi second group L<sub>25</sub> (OA) for roughing

		Factor 1	Factor 2	Factor 3	Factor 1	Factor 2	Factor 3
Std	Run	A:A	B:B	C:C	<i>I</i>	<i>T<sub>on</sub></i>	<i>T<sub>off</sub></i>
9	26	2	4	5	9	400	200
25	27	5	5	4	25	800	100
13	28	3	3	5	12	200	200
24	29	5	4	3	25	400	50
8	30	2	3	4	9	200	100
14	31	3	4	1	12	400	12
15	32	3	5	2	12	800	25
12	33	3	2	4	12	100	100
22	34	5	2	1	25	100	12
10	35	2	5	1	9	800	12
2	36	1	2	2	6	100	25
7	37	2	2	3	9	100	50
6	38	2	1	2	9	50	25
11	39	3	1	3	12	50	50
23	40	5	3	2	25	200	25
5	41	1	5	5	6	800	200
20	42	4	5	3	18	800	50
19	43	4	4	2	18	400	25
4	44	1	4	4	6	400	100
3	45	1	3	3	6	200	50
16	46	4	1	4	18	50	100
17	47	4	2	5	18	100	200
21	48	5	1	5	25	50	200
1	49	1	1	1	6	50	12
18	50	4	3	1	18	200	12

**Table 4.8** EDM parameters and levels for first group L<sub>25</sub> for finishing

<b><i>I</i> (A)</b>	3	6	12	18	25
<b><i>T<sub>on</sub></i> (μs)</b>	6	12	25	50	100
<b><i>T<sub>off</sub></i> (μs)</b>	3	6	12	25	50

**Table 4.9** EDM parameters and levels for second group L<sub>25</sub> for roughing

<b><i>I</i> (A)</b>	6	9	12	18	25
<b><i>T<sub>on</sub></i> (μs)</b>	50	100	200	400	800
<b><i>T<sub>off</sub></i> (μs)</b>	12	25	50	100	200

## 4.8 Experimental Procedure

A series of experiments was conducted to make out the effects of EDM machining parameters such as; discharge current ( $I$ ), pulse on-time ( $T_{on}$ ) and pulse off-time ( $T_{off}$ ) to surface roughness values ( $R_a$ ), material removal rate (MRR), electrode wear ratio (EWR) and average white layer thickness (AWLT) on the X40CrMoV5.1 hot work tool steel (DIN 1.2344).

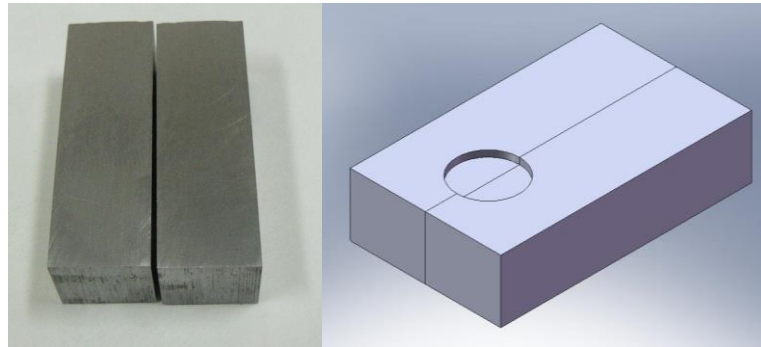


**Figure 4.2** View of Specimens

The specimens were prepared with a size of 12×10×40 mm. The aligned surfaces of the two specimens were clamped to each other, and 10 and 20 mm in diameter and 4 mm in depth blind holes were machined on the line of intersection as shown in Figure 4.2 with a precise adjustment. Before the experimentation, the workpiece top, bottom and joined surfaces were ground.

## 4.9 Measurements of Output Parameters

EDM performance, regardless of the type of the electrode material and dielectric fluid, is measured usually by the following output parameters:

- Material removal rate (MRR)
- Electrode wear ratio (EWR)
- Surface quality of workpiece
  - Surface roughness ( $R_a$ )
  - White layer thickness

To measure the above parameters, a digital weighing machine, an electronic timer, a metallographic microscope, and Mahr-stylus surface roughness measurement machine were used.



#### 4.9.1 Measurement of Material Removal Rate

Material removal rate is commonly described as removed material volume per minute ( $\text{mm}^3/\text{min}$ ). MRR is calculated as dividing the machining time and density of the workpiece by the difference in weight between the initial and final weight of the workpiece. The following equation is used to determine the MRR value;

$$MRR = \frac{W_f - W_i}{t \times \rho} (\text{mm}^3/\text{min}) \quad 4.1$$

where  $W_i$  = Initial weight of workpiece material (g),  $W_f$  = Final weight of workpiece material (g),  $t$  = Machining time (min) and  $\rho$  = Density of workpiece ( $\text{g}/\text{mm}^3$ )



**Figure 4.3** Digital weighing machine (Radwag WTB 200)

So, to calculate the loss of mass for the material during EDM operation, the weights of the workpiece, before and after the machining, must be measured. The specimens and electrodes must be weighed before and after EDM operation with an accurate digital weighing machine (Radwag WTB 200) (Figure 4.3).

#### 4.9.2 Electrode Wear Ratio (EWR)

The electrode wear ratio (EWR) is defined by the ratio of the electrode wear weight to the work piece removal weight and usually expressed as a percentage, that is calculated by following formula;

$$EWR(\%) = \frac{\text{Wear weight of electrode}}{\text{Wear weight of workpiece}} \times 100 \quad 4.2$$

Minimum value of EWR is important for the better accuracy in the product because minimum wear means a minimum difference in the shape of electrode.

#### 4.9.3 Surface Quality

Surface roughness is an important index for product quality and technical needed for mechanical parts and it is related to functional behaviour of a part. Surface quality is defined with two main factors which are texture and integrity of surface (Hasçalık and

Çaydaş, 2007). Surface texture is related to geometric irregularities of the solid surface, which is generally described as surface roughness. Surface integrity comprises the metallurgical changes of the surface and surface beneath layer. The exposed discharge energy of EDM process creates very high temperature at the spark point. This melts and vaporises a minute part of the workpiece and a crater is formed on the machined surface. Therefore the surface texture is characterized by these craters and it is determined by EDM parameters ( $I$ ,  $T_{on}$ ,  $T_{off}$ , etc.). Surface morphology plays an important part in understanding the characteristics of machined surfaces.

#### 4.9.3.1 Surface Roughness

Throughout the EDM process, the discharged energy causes a small part of the specimen to melt and vaporize due to high temperatures at the point of the spark. A crater is shaped on the workpiece surface at each discharge. The distinctive discharge craters characterize surface roughness in EDM. There are various simple surface roughness amplitude parameters used in industry, such as roughness average ( $R_a$ ), root-mean-square (rms) roughness ( $R_q$ ), and maximum peak-to-valley roughness ( $R_t$ ), etc.

- **Roughness average  $R_a$**  is the arithmetic average of the absolute values of the roughness profile ordinates.
- **$R_t$ , maximum peak to valley**, the maximum peak to valley height of the filtered profile over the evaluation length; it is very sensitive to large deviations from the mean line and scratches.

The parameter  $R_a$  and  $R_t$  was examined in this study. The  $R_a$  is specified by the following equation:

$$R_a = \frac{1}{l} \int_0^l |Z(x)| dx \quad 4.3$$

where  $R_a$  : is the arithmetic average deviation from the mean line,  $l$  : the sampling length, and  $Z(x)$ : profile ordinates of the roughness profile.

**Table 4.10** Measuring Parameters

Software	MarTalk®
Drive Unit	GD 25
Probe	MFW-250:1(#6851855)-1.0%
Traversing Speed ( $V_t$ ) (mm/sec)	0.5
Traversing Length ( $L_t$ ) (mm)	5.8
Cut off length ( $\lambda_c$ ) (mm)	0.8

There are many methods to measure surface roughness such as; image processing, microscopes, stylus type instruments, profile tracing instruments, etc. In this study, so as to measure surface roughness of machined samples, Mahr stylus instrument (MarSurf XR 20 with GD 25) was used (Figure 4.4). Some properties of the instrument and its setting parameters used in the measurements are given in Table 4.10

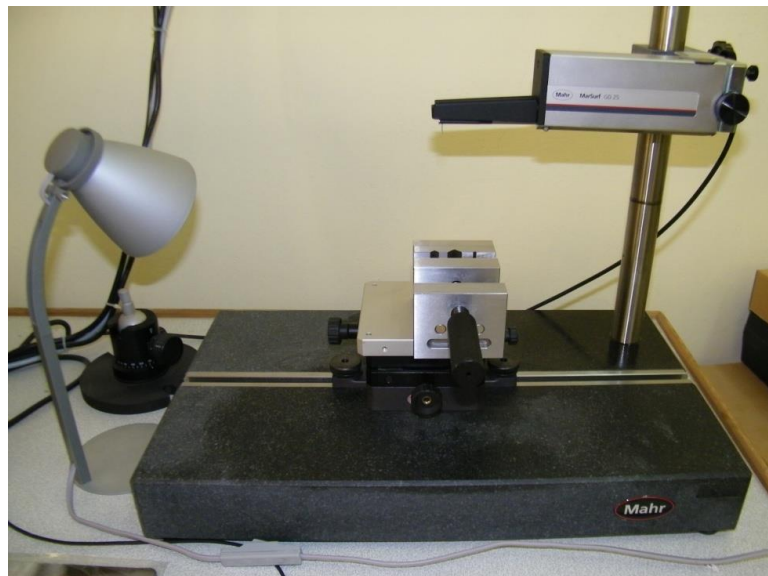


**Figure 4.4** View of Mahr stylus instrument

#### **4.9.3.2 White Layer Thickness**

EDM changes the metallurgical structure of the machined workpiece surface. There are essentially three layers: a melted and redeposited layer (recast layer), a heat-affected layer and the bulk material. The outer layer consists of a resolidified layer. The recast layer is formed by the re-solidifying of the melted material which was not cleaned up from the machined surface by the dielectric fluid through the EDM process. The recast layer also called the white layer, since it is very difficult to etch and as its appearance is white when observed through an optical microscope (Figure 4.5).

Underneath the recast layer a heat affected zone (HAZ) is present. This zone comprises the workpiece material that has undergone a thermal influence, but has not been molten. The HAZ usually consists of several layers, although it is not always easy to distinguish them. In the case of steel, usually a hardened (martensitic) and an annealed layer exist.

The white layer is normally different in character from the parent material, consists of micro-cracks, voids, impurities, stress and several other defects and is responsible for the deterioration the mechanical properties of the machined components (Lee and Tai, 2003). Micro-cracks can take place in this layer because of an increase in non-homogeneities of metallurgical phases within the white layer (Ekmekçi, 2009). Surface crack is a vital defect, which certainly affects the fatigue life of the components (Lee et al., 1998), and these are generally formed when the induced stress exceeds the ultimate stress (Lee et al., 2004). The EDM process conditions directly affect thickness and density of the white layer (Ramasawmy et al., 2005; Lee and Tai, 2003).

The recast layer increases surface roughness, makes the surface become hard and brittle, and decreases the fatigue strength due to the presence of micro-cracks and micro-voids (Liao et al., 2004).

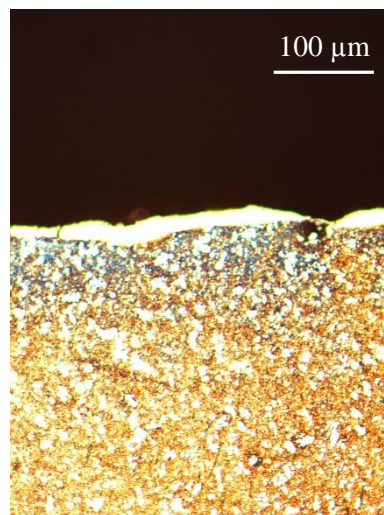


**Figure 4.5** View of EDMed surface

The roughness of the surface machined with EDM is also related to the spreading of the craters. To increase the EDMed product lifelong, the recast layer is normally removed. Because the layer has a vital role for applications in which the part is subjected to cyclical stress or fluctuating loads (Lee et al., 2004).

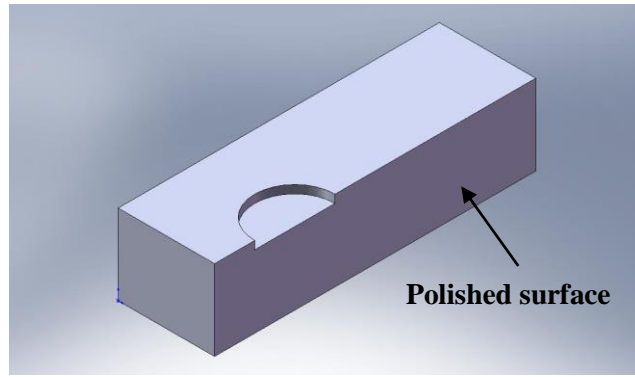


**Figure 4.6** Transverse section of specimen



**Figure 4.7** Forcipol 2V grinder polisher



**Figure 4.8** View of Nikon Ma100 metallographic microscope

In order to measure white layer thickness of the EDMed specimens, the transverse section of specimens (Figure 4.6) was ground with silicon carbide paper (having 200 to 600 grit size) by using grinder polisher machine in which water is used as lubricant (Figure 4.7). Then these faces were polished with diamond paste and alumina oxide

and etched with 5% nital solution for inspection of specimens by metallographic microscope. Topographic observations throughout the EDM surfaces were carried out with a Nikon Ma100 Metallographic Microscope (Figure 4.8) to observe the thickness of the recast layer. The microscope is equipped with various objectives which are capable to capture online image of the EDMed workpiece surface. The white layers from the online photographs are easily identified. The samples were viewed with 100 (100x) and 200 times magnification (200×). The depths (thickness) of white layers were measured carefully from the micrographs and an average of 8 readings was taken from each specimen.

#### **4.10 Results and Discussion of Experimental Studies**

In this chapter, the results of experiments are tabulated in Appendix A (Table A.1 to Table A.2). The analysis of the results obtained from the experimental research about the material removal rate (MRR), electrode wear ratio (EWR), surface roughness ( $R_a$ ) and average white layer thickness (AWLT) will be discussed in this section. According to the experimental results and the effects of EDM machining parameters to the EDM performances are graphically represented.

##### **4.10.1 Influences of Process Parameters on MRR**

In EDM process, the melt removal causes a crater shape on the machined surface, since the process of electrical spark erosion takes place repeatedly. The total mass of the molten metal concludes the amount of material removal rate. Generally, when the discharge current increases, MRR also rises. This is clearly observed in Figures 4.9 and 4.10. As the discharge current increases, the energy density on the workpiece material also increases; this increases the amount of molten and vaporized metal as well.

Figure 4.9 presents the relationship between the pulse on-time and the material removal rate for various discharge currents at a constant pulse off-time ( $T_{off}=12\mu s$ ) for finish machining stage. It can be seen that the most significant parameter on MRR is discharge current, the pulse on-time just affects the *MRR* slightly. As a consequence, for lower discharge currents (3-12 amperes) the discharge energy is insufficient to melt the material; therefore, *MRR* cannot increase with longer  $T_{on}$ .

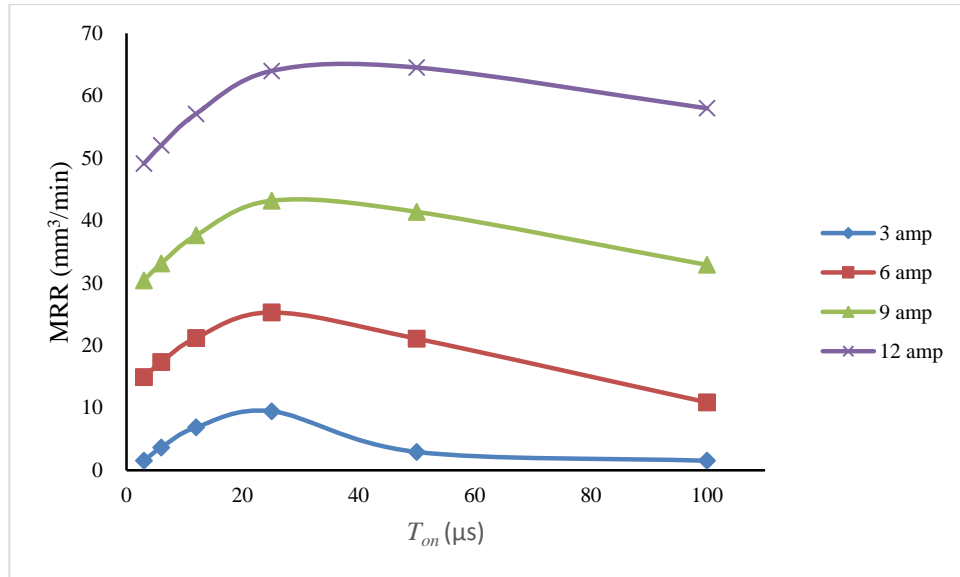


**Figure 4.9** The influences of both discharge current and pulse on-time (at  $T_{off}=12 \mu s$ ) on MRR at finishing stage

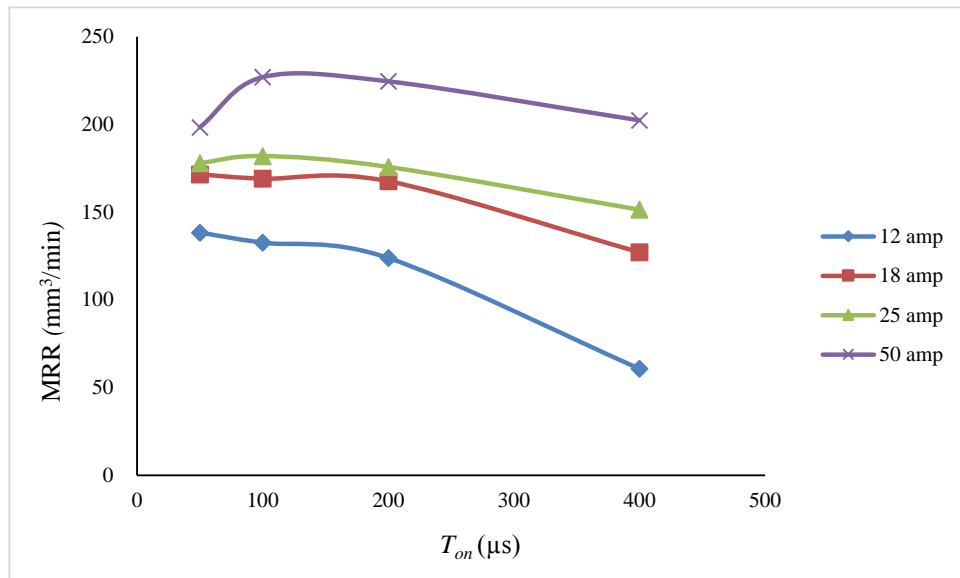


**Figure 4.10.** The influences of both discharge current and pulse on-time (at  $T_{off}=50 \mu s$ ) on MRR at roughing stage

It can be concluded from Figures 4.9 and 4.10 that as the pulse on-time increases,  $MRR$  also increases up to a maximum value for a specific optimum  $T_{on}$ . For each discharge current there is a consistent optimum  $T_{on}$  which permits maximum  $MRR$ . After this point,  $MRR$  tends to decrease. This optimum point changes with pulse off-time and discharge current. For example, for  $I=50$  amperes, maximum  $MRR$  is  $226 \text{ mm}^3/\text{min}$  at  $T_{on}=100\mu s$  and  $T_{off}=50\mu s$  and for  $I=18$  amperes maximum  $MRR$  is  $171 \text{ mm}^3/\text{min}$  at  $T_{on}=50\mu s$  and  $T_{off}=50\mu s$  and for  $I=12$  amperes, maximum  $MRR$  is  $64.5 \text{ mm}^3/\text{min}$  at  $T_{on}=50\mu s$  and  $T_{off}=12\mu s$ . The explanation for  $MRR$  behaviour after its optimum point

is due to longer  $T_{on}$  that causes instability, i.e., diminishing pressure and energy of the plasma channel between the molten material and the electrode (Amorim et al., 2010). For higher values from optimal  $T_{on}$  values, the plasma that is formed among electrodes' gap impedes energy transfer thus, it causes MRR to decrease.

The effect of pulse off-time on  $MRR$  for a constant pulse-on time ( $T_{on}=100 \mu s$ ) is shown in Figure 4.11. According to the Figure 4.11  $MRR$  increases up to when  $T_{off}$  is  $30 \mu s$  for the values 25 and 50 amp, however, for 12 and 18 amp, it increases up to when  $T_{off}$  reaches to  $50 \mu s$ .  $T_{off}$  time provides suitable environment to be removed the molten particles, this causes the increase of  $MRR$  up to these points. After these points, since a slight increase in  $T_{off}$  causes a considerable increase in machining time,  $MRR$  decreases based on this cases. The  $T_{off}$  time is necessary to stabilize the EDM process at the end of each discharge. In the time, the reconstruction of insulation in the working gap occurs (Lee and Li, 2001). However, there exists a restriction to decrease the  $T_{off}$ , because each discharge needs enough time to deionize dielectric. This limit value changes based upon the  $T_{on}$  and the discharge current. Throughout machining,  $T_{off}$  is to be set accurately to avoid arcing, which helps to achieve high  $MRR$ . Moreover, too-short  $T_{off}$  causes a lack of time to flush away debris from the gap amongst electrode and workpiece.

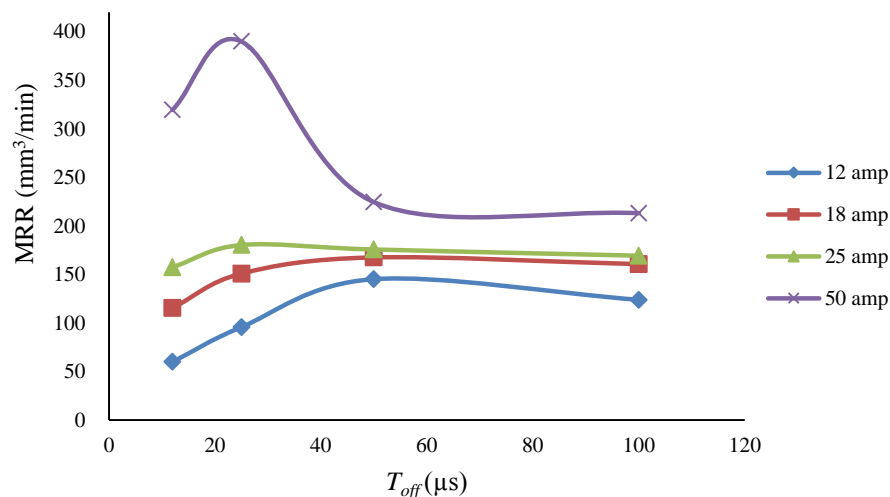
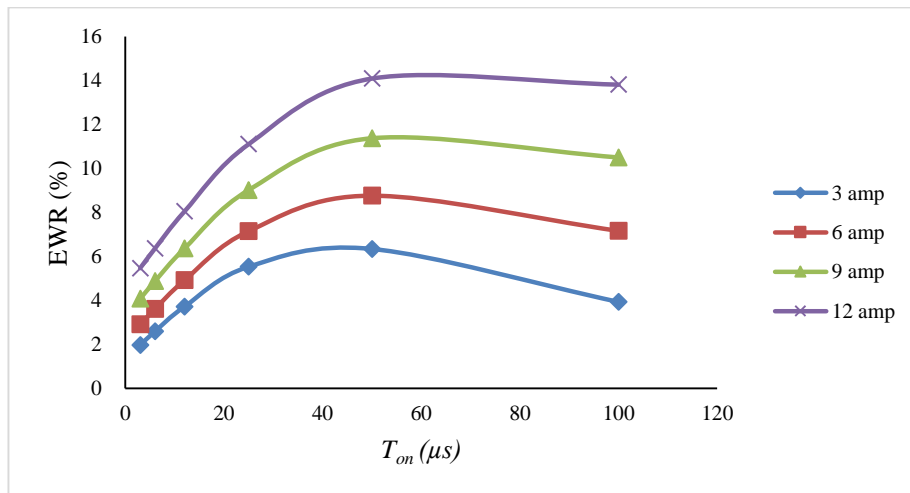


**Figure 4.11** The influences of both discharge current and pulse off-time (at  $T_{on} = 100 \mu s$ ) on  $MRR$  at roughing stage

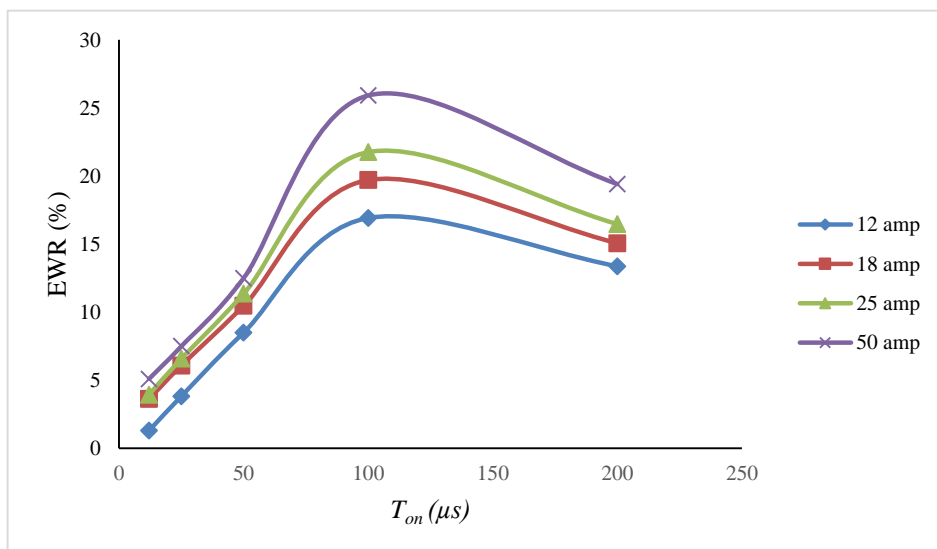


#### 4.10.2 Influences of Process Parameters on EWR

Electrode wear takes place during the electrical discharge erosion process. This is because spark discharge removes material not only from the workpiece but also from the electrode. The ratio of the loss of tool material to loss of workpiece material in the process of machining is known as electrode wear ratio (EWR). The electrode wear makes the geometry of the electrode unstable and affects the dimensional accuracy of the workpiece. Reducing the electrode wear ratio in the EDM process causes a better the machining performance. Therefore, the electrode wear ratio is an important parameter for evaluating machining performance in the electrical discharge machining operation.

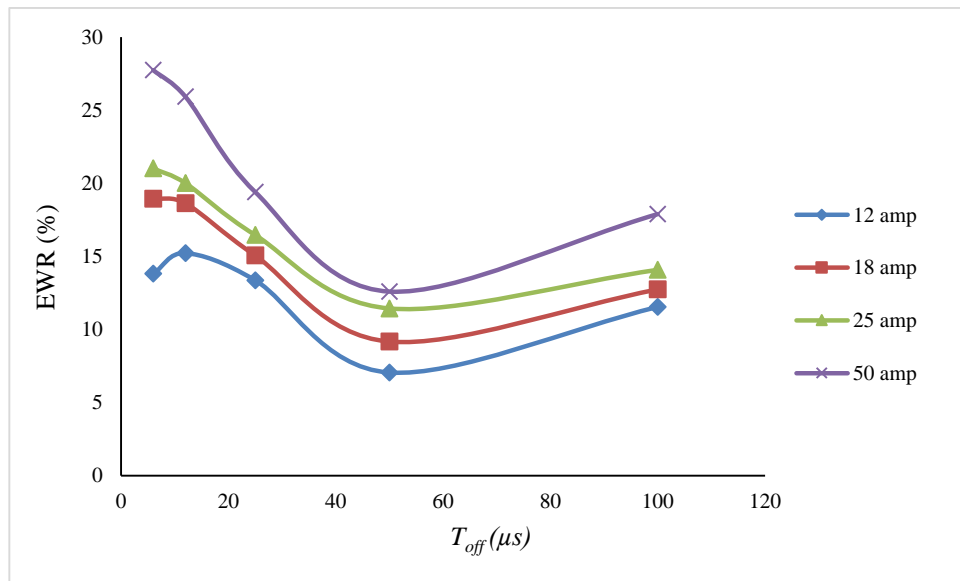


**Figure 4.12** The influences of both discharge current and pulse on-time (at  $T_{off}=6 \mu s$ ) on EWR at finishing stage



**Figure 4.13** The influences of both discharge current and pulse on-time (at  $T_{off}=25 \mu s$ ) on EWR at roughing stage

The effect of pulse-on duration on the EWR at different discharge currents is shown in Figures 4.12 and 4.13. As the discharge current increases, discharge energy and sparking increase. So this causes to remove more molten material from both work-piece and electrode which increases the EWR. The increase in EWR with the increasing pulse on-time is seen until the  $T_{on} = 50 \mu s$  for finishing and  $T_{on} = 100 \mu s$  for roughing stage. Further rise in  $T_{on}$  decreases the EWR. The EWR decreases with longer  $T_{on}$  since the material removal rate rises at a faster rate than the tool wear rate (Ozgedik and Cogun, 2006).



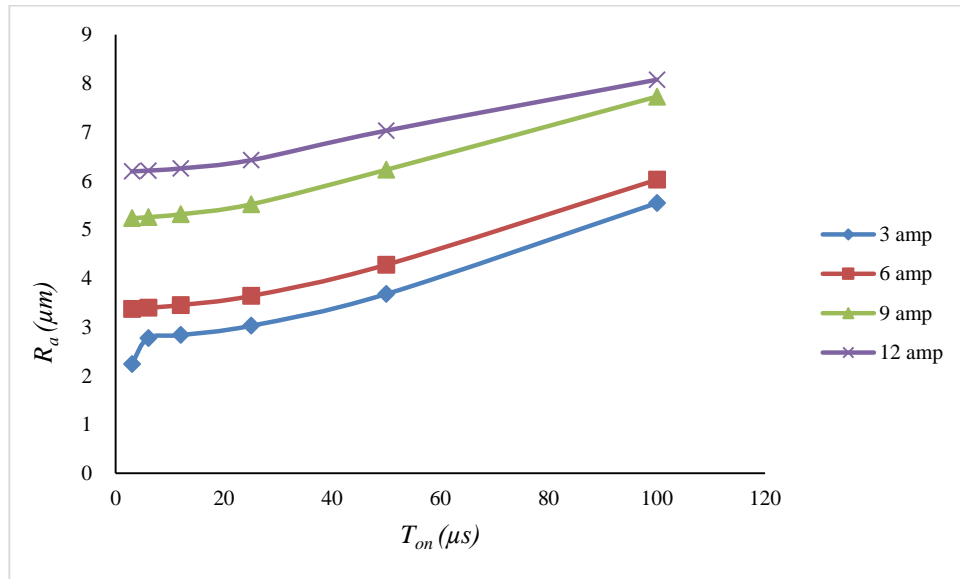
**Figure 4.14** The influences of both discharge current and pulse off-time (at  $T_{on} = 100 \mu s$ ) on EWR at roughing stage

Figure 4.14 shows that the variation of  $T_{off}$  for rough machining affects meaningfully EWR values. For the discharge current  $I = 50 A$  the increase in  $T_{off}$  from  $6 \mu s$  to  $50 \mu s$  reduces EWR up to about 50%. This is owing to the low  $T_{off}$  that helps high concentration of EDM by-products in the sparking gap, reducing the material removal rate. Here it occurs because long  $T_{off}$  develops the flushing conditions by reducing the occurrence of arc-discharges and short-circuits encouraging more stability to the machining (Amorim, 2010). Moreover, during the pulse off-time the carbon transmits from the dielectric to the copper electrode and it causes a black layer on the tool surface which prevents tool wear.

#### 4.10.3 Influences of Process Parameters on Surface Roughness

Figures 4.15 and 4.16 show the results of surface roughness measurements. As the discharge current increases, it does the discharge heat concentration on the workpiece

surface, which results in larger craters, i.e., surface roughness. The higher discharge current causes more MRR, leading to the creation of a deeper and greater crater on the surface of the workpiece and results in a worse surface finish. At a constant current, it was observed that  $R_a$  increased when increase in pulse on-time. Because, when pulse on-time increased, spark energy will also increase and hence increases the surface roughness.



**Figure 4.15** The influences of both discharge current and pulse on-time (at  $T_{off} = 6 \mu s$ ) on  $R_a$  at finishing stage

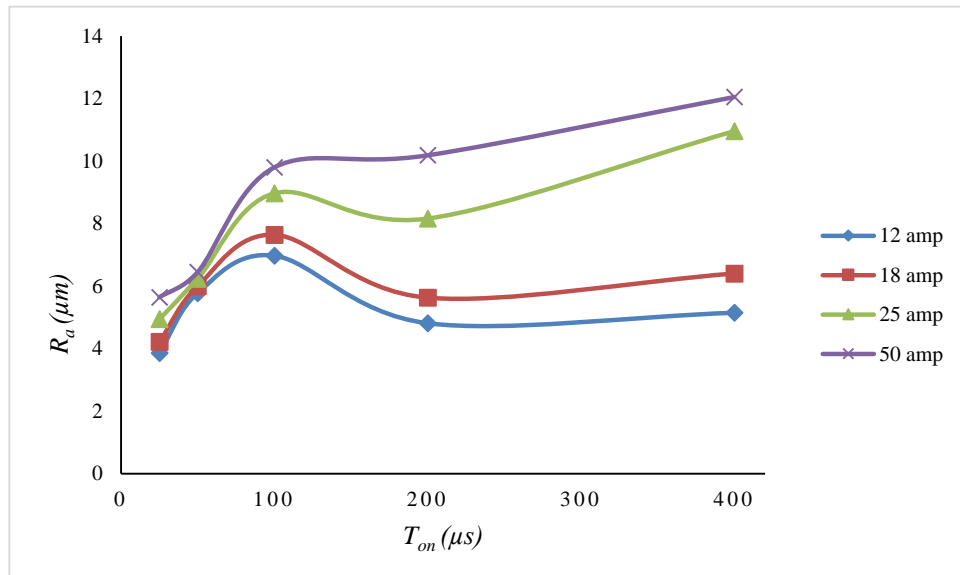


**Figure 4.16** The influences of both discharge current and pulse on-time (at  $T_{off} = 12 \mu s$ ) on  $R_a$  at roughing stage

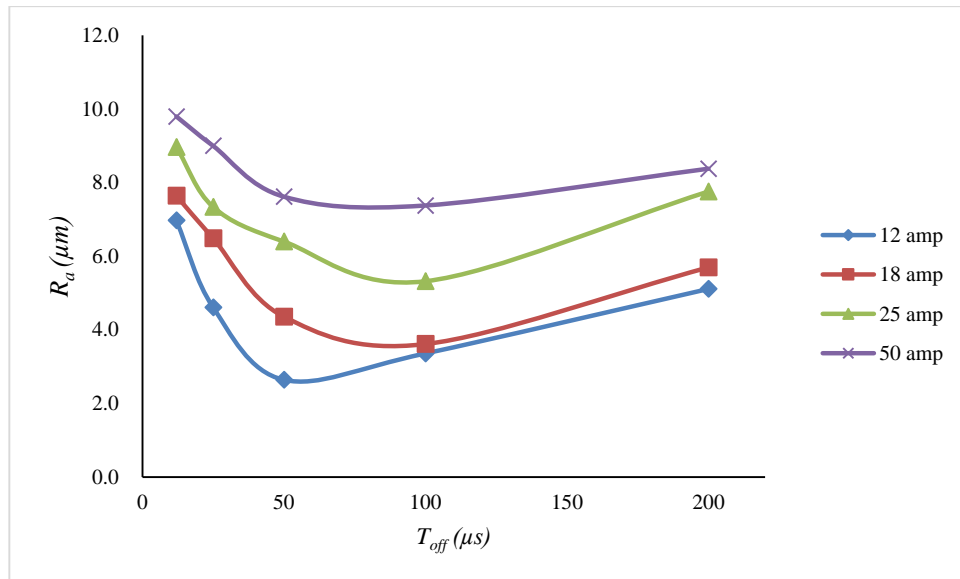


**Figure 4.17** The influences of both discharge current and pulse off-time (at  $T_{on}= 100 \mu s$ ) on  $R_a$  at roughing stage

According to Figure 4.17,  $R_a$  is high when  $T_{off}$  is about  $12 \mu s$ , since too-short  $T_{off}$  causes a lack of time to flush away debris from the gap and these cause recast layer and also cause the second arcing, which consequently results higher surface roughness. When  $T_{off}$  time is  $50 \mu s$ , it provides suitable environment to be removed the molten particles from the gap and a smoother surface occurs. However, after this optimum point, it is obviously seen that the  $R_a$  is comprehensively affected by  $T_{off}$  values. The reason is that the  $T_{off}$  does not affect the energy supplied to the EDM machining process. As a general trend the increase in pulse off time reduces slightly surface roughness. However, the long pulse off time increases machining time hence it is desired that the pulse off-time should be as low as possible, but in most cases it should be selected based on the pulse on-time used for machining.

#### 4.10.4 Influences of Process Parameters on White Layer Thickness

It can be clearly seen from Figures 4.18 and 4.19 that the white layer thickness increases significantly by the increase in  $T_{on}$ . The white layer is generally formed by the sticking of the non-removed debris and also the depth of material affected from high temperature. The increase in  $T_{on}$  for the period of each discharge is the reason why the heat conduction throughout workpiece increases. Thus, the high temperature influences widespread zone on workpiece material and the white layer gets thicker as well.

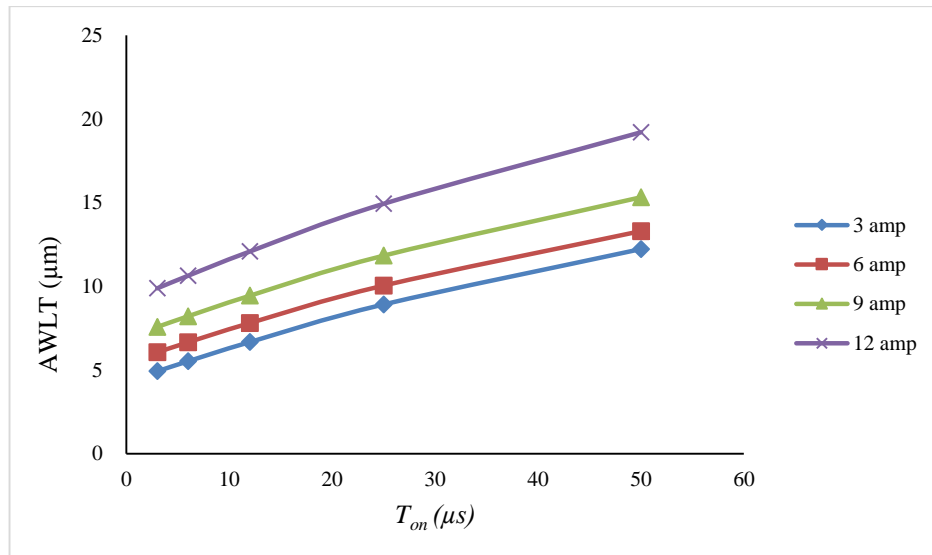


**Figure 4.18** The influences of both discharge current and pulse on-time (at  $T_{off} = 3 \mu s$ ) on AWLT at finishing stage

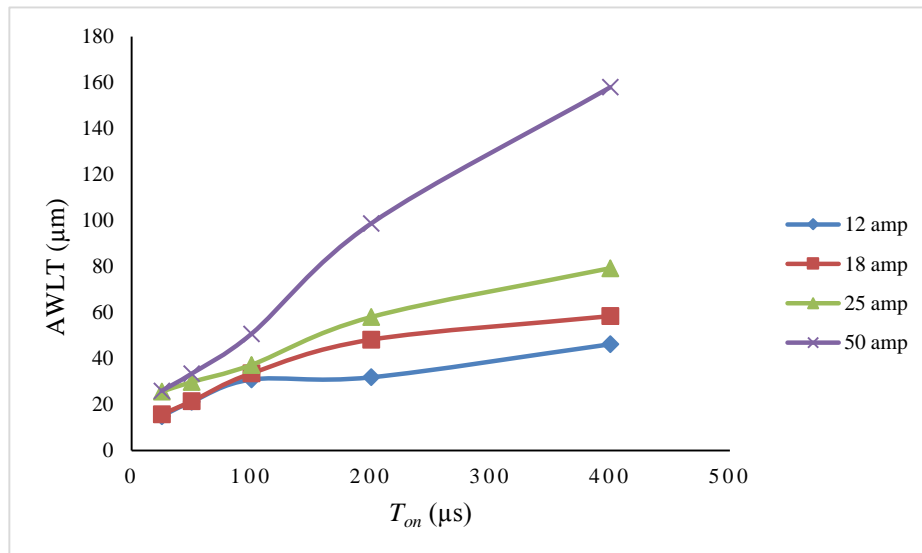


**Figure 4.19** The influences of both discharge current and pulse on-time (at  $T_{off} = 12 \mu s$ ) on AWLT at roughing stage

It is clear that the discharge current has a less effect than the pulse on-time on the white layer thickness (see Figures 4.18 and 4.20). Despite of the fact that an increase in discharge current results in an increase in the dimensions of the craters and the heat penetrating thickness, it also causes more molten material to be cleared away from the molten crater; therefore, a thin white layer appears on the surface of the workpiece.

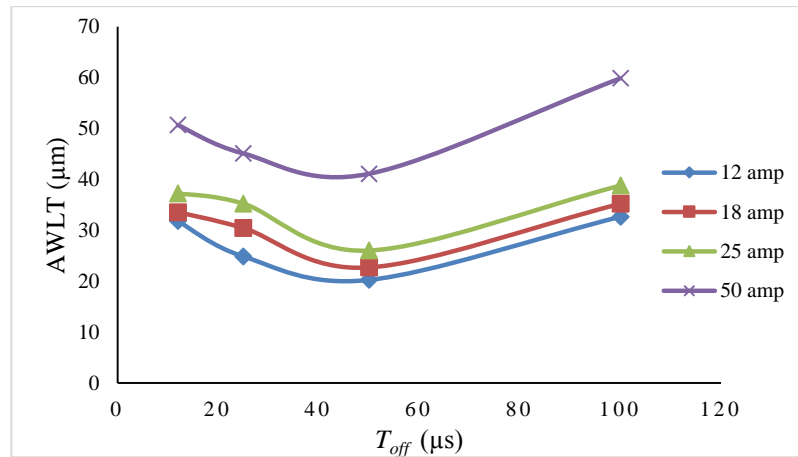


**Figure 4.20** The influences of both discharge current and pulse off-time (at  $T_{on} = 100 \mu s$ ) on AWLT at roughing stage

#### 4.11 Conclusions based on the Experimental Study

In this section of the thesis, a series of experiment was carried out and MRR, EWR, Ra and AWLT were measured. The following may be concluded from the experimental results;

1. The increase in pulse on-time leads to an increase in the material removal rate, surface roughness, as well the white layer thickness.
2. The increase in discharge current leads to a sharp increase in the material removal rate and surface roughness.
3. Electrode wear ratio decreases by an increase of pulse on-time, and EWR increases by an increase in the pulse current.
4. A slight decrease could be observed in the white layer thickness by an increase in the pulse current.
5. High discharge current and  $T_{on}$  provide low surface finish quality but this combination would increase material removal rate and reduce machining cost. As a result, this parameter set should be used for rough machining stages in EDM process.
6. Better surface quality was obtained when lower discharge current and shorter pulse on-time are applied. Machining time and surface quality are the two conflicting requirements. A compromise must be found by adjusting the values of these parameters. The MRR rate will be low and thus machining cost increases. The situation can be used for a higher surface quality is needed at finish machining stage of EDM process.

## **CHAPTER 5**

### **MODELING OF EDM PARAMETERS**

#### **5.1 Introduction**

The purpose of this chapter is to present a proficient and incorporated approach to establish a model that can accurately predict the performances of EDM process by correlating input parameters. In this chapter, the well-known soft computing methods such as adaptive neuro-fuzzy inference system (ANFIS), genetic expression programming (GEP) and artificial neural networks (ANN) were compared for predicting EDM performances. Thus the precision, efficiency and quality of EDM process can be improved by choosing the best model. The data set used in the study comprises EDM processing parameters and responses obtained from real experimental studies.

Selection of appropriate operating conditions is an important attribute to be paid attention in EDM. Lots of experiments can be done to get many machining parameter set alternatives but it takes a lot of time and cost, therefore the computational relations between the output responses and controllable input parameters must be needed. However, the proper selection of these parameters is a complex task and it is generally made with the help of sophisticated numerical models. The artificial intelligence approaches have lately emerged as promising for developing a useful model for the complex systems.

#### **5.2 Fundamentals of Artificial Intelligence**

Artificial intelligence is defined as the study of thinking that enable computers to be intelligent. In the last decade, there has been an increasing interest in the area of artificial intelligence, where the aim is to find out useful models from experimental data. Because of the advantages of the artificial intelligence systems, many researchers studied to find the relationships between input and output parameters in EDM process by using soft computing techniques.

### 5.2.1 Overview of Genetic Programming (GP) Models

GP is an artificial intelligence method which has many application areas like engineering and science, industrial and mechanical models (Ong et al., 2005; Cevik and Guzelbey, 2007; Kok et al., 2011). GP proffers a solution as a result of the evolution of computer programs by using natural selection methods. Genetic programming (GP) was developed by Koza, 1992. GP is a propagation of the traditional genetic algorithm (GA). Ferreira (2001) invented an evolutionary algorithm called as Gene Expression Programming (GEP) to predict mathematical models by using experimental data in 2001. GEP includes simple linear chromosomes of fixed length like as used in GA and forked forms of various sizes and shapes similar to the parse trees of GP (Cevik, 2007).

### 5.2.2 Overview of Artificial Neural Networks (ANNs) Models

An artificial neural network consists of a number of neurons similar the biological neurons in the brain (Kim and Kasabov, 1999). ANNs can solve complex problems that are analytically hard to solve with its capability of adaptive learning (Sugeno and Kang, 1988). ANNs are preferred to solve such problems of interest to computer scientists and engineers as pattern classification, clustering, function approximation, forecasting, optimization and control etc.

After simple neurons were introduced by McCulloch and Pitts (1943), connected model or ANN that is known as parallel distributed processing has become focus of interest. ANN is composed of simple processing units called neurons and signals are passed between them through a series of weighted connections. Processing units, connection pattern and activation are the main concepts of ANN (Haykin, 2009). Main neuron model is shown in Figure 5.1.

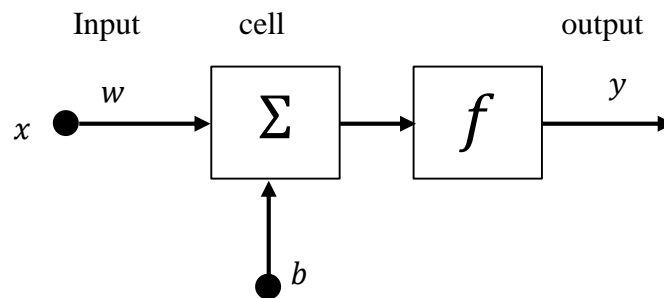


**Figure 5.1** Main neuron model



Each neuron computes in similar way an output signal that will be transferred into other neurons. System runs parallel and neurons in the same layer calculate concurrently. The input data for a neuron is the sum of weighted output data which is transferred from its own to other connected neurons and threshold value:

$$S_k = \sum_{k=1} x_i w_{ik} + \theta_k \quad 5.1$$

Input data ( $x_i$ ), weights ( $w_{ik}$ ), threshold value ( $\theta_k$ ). There is a rule that gives influence of input data on each neuron.

$$y_j(t+1) = a_k(y_j(t), s_k(t)) \quad 5.2$$

Here, activation function  $a_k$ , the last input value  $s_k$  and last activation  $y_j$  generate new activation value of  $k^{\text{th}}$  neuron.

Neural networks can be grouped into two categories, based on the connection architecture. These are feedforward and recurrent (feedback) networks. In feedforward networks, neurons are organized into layers that have unidirectional connections between them. There are three main learning paradigms (supervised, unsupervised and hybrid) for ANNs, in which learning rules are used for adjusting weights. In supervised learning paradigm the network is given a desired output for each input pattern. During the learning process, the actual output  $y$  generated by the network may not equal to the desired output  $d$ . The basic principle of error-correction learning rules is to use the error signal ( $d-y$ ), to modify connection weights and to gradually reduce this error. Another error-correction algorithm is the back propagation algorithm which is gradient-descent method to minimize the squared error cost function in eq. 5.2. The development of the backpropagation learning algorithm for determining (or updating) weights in a Multilayer perceptron which is a feedforward and supervised network has made these networks the most popular among researches.

Normally, the network consists of an input layer of source neurons, at least one middle layer or hidden layer of computational neurons, and an output layer of computational neurons. A multilayer perceptron with one hidden layers is shown in Figure 5.2. Each layer in a multilayer neural network has its own specific function. The function of input layer accepting the input signals from environment and redistributing these signals to each neuron in the hidden layer. The function of output layer is receiving

the output signals from the hidden layer and creating the output model of the entire network. Neurons in the hidden layer perceive the features; the weights of the neurons represent the features hidden in the input patterns. These features are then used for determining of the output pattern by the output layer.

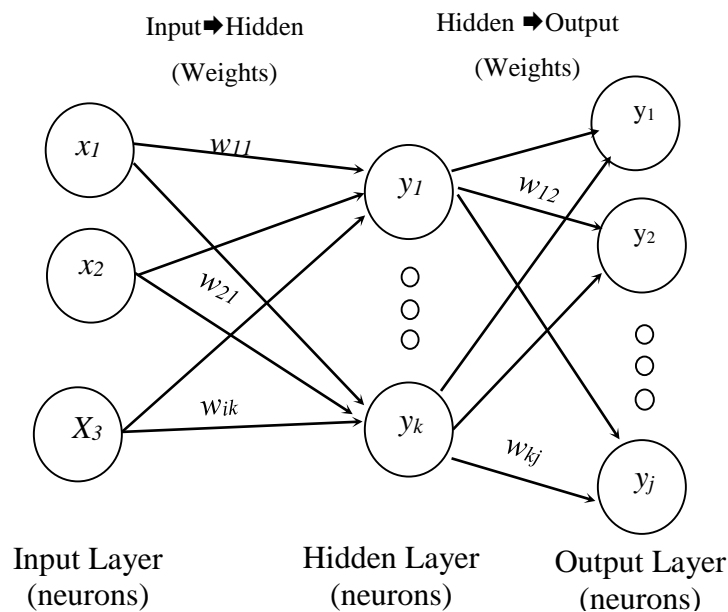


**Figure 5.2** Three-layered feed forward neural network topology

### 5.2.3 Overview of Adaptive Neuro-Fuzzy Inference System (ANFIS) Models

Fuzzy logic (FL) and neural networks (NN) supply two different methodologies to achieve appropriate solution for uncertainty. Appropriate hybridization of fuzzy logic and neural networks technologies leads to overcome the weakness of one with the strength of other and so provide efficient solution to range of problems belonging to different domains. A specific approach in neuro-fuzzy development is the Adaptive Neuro-Fuzzy Inference System (ANFIS) (Jang and Sun, 1997; Kim and Kasabov, 1999).

The ANFIS learning method works similarly to the neural networks one. In ANFIS system, membership functions parameters are adjusted using either a backpropagation algorithm alone or in combination with a least squares type of method by using a given input/output data set. This adjustment allows your fuzzy systems to learn from the data to be modelled (Jang, 1993).

Figure 5.3 shows a typical ANFIS architecture with two inputs ( $x$  and  $y$ ), the linguistic labels (A1, A2, B1 and B2) associated with the node function, the normalized firing

strengths ( $W_i$ ) and the node label ( $\Pi$ ). ANFIS is a Sugeno-type fuzzy system in five-layered feed-forward network structure. A fuzzification process is performed in the first layer, the second layer is the rule layer, and each neuron in this layer corresponds to a single Sugeno-type fuzzy rule. The membership functions (MFs) are normalized in the third layer. The fourth layer is defuzzification layer where the consequent parts of the rules are executed. The fifth layer computes the overall ANFIS output as the summation of all input signals (Sugeno and Kang, 1988).

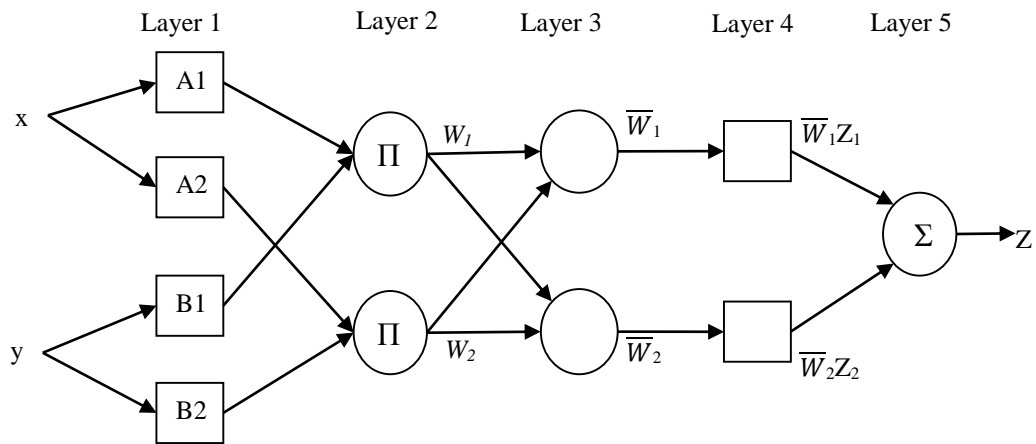


**Figure 5.3** A typical ANFIS architecture (Jang, 1993).

### 5.3 Development of Models

As a preliminary study, GEP, ANN and ANFIS methods were applied to determine their success in prediction of EDM output parameters. Discharge current, pulse on-time and pulse off-time were taken as input parameters and electrode wear ratio and material removal rate are taken the output parameters. Using the experimental data set, ANFIS, ANN and GEP models are developed and then their performances were compared.

**Table 5.1** Training data

Exp No	<i>I</i> (Amp)	<i>T<sub>on</sub></i> (μs)	<i>T<sub>off</sub></i> (μs)	MRR (mm <sup>3</sup> /min)	EWR (%)	<i>R<sub>a</sub></i> (μm)	AWLT (μm)
51	3	3	3	0.7	3.3	2.18	6.7
52	6	3	6	9.2	2.7	3.43	2.0
8	12	12	25	95.7	1.3	4.96	11.6
20	3	25	12	7.1	4.3	2.85	7.5
14	12	3	12	49.3	0.7	5.57	11.4
5	6	25	25	43.3	2.6	3.74	12.8
54	25	3	25	160.7	2.1	2.25	9.4
55	6	50	12	19.8	9.1	4.60	11.1
56	25	12	12	146.9	4.3	3.86	11.5
57	6	12	3	19.5	6.3	2.80	10.0
58	25	50	3	148.9	21.4	6.50	21.8
59	12	25	3	59.1	12.8	6.28	12.2
11	3	12	6	6.3	3.7	2.80	7.8
16	3	100	50	52.2	2.4	2.51	20.6
12	6	12	12	22.1	2.7	3.75	8.8
1	6	50	50	92.8	1.0	3.16	21.2
10	6	100	3	22.2	5.7	5.56	14.5
6	12	50	3	58.5	14.7	6.90	22.3
7	12	100	6	49.2	13.6	8.08	17.4
21	18	3	25	129.6	2.1	3.35	17.1
22	18	12	50	179.6	4.6	2.68	11.7
18	18	50	6	104.2	18.3	6.87	17.1
17	18	100	12	101.6	18.7	7.65	36.6
23	25	3	50	201.6	9.6	2.88	8.2
9	25	12	3	117.4	14.7	4.80	13.6
2	25	100	25	170.2	16.5	9.00	35.2
60	3	12	3	8.6	4.9	2.38	2.8
62	3	50	12	4.7	7.0	3.41	25.4
63	3	100	25	7.2	8.6	3.89	11.9
45	6	200	50	51.3	7.9	6.22	19.5
44	6	400	100	110.1	17.4	3.33	24.3
30	9	200	100	171.3	7.9	2.15	16.5
26	9	400	200	222.8	0.3	6.65	33.4
34	25	100	12	152.1	19.9	9.80	33.9
29	25	400	50	154.1	0.4	6.32	46.5
39	12	50	50	140.4	2.5	3.92	20.6
50	18	200	12	77.4	25.0	6.40	46.3
27	25	800	100	156.8	0.2	5.49	62.7
38	9	50	25	62.8	7.3	5.05	20.2
37	9	100	50	105.3	5.7	3.02	24.2
47	18	100	200	234.2	1.5	7.93	27.1
28	12	200	200	230.4	1.5	7.57	28.6
33	12	100	100	195.9	1.6	3.36	18.6
69	9	100	12	30.1	12.9	6.92	31.7
70	9	400	50	25.4	14.1	5.70	25.0
71	12	400	25	7.9	28.4	7.22	35.7

74	18	400	12	40.4	83.3	5.63	30.9
75	25	200	12	131.9	28.1	10.96	58.1
76	50	200	25	390.0	25.9	8.80	62.4
77	50	100	12	371.8	25.9	8.97	50.7
79	50	50	6	349.0	26.9	6.53	33.7
80	50	100	50	228.9	9.7	7.09	41.1
81	50	200	200	237.5	0.1	6.80	52.7
82	50	1600	200	158.3	41.9	14.74	119.4
83	50	800	100	315.6	35.5	15.20	158.1
84	50	400	100	232.8	16.7	10.93	111.1

**Table 5.2** Testing data

Exp No	<i>I</i> (Amp)	<i>T<sub>on</sub></i> (μs)	<i>T<sub>off</sub></i> (μs)	MRR (mm <sup>3</sup> /min)	EWR (%)	<i>R<sub>a</sub></i> (μm)	AWLT (μm)
15	25	25	6	151.1	17.1	5.00	13.8
53	12	50	6	57.8	14.5	6.84	14.3
85	50	200	50	232.6	17.6	10.10	104.8
25	18	25	3	101.0	17.6	6.48	17.9
4	25	50	12	160.9	16.4	5.60	32.2
24	3	6	3	3.9	3.9	2.25	6.0
64	6	3	3	8.0	4.3	2.75	3.6
13	6	6	3	12.5	5.0	3.00	6.5
65	6	25	6	22.1	7.4	3.60	14.3
66	6	50	6	20.6	9.2	4.10	24.8
67	6	100	12	12.6	10.1	5.73	20.8
36	6	100	25	25.8	10.5	4.84	22.5
40	25	200	25	152.9	20.6	9.01	52.2
61	3	25	6	8.6	5.6	2.73	17.7
43	18	400	25	48.6	38.2	8.45	27.0
73	18	200	25	101.3	15.6	5.75	33.5
3	12	25	50	145.5	0.0	3.91	8.8
72	18	100	50	167.3	9.8	4.00	23.4
78	50	25	6	313.1	17.9	4.45	24.8
48	25	50	200	236.0	0.1	4.25	22.4
19	3	50	25	15.9	5.6	2.65	6.6
68	12	3	3	26.7	7.5	5.92	14.8

78 experimental data were used for modelling study. Testing and training data sets used for construction of all models are selected randomly. Table 5.1 and Table 5.2 show training and testing data sets. Regarding the MRR and EWR formulation, 56 training data (72 % of all data) and 22 (28 % of all data) testing data were used.

### 5.3.1 Development of Genetic Programming (GP) Models

In this study GeneXproTools 4.0 program was used to develop mathematical models which is used to estimate MRR, EWR values. Primarily the chromosomes of a number of individuals are produced fortuitously in the GEP process. Then the chromosomes

are stated as expression trees (ETs), evaluated based on a fitness function and selected by fitness to reproduce with modification by means of genetic operations. The new generation of solutions experiences the same process and the process is repeated until the stop condition is fulfilled. The fittest individual is used as the final solution (Haykin, 2009).

**Table 5.3** Input and output parameters of GEP models

	Code	Variables	Symbol	Range
Input	d0	Discharge current (Ampere)	$I$	3-50
Input	d1	Pulse on-time ( $\mu$ s)	$T_{on}$	3-1600
Input	d2	Pulse off-time ( $\mu$ s)	$T_{off}$	3-200
Output 1	F1	Material Removal Rate ( $\text{mm}^3/\text{min}$ )	$MRR$	0.7-390
Output 2	F2	Electrode Wear Ratio (%)	$EWR$	0.01-83

**Table 5.4** GEP model parameters

P1	Function Set	$\ln, \log, 1/X, \tan, \sqrt[3]{}, X^3, X^2, e^x, \sqrt{}/, *, -, +,$
P2	Gene number	5,4,3,2,1
P3	Head Size	15, 10, 8, 5
P4	Linking Function	(+), (*)
P5	Number of Generation	10000- 20000
P6	Chromosomes	28-45
P7	Mutation Rate	0.044
P8	Inversion Rate	0.1
P9	One-point Recombination Rate	0.3
P10	Two-point Recombination Rate	0.1
P11	Gene Recombination Rate	0.1
P12	Gene transposition Rate	0.1

**Table 5.5** Function set's list

Code	Function Set
S1	$\tan, \sqrt[3]{}, X^3, X^2, \log, \ln, e^x, \sqrt{}/, *, -, +, 1/x, 10^x$
S2	$\sqrt[3]{}, X^3, X^2, \log, \ln, e^x, \sqrt{}/, *, -, +, \tan$
S3	$\ln, e^x, \sqrt{}/, *, -, +, \sqrt[3]{}, X^2$
S4	$e^x, \sqrt{}/, *, -, +$
S5	$/, *, -, +$

Experimental parameters and their ranges are shown in Table 5.3, parameters which are used for construction of GEP models are specified in Table 5.4. The list of function set is presented in Table 5.5. The data obtained from experimental study is separated into two parts as training and test sets to find out explicit formulations. The results of GEP models obtained from different combinations are presented in Table 5.6. Longer computational time was needed for training all of these combinations. Hence a subset of these combinations was chosen to analyse the GEP performance's algorithm for estimating the MRR and EWR. The optimal settings obtained from GEP models are

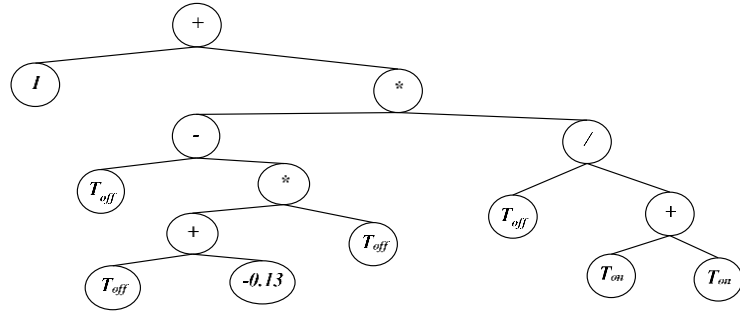
shown as bold in Table 5.6. Consequently, these optimal settings are used for the estimation of all performances.

**Table 5.6** Results obtained from GEP models

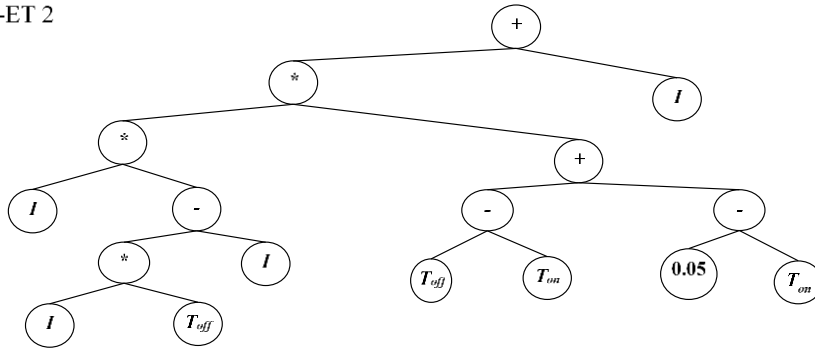
P1	P2	P3	P4	MRR			EWR		
				P5	R <sup>2</sup> Error		P5	R <sup>2</sup> Error	
					Train	Test		Train	Test
S1	2	5	+	13939	0.939	0.926	15408	0.925	0.855
S1	2	5	*	13293	0.941	0.938	16779	0.896	0.810
S1	3	8	+	14366	0.940	0.932	18069	0.902	0.880
S1	3	8	*	19949	0.926	0.924	17732	0.906	0.842
S1	4	10	+	18083	0.962	0.946	19231	0.875	0.862
S1	4	10	*	15231	0.948	0.926	18962	0.884	0.843
S1	5	15	+	15743	0.947	0.943	18675	0.908	0.876
S1	5	15	*	17607	0.953	0.932	19138	0.905	0.900
S2	2	5	+	15609	0.944	0.923	14693	0.920	0.836
S2	2	5	*	17428	0.939	0.936	15561	0.945	0.791
S2	3	8	+	19163	0.947	0.938	16395	0.858	0.831
S2	3	8	*	12971	0.923	0.898	16793	0.946	0.829
S2	4	10	+	19581	0.949	0.940	13846	0.854	0.822
S2	4	10	*	17086	0.905	0.898	12196	0.892	0.828
S2	5	15	+	10655	0.954	0.941	17688	0.919	0.887
S2	5	15	*	15783	0.947	0.945	19707	0.867	0.834
S3	2	5	+	16861	0.943	0.927	17250	0.934	0.796
S3	2	5	*	13278	0.927	0.899	18324	0.926	0.819
S3	3	8	+	10200	0.937	0.932	11538	0.923	0.834
S3	3	8	*	16575	0.933	0.929	11538	0.923	0.834
S3	4	10	+	10385	0.936	0.927	16795	0.910	0.903
S3	4	10	*	19919	0.932	0.920	16889	0.927	0.843
S3	5	15	+	18944	0.912	0.903	16303	0.873	0.857
S3	5	15	*	16512	0.945	0.945	17762	0.944	0.851
S4	2	5	+	19303	0.954	0.938	12609	0.826	0.775
S4	2	5	*	16380	0.952	0.941	13628	0.930	0.793
S4	3	8	+	14957	0.926	0.913	16868	0.912	0.845
S4	3	8	*	16529	0.935	0.931	13853	0.928	0.835
S4	4	10	+	17392	0.948	0.939	19498	0.910	0.801
S4	4	10	*	10454	0.954	0.946	19197	0.933	0.883
S4	5	15	+	15284	0.940	0.916	18276	0.883	0.880
S4	5	15	*	12844	0.930	0.921	18179	0.852	0.849
S5	2	5	+	16650	0.921	0.911	19335	0.946	0.783
S5	2	5	*	11804	0.956	0.930	13773	0.913	0.808
S5	3	8	+	19855	0.939	0.928	18166	0.936	0.815
S5	3	8	*	12957	0.952	0.934	13912	0.907	0.826
S5	4	10	+	12365	<b>0.962</b>	<b>0.950</b>	11323	0.888	0.855
S5	4	10	*	15066	0.950	0.943	16344	0.903	0.851
S5	5	15	+	10322	0.937	0.936	19868	<b>0.926</b>	<b>0.911</b>
S5	5	15	*	17445	0.927	0.920	17112	0.894	0.883

In this study three statistical parameters were used for measuring performance of GEP models. They are coefficients of correlation ( $R^2$ ), mean square error (MSE) and mean absolute error (MAE). Table 5.7 shows best statistical results obtained from GEP formulation.

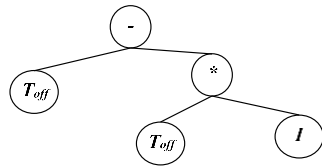
Sub-ET 1



Sub-ET 2



Sub-ET 3



Sub-ET 4

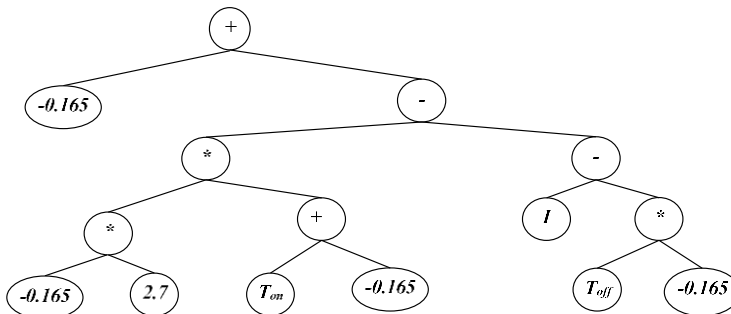


**Figure 5.4** Expression tree for MRR



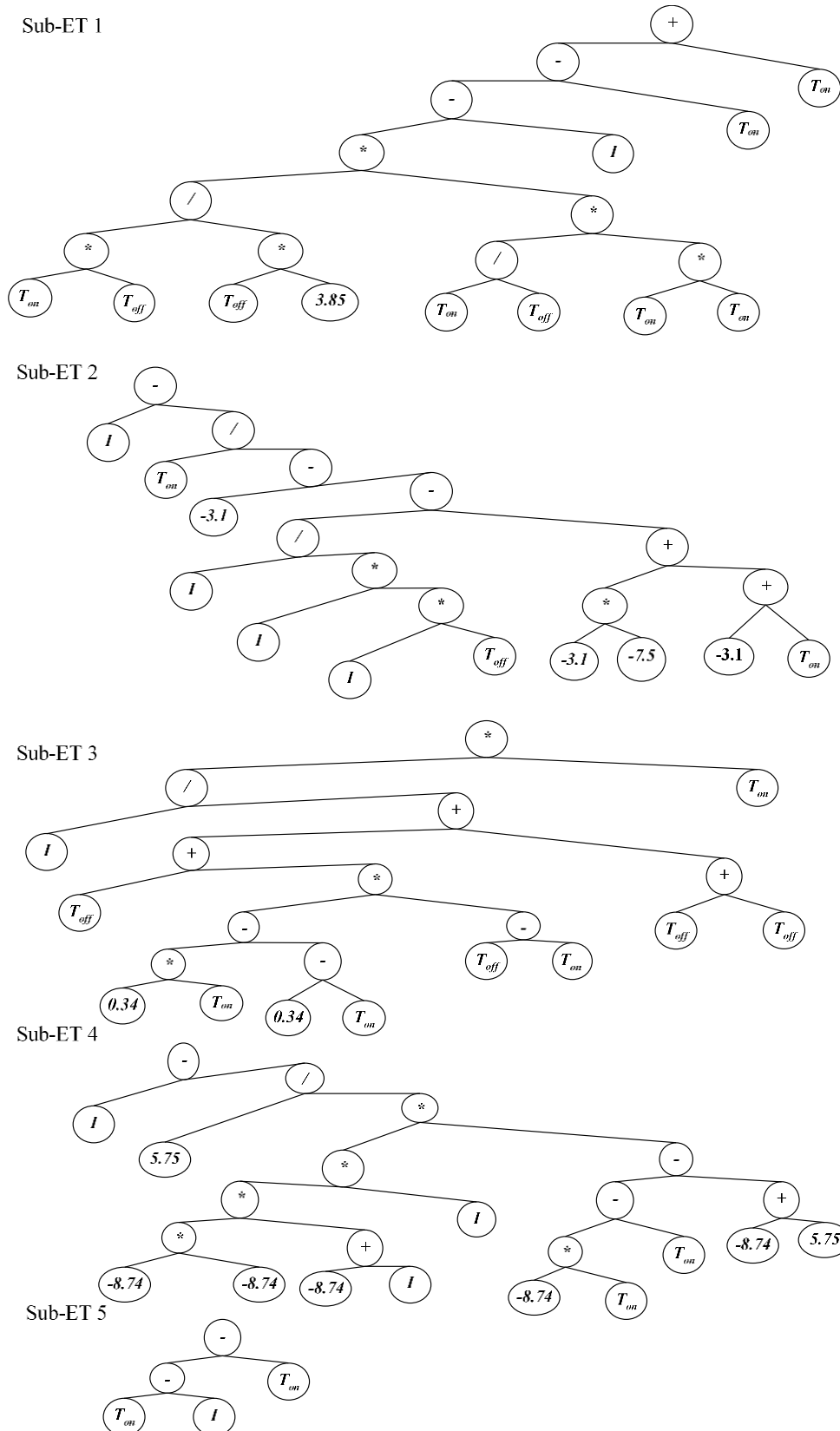


**Figure 5.5** Expression tree for EWR

**Table 5.7** Best statistical results obtained from GEP formulation

Statistical parameters	(MRR)		(EWR)	
	Training	Testing	Training	Testing
MSE	384.22	709.92	19.23	20.13
MAE	14.5	18.27	3.45	4.14
R <sup>2</sup>	0.962	0.951	0.926	0.911

The offered GP formulations must be suitable range as remarked in Table 5.3. The formulations resulting from training values are checked by test values. The GEP modelling results in the expression tree form are presented in Figure 5.4 and Figure 5.5 which correspond to the following equations, respectively:

$$MRR = 1 + [(0.87 \times T_{off} - T_{off}^2) \times (T_{off} - 2 \times T_{on})] + [(I^2 \times T_{off} - I^2) \times (T_{off} - 2 \times T_{on} + 0.5)] + T_{off} - (I \times T_{off}) - 0.45 \times T_{on} - 0.165 \times T_{off} - 0.0915 \quad 5.3$$

$$EWR = \frac{(I \times T_{on}^5)}{(3.85 \times T_{off}^3)} - \left( \frac{I \times T_{on} \times T_{off}}{9.508 \times I \times T_{off} - 1} \right) + \left( \frac{I \times T_{on}}{3 \times T_{off} + [(1.34 \times T_{on} - 0.34) \times (T_{off} - T_{on})]} \right) + \left( \frac{5.75}{[(76.38 \times I^2 - 6.67 \times I) \times (-9.74 \times T_{on} + 2.99)]} \right) \quad 5.4$$

### 5.3.2 Development of Artificial Neural Networks (ANNs) Models

In this study, an ANN model was designed in MATLAB (version 7.0) environment. This developed ANN model's specifications are listed in Table 5.8. The developed ANN model consists of one input layer, one hidden layer and one output layer. The inputs to be used in the ANN are the same as ones in GEP models.

**Table 5.8** ANN model's specifications

Paradigm	Supervised
Learning Rule	Error-correction (Levenberg–Marquardt)
Architecture	Feed-forward Multilayer perceptron
Learning algorithm	Back-propagation
Performance Function	MSE
Model	3-4-1 and 3-5-1
Neurons of Input layer	3
No of Hidden Layer	1
Neurons of Hidden Layer	4 and 5 (compared to each)
Activation of Hidden Layer	TanhAxon
Neurons of Output	1
Activation of Output Layer	TanhAxon

Firstly training and test data sets were created, then the best structure of MLP for this application was developed by training different types of transfer and output functions

for layers and also different numbers of hidden layers and its neurons were developed as well, at the end, the neural network model was established by comparing the network prediction to validation data (10 % of the data). In this study, the neuron numbers in the hidden layer were used as a main parameter to obtain the best ANN structure. Therefore, they were changed until the minimum mean squared error is achieved. Regarding the MRR and EWR formulation, 56 training, 7 validation and 15 tests data were used as training and testing sets, respectively. From this trial and error study, TanhAxon function was found that the most compatible one for the hidden layer and output layer in all tested ANN models. TanhAxon squash the range of each neuron in the layer to between -1 and 1. Such nonlinear elements provide a network with the ability to make soft decisions. The output of the  $j^{\text{th}}$  neuron after activation can be evaluated by using following equation;

$$f(x) = \frac{e^{2x} + 1}{e^{2x} - 1} \text{ and } f(x) \in (-1,1) \quad 5.5$$

Before training ANN, input data set was scaled between 0 and 1 for normalization. There are a variety of practical reasons why standardizing the inputs can make training faster and reduce the chances of getting stuck in local optima. Normalization was done by using following equation;

$$U_{Nor} = \frac{U_{actual}}{U_{max}} \quad 5.6$$

where  $U_{Nor}$  is the normalized value,  $U_{actual}$  is the actual value obtained from experiment;  $U_{max}$  is the maximum observation value of the data set. The normalized data set was then used as inputs to ANN.

Statistical parameters of ANN models are presented in Table 5.9 and Table 5.10 where;  $R^2$ , MSE and MAE correspond to the coefficient of correlation, mean square error and the mean absolute error. Table 5.9 shows the performances of the best ANN models for training phase. Table 5.10 shows the performances of the best ANN models for test data which consists of test and validation data. The patterns used in test and training sets are selected in systematic randomly. It seems that the network with 5 neurons in its hidden layer has better performance than the network with 4 neurons in its hidden layer for all training phase. On the other hand, though, the former has better performance for MRR and EWR test data.

**Table 5.9** Statistical values of the best results of ANN modelling for training data

Statistical Parameters	MRR Train Data		EWR Train Data	
	4 neuron	5 neuron	4 neuron	5 neuron
MSE	42.48	<b>14.50</b>	3.32	<b>1.55</b>
MAE	4.55	<b>2.72</b>	1.43	<b>0.93</b>
R <sup>2</sup>	0.9956	<b>0.9985</b>	0.9825	<b>0.9918</b>

**Table 5.10** Statistical values of the best results of ANN modelling for testing data

Statistical Parameters	MRR Test Data		EWR Test Data	
	4 neuron	5 neuron	4 neuron	5 neuron
MSE	271.36	<b>207.43</b>	5.43	<b>3.86</b>
MAE	9.86	<b>6.35</b>	1.75	<b>1.33</b>
R <sup>2</sup>	0.9699	<b>0.9785</b>	0.9297	<b>0.9604</b>

### 5.3.3 Development of ANFIS Models

In this study, to build an ANFIS model and to predict the MRR and EWR, the Adaptive Neuro-Fuzzy Inference System (ANFIS) editor of MATLAB was used. The toolbox helps you to create fuzzy systems by using a back propagation algorithm alone or in combination with a least squares method. Training and testing data set used in ANFIS models are the same as used ANN and GEP models. Here, testing data set was used as a checking data set. A checking data set is employed for verifying the ANFIS model generalization capabilities, except for training set. An initial FIS for training of ANFIS implementing subtractive clustering on the input/output data given is created by the model. A fast identification of parameters is obtained by using the hybrid learning algorithm so the necessary time to approach the convergence is reduced.

A membership function (MF) is a curve that defines how each point in the input space is mapped to a membership value (or degree of membership) between 0 and 1. The ANFIS toolbox includes 11 built-in membership function types; trimf, trapmf, gauss, and bell etc. The number of membership functions, MFs, and the type of input and output membership functions are chosen in the toolbox. In this study, due to their smoothness and concise notation, **Gaussian** and **bell** membership functions were chosen for inputs. The numbers of MFs were changed 3-3-3 to 6-6-6. It means that  $64 \times 2 = 128$  tries were carried out for each performance parameters. MF type was selected linear as the output membership function and epoch number was taken as 100.

**Table 5.11** Statistical values of the best results of ANFIS modelling for training data

Statistical Parameters	MRR Train Data		EWR Train Data	
	GbellMF's (365)	GaussMF's (356)	GbellMF's (433)	GaussMF's (355)
MSE	0.43	<b>0.39</b>	0.032	<b>0.019</b>
MAE	0.44	<b>0.40</b>	0.089	<b>0.067</b>
R <sup>2</sup>	0.999955	<b>0.999959</b>	0.9998	<b>0.9999</b>

**Table 5.12** Statistical values of the best results of ANFIS modelling for testing data

Statistical Parameters	MRR Test Data		EWR Test Data	
	GbellMF's (365)	GaussMF's (356)	GbellMF's (433)	GaussMF's (355)
MSE	107.57	<b>42.25</b>	10.75	<b>6.43</b>
MAE	6.25	<b>4.36</b>	1.98	<b>1.33</b>
R <sup>2</sup>	0.9889	<b>0.9979</b>	0.8600	<b>0.9511</b>

Tables 5.11 and 5.12 show statistically the performances of the best ANFIS models that have Gaussian and bell membership functions for training and test phase respectively. After training and testing, the number of MFs was fixed for each input variable, when the ANFIS model reaches to the more acceptable satisfactory level at gauss MFs. For the best models, ANFIS architectures are illustrated in Table 5.13.

**Table 5.13** ANFIS architecture and training parameters for MRR and EWR

	MRR	EWR
MFs type	Gauss	Gauss
Number of nodes	214	182
Number of linear parameters	360	300
Number of nonlinear parameters	28	26
Total number of parameters	388	326
Number of fuzzy rules	90	75
NumMFs input 1	3	3
NumMFs input 2	5	5
NumMFs input 3	6	5

### 5.3.4 Comparisons of MRR and EWR parameters modelling study

The results obtained from the modelling and experimental studies are compared in this section. Comparisons of the training performances and testing performances of GEP, ANN and ANFIS models for MRR and EWR parameters with the experimental equivalents are represented graphically in Figures 5.6 and 5.7. As shown in Figure 5.6,

there is a little deviation between the real and predicted values. It means that, all of these models can predict accurately and satisfactorily MRR parameter by learning complex relationship between the input and output parameters. However, for modelling EWR, GEP model is not very successful (see Table 5.15 and Figure 5.7).

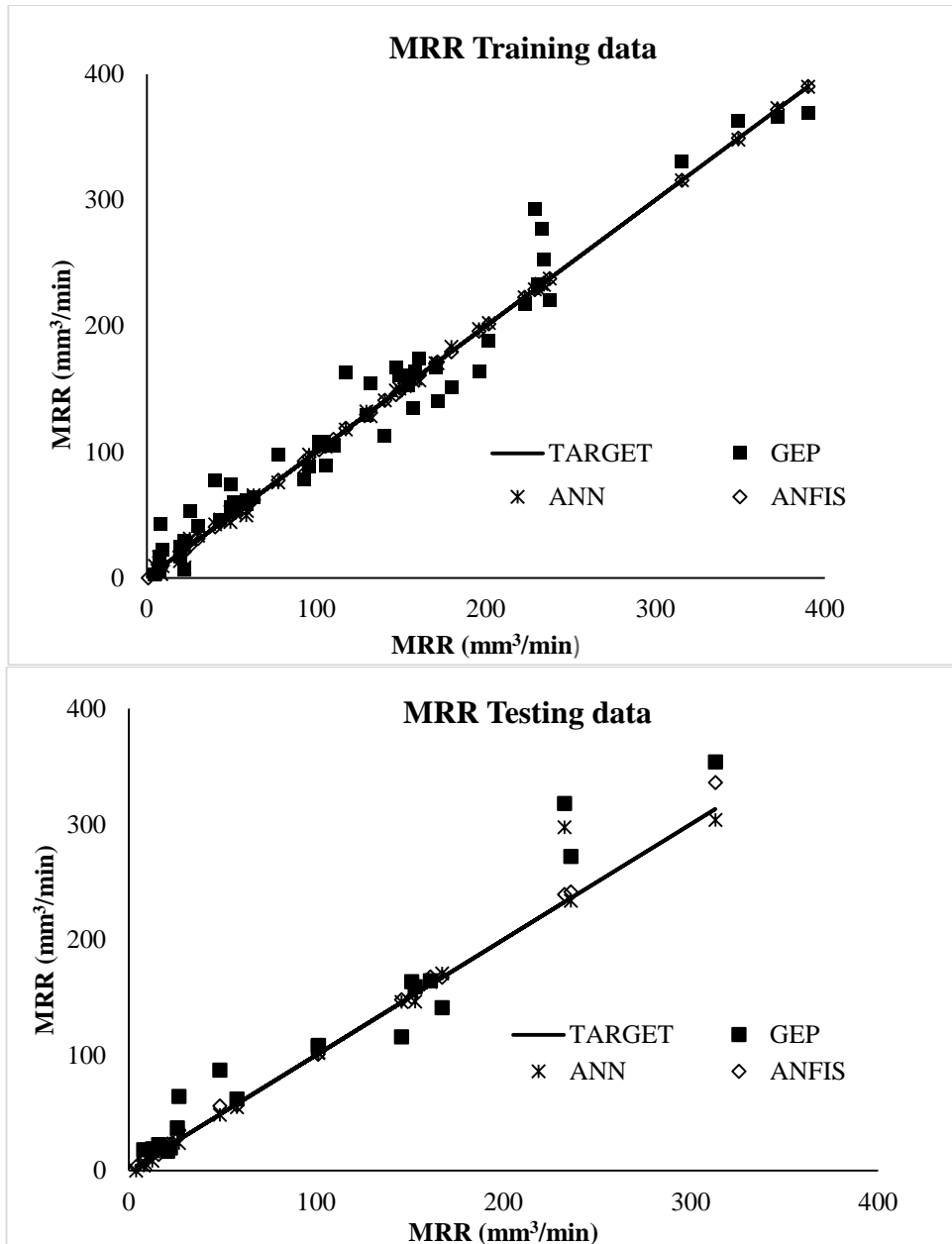


**Figure 5.6** Comparisons of training and testing performances of all methods for MRR

**Table 5.14** Statistical values of MRR modelling for training and testing sets

Statistical Parameters	MRR Training Sets			MRR Test sets		
	GEP	ANN	ANFIS	GEP	ANN	ANFIS
MSE	384.22	14.50	<b>0.39</b>	709.92	207.43	<b>42.25</b>
MAE	14.5	2.72	<b>0.40</b>	18.27	6.35	<b>4.36</b>
R <sup>2</sup>	0.9620	0.9985	<b>0.9999</b>	0.9510	0.9785	<b>0.9979</b>

**Table 5.15** Statistical values of EWR modelling for training and testing sets

Statistical Parameters	EWR Training Sets			EWR Testing sets		
	GEP	ANN	ANFIS	GEP	ANN	ANFIS
MSE	19.23	1.55	<b>0.019</b>	20.13	<b>3.86</b>	6.43
MAE	3.45	0.93	<b>0.067</b>	4.14	<b>1.33</b>	1.33
R <sup>2</sup>	0.926	0.991	<b>0.999</b>	0.911	<b>0.9604</b>	0.9511

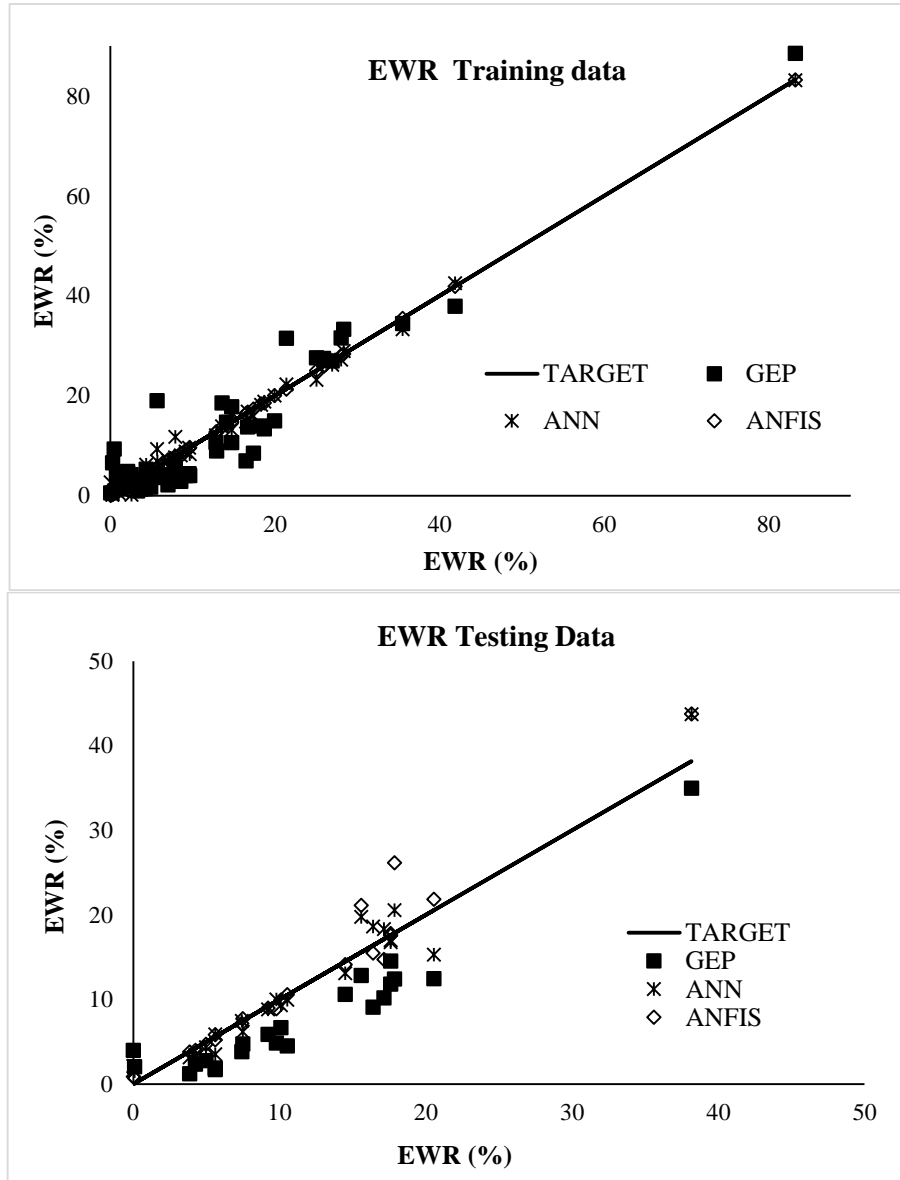


**Figure 5.7** Comparisons of training and testing performance of all methods for EWR. MSE, MAE and R<sup>2</sup> values are used to compare statistically the created models. Statistical performances of MRR and EWR modelling for training and testing sets are given in Tables 5.14 and 5.15 respectively. ANFIS model is very successful in training (R<sup>2</sup>=0.9999, MAE=0.40, and MSE=0.39), and testing of MRR (R<sup>2</sup>=0.9979, MAE=4.36, and MSE=42.25) (Table 5.14). For EWR modelling the ANFIS model is

more successful in training than the ANN model but the ANN model is slightly better in prediction of EWR than the ANFIS model (Table 5.15).

GEP model is less successful compared with other models and GEP models needed more calculation time than the others. The differences between the ANN and the ANFIS results in terms of  $R^2$ , MSE, and MAE, are very close, so that both models may be accepted as successful. However, the ANFIS model is slightly better than the ANN and the GEP model. Therefore, it is decided to model other performance parameters ( $R_a$  and AWLT), by using ANN and ANFIS methods.

#### 5.4 Modelling of $R_a$ and AWLT Parameters

Using the experimental data set, ANFIS, ANN models are developed for  $R_a$  and AWLT parameters. Same ANN models specifications (Table 5.8) were used to develop  $R_a$  and AWLT models. The developed ANN models consist of one input layer, one hidden layer and one output layer like as MRR and EWR models and , the neuron numbers in the hidden layer were used as a main parameter to obtain the best ANN structure.

**Table 5.16** ANFIS architecture and training parameters for  $R_a$  and AWLT

	$R_a$	AWLT
MFs type	Gbell	Gbell
Number of nodes	338	118
Number of linear parameters	600	180
Number of nonlinear parameters	48	33
Total number of parameters	648	213
Number of fuzzy rules	150	45
NumMFs input 1	5	3
NumMFs input 2	5	3
NumMFs input 3	6	5

At the end of the study it was found that ANN models with 5 neurons were better than ones with 4 neurons both  $R_a$  and AWLT models. Best ANFIS models architecture of  $R_a$  and AWLT parameters are given in Table 5.16. After training and testing, the number of MFs was fixed for each input variable, when the ANFIS model reaches to the more acceptable satisfactory level at gbell MFs for both models.



MSE, MAE and  $R^2$  values are used to compare statistically the created  $R_a$  and AWLT models. Statistical performances of  $R_a$  and AWLT modelling for training and testing sets are given in Tables 5.17 and 5.18 respectively. ANFIS model is very successful in training and testing of both  $R_a$  and AWLT (Tables 5.17 and 5.18).

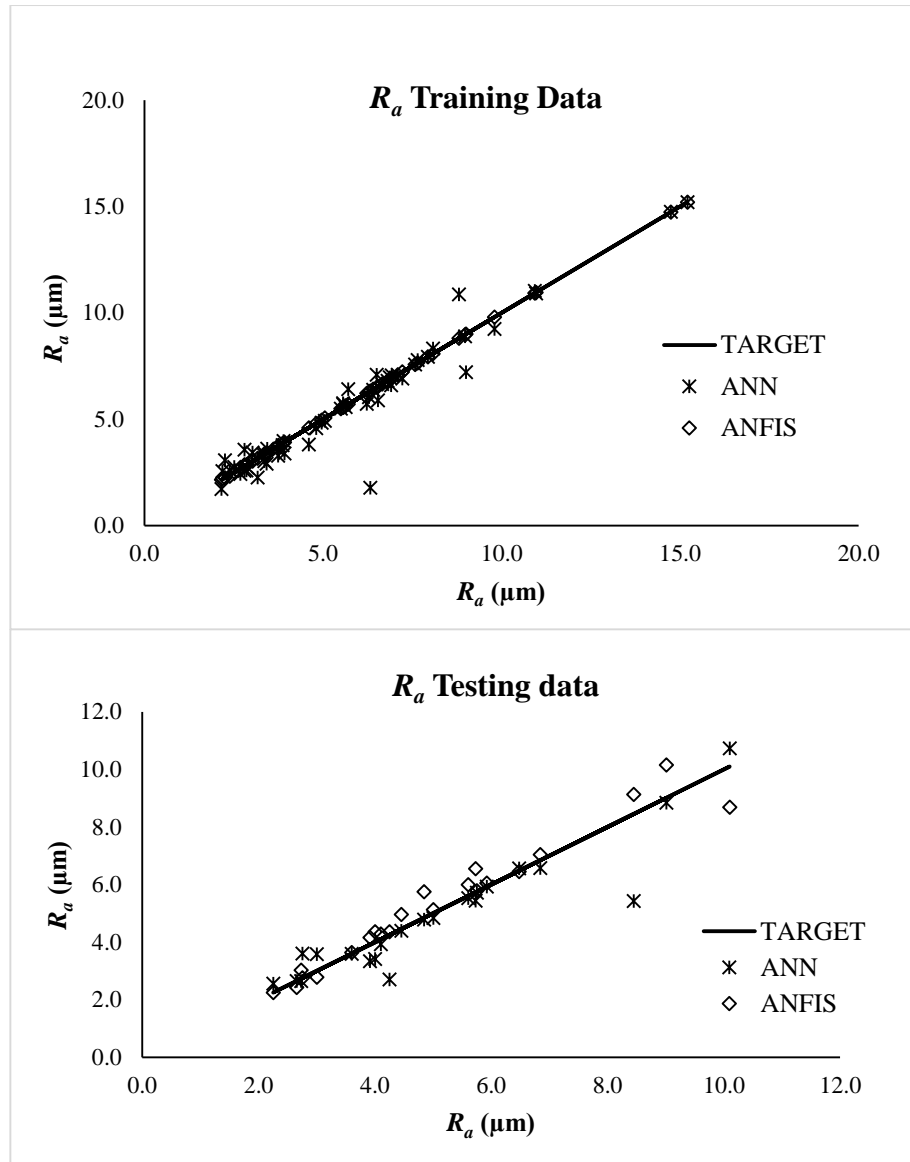


**Figure 5.8** Training and testing performances of ANN and ANFIS methods for  $R_a$

**Table 5.17** Statistical values of  $R_a$  modelling for training and testing sets

Statistical Parameters	$R_a$ training sets		$R_a$ testing sets	
	ANN	ANFIS	ANN	ANFIS
MSE	0.62	<b>0.0002</b>	0.64	<b>0.28</b>
MAE	0.40	<b>0.0065</b>	0.43	<b>0.37</b>
$R^2$	0.93186	<b>0.99997</b>	0.8640	<b>0.9464</b>

**Table 5.18** Statistical values of AWLT modelling for training and testing sets

Statistical Parameters	AWLT training sets		AWLT Testing sets	
	ANN	ANFIS	ANN	ANFIS
MSE	11.34	<b>3.08</b>	50.46	<b>76.14</b>
MAE	2.32	<b>1.00</b>	5.62	<b>6.65</b>
R <sup>2</sup>	0.9859	<b>0.9962</b>	0.8878	<b>0.9334</b>

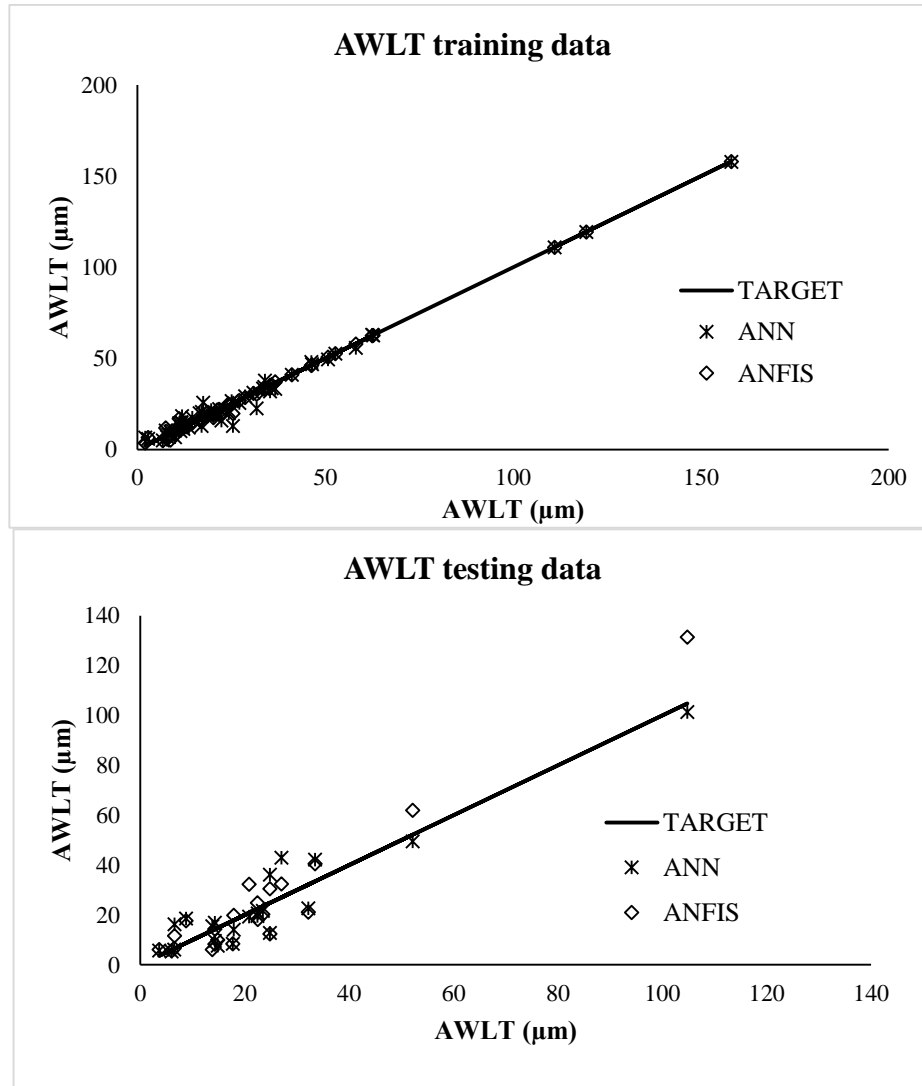


**Figure 5.9** Training and testing performances of ANN and ANFIS methods for AWLT  
 Training and testing performances off ANN and ANFIS models for Ra and AWLT parameters with the experimental equivalents are given as graphically in Figures 5.8 and 5.9. There is a little deviation between the real and predicted values of ANFIS models.

## 5.5 Discussions and Conclusions of Modelling Studies

The results obtained from the modelling and experimental studies are compared in this section. Experimental data are illustrated experiment, and data obtained from modelling studies are illustrated as guess value in Tables 5.19-5.26. Training data sets for MRR, EWR,  $R_a$  and AWLT parameters are given in Tables 5.19-5.22 and testing data are given in Tables 5.23-5.26 respectively. E/M ratio means the ratio of the experimental data to the predicted value obtained from modelling study. Estimation capabilities of all artificial models for each experimental data can be evaluated as quantitatively with the help of ratio values.

The training performances and testing performances of all models with the experimental equivalents are given as graphically in Figures 5.6 to 5.9. There is a little deviation between the real and predicted values. It means that, all of these models can predict accurately and satisfactorily EDM performances by learning complex relationship between the input and output parameters. The data set obtained from experimental study was used to develop mathematical models.

- As the results show that all approaches are successful for prediction of EDM performances by learning complex relationship between the input and output parameters in terms of statistical parameters.
- GEP model was less successful among others; however, it has a simple and explicit mathematical formulation.
- The results produced by both ANN and ANFIS models also presents relatively good level of accuracy. However, the ANFIS model is **more** successful than the ANN model.
- Using of MLP with back-propagation learning algorithm (while it has one hidden layer, tanhaxon and 5 neurons) is successful for modelling EDM performances.
- Selection of gauss MFs type and Gbell MFs type gives better results than the others MFs types for modelling of EDM performances by using ANFIS method.

**Table 5.19** Training values of material removal rate (MRR) (mm<sup>3</sup>/min)

Exp No	I Amp	Ton $\mu$ s	Toff $\mu$ s	EXP.	GEP		ANN		ANFIS	
					MODEL	E/M	MODEL	E/M	MODEL	E/M
51	3	3	3	0.7	-4.9	-0.2	-2.5	-0.3	0.1	13.6
52	6	3	6	9.2	22.3	0.4	9.3	1.0	10.1	0.9
8	12	12	25	95.7	88.4	1.1	97.9	1.0	95.9	1.0
20	3	25	12	7.1	6.0	1.2	11.8	0.6	6.7	1.1
14	12	3	12	49.3	74.5	0.7	52.3	0.9	48.9	1.0
5	6	25	25	43.3	46.1	0.9	46.2	0.9	44.1	1.0
54	25	3	25	160.7	174.1	0.9	156.8	1.0	160.9	1.0
55	6	50	12	19.8	25.0	0.8	23.5	0.8	20.4	1.0
56	25	12	12	146.9	167.1	0.9	148.6	1.0	145.4	1.0
57	6	12	3	19.5	17.1	1.1	13.3	1.5	21.0	0.9
58	25	50	3	148.9	160.8	0.9	150.2	1.0	147.6	1.0
59	12	25	3	59.1	61.7	1.0	53.0	1.1	58.2	1.0
11	3	12	6	6.3	-1.5	-4.3	5.7	1.1	5.9	1.1
16	3	100	50	52.2	54.3	1.0	51.0	1.0	52.4	1.0
12	6	12	12	22.1	29.6	0.7	25.8	0.9	20.9	1.1
1	6	50	50	92.8	77.9	1.2	88.1	1.1	92.6	1.0
10	6	100	3	22.2	6.5	3.4	8.3	2.7	21.4	1.0
6	12	50	3	58.5	58.8	1.0	49.7	1.2	58.9	1.0
7	12	100	6	49.2	56.4	0.9	44.3	1.1	48.7	1.0
21	18	3	25	129.6	129.3	1.0	132.1	1.0	129.5	1.0
22	18	12	50	179.6	151.2	1.2	183.6	1.0	179.4	1.0
18	18	50	6	104.2	108.0	1.0	105.7	1.0	104.6	1.0
17	18	100	12	101.6	108.0	0.9	104.5	1.0	101.5	1.0
23	25	3	50	201.6	188.6	1.1	202.4	1.0	201.7	1.0
9	25	12	3	117.4	163.1	0.7	117.8	1.0	118.8	1.0
2	25	100	25	170.2	166.8	1.0	170.3	1.0	170.1	1.0
60	3	12	3	8.6	-6.0	-1.4	3.0	2.9	8.9	1.0
62	3	50	12	4.7	3.0	1.6	9.6	0.5	4.9	1.0
63	3	100	25	7.2	16.6	0.4	16.4	0.4	6.9	1.0
45	6	200	50	51.3	59.8	0.9	54.4	0.9	51.6	1.0
44	6	400	100	110.1	105.3	1.0	104.9	1.0	110.1	1.0
30	9	200	100	171.3	140.2	1.2	170.3	1.0	171.3	1.0
26	9	400	200	222.8	217.5	1.0	222.6	1.0	222.8	1.0
34	25	100	12	152.1	161.1	0.9	152.2	1.0	154.2	1.0
29	25	400	50	154.1	153.1	1.0	153.1	1.0	154.1	1.0
39	12	50	50	140.4	112.9	1.2	141.0	1.0	141.0	1.0
50	18	200	12	77.4	97.7	0.8	75.8	1.0	77.6	1.0
27	25	800	100	156.8	135.0	1.2	156.5	1.0	156.8	1.0
38	9	50	25	62.8	63.5	1.0	65.7	1.0	62.1	1.0
37	9	100	50	105.3	89.4	1.2	104.0	1.0	104.6	1.0
47	18	100	200	234.2	252.7	0.9	232.7	1.0	234.2	1.0
28	12	200	200	230.4	233.2	1.0	229.8	1.0	230.4	1.0
33	12	100	100	195.9	164.1	1.2	197.4	1.0	195.9	1.0
69	9	100	12	30.1	41.0	0.7	33.4	0.9	31.2	1.0
70	9	400	50	25.4	53.2	0.5	31.1	0.8	25.3	1.0
71	12	400	25	7.9	42.7	0.2	12.5	0.6	8.0	1.0
74	18	400	12	40.4	77.3	0.5	42.4	1.0	40.4	1.0
75	25	200	12	131.9	154.4	0.9	128.3	1.0	131.1	1.0
76	50	200	25	390.0	368.8	1.1	390.0	1.0	390.0	1.0
77	50	100	12	371.8	366.3	1.0	373.0	1.0	371.8	1.0
79	50	50	6	349.0	362.8	1.0	347.8	1.0	349.0	1.0
80	50	100	50	228.9	293.3	0.8	229.0	1.0	228.9	1.0
81	50	200	200	237.5	220.5	1.1	237.7	1.0	237.5	1.0
82	50	1600	200	158.3	163.9	1.0	158.3	1.0	158.3	1.0
83	50	800	100	315.6	330.5	1.0	315.5	1.0	315.6	1.0
84	50	400	100	232.8	277.3	0.8	233.4	1.0	232.8	1.0

**Table 5.20** Training values of electrode wear ratio (EWR) (%)

Exp No	I Amp	Ton $\mu$ s	Toff $\mu$ s	EXP.	GEP		ANN		ANFIS	
					MODEL	E/M	MODEL	E/M	MODEL	E/M
51	3	3	3	3.3	1.0	3.4	2.4	1.4	3.1	1.1
52	6	3	6	1.7	2.1	0.8	1.8	0.9	2.3	0.7
8	12	12	25	1.3	4.1	0.3	1.4	0.9	1.3	1.0
20	3	25	12	4.3	1.4	3.0	3.5	1.2	4.4	1.0
14	12	3	12	0.7	4.1	0.2	1.8	0.4	0.9	0.9
5	6	25	25	2.6	2.4	1.1	0.2	12.4	2.6	1.0
54	25	3	25	2.1	4.5	0.5	2.3	0.9	2.2	1.0
55	6	50	12	9.1	4.0	2.3	8.8	1.0	9.1	1.0
56	25	12	12	4.3	5.3	0.8	6.2	0.7	4.3	1.0
57	6	12	3	6.3	3.7	1.7	6.0	1.1	6.0	1.0
58	25	50	3	21.4	31.5	0.7	22.3	1.0	21.3	1.0
59	12	25	3	12.8	10.7	1.2	12.1	1.1	12.8	1.0
11	3	12	6	3.7	1.3	2.9	3.2	1.2	3.7	1.0
16	3	100	50	2.4	2.3	1.0	4.1	0.6	2.4	1.0
12	6	12	12	2.7	2.4	1.2	1.3	2.1	2.2	1.3
1	6	50	50	1.0	2.6	0.4	0.5	1.9	1.0	1.0
10	6	100	3	5.7	19.0	0.3	9.4	0.6	5.6	1.0
6	12	50	3	14.7	17.8	0.8	13.2	1.1	14.7	1.0
7	12	100	6	13.6	18.6	0.7	13.9	1.0	13.8	1.0
21	18	3	25	2.1	4.8	0.4	3.0	0.7	2.0	1.1
22	18	12	50	4.6	4.5	1.0	3.0	1.5	4.7	1.0
18	18	50	6	18.3	14.0	1.3	18.2	1.0	18.4	1.0
17	18	100	12	18.7	13.4	1.4	18.8	1.0	18.6	1.0
23	25	3	50	9.6	4.4	2.2	9.6	1.0	9.5	1.0
9	25	12	3	14.7	10.6	1.4	16.6	0.9	14.8	1.0
2	25	100	25	16.5	7.0	2.4	14.8	1.1	16.5	1.0
60	3	12	3	4.9	1.7	2.9	4.6	1.1	4.9	1.0
62	3	50	12	7.0	2.2	3.2	7.1	1.0	7.1	1.0
63	3	100	25	8.6	2.9	3.0	8.1	1.1	8.5	1.0
45	6	200	50	7.9	5.8	1.4	11.8	0.7	7.9	1.0
44	6	400	100	17.4	8.5	2.0	16.0	1.1	17.4	1.0
30	9	200	100	7.9	5.0	1.6	7.7	1.0	7.9	1.0
26	9	400	200	0.3	6.6	0.0	0.3	1.1	0.3	1.0
34	25	100	12	19.9	15.0	1.3	20.0	1.0	20.0	1.0
29	25	400	50	0.4	9.3	0.0	1.1	0.4	0.4	1.0
39	12	50	50	2.5	4.2	0.6	2.1	1.2	2.5	1.0
50	18	200	12	25.0	27.6	0.9	23.2	1.1	25.1	1.0
27	25	800	100	0.2	-2.9	-0.1	0.2	1.3	0.2	1.0
38	9	50	25	7.3	4.2	1.7	6.2	1.2	7.4	1.0
37	9	100	50	5.7	4.4	1.3	6.8	0.8	5.7	1.0
47	18	100	200	1.5	2.9	0.5	0.9	1.6	1.5	1.0
28	12	200	200	1.5	4.0	0.4	1.6	0.9	1.5	1.0
33	12	100	100	1.6	4.1	0.4	2.4	0.6	1.6	1.0
69	9	100	12	12.9	8.9	1.4	11.4	1.1	12.8	1.0
70	9	400	50	14.1	14.8	1.0	14.5	1.0	14.1	1.0
71	12	400	25	28.4	33.3	0.9	28.9	1.0	28.4	1.0
74	18	400	12	83.3	88.5	0.9	83.2	1.0	83.2	1.0
75	25	200	12	28.1	31.6	0.9	27.3	1.0	28.0	1.0
76	50	200	25	25.9	27.5	0.9	27.4	0.9	25.9	1.0
77	50	100	12	25.9	27.1	1.0	27.1	1.0	25.9	1.0
79	50	50	6	26.9	27.0	1.0	26.2	1.0	26.9	1.0
80	50	100	50	9.7	4.0	2.4	8.3	1.2	9.7	1.0
81	50	200	200	0.1	0.6	0.1	2.7	0.0	0.1	1.0
82	50	1600	200	41.9	37.9	1.1	42.6	1.0	41.9	1.0
83	50	800	100	35.5	34.4	1.0	33.3	1.1	35.5	1.0
84	50	400	100	16.7	13.8	1.2	16.8	1.0	16.7	1.0

**Table 5.21** Training values of surface roughness ( $R_a$ ) ( $\mu\text{m}$ )

Exp No	I Amp	Ton $\mu\text{s}$	Toff $\mu\text{s}$	EXP.	ANN		ANFIS	
					MODEL	E/M	MODEL	E/M
51	3	3	3	2.2	2.6	0.9	2.2	1.0
52	6	3	6	3.4	3.6	0.9	3.4	1.0
8	12	12	25	5.0	4.8	1.0	5.0	1.0
20	3	25	12	2.9	2.6	1.1	2.8	1.0
14	12	3	12	5.6	5.7	1.0	5.6	1.0
5	6	25	25	3.7	3.3	1.1	3.7	1.0
54	25	3	25	2.3	3.1	0.7	2.2	1.0
55	6	50	12	4.6	3.8	1.2	4.6	1.0
56	25	12	12	3.9	3.8	1.0	3.9	1.0
57	6	12	3	2.8	3.6	0.8	2.8	1.0
58	25	50	3	6.5	7.1	0.9	6.5	1.0
59	12	25	3	6.3	6.0	1.0	6.3	1.0
11	3	12	6	2.8	2.6	1.1	2.8	1.0
16	3	100	50	2.5	2.8	0.9	2.5	1.0
12	6	12	12	3.8	3.6	1.1	3.8	1.0
1	6	50	50	3.2	2.3	1.4	3.2	1.0
10	6	100	3	5.6	5.7	1.0	5.6	1.0
6	12	50	3	6.9	6.6	1.0	6.9	1.0
7	12	100	6	8.1	8.3	1.0	8.1	1.0
21	18	3	25	3.4	3.0	1.1	3.4	1.0
22	18	12	50	2.7	2.4	1.1	2.7	1.0
18	18	50	6	6.9	7.0	1.0	6.9	1.0
17	18	100	12	7.7	7.8	1.0	7.6	1.0
23	25	3	50	2.9	2.7	1.1	2.9	1.0
9	25	12	3	4.8	4.6	1.0	4.8	1.0
2	25	100	25	9.0	7.2	1.2	9.0	1.0
60	3	12	3	2.4	2.6	0.9	2.3	1.0
62	3	50	12	3.4	2.9	1.2	3.4	1.0
63	3	100	25	3.9	4.0	1.0	3.9	1.0
45	6	200	50	6.2	5.7	1.1	6.2	1.0
44	6	400	100	3.3	3.3	1.0	3.3	1.0
30	9	200	100	2.2	1.7	1.3	2.2	1.0
26	9	400	200	6.7	6.6	1.0	6.6	1.0
34	25	100	12	9.8	9.2	1.1	9.8	1.0
29	25	400	50	6.3	1.8	3.5	6.3	1.0
39	12	50	50	3.9	3.4	1.2	3.9	1.0
50	18	200	12	6.4	6.4	1.0	6.4	1.0
27	25	800	100	5.5	5.5	1.0	5.5	1.0
38	9	50	25	5.1	4.9	1.0	5.1	1.0
37	9	100	50	3.0	3.4	0.9	3.0	1.0
47	18	100	200	7.9	7.9	1.0	7.9	1.0
28	12	200	200	7.6	7.6	1.0	7.6	1.0
33	12	100	100	3.4	3.4	1.0	3.4	1.0
69	9	100	12	6.9	7.1	1.0	6.9	1.0
70	9	400	50	5.7	6.4	0.9	5.7	1.0
71	12	400	25	7.2	6.9	1.0	7.2	1.0
74	18	400	12	5.6	5.6	1.0	5.6	1.0
75	25	200	12	11.0	10.9	1.0	11.0	1.0
76	50	200	25	8.8	10.9	0.8	8.8	1.0
77	50	100	12	9.0	8.9	1.0	9.0	1.0
79	50	50	6	6.5	5.9	1.1	6.5	1.0
80	50	100	50	7.1	7.1	1.0	7.1	1.0
81	50	200	200	6.8	6.8	1.0	6.8	1.0
82	50	1600	200	14.7	14.7	1.0	14.7	1.0
83	50	800	100	15.2	15.2	1.0	15.2	1.0
84	50	400	100	10.9	11.0	1.0	10.9	1.0

**Table 5.22** Training values of average white layer thickness (AWLT) ( $\mu\text{m}$ )

EXP NO	I Amp	Ton $\mu\text{s}$	Toff $\mu\text{s}$	EXP.	ANN		ANFIS	
					MODEL	E/M	MODEL	E/M
51	3	3	3	6.7	5.0	1.3	4.9	1.4
52	6	3	6	2.0	6.7	0.3	3.7	0.5
8	12	12	25	11.6	14.7	0.8	14.4	0.8
20	3	25	12	7.5	10.4	0.7	12.0	0.6
14	12	3	12	11.4	10.1	1.1	10.7	1.1
5	6	25	25	12.8	15.2	0.8	12.6	1.0
54	25	3	25	9.4	10.2	0.9	10.3	0.9
55	6	50	12	11.1	14.5	0.8	17.0	0.7
56	25	12	12	11.5	12.3	0.9	11.8	1.0
57	6	12	3	10.0	6.8	1.5	7.8	1.3
58	25	50	3	21.8	22.4	1.0	22.1	1.0
59	12	25	3	12.2	11.3	1.1	14.9	0.8
11	3	12	6	7.8	7.0	1.1	5.8	1.4
16	3	100	50	20.6	20.3	1.0	19.7	1.0
12	6	12	12	8.8	9.8	0.9	5.3	1.7
1	6	50	50	21.2	20.1	1.1	21.7	1.0
10	6	100	3	14.5	17.6	0.8	14.6	1.0
6	12	50	3	22.3	16.0	1.4	19.2	1.2
7	12	100	6	17.4	25.9	0.7	18.4	0.9
21	18	3	25	17.1	12.9	1.3	15.3	1.1
22	18	12	50	11.7	15.1	0.8	12.5	0.9
18	18	50	6	17.1	20.8	0.8	16.7	1.0
17	18	100	12	36.6	33.3	1.1	37.2	1.0
23	25	3	50	8.2	8.4	1.0	7.6	1.1
9	25	12	3	13.6	12.1	1.1	13.4	1.0
2	25	100	25	35.2	32.0	1.1	35.2	1.0
60	3	12	3	2.8	5.9	0.5	6.7	0.4
62	3	50	12	25.4	12.9	2.0	19.8	1.3
63	3	100	25	11.9	18.4	0.6	12.9	0.9
45	6	200	50	19.5	21.8	0.9	19.7	1.0
44	6	400	100	24.3	20.0	1.2	24.3	1.0
30	9	200	100	16.5	20.0	0.8	16.5	1.0
26	9	400	200	33.4	33.6	1.0	33.4	1.0
34	25	100	12	33.9	37.8	0.9	33.5	1.0
29	25	400	50	46.5	46.9	1.0	46.5	1.0
39	12	50	50	20.6	20.0	1.0	19.8	1.0
50	18	200	12	46.3	48.0	1.0	46.2	1.0
27	25	800	100	62.7	62.8	1.0	62.7	1.0
38	9	50	25	20.2	18.8	1.1	17.5	1.2
37	9	100	50	24.2	21.7	1.1	25.0	1.0
47	18	100	200	27.1	25.6	1.1	27.1	1.0
28	12	200	200	28.6	29.3	1.0	28.6	1.0
33	12	100	100	18.6	18.7	1.0	18.6	1.0
69	9	100	12	31.7	22.7	1.4	30.4	1.0
70	9	400	50	25.0	26.7	0.9	24.9	1.0
71	12	400	25	35.7	33.8	1.1	35.7	1.0
74	18	400	12	30.9	31.3	1.0	30.9	1.0
75	25	200	12	58.1	55.8	1.0	58.0	1.0
76	50	200	25	62.4	63.0	1.0	62.4	1.0
77	50	100	12	50.7	49.6	1.0	50.7	1.0
79	50	50	6	33.7	34.4	1.0	33.7	1.0
80	50	100	50	41.1	41.1	1.0	41.1	1.0
81	50	200	200	52.7	52.7	1.0	52.7	1.0
82	50	1600	200	119.4	119.4	1.0	119.4	1.0
83	50	800	100	158.1	158.0	1.0	158.1	1.0
84	50	400	100	111.1	111.1	1.0	111.1	1.0

**Table 5.23** Testing values of material removal rate (MRR) (mm<sup>3</sup>/min)

Exp No	I Amp	Ton $\mu$ s	Toff $\mu$ s	EXP.	GEP		ANN		ANFIS	
					MODEL	E/M	MODEL	E/M	MODEL	E/M
15	25	25	6	151.1	163.6	0.9	154.6	1.0	149.9	1.0
53	12	50	6	57.8	62.2	0.9	55.0	1.1	56.6	1.0
85	50	200	50	232.6	317.9	0.7	297.3	0.8	239.2	1.0
25	18	25	3	101.0	108.0	0.9	102.0	1.0	100.9	1.0
4	25	50	12	160.9	164.5	1.0	163.5	1.0	167.8	1.0
24	3	6	3	3.9	-5.3	-0.7	0.0	135.9	3.7	1.0
64	6	3	3	8.0	18.1	0.4	4.4	1.8	11.1	0.7
13	6	6	3	12.5	17.8	0.7	8.4	1.5	15.2	0.8
65	6	25	6	22.1	19.7	1.1	19.2	1.2	23.1	1.0
66	6	50	6	20.7	16.7	1.2	16.7	1.2	23.1	0.9
67	6	100	12	12.6	19.0	0.7	16.8	0.8	14.3	0.9
36	6	100	25	25.9	37.1	0.7	33.0	0.8	31.2	0.8
40	25	200	25	152.9	159.3	1.0	146.3	1.0	160.1	1.0
61	3	25	6	8.6	-3.0	-2.8	6.7	1.3	10.0	0.9
43	18	400	25	48.6	87.2	0.6	48.4	1.0	56.2	0.9
73	18	200	25	101.3	108.4	0.9	102.4	1.0	107.6	0.9
3	12	25	50	145.5	115.9	1.3	146.0	1.0	148.0	1.0
72	18	100	50	167.3	141.3	1.2	170.8	1.0	167.4	1.0
78	50	25	6	313.1	354.0	0.9	303.7	1.0	336.0	0.9
48	25	50	200	236.0	272.1	0.9	233.7	1.0	241.4	1.0
19	3	50	25	15.9	22.6	0.7	22.8	0.7	13.9	1.1
68	12	3	3	26.7	64.2	0.4	23.9	1.1	35.0	0.8

**Table 5.24** Training values of electrode wear ratio (EWR) (%)

Exp No	I Amp	Ton $\mu$ s	Toff $\mu$ s	EXP.	GEP		ANN		ANFIS	
					MODEL	E/M	MODEL	E/M	MODEL	E/M
15	25	25	6	17.1	10.2	1.7	18.3	0.9	14.7	1.2
53	12	50	6	14.5	10.6	1.4	13.1	1.1	14.1	1.0
85	50	200	50	17.6	11.8	1.5	16.8	1.1	17.8	1.0
25	18	25	3	17.6	14.5	1.2	17.0	1.0	17.6	1.0
4	25	50	12	16.4	9.1	1.8	18.6	0.9	15.5	1.1
24	3	6	3	3.9	1.2	3.2	3.1	1.2	3.8	1.0
64	6	3	3	4.3	2.3	1.8	3.4	1.2	4.0	1.1
13	6	6	3	5.0	2.8	1.8	4.3	1.1	4.7	1.1
65	6	25	6	7.4	3.8	2.0	7.4	1.0	7.2	1.0
66	6	50	6	9.2	5.8	1.6	8.8	1.0	9.0	1.0
67	6	100	12	10.1	6.6	1.5	9.3	1.1	9.9	1.0
36	6	100	25	10.5	4.5	2.3	9.9	1.1	10.5	1.0
40	25	200	25	20.6	12.5	1.7	15.3	1.3	21.8	0.9
61	3	25	6	5.6	1.9	3.0	5.9	1.0	5.8	1.0
43	18	400	25	38.2	35.0	1.1	43.7	0.9	43.8	0.9
73	18	200	25	15.6	12.8	1.2	19.8	0.8	21.1	0.7
3	12	25	50	0.0	4.0	0.0	2.1	0.0	0.9	0.0
72	18	100	50	9.8	4.8	2.0	10.0	1.0	8.9	1.1
78	50	25	6	17.9	12.4	1.4	20.5	0.9	26.1	0.7
48	25	50	200	0.1	2.0	0.0	1.5	0.1	0.7	0.1
19	3	50	25	5.6	1.7	3.3	3.5	1.6	5.2	1.1
68	12	3	3	7.5	4.7	1.6	6.2	1.2	7.7	1.0



**Table 5.25** Testing values of surface roughness ( $R_a$ ) ( $\mu\text{m}$ )

Exp No	I Amp	Ton $\mu\text{s}$	Toff $\mu\text{s}$	EXP.	ANN		ANFIS	
					MODEL	E/M	MODEL	E/M
15	25	25	6	5.0	4.8	1.0	5.1	1.0
53	12	50	6	6.8	6.6	1.0	7.0	1.0
85	50	200	50	10.1	10.7	0.9	8.7	1.2
25	18	25	3	6.5	6.6	1.0	6.5	1.0
4	25	50	12	5.6	5.5	1.0	6.0	0.9
24	3	6	3	2.3	2.6	0.9	2.2	1.0
64	6	3	3	2.8	3.6	0.8	2.8	1.0
13	6	6	3	3.0	3.6	0.8	2.8	1.1
65	6	25	6	3.6	3.6	1.0	3.6	1.0
66	6	50	6	4.1	3.9	1.0	4.3	1.0
67	6	100	12	5.7	5.4	1.1	6.5	0.9
36	6	100	25	4.8	4.8	1.0	5.8	0.8
40	25	200	25	9.0	8.8	1.0	10.1	0.9
61	3	25	6	2.7	2.7	1.0	3.0	0.9
43	18	400	25	8.5	5.4	1.6	9.1	0.9
73	18	200	25	5.8	5.7	1.0	5.8	1.0
3	12	25	50	3.9	3.3	1.2	4.2	0.9
72	18	100	50	4.0	3.4	1.2	4.4	0.9
78	50	25	6	4.5	4.4	1.0	5.0	0.9
48	25	50	200	4.3	2.7	1.6	4.4	1.0
19	3	50	25	2.7	2.6	1.0	2.4	1.1
68	12	3	3	5.9	5.9	1.0	6.0	1.0

**Table 5.26** Testing values of average white layer thickness (AWLT) ( $\mu\text{m}$ )

EXP NO	I Amp	Ton $\mu\text{s}$	Toff $\mu\text{s}$	EXP.	ANN		ANFIS	
					MODEL	E/M	MODEL	E/M
15	25	25	6	13.8	15.4	0.9	6.1	2.2
53	12	50	6	14.3	16.8	0.8	14.3	1.0
85	50	200	50	104.8	101.3	1.0	131.4	0.8
25	18	25	3	17.9	14.0	1.3	19.9	0.9
4	25	50	12	32.2	22.7	1.4	21.1	1.5
24	3	6	3	6.0	5.3	1.1	5.5	1.1
64	6	3	3	3.6	5.8	0.6	6.1	0.6
13	6	6	3	6.5	6.1	1.1	6.7	1.0
65	6	25	6	14.3	9.5	1.5	8.2	1.7
66	6	50	6	24.8	12.7	2.0	12.4	2.0
67	6	100	12	20.8	19.3	1.1	32.3	0.6
36	6	100	25	22.5	20.6	1.1	18.1	1.2
40	25	200	25	52.2	49.5	1.1	62.0	0.8
61	3	25	6	17.7	8.4	2.1	8.4	2.1
43	18	400	25	27.0	43.0	0.6	32.4	0.8
73	18	200	25	33.5	42.2	0.8	40.5	0.8
3	12	25	50	8.8	18.6	0.5	17.7	0.5
72	18	100	50	23.4	21.6	1.1	20.2	1.2
78	50	25	6	24.8	36.1	0.7	30.5	0.8
48	25	50	200	22.4	19.6	1.1	24.9	0.9
19	3	50	25	6.6	16.2	0.4	11.6	0.6
68	12	3	3	14.8	7.7	1.9	9.9	1.5

## CHAPTER 6

### MULTI-STAGE EDM STRATEGY AND PROGRAMMING

#### 6.1 Introduction

In this chapter, a multistage strategy was developed to determine the required number of stages for minimum machining time. Then, a multi-stage EDM selection program was developed by using MATLAB package program. The developed program computes the number of stages required to complete the operation, the sequence of them from rough to finish and the machining parameter sets for each stage according to minimum machining time. The resulting average white layer thickness of the previous stage was taken as a criterion to determine the machining depth. The machining depth and the corresponding parameters set in each stage according to the desired surface quality, volume and area of the workpiece can be defined by using the alternative EDM parameter sets which were generated by the models. Some case studies and a verification experiment were performed to explain the developed multi-stage strategy and the computer program.

#### 6.2 Development of A Multi-Stage Strategy

Multi-stage machining process refers to a part that is machined through different setups (Loose et al., 2007). A multi-stage machining process includes at least two stages, i.e. roughing and finishing stages. The main aim of any roughing operation is to remove maximum material from the workpiece with a minimum machining time and cost. Here, surface quality and dimensional accuracy are of a minor importance. The objective of a finishing operation is to accomplish the desired final dimension and surface quality of the machined part. In finishing operation, the quality is of major concern.

The results of the experimental studies given in the previous chapter show that EDM is a highly nonlinear process and its performance is influenced by various machining parameters. For example, increasing discharge current and pulse on-time increases

surface roughness. However, this parameter set will decrease machining time and increase MRR. So, selection of this parameter set is suitable for rough-stage of EDM process. Low discharge current, low pulse on-time and large pulse off-time cause minimum surface roughness. But, this parameter set is not profitable since machining time will increase. So, this parameter set can be used in finish-stage of EDM process. Properly selection of machining parameters at any machining stages is vitally important to encourage efficiency. However, it is very difficult to attain high MRR and excellent surface feature in the same breath in one-stage machining. Therefore, in a whole EDM process, machining stages that usually consist of rough-stage, middle-stage and finish-stage are realized one after the other (Su et al., 2004).

The multi-stage machining is the impressive method to overcome the contradiction between the machining speed and surface feature, and to achieve the higher output performances (Li et al., 2003; Guo and Xing, 2000). In addition, this method permits the operator to reduce machining costs by decreasing the amount of electrodes needed to complete the machining process.

In Ram EDM process, processing conditions are determined according to the processing parameters which are electrode and workpiece material, electrode discharge area, cutting depth, final surface quality, electrode wear necessity, etc. The operator defines the processing conditions from rough stage to finish stage according to the parameters. Determination of the number of stages, depth of material removal and machine parameter set for each stage are considered as a crucial period of EDM process planning.

Generally classification of stages from rough to finish is made according to average surface roughness values. For instance, machining stages were classified as finishing (if  $Ra \leq 2 \mu\text{m}$ ), semi-finishing (if  $2 < Ra \leq 4.5 \mu\text{m}$ ) and roughing (if  $4.5 < Ra \leq 7 \mu\text{m}$ ) by Assarzadeh et al. (2008). Helmi (2008) defined EDM machining stages as gentle (if  $Ra < 1.6 \mu\text{m}$ ), finishing (if  $1.6 \mu\text{m} < Ra < 3.2 \mu\text{m}$ ), normal (if  $3.2 \mu\text{m} < Ra < 6.3 \mu\text{m}$ ), roughing (if  $6.3 \mu\text{m} < Ra < 12.3 \mu\text{m}$ ) and abusive (if  $Ra > 12.5 \mu\text{m}$ ). Su et al. (2004) defined machining stages with respect to machined area and surface roughness together as shown in Table 6.1

**Table 6.1** Classification of EDM stages (Su et al., 2004)

Classification of Machined area	Finishing $R_a$ ( $\mu m$ )	Middle $R_a$ ( $\mu m$ )	Roughing $R_a$ ( $\mu m$ )
Very small	0.6-3.0	3.0-4.4	4.4-6.0
Small	4.0-6.0	6.0-9.0	9.0-13.0
Middle	5.5-7.5	7.5-11	11.0-16.0
Large	5.5-8.0	8.0-14	14.0-23.0
Very large	-	-	19.0-24.0

In multi stage EDM, researches developed different strategies to describe operation sequences. Sanchez et al. (2002) proposed a strategy based on complete removal of  $R_t$ , at each stage of planetary EDM. They reported that this strategy gave the best results in machining time, but it could not assure the required surface roughness.

Huang et al. (1999) defined a strategy considering the removal of the heat-affected zone and surface roughness together to determine number of stages and parameters settings in WEDM. Minimum machining time is the main objective and surface quality and white layer depth are constraints.

Surface integrity has always been of concern in EDM. Surface roughness is an important criteria for product quality and technical requirement for mechanical parts and it is related to functional behaviour of a part. Beneath the surface are the metallurgically and chemically affected zones. There are basically three layers: a recast (white) layer, a heat-affected layer and the bulk material. The outer layer consists of a resolidified layer that has a recast structure. In most functional performance situations, the sub-surface features are the most influential.

In this thesis, the thickness of white (recast) layer was taken as a main criteria in determination of machining stages. The reasons are summarised as follows;

- The white layer has normally different characteristic from the parent material, it consists of micro-cracks, voids, impurities, stress and several other defects and causes the deterioration of the mechanical properties of the machined components (Lee and Tai, 2003).
- Surface crack is a vital defect, which certainly affects the fatigue life of the components (Lee et al., 1998), and these are generally formed when the

induced stress exceeds the ultimate stress (Lee et al., 2004). Moreover, the surface cracks in EDMed surfaces are restricted to the white layers only; therefore, removing the white layers also clears the surface cracks on the surface (Pradhan, 2013).

- The recast layer increases surface roughness, since the roughness of the surface machined with EDM is related to the spreading of the craters. Therefore, removing the white layer increases the surface quality.
- To obtain fatigue properties representative of the bulk material, however, both the recast layer and the HAZ must be removed. (ASM handbook). The depth of the HAZ is approximately twice the white layer depth (Griffiths, 2001).

The experimental studies show that the white layer in roughing stage was mainly discontinuous and non-uniform and much more than that in finishing stage. However, in finishing stage, the thickness of the white layer was very small for all EDMed surfaces (Figure 6.1). It shows that, the white layer in previous-stages can be removed or minimized by using multi-stage machining strategy. So, in this thesis, the thickness of white (recast) layer was taken as a main criteria in determination of machining stages.

EDM machining settings are made depending on the aim of machining. The suitable machining sets vary according to the machining content such as rough machining and finish machining etc. To complete the desired shape of workpiece accurately and reaching the final surface quality in a minimum machining time are the main objectives of the EDM machining. To begin with EDM machining, initially following have to be determined;

- Total machining volume
- Depth of cut
- Final surface quality
- Discharge area (projection or frontal surface of workpiece area)

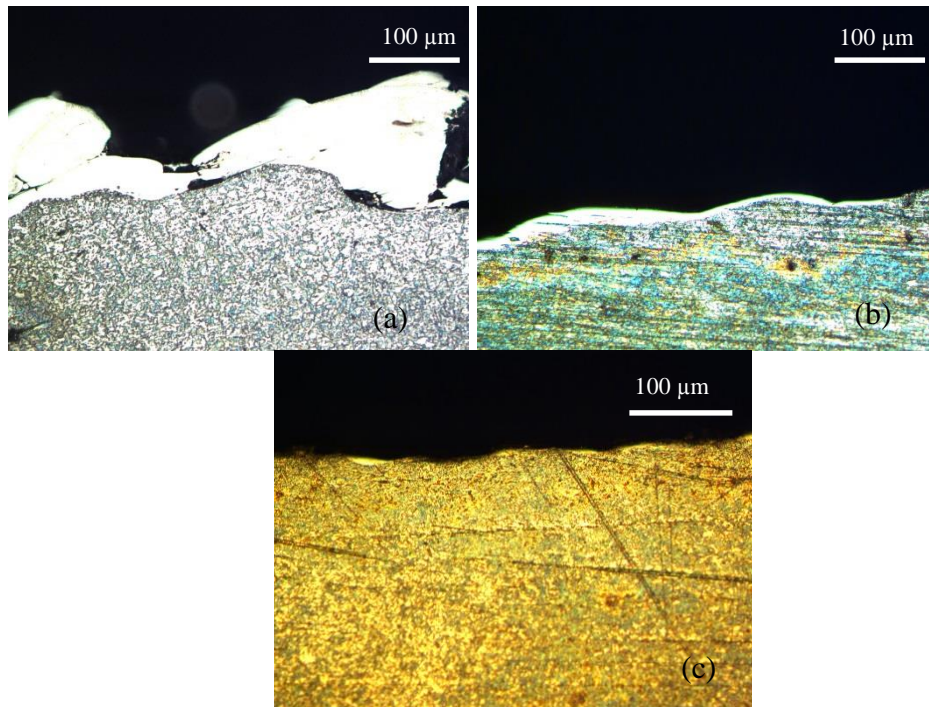


**Figure 6.1** Views of white layer on various stage where a)  $I=50$  A,  $T_{on}=400\mu s$ ,  $T_{off}=100\mu s$ ,  $AWLT=111.1\mu m$ ,  $R_a=10.9 \mu m$  b)  $I=12$  A,  $T_{on}=50 \mu s$ ,  $T_{off}=3 \mu s$ ,  $AWLT=22.3 \mu m$ ,  $R_a=6.9 \mu m$  c)  $I=3$  A,  $T_{on}=3 \mu s$ ,  $T_{off}=3\mu s$ ,  $AWLT=6.7 \mu m$ ,  $R_a=2.18 \mu m$

The discharge current value for rough machining is one of the important parameters that have great impact on the processing efficiency and accuracy. The discharge area limits the maximum value of the discharge current. Because, if high current is passed through the thin electrode (has a small front area), electrode will be worn excessively. In the previous chapter, the suggested maximum value of discharge current according to discharge area was given (see Table 4.5).

The desired surface quality limits the finishing discharge current. The finish machining discharge current value is determined by the required final surface roughness which determines the quality of a product.

Usually, to obtain a precise workpiece in good surface quality, some extra middle-stages may be needed. Effective middle-stages are the keys to successful finish machining. But, the number of stages and parameters set of each stage which satisfy the specified quality restrictions (i.e. surface finish, accuracy and surface integrity) and minimum machining time must be determined.

To determine the depth of cut for each stage, as a strategy, we suggest that the AWLT of the previous machining stage is taken as a criterion. The machining depth of any

subsequent stage can be chosen as 2-3 times larger than the previous AWLT. Because, the depth of the HAZ is approximately twice the white layer depth (Griffiths, 2001). By doing this, the negative effects of the white layer and HAZ can be eliminated. In our strategy, the most of the thickness of the white layer and HAZ produced by previous machining stage is removed by subsequent machining stage.

Ram EDM is a type of machining of copying the shape of the electrode to the workpiece, but the dimension of the electrode changes, it is damaged by sparks. This change is named of electrode wear. The electrode wear causes some amount of uncut (rest) stock (Figure 6.2). One of the aims of our strategy is to machine the rest material in the subsequent machining stage.

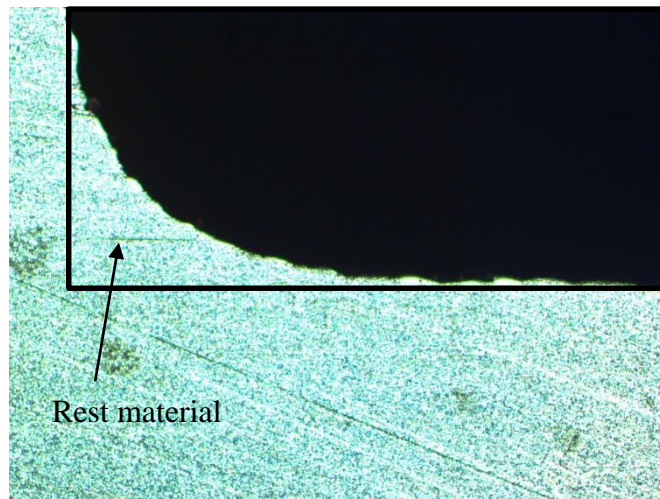


**Figure 6.2** A section view of rest material from previous machining stage

Calculating of the amount of rest material can be done by using amount of electrode wear, because the volume of tool wear ( $\text{mm}^3$ ) is nearly equal to rest material. Volume of the tool wear (TW) or the rest material is calculated by using following equations.

The equation 4.2 is rearranged as

$$EWR(\%) = \frac{TWR \left( \frac{\text{mm}^3}{\text{min}} \right)}{MRR \left( \frac{\text{mm}^3}{\text{min}} \right)} \times \frac{\rho_e}{\rho_m} \times 100 \quad 6.1$$

where TWR, and MRR are the volume material removed per unit time from the tool (electrode) and from the workpiece, respectively.  $\rho_m$  and  $\rho_e$ , are the densities of workpiece and the electrode materials, respectively. And TWR (tool wear rate) can be calculated as

$$TWR \left( \frac{mm^3}{min} \right) = \frac{EWR(\%) \times MRR \left( \frac{mm^3}{min} \right)}{100} \times \frac{\rho_m}{\rho_e} \quad 6.2$$

MRR, EWR (%) of each stage can be found from the data table. Machining time ( $t$ ) of previous stage times TWR gives the volume of tool wear (TW) or rest material volume (RV) in  $mm^3$ , it can be seen at equation 6.3

$$RV (mm^3) = \frac{EWR(\%) \times MRR \left( \frac{mm^3}{min} \right)}{100} \times \frac{\rho_m}{\rho_e} \times t (min) \quad 6.3$$

### 6.2.1 An illustrative example of Multi-Stage strategy

An illustrative example was carried out to show the multi-stage machining strategy. Table 6.2 shows the specifications of the example.

**Table 6.2** Specifications of the example

Material	1.2344 tool steel
Electrode	Copper
Machining Geometry	60x60x30 mm prismatic blind hole
Objective	Number of stages, EDM parameter set ( $I$ , $T_{on}$ , $T_{off}$ ) in each stage
Output	Minimum machining time
Desired surface quality $R_{af}$	2.7 $\mu m$ .
Parameters	MRR, EWR, Surface quality
Controllable parameters	Pulse on-time ( $T_{on}$ ), pulse off-time ( $T_{off}$ ), discharge current ( $I$ )
Criteria	White layer thickness (WLT), machining surface area

For this example, the levels of electrical parameter of the EDM machine are given in Table 6.3.

**Table 6.3** Levels of electrical parameters of the EDM machine

$I$ (amp)	3,6,9,12,18,25,31,37,44,50
$T_{on}$ ( $\mu s$ )	3,6,12,25,50,100,200,400,800,1600
$T_{off}$ ( $\mu s$ )	3,6,12,25,50,100,200

A backward-chain strategy was developed to define the stages of the EDM. According to the final surface roughness requirement, the machining parameters of the last (finishing) stage are determined first. The desired surface quality in this study is  $R_{af} = 2.7 \mu m$ , the database model gives us 3 alternatives as shown in Table 6.4.



**Table 6.4** Different choice for  $R_a = 2.7 \mu\text{m}$ 

$I$ (amp)	$T_{on}$ ( $\mu\text{s}$ )	$T_{off}$ ( $\mu\text{s}$ )	MRR ( $\text{mm}^3/\text{min}$ )	$R_a$ ( $\mu\text{m}$ )	EWR (%)	AWLT ( $\mu\text{m}$ )
3	12	12	6.1	2.7	1.7	7.9
3	25	6	8.6	2.7	5.6	17.7
3	50	25	15.9	2.7	5.6	6.6

It is seen that MRR is different for each parameter set but the maximum MRR is  $15.9 \text{ mm}^3/\text{min}$ . Owing to the lowest machining time (i.e max MRR), the suitable EDM parameters set is taken where  $I = 3 \text{ amps}$ ,  $T_{on} = 50 \mu\text{s}$  and  $T_{off} = 25 \mu\text{s}$ .

When one stage EDM is applied to attain final surface quality and to machine desired shape by EDM, machining time is calculated as;

$$\text{Machining time} = \frac{\text{Machining volume}}{\text{MRR of finish-cut}} = \frac{108000 \text{ mm}^3}{15.9 \text{ mm}^3/\text{min}} = 6792.45 \text{ min}$$

When two stage (rough and finish) EDM is chosen, the amount of material to be removed in the last stage must be determined. As a strategy, we suggest that the AWLT of the previous machining stage is taken as a criterion. The machining depth of any subsequent stage must be chosen as two times larger than the previous AWLT. Therefore, the AWLT of the first (rough) stage needed to be determined first. To find resulting AWLT of first-stage, parameters set of first-stage must be determined. Firstly, the discharge current is selected according to discharge area (Table 6.5).

**Table 6.5** A contrast of machined area to current

Electrode front area (machined surface area) ( $\text{cm}^2$ )	Recommended current for copper electrode (amp)
0-0.25	1-6
0.25-1	6-10
1-4	10-25
4-16	25-50
>16	50

Here, to obtain minimum machining time MRR must be high, it means that initial discharge current must be high as well. In this example machined surface area is  $36 \text{ cm}^2$  so recommended initial current is 50 amps for first-stage (rough-stage). The parameters set is chosen where MRR is max ( $390 \text{ mm}^3/\text{min}$ ) in  $I = 50 \text{ amps}$  as shown in Table 6.6.

**Table 6.6** Set of process parameters for  $I= 50$  amp

$I$ (amp)	$T_{on}$ ( $\mu s$ )	$T_{off}$ ( $\mu s$ )	MRR ( $mm^3/min$ )	$R_a$ ( $\mu m$ )	EWR (%)	AWLT ( $\mu m$ )
50	50	12	360.6	5.8	21.2	33.4
50	50	25	372.5	5.1	9.7	62.8
50	100	12	371.8	9	25.9	50.7
50	100	25	379.4	7.3	18.3	88.2
50	100	50	228.9	7.1	9.7	41.1
<b>50</b>	<b>200</b>	<b>25</b>	<b>390</b>	<b>10.9</b>	<b>25.9</b>	<b>62.4</b>
50	200	50	232.6	10.1	17.6	104.8
50	200	200	237.5	6.8	0.1	52.7
50	400	100	232.8	10.9	16.7	111.1
50	400	200	209.1	6.3	0.1	49.4
50	1600	200	158.3	14.7	41.9	119.4

Therefore these parameter set ( $I = 50$  amps,  $T_{on}=200 \mu s$  and  $T_{off}=25 \mu s$ ,  $MRR=390 mm^3/min$ ,  $R_a=10.9 \mu m$  and  $AWLT=62.4 \mu m$  (see Table 6.7) is taken as first-stage (rough-stage) parameter set. AWLT is important because it is a limiting factor in our study and the depth of cut is described dependently.

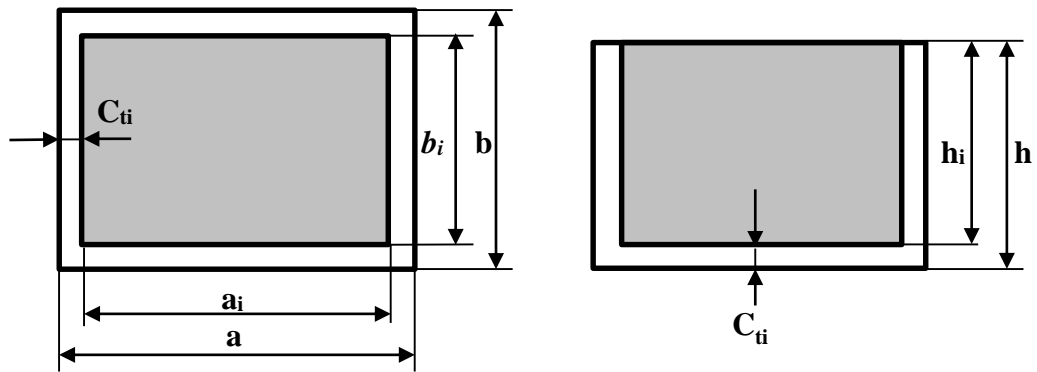


**Figure 6.3** View of two-stage machining

$$h_n = h - \sum_i^n C_{ti} \quad 6.4$$

$$C_{ti} = AWLT_i \times k \quad (i=1,2,3,\dots,n) \quad 6.5$$

$$SA = a \times b \quad 6.6$$

$$V_T = SA \times h \quad 6.7$$

$$SA_i = a_i \times b_i \quad 6.8$$

$$a_n = a - 2 \times \sum_i^n C_{ti} \quad 6.9$$

$$b_n = b - 2 \times \sum_i^n C_{ti}$$

$$V_i = SA_i \times h_i \tag{6.10}$$

$$RV_i = \frac{EWR_i(\%) \times MRR_i \left( \frac{mm^3}{min} \right)}{100} \times \frac{7.8}{8.9} \times t_i \tag{6.11}$$

$$V_{n+1} = V_T - \sum_i^n V_i \tag{6.12}$$

$$V'_{n+1} = V_{n+1} + RV_n \tag{6.13}$$

$$t_1 = \frac{V_1}{MRR_1} \tag{6.14}$$

$$t_{i+1} = \frac{V'_{i+1}}{MRR_{i+1}} \tag{6.15}$$

$$t_T = \sum_i^n t_i \tag{6.16}$$

where (see Figure 6.2);

$n$ : Number of the stage

$C_{ti}$ : The cutting thickness of  $i^{th}$  stage

$k$ : The cutting thickness coefficient

$h_i$ : Cutting depth of  $i^{th}$  stage

$h$ : Total machining depth

$AWLT_i$ : Average white layer thickness of  $i^{th}$  stage

$SA$ : Frontal area of workpiece

$SA_i$ : Frontal area of  $i^{th}$  stage electrode

$a$ : Length of workpiece

$b$ : Width of workpiece

$a_i$ : Length of  $i^{th}$  stage

$b_i$ : Width of  $i^{th}$  stage

$V_i$ : Volume of the  $i^{th}$  stage

$V_{i+1}$ : Volume of  $(i+1)^{th}$  stage

$RV_i$  : Rest (uncut ) volume of  $i^{\text{th}}$  stage

$V'_{i+1}$ : Real machining volume of  $(i+1)^{\text{th}}$  stage

$V_T$ : Total machining volume

$t_i$ : Machining time of  $i^{\text{th}}$  stage

$t_{i+1}$ : Machining time of  $(i+1)^{\text{th}}$  stage

$t_T$ : total machining time

$MRR_i$ : material removal rate of  $i^{\text{th}}$  stage

$MRR_{i+1}$ : material removal rate of  $(i+1)^{\text{th}}$  stage

$EWR_i$  : EWR (%) of the  $i^{\text{th}}$  stage

If the machining depth of any subsequent stage is chosen two times larger than the previous AWLT, then  $k=2$ .

$$C_{t1} = AWLT_1 \times k = 62.4 \mu\text{m} \times \frac{0.001 \text{mm}}{1 \mu\text{m}} \times 2 = 0.1248 \text{ mm}$$

$$h_l = 30 \text{ mm} - 0.1248 = 29.875 \text{ mm}$$

To calculate the volume of first-stage, frontal area of first-stage electrode must be taken into account, because, WLT occurs on each side of electrode; wall and end side so it causes decreasing of frontal area of first-stage electrode (see Figure 6.2)

In this example  $a=b$  (squared area) so;

$$a_1 = b_1 = a - 2 \times C_1 = 60 - 2 \times 0.1248 = 59.75 \text{ mm}$$

$$SA_1 = 59.75 \text{ mm} \times 59.75 \text{ mm} = 3570.11 \text{ mm}^2 \text{ and}$$

$$V_1 = SA_1 \times h_l = 3570.11 \text{ mm}^2 \times 29.875 \text{ mm} = 106657.03 \text{ mm}^3$$

$$t_1 = \frac{V_1}{MRR_1} = \frac{106657.03 \text{ mm}^3}{390 \text{ mm}^3/\text{min}} = 273.479 \text{ min}$$

$$RV_1 = \frac{EWR_1(\%) \times MRR_1 \left(\frac{\text{mm}^3}{\text{min}}\right)}{100} \times \frac{7.8}{8.9} \times t_1 = \frac{25.9 \times 390 \left(\frac{\text{mm}^3}{\text{min}}\right)}{100} \times \frac{7.8}{8.9} \times 273.479 = 24209.897 \text{ mm}^3$$

$$V_2 = V_T - V_1 = 108000 - 106657 = 1343 \text{ mm}^3$$

$$V'_2 = V_2 + RV_1 = 1343 + 24209.897 \text{ mm}^3 = 25552.89 \text{ mm}^3$$

$$t_2 = \frac{V_2}{MRR_2} = \frac{25552.89 \text{ mm}^3}{15.9 \frac{\text{mm}^3}{\text{min}}} = 1607.1 \text{ min}$$

$$t_T = t_1 + t_2 = 273.479 + 1607.1 = 1880.57 \text{ min}$$

The time difference between two-stage and one-stage machining is;

$$6792.45 - 1880.57 = 4911.87 \text{ min}$$

It can be seen that two-stages machining reduces machining time 75% compared to one-stage machining.

For this example, if three stages are applied to machine, a middle stage must be selected from the data table. Selection of middle stage parameters set is done according to  $I$  (discharge current) range.  $I$  range between the rough and finish stage is 50, 44, 37, 31, 25, 18, 12, 9, 6 and 3 amperes for this example. If 44 amp is selected for middle stage, parameter set must be selected at third row to obtain minimum machining time where MRR is maximum (see Table 6.8).

**Table 6.7** Set of process parameters for  $I= 44$  amp

$I$ (amp)	$T_{on}$ ( $\mu$ s)	$T_{off}$ ( $\mu$ s)	MRR ( $\text{mm}^3/\text{min}$ )	$R_a$ ( $\mu$ m)	EWR (%)	AWLT ( $\mu$ m)
44	12	3	325.7	3.8	17.0	16.8
44	50	6	363.6	5.7	14.6	25.3
<b>44</b>	<b>100</b>	<b>12</b>	<b>375.2</b>	<b>8.7</b>	<b>13.3</b>	<b>19.7</b>
44	100	25	343.6	8.1	11.4	47.6
44	100	50	223.7	6.9	7.8	10.2
44	200	25	352.0	10.9	18.5	39.0
44	200	50	231.8	10.7	14.6	99.0
44	200	200	231.8	6.6	0.2	47.8
44	400	200	204.1	15.8	0.2	46.3
44	800	200	14.1	15.9	17.3	50.9
44	1600	200	136.8	15.3	35.3	105.4

Parameters sets of each stage for this example when 3-stages machining is applied are seen in Table 6.8

**Table 6.8** Process parameter set and machining time for each stages

Stages	$I$ (amp)	$T_{on}$ ( $\mu$ s)	$T_{off}$ ( $\mu$ s)	MRR ( $\text{mm}^3/\text{min}$ )	$R_a$ ( $\mu$ m)	EWR (%)	AWLT ( $\mu$ m)
First	50	200	25	390	10.9	25.9	62.4
Second	44	100	12	375.2	8.7	13.3	19.7
Third	3	50	25	15.9	2.7	5.6	6.6

The calculation of 3-stage machining are done according to Figure 6.4.

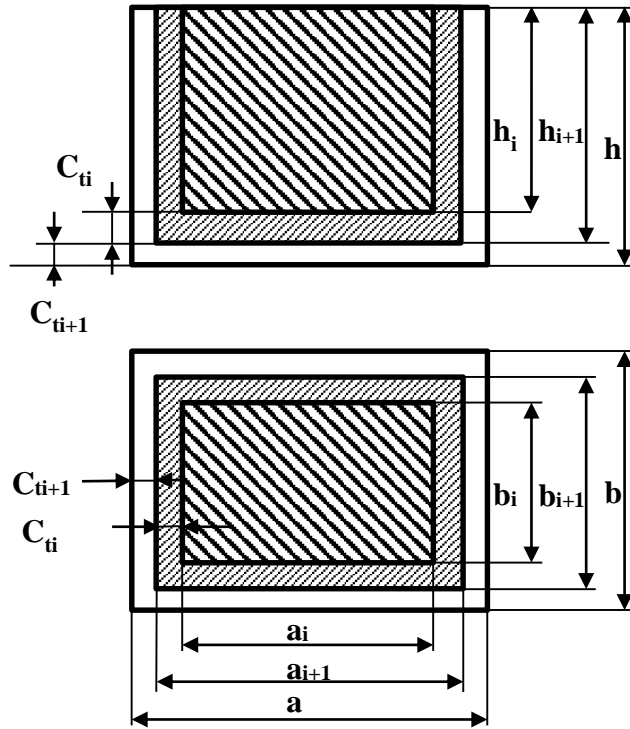


**Figure 6.4** View of three-stage machining for prismatic parts

$$C_{t1} = AWLT_1 \times k = 62.4 \mu m \times \frac{0.001 mm}{1 \mu m} \times 2 = 0.1248 \text{ mm}$$

$$C_{t2} = AWLT_2 \times k = 19.7 \mu m \times \frac{0.001 mm}{1 \mu m} \times 2 = 0.0394 \text{ mm}$$

$$a_1 = a - 2 \times (C_{t1} + C_{t2}) = 60 - 2 \times (0.1248 + 0.0394) = 59.6716 \text{ mm}$$

$$b_1 = b - 2 \times (C_{t1} + C_{t2}) = 60 - 2 \times (0.1248 + 0.0394) = 59.6716 \text{ mm}$$

$$a_2 = a - 2 \times C_{t2} = 60 - 2 \times (0.0394) = 59.9212 \text{ mm}$$

$$b_2 = b - 2 \times C_{t2} = 60 - 2 \times (0.0394) = 59.9212 \text{ mm}$$

$$h_1 = h - (C_{t1} + C_{t2}) = 30 - (0.1248 + 0.0394) = 29.8358 \text{ mm}$$

$$h_2 = h - C_{t2} = 30 - 0.0394 = 29.9606 \text{ mm}$$

$$SA_1 = a_1 \times b_1 = 59.67 \times 59.67 = 3560.699847 \text{ mm}^2$$

$$SA_2 = a_2 \times b_2 = 59.9212 \times 59.9212 = 3590.550209 \text{ mm}^2$$

$$V_I = SA_1 \times h_1 = 3560.699847 \times 29.8358 = 106236.3285$$

$$V_2 = (SA_2 \times h_2) - V_1 = (3590.550209 \times 29.9606) - 106236.3285 = 1338.710123 \text{ mm}^3$$

$$V_T = a \times b \times h = 60 \times 60 \times 30 = 108000 \text{ mm}^3$$

$$t_1 = \frac{V_1}{MRR_1} = \frac{106236.3285}{390} = 272.4 \text{ min}$$

$$RV_1 = \frac{EWR_1 \times MRR_1 \left(\frac{\text{mm}^3}{\text{min}}\right)}{100} \times \frac{7.8}{8.9} \times t_1 = \frac{25.9 \times 390 \left(\frac{\text{mm}^3}{\text{min}}\right)}{100} \times \frac{7.8}{8.9} \times 272.4 = 24114.44916 \text{ mm}^3$$

$$V'_2 = V_2 + RV_1 = 1338.710123 + 24114.44916 = 25453.15928 \text{ mm}^3$$

$$t_2 = \frac{V'_2}{MRR_2} = \frac{25453.15928}{375.2} = 67.84 \text{ min}$$

$$RV_2 = \frac{EWR_2 \times MRR_2 \left(\frac{\text{mm}^3}{\text{min}}\right)}{100} \times \frac{7.8}{8.9} \times t_2 = \frac{13.3 \times 375.2 \left(\frac{\text{mm}^3}{\text{min}}\right)}{100} \times \frac{7.8}{8.9} \times 67.84 = 2966.865538 \text{ mm}^3$$

$$V_3 = V_T - (V_1 + V_2) = 108000 - (106236.3285 + 1338.710123) = 424.9613951 \text{ mm}^3$$

$$V'_3 = V_3 + RV_2 = 424.9614 + 2966.8655 = 3391.826933 \text{ mm}^3$$

$$t_3 = \frac{V'_3}{MRR_3} = \frac{3391.826933}{15.9} = 213.32 \text{ min}$$

$$t_T = t_1 + t_2 + t_3 = 272.4 + 67.84 + 213.32 = 553.56 \text{ min}$$

The time difference between 3-stages and 1-stage machining is;

$$6792.45 - 553.56 = 6238.89 \text{ min}$$

The time difference between 3-stages and 2-stage machining is

$$1880.57 - 553.56 = 1327.01 \text{ min}$$

It can be seen clearly that 3-stages machining reduces machining time remarkably. These calculations can be done for 4-stages machining and 5-stages machining also by using the same way but *I* range between the rough and finish stage is 50, 44, 37, 31, 25, 18, 12, 9, 6 and 3 amperes for this example. So, many various groups can be generated for two, three, four and five stages machining. Such as; groups of two-stage machining can be generated as: (50, 3), (44, 3), (37, 3), (31, 3), (25, 3), (18, 3), (12, 3), (9, 3), (6, 3) totally 9 groups. Some groups of three-stages are (50, 44, 3), (50, 37, 3), (50, 31, 3), and etc. Some groups of four-stages are (50, 44, 37, 3), (50, 44, 31, 3), (50, 44, 25, 3) and etc. Some groups of five-stages are (50, 44, 37, 31, 3), (50, 44, 31, 25, 3), (50, 44, 25, 18, 3) and etc. It is seen that, it consumes a lot of time to generate

all groups. The combination may be used for the purpose and the formula in mathematics is given as

$$\binom{n}{r} = \frac{n!}{r!(n-r)!} \quad 6.17$$

where  $n$  is the number of things to choose from, and you choose  $r$  of them (No repetition, order doesn't matter). In this study,  $n$  refers to  $I$  range, it means 10 and  $r$  is the number of stage but finishing stages  $I$  is repeated so for this study combination formulation changes as below:

$$\binom{n-1}{r-1} = \frac{(n-1)!}{(r-1)![(n-1)-(r-1)]!} \quad 6.18$$

According to this formula number of two stages is

$$\binom{10-1}{2-1} = \frac{(10-1)!}{(2-1)![(10-1)-(2-1)]!} = \frac{9!}{8!} = 9$$

Number of three-stages is calculated as:

$$\binom{10-1}{3-1} = \frac{(10-1)!}{(3-1)![(10-1)-(3-1)]!} = \frac{9!}{2! \times 7!} = 36$$

Number of four-stages is calculated as:

$$\binom{10-1}{4-1} = \frac{(10-1)!}{(4-1)![(10-1)-(4-1)]!} = \frac{9!}{3! \times 6!} = 84$$

And number of five-stages is calculated as:

$$\binom{10-1}{5-1} = \frac{(10-1)!}{(5-1)![(10-1)-(5-1)]!} = \frac{9!}{4! \times 5!} = 126$$

To generate all of these combinations and to select parameters from these alternatives takes a lot of time for manual calculation. For this reason, a multi-stage EDM selection program was developed to do these works by using MATLAB package program. This multi-stage program is supposed to select the process parameter set from the data table which is produced from the artificial intelligent models given in Chapter 5. Phases of the developed multi stage machining program and its algorithm is given in the following sections.



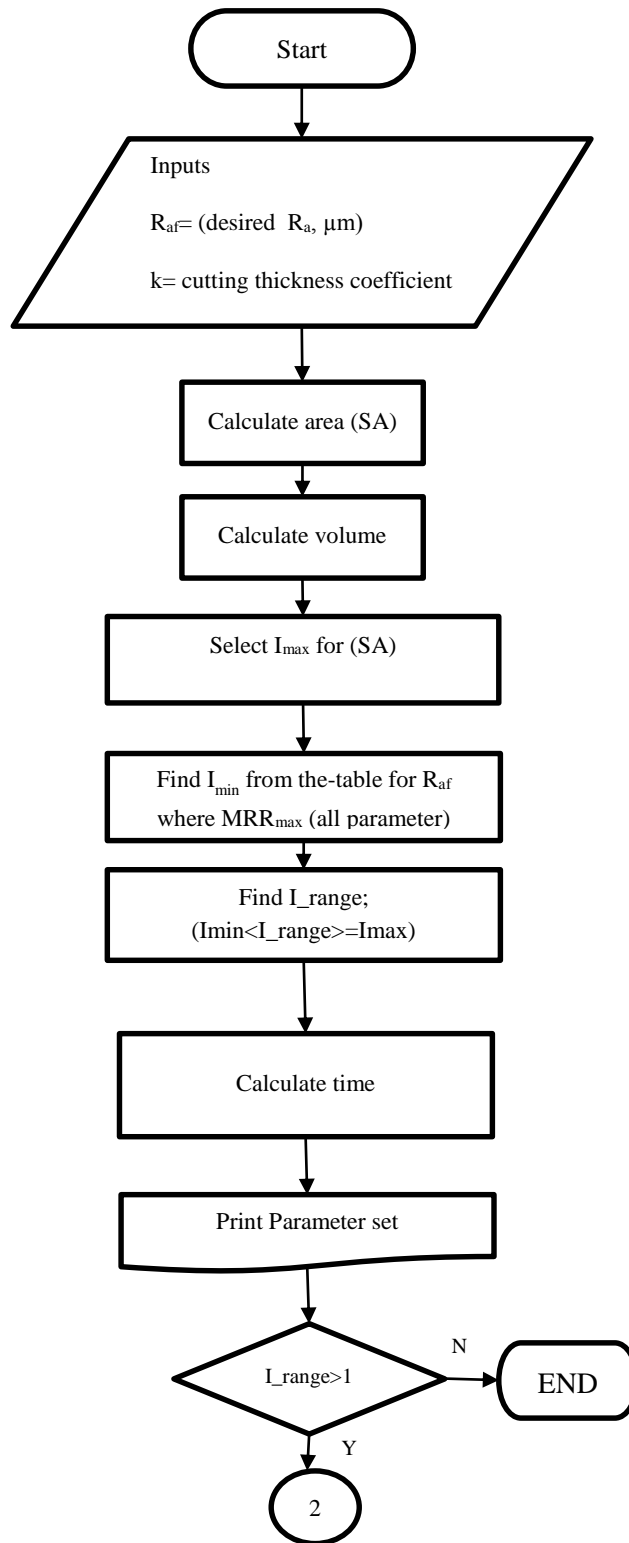
### 6.3 Procedure of Multi-Stage Machining Strategy

The developed multi-stage strategy is a backward-chain strategy. Stages of the strategy are summarised as following;

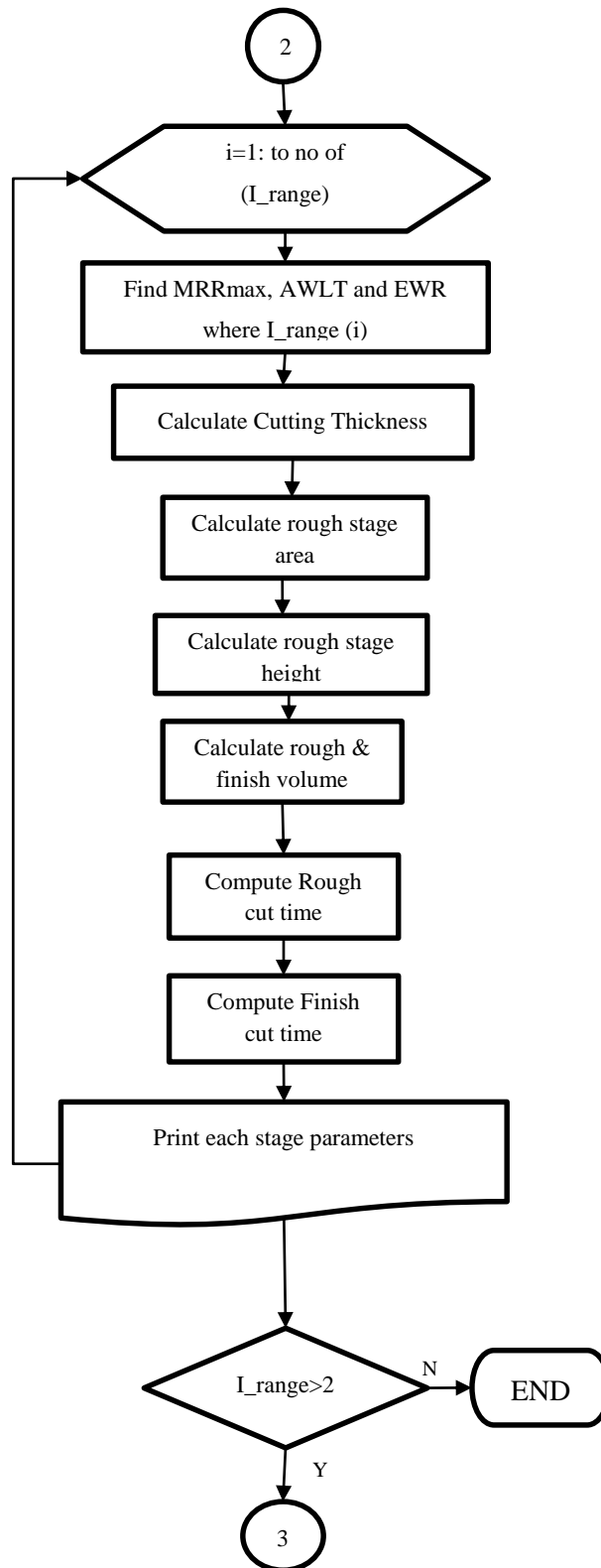
- According to the final (desired) surface roughness requirement ( $R_{af}$ ), the machining parameters of the last (finishing) stage are determined first.
- Then, the discharge current of the rough (initial) stage is determined according to the discharge area, because the discharge area limits the maximum value of the discharge current.
- After that, from the data table, the parameters set of rough stage is selected according to the discharge current which has maximum MRR value.
- The combinations of machining stages are determined as the current range between the discharge current of initial and finish stage.
- Machining parameters set are selected to discharge current values which give maximum MRR to provide minimum machining time at each stage.
- The cutting thickness (machining depth) of each stages is calculated to  $k \times \text{AWLT}$  of the previous stage.
- EWR of the previous stage is found from the data table and the rest (uncut) material volume is calculated.
- And the real machining volume and machining times of each stage are calculated from the real volume per MRR values of each stage.
- Multi-stage program calculates all combinations and sequence them according to minimum machining time.
- Consequently, the program gives the number of stages (electrodes) required to complete the operation, their sequence from rough to finish and the machining parameters set for each stage according to minimum machining time under the constraints of surface quality and white layer thickness.

## 6.4 Multi-Stage Algorithm

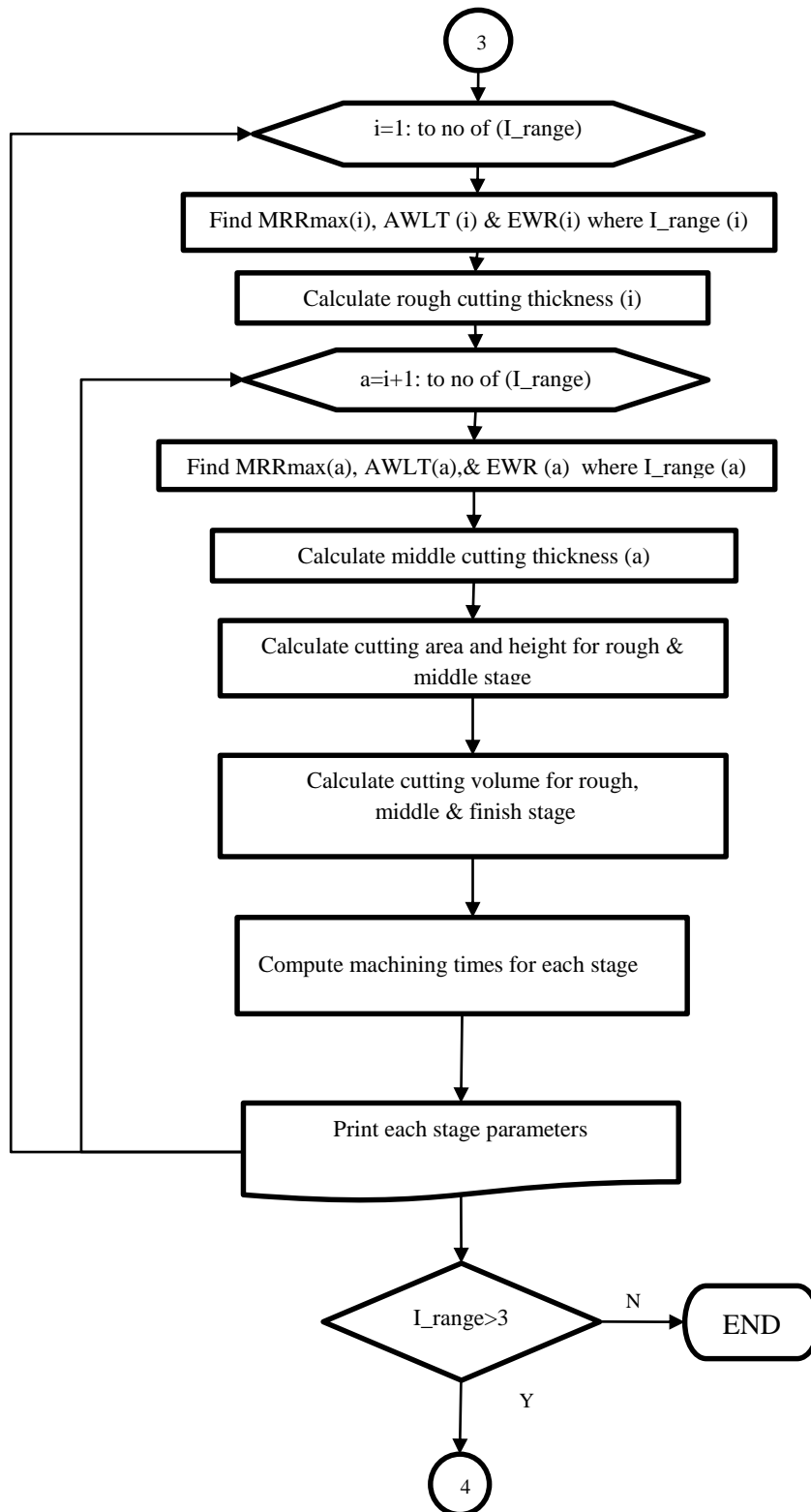
The developed program algorithm is charted below;



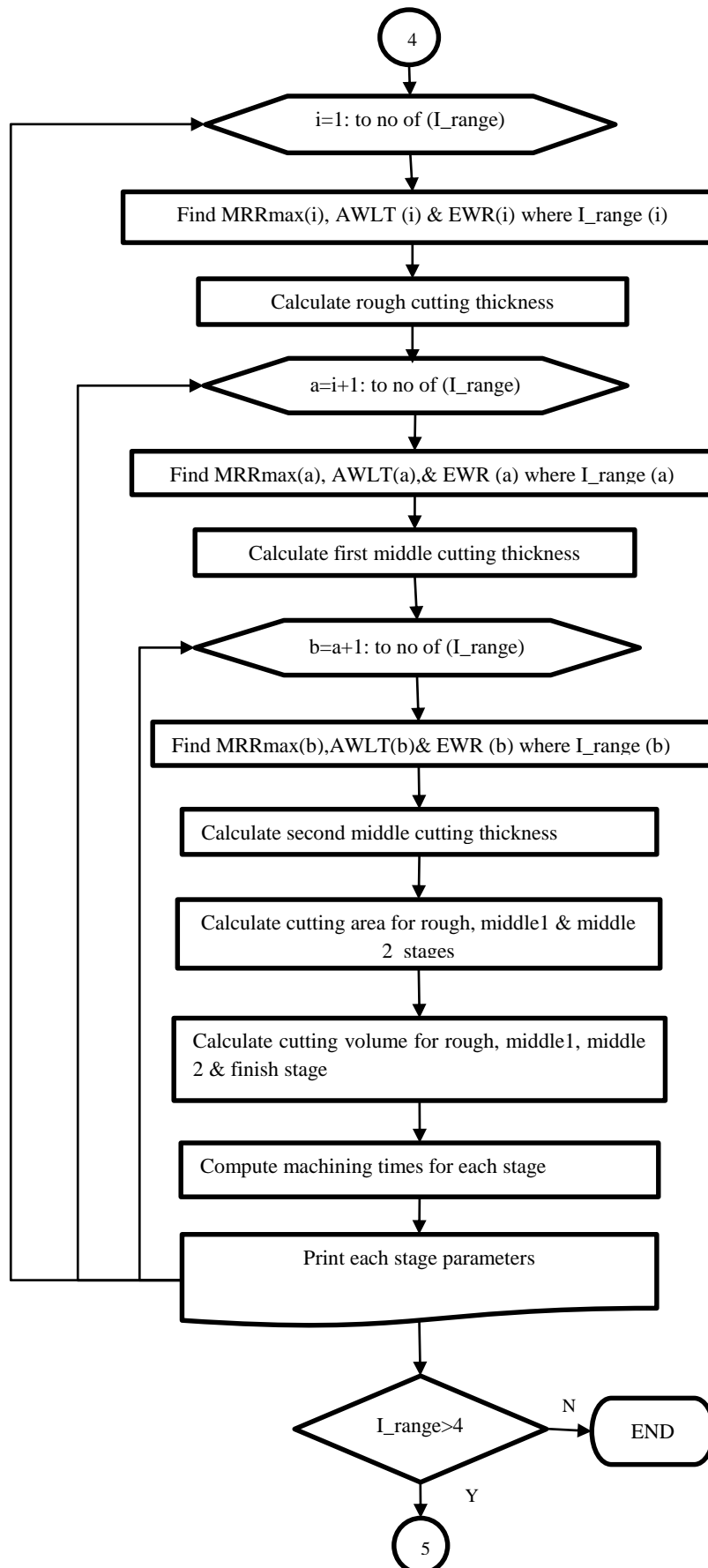
The 2<sup>nd</sup> stage



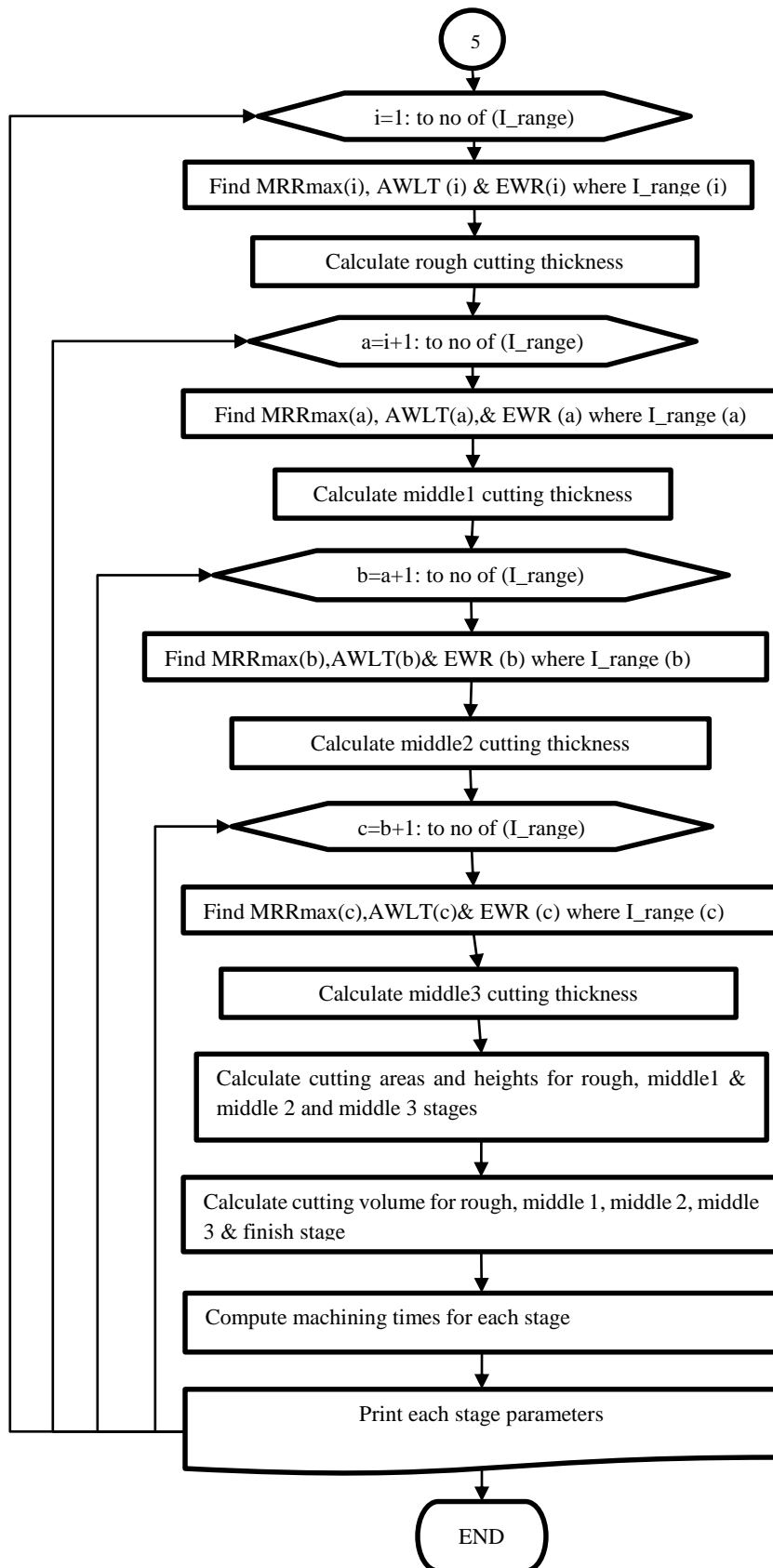
The 3<sup>rd</sup> stage



The 4<sup>th</sup> stage

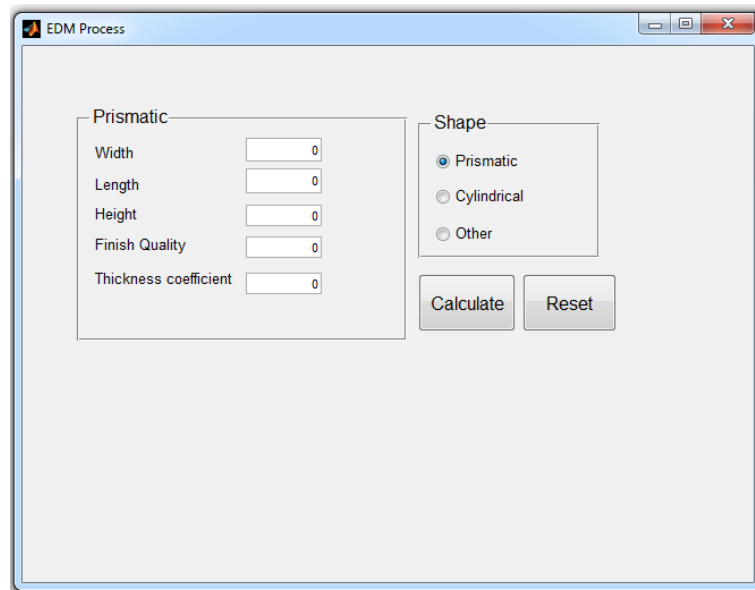


The 5<sup>th</sup> stage



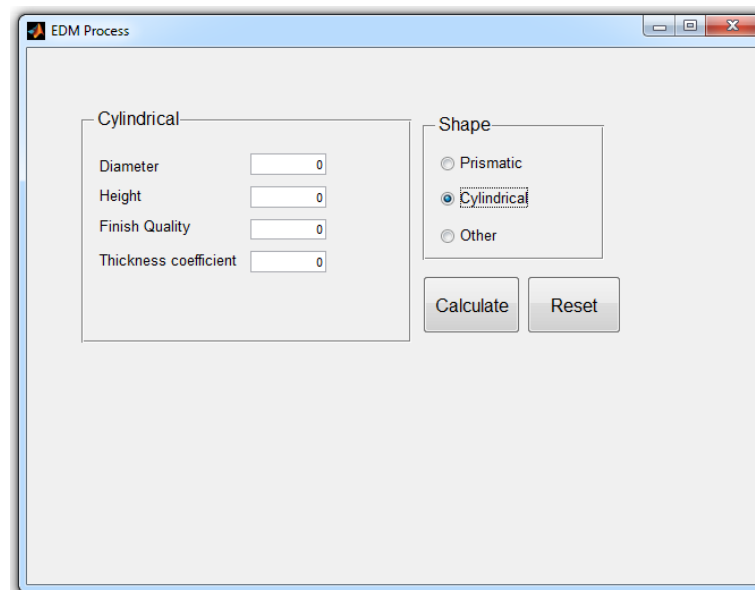
## 6.5 Program Description

According to the algorithm given in the previous section, the surface area, volume and depth of machining stock, the desired surface roughness and cutting thickness coefficient ( $k$ ) are defined using the input menu of the program. The input menu is arranged for *rectangular*, *circular* and *other* choices to define these parameters easily. In rectangular data input menu, width, length and height of machining stock (in mm) and desired average final surface quality ( $R_{af}$ , in  $\mu\text{m}$ ) and cutting thickness coefficient  $k$  (it shows percentage of AWLT) are given as inputs (Figure 6.5).



The screenshot shows the 'EDM Process' window with the 'Prismatic' shape selected. The 'Prismatic' section contains five input fields: Width, Length, Height, Finish Quality, and Thickness coefficient, all with a value of 0. The 'Shape' section has three radio buttons: 'Prismatic' (selected), 'Cylindrical', and 'Other'. Below the 'Shape' section are 'Calculate' and 'Reset' buttons.

**Figure 6.5** Main menu of program for rectangular shapes



The screenshot shows the 'EDM Process' window with the 'Cylindrical' shape selected. The 'Cylindrical' section contains four input fields: Diameter, Height, Finish Quality, and Thickness coefficient, all with a value of 0. The 'Shape' section has three radio buttons: 'Prismatic', 'Cylindrical' (selected), and 'Other'. Below the 'Shape' section are 'Calculate' and 'Reset' buttons.

**Figure 6.6** Main menu of program for circular shapes

In circular data input menu, the input data are diameter and height of machining stock and  $k$  and  $R_{af}$  (Figure 6.6).

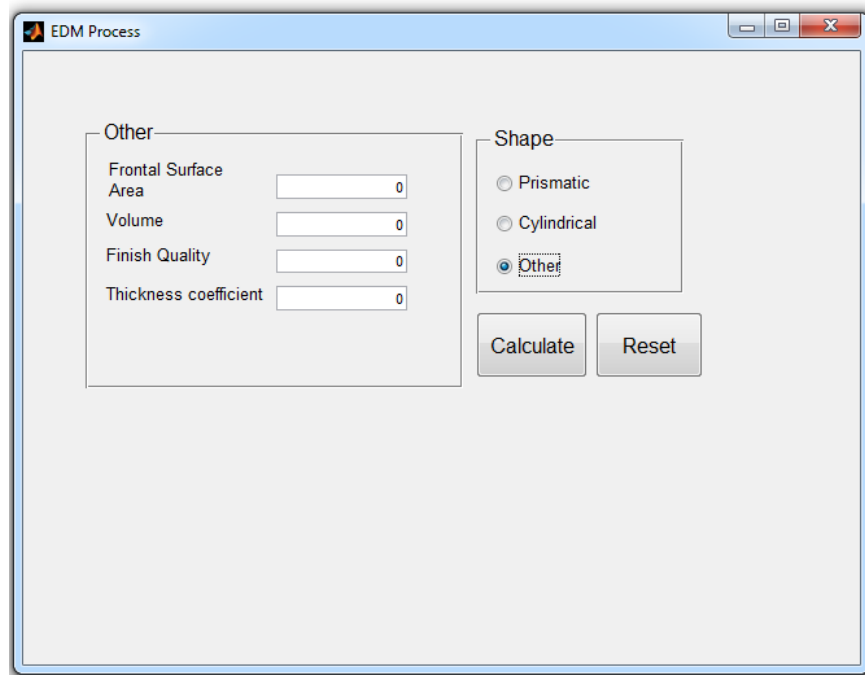


**Figure 6.7** Main menu of program for complex shapes

In other input menu, inputs are frontal surface area of machining stock as  $\text{mm}^2$  and volume of workpiece as  $\text{mm}^3$  and also  $k$  and  $R_{af}$  (Figure 6.7). In the following section, four case studies are given to show how the program works.

## 6.6 Case Studies

### 6.6.1 Case Study 1

The illustrative example given in the section 6.2.1 was carried out using the program. The specifications were taken from Table 6.2. The machining stock size was  $60 \times 60 \times 30$  mm, cutting thickness coefficient ( $k$ ) was 2 and desired surface quality ( $R_{af}$ ) was  $2.7 \mu\text{m}$ . After running the program by clicking on calculate button the outputs were calculated as shown in Figures 6.9 to 6.13. The corresponding EDM parameter sets ( $I$ ,  $T_{on}$ ,  $T_{off}$ , MRR,  $R_a$ , EWR, AWLT) and machining time of alternatives are displayed for one to five stages. For one stage machining there is only one setting which gives maximum MRR (Figure 6.9). In two, three, four and five stages, 9, 36, 83 and 120 alternatives are available, respectively.



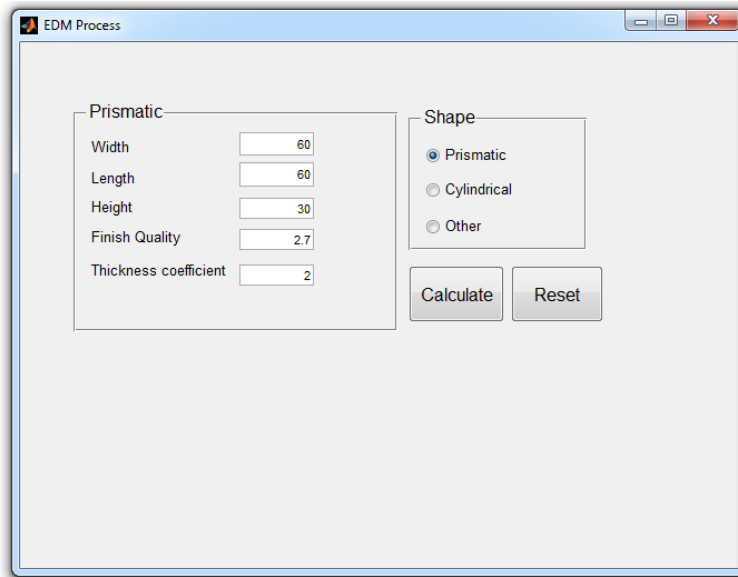


**Figure 6.8** Entering input data into the program for rectangular part

	I	Ton	Toff	MRR	Ra	EWR	AWLT	Time
1	3	50	25	15.9000	2.7000	5.6000	6.6000	6.7925e+03

**Figure 6.9** Output display from program for one-stage

	I	Ton	Toff	MRR	Ra	EWR	AWLT	Time
1	50	200	25	390	10.9000	25.9000	62.4000	273.4814
2	3	50	25	15.9000	2.7000	5.6000	6.6000	1.6071e+03
3	44	100	12	375.2000	8.7000	13.3000	19.7000	286.7139
4	3	50	25	15.9000	2.7000	5.6000	6.6000	815.3523
5	37	50	12	300.1000	5.2000	7.5000	20.7000	358.3922
6	3	50	25	15.9000	2.7000	5.6000	6.6000	472.7063
7	31	50	50	244.2000	6.1000	5.3000	10.7000	441.3147
8	3	50	25	15.9000	2.7000	5.6000	6.6000	329.3564
9	25	100	200	241.5000	5.7000	1.3000	25.1000	444.9638

**Figure 6.10** Output display from program for two-stage

	I	Ton	Toff	MRR	Ra	EWR	AWLT	Time
1	50	200	25	390	10.9000	25.9000	62.4000	272.40
2	44	100	12	375.2000	8.7000	13.3000	19.7000	67.83
3	3	50	25	15.9000	2.7000	5.6000	6.6000	213.32
4	50	200	25	390	10.9000	25.9000	62.4000	272.34
5	37	50	12	300.1000	5.2000	7.5000	20.7000	84.79
6	3	50	25	15.9000	2.7000	5.6000	6.6000	133.28
7	50	200	25	390	10.9000	25.9000	62.4000	272.89
8	31	50	50	244.2000	6.1000	5.3000	10.7000	104.41
9	3	50	25	15.9000	2.7000	5.6000	6.6000	89.01

Figure 6.11 Output display from program for third-stage

	I	Ton	Toff	MRR	Ra	EWR	AWLT	Time
1	50	200	25	390	10.9000	25.9000	62.4000	271.26
2	44	100	12	375.2000	8.7000	13.3000	19.7000	67.56
3	37	50	12	300.1000	5.2000	7.5000	20.7000	11.25
4	3	50	25	15.9000	2.7000	5.6000	6.6000	42.04
5	50	200	25	390	10.9000	25.9000	62.4000	271.81
6	44	100	12	375.2000	8.7000	13.3000	19.7000	67.69
7	31	50	50	244.2000	6.1000	5.3000	10.7000	13.86
8	3	50	25	15.9000	2.7000	5.6000	6.6000	24.41
9	50	200	25	390	10.9000	25.9000	62.4000	271.02

Figure 6.12 Output display from program for four-stage

	I	Ton	Toff	MRR	Ra	EWR	AWLT	Time
1	50	200	25	390	10.9000	25.9000	62.4000	269.91
2	44	100	12	375.2000	8.7000	13.3000	19.7000	67.23
3	37	50	12	300.1000	5.2000	7.5000	20.7000	11.20
4	31	50	200	243.4000	3.2000	0.5000	24.8000	2.73
5	3	50	25	15.9000	2.7000	5.6000	6.6000	33.81
6	50	200	25	390	10.9000	25.9000	62.4000	270.04
7	44	100	12	375.2000	8.7000	13.3000	19.7000	67.26
8	37	50	12	300.1000	5.2000	7.5000	20.7000	11.21
9	25	50	200	236	4.3000	0.1000	22.4000	2.82

Figure 6.13 Output display from program for five-stage

	Stage-5	Stage-4	Stage-3	Stage-2	Stage-1
1	349	360	382	556	6.7925e+03
2	358	361	388	584	0
3	359	363	390	594	0
4	361	363	391	771	0
5	362	366	410	831	0
6	362	366	414	882	0
7	363	366	419	1102	0
8	363	367	423	1108	0
9	364	367	427	1881	0
10	366	368	430	0	0

**Figure 6.14** Display of minimum machining time tables for all trials

Figure 6.14 shows total machining times for all alternatives, wherein, times are sequenced from minimum to maximum. The parameter sets of sub-stages can be displayed by click on any of the time value as shown in Figure 6.15.

	Stage-5	Stage-4	Stage-3	Stage-2	Stage-1
1	349	360	382	556	6.7925e+03
2	358	361	388	584	0
3	359	363	390	594	0
4	361	363	391	771	0
5	362	366	410	831	0
6	362	366	414	882	0

	I	Ton	Toff	MRR	Ra	EWR	AWLT	Time
1	44	100	12	375.2000	8.7000	13.3000	19.7000	284.4632
2	37	50	12	300.1000	5.2000	7.5000	20.7000	42.8639
3	12	100	100	195.9000	3.4000	1.6000	18.6000	6.5897
4	3	50	25	15.9000	2.7000	5.6000	6.6000	26.3751

**Figure 6.15** Display of optimum machining time for each stage

Nearly 255 alternatives were generated by the computer program for these examples. Tables B.1 to B.4 in Appendix B show the all alternatives for 2, 3, 4 and 5 stages, last column of these tables show the total machining time of each group. Some of these alternatives are summarised in Tables 6.9 to 6.12.

**Table 6.9** Some trials of two-stages machining

<i>No</i>	<i>I</i> (amp)	<i>T<sub>on</sub></i> ( $\mu$ s)	<i>T<sub>off</sub></i> ( $\mu$ s)	MRR (mm <sup>3</sup> /min)	<i>R<sub>a</sub></i> ( $\mu$ m)	EWR (%)	AWLT ( $\mu$ m)	Time (min)	Mach-time (min)
1	50	200	25	390	10.9	25.9	62.4	273.5	1880.6
	3	50	25	15.9	2.7	5.6	6.6	1607.1	
2	44	100	12	375.2	8.7	13.3	19.7	286.7	1102.1
	3	50	25	15.9	2.7	5.6	6.6	815.4	
3	37	50	12	300.1	5.2	7.5	20.7	358.4	831.1
	3	50	25	15.9	2.7	5.6	6.6	472.7	
4	31	50	50	244.2	6.1	5.3	10.7	441.3	770.7
	3	50	25	15.9	2.7	5.6	6.6	329.4	
5	25	100	200	241.5	5.7	1.3	25.1	445.0	556.0
	3	50	25	15.9	2.7	5.6	6.6	111.0	
6	18	100	200	234.2	7.9	1.5	27.1	458.6	584.2
	3	50	25	15.9	2.7	5.6	6.6	125.6	

**Table 6.10** Some trials of three-stages machining

<i>No</i>	<i>I</i> (amp)	<i>T<sub>on</sub></i> ( $\mu$ s)	<i>T<sub>off</sub></i> ( $\mu$ s)	MRR (mm <sup>3</sup> /min)	<i>R<sub>a</sub></i> ( $\mu$ m)	EWR (%)	AWLT ( $\mu$ m)	Time (min)	Mach-time (min)
4	50	200	25	390	10.9	25.9	62.4	272.11	429.6
	25	100	200	241.5	5.7	1.3	25.1	105.28	
	3	50	25	15.9	2.7	5.6	6.6	52.26	
11	44	100	12	375.2	8.7	13.3	19.7	285.28	382.0
	25	100	200	241.5	5.7	1.3	25.1	53.42	
	3	50	25	15.9	2.7	5.6	6.6	43.28	
22	31	50	50	244.2	6.1	5.3	10.7	439.10	498.5
	25	100	200	241.5	5.7	1.3	25.1	21.58	
	3	50	25	15.9	2.7	5.6	6.6	37.78	

**Table 6.11** Some trials of four-stages machining

<i>No</i>	<i>I</i> (amp)	<i>T<sub>on</sub></i> ( $\mu$ s)	<i>T<sub>off</sub></i> ( $\mu$ s)	MRR (mm <sup>3</sup> /min)	<i>R<sub>a</sub></i> ( $\mu$ m)	EWR (%)	AWLT ( $\mu$ m)	Time (min)	Mach-time (min)
1	50	200	25	390	10.9	25.9	62.4	271.3	392.1
	44	100	12	375.2	8.7	13.3	19.7	67.6	
	37	50	12	300.1	5.2	7.5	20.7	11.3	
	3	50	25	15.9	2.7	5.6	6.6	42.0	
32	44	100	12	375.2	8.7	13.3	19.7	284.5	360.3
	37	50	12	300.1	5.2	7.5	20.7	42.9	
	12	100	100	195.9	3.4	1.6	18.6	6.6	
	3	50	25	15.9	2.7	5.6	6.6	26.4	
76	25	100	200	241.5	5.7	1.3	25.1	441.8	482.3
	18	50	50	175.4	3.5	5.2	16.5	10.0	
	6	12	50	107.7	2.9	1.4	19.3	4.0	
	3	50	25	15.9	2.7	5.6	6.6	26.5	

**Table 6.12** Some trials of five-stages machining

<i>No</i>	<i>I</i> (amp)	<i>T<sub>on</sub></i> ( $\mu$ s)	<i>T<sub>off</sub></i> ( $\mu$ s)	<b>MRR</b> (mm <sup>3</sup> /min)	<i>R<sub>a</sub></i> ( $\mu$ m)	<b>EWR</b> (%)	<b>AWLT</b> ( $\mu$ m)	<b>Time</b> (min)	<b>Mach-time</b> (min)
1	50	200	25	390	10.9	25.9	62.4	269.9	384.9
	44	100	12	375.2	8.7	13.3	19.7	67.2	
	37	50	12	300.1	5.2	7.5	20.7	11.2	
	31	50	200	243.4	3.2	0.5	24.8	2.7	
	3	50	25	15.9	2.7	5.6	6.6	33.8	
56	44	100	12	375.2	8.7	13.3	19.7	283.6	349.5
	37	50	12	300.1	5.2	7.5	20.7	42.7	
	31	50	200	243.4	3.2	0.5	24.8	5.3	
	25	12	50	209.2	3.1	8.6	9.4	2.6	
	3	50	25	15.9	2.7	5.6	6.6	15.3	
109	31	50	50	244.2	6.1	5.3	10.7	435.3	497.8
	25	100	200	241.5	5.7	1.3	25.1	21.4	
	12	100	100	195.9	3.4	1.6	18.6	3.0	
	9	100	50	105.3	3	5.7	24.2	3.9	
	3	50	25	15.9	2.7	5.6	6.6	34.1	

It can be seen from these tables, the corresponding minimum machining times are 6792.5, 556, 382, 360 and 349 minutes for 1, 2, 3, 4 and 5 stage machining respectively. The parameter set of these stages are shown in Table 6.13.

**Table 6.13** Parameter sets for optimum sub-stages for Case Study-1

<b>No of trial</b>	<b>No of stages</b>	<i>I</i> (amp)	<i>T<sub>on</sub></i> ( $\mu$ s)	<i>T<sub>off</sub></i> ( $\mu$ s)	<b>MRR</b> (mm <sup>3</sup> /min)	<i>R<sub>a</sub></i> ( $\mu$ m)	<b>EWR</b> (%)	<b>AWLT</b> ( $\mu$ m)	<b>Time</b> (min)	<b>Total Mach-time</b> (min)
56	5	44	100	12	375.2	8.7	13.3	19.7	283.6	349.5
		37	50	12	300.1	5.2	7.5	20.7	42.7	
		31	50	200	243.4	3.2	0.5	24.8	5.3	
		25	12	50	209.2	3.1	8.6	9.4	2.6	
		3	50	25	15.9	2.7	5.6	6.6	15.3	
32	4	44	100	12	375.2	8.7	13.3	19.7	284.5	360.3
		37	50	12	300.1	5.2	7.5	20.7	42.9	
		12	100	100	195.9	3.4	1.6	18.6	6.6	
		3	50	25	15.9	2.7	5.6	6.6	26.4	
11	3	44	100	12	375.2	8.7	13.3	19.7	285.3	382.0
		25	100	200	241.5	5.7	1.3	25.1	53.4	
		3	50	25	15.9	2.7	5.6	6.6	43.3	
5	2	25	100	200	241.5	5.7	1.3	25.1	445.0	556.0
		3	50	25	15.9	2.7	5.6	6.6	111.0	
1	1	3	50	25	15.9	2.7	5.6	6.6	6792.5	6792.5

Comparing to the results of manual calculation (see Table 6.14) which was given in Section 6.2.1, the computer program generates better alternatives in terms of less machining time.

**Table 6.14** Manual calculation results for Case Study-1

<i>No of trial</i>	<i>I (amp)</i>	<i>T<sub>on</sub> (μs)</i>	<i>T<sub>off</sub> (μs)</i>	<b>MRR (mm<sup>3</sup>/min)</b>	<i>R<sub>a</sub> (μm)</i>	<b>EWR (%)</b>	<b>AWLT (μm)</b>	<b>Time (min)</b>	<b>Mach-time (min)</b>
1	50	200	25	390	10.9	25.9	62.4	272.40	
	44	100	12	375.2	8.7	13.3	19.7	67.84	
	3	50	25	15.9	2.7	5.6	6.6	213.32	553.6

In Figure 6.16, the machining times are plotted versus the number of machining stages. The curve is sharply decreasing from 2 to 3 stages and then decreasing smoothly with increasing number of machining stages. Although the minimum machining time is 349.5 minutes (5-stage), the difference between the 5-stage and 4-stage machining is only 10.8 minutes (see Table 6.13). In the cost analysis of EDM machining, set-up time and cost of electrodes must be taken into account. Generally, each machining-stage needs a new electrode and set-up time. If the set-up time is taken as 10 minutes for each stage, the total time changes as seen in Table 6.15. According to this table the difference between the 5 and 4-stages is 0.8 minutes.

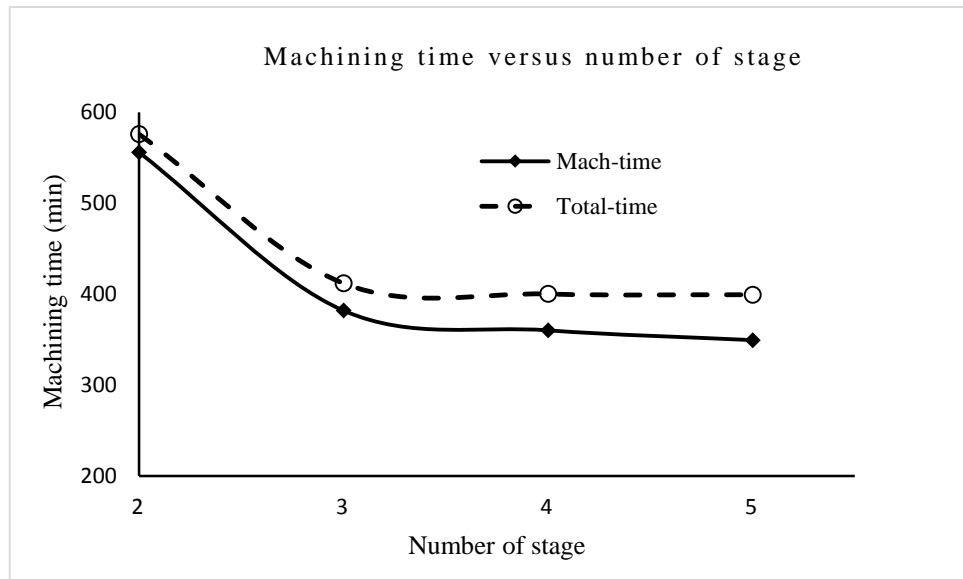


**Figure 6.16** Effect of number of stages on machining time

It is also seen from this example, for 5-stage machining, 5 electrodes must be prepared, and the machining times of 3<sup>rd</sup> and 4<sup>th</sup> stage are 5.3 and 2.6 minutes, respectively. And for 4-stage machining, the time of 3<sup>rd</sup> stage is 6.6 minutes. The final decision must be reached by taking the cost of the electrode and set-up time into account. For this example 3-stage machining may be considered as the final choice.

**Table 6.15** Effects of machining set-up time

Stage No	Mach-time	Set-up time	Total-time
2	556.0	20	576.0
3	382.0	30	412.0
4	360.3	40	400.3
5	349.5	50	399.5

Increasing cutting thickness coefficient ( $k$ ) increases total machining time proportionally (see Figure 6.17 and Table 6.16). Keeping in mind that the total machining volume is constant, higher ( $k$ ) means more material stock removal in final (finishing) stage, i.e. longer time, but less material stock for the previous (rough) stage.

**Table 6.16** Cutting thickness coefficient and machining time

Cutting coefficient	$I$ (amp)	$T_{on}$ ( $\mu$ s)	$T_{off}$ ( $\mu$ s)	MRR ( $\text{mm}^3/\text{min}$ )	$R_a$ ( $\mu$ m)	EWR (%)	AWLT ( $\mu$ m)	Time (min)	Total Mach-time (min)
k=2	44	100	12	375.2	8.7	13.3	19.7	284.5	360.3
	37	50	12	300.1	5.2	7.5	20.7	42.9	
	12	100	100	195.9	3.4	1.6	18.6	6.6	
	3	50	25	15.9	2.7	5.6	6.6	26.4	
k=2.5	44	100	12	375.2	8.7	13.3	19.7	283.6	366.7
	37	50	12	300.1	5.2	7.5	20.7	43.1	
	12	100	100	195.9	3.4	1.6	18.6	7.2	
	3	50	25	15.9	2.7	5.6	6.6	32.8	
k=3	44	100	12	375.2	8.7	13.3	19.7	283.0	372.9
	37	50	12	300.1	5.2	7.5	20.7	43.3	
	18	50	50	175.4	3.5	5.2	16.5	8.7	
	3	50	25	15.9	2.7	5.6	6.6	37.9	
k=3.5	44	100	12	375.2	8.7	13.3	19.7	282.2	378.9
	37	50	12	300.1	5.2	7.5	20.7	43.6	
	18	50	50	175.4	3.5	5.2	16.5	9.3	
	3	50	25	15.9	2.7	5.6	6.6	43.8	

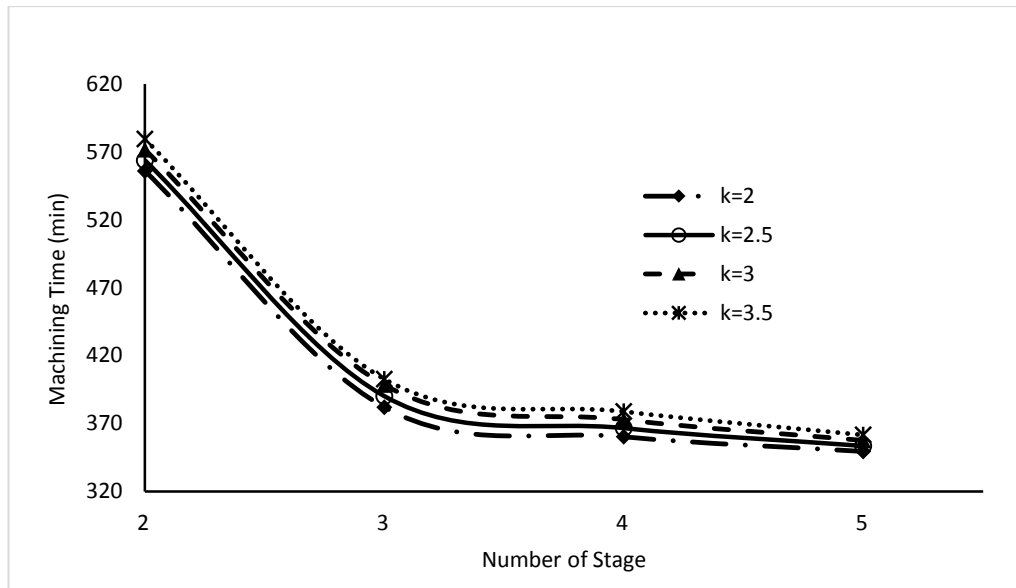


**Figure 6.17** Effect of cutting thickness coefficient ( $k$ ) on machining time

The final surface quality is also effective in determination of number of machining stages. The required machining time versus number of machining stages for different final surface roughness ( $R_a$ ) are shown in Table 6.17 and Figure 6.18.

**Table 6.17** Changing machining times with  $R_{af}$

$R_{af}$ ( $\mu\text{m}$ )	Machining time (min)			
	2 stage	3 stage	4 stage	5 stage
$R_a$ 2.1 $\mu\text{m}$	2340.5	1054.5	740.2	682.2
$R_a$ 2.2 $\mu\text{m}$	897.7	508.3	440.8	396.6
$R_a$ 2.3 $\mu\text{m}$	650.3	418.7	382.7	362.5
$R_a$ 2.7 $\mu\text{m}$	556.0	382.0	360.3	349.5
$R_a$ 2.9 $\mu\text{m}$	407.1	340.6	337.0	336.4
$R_a$ 3.1 $\mu\text{m}$	348.7	334.7	334.8	353.7



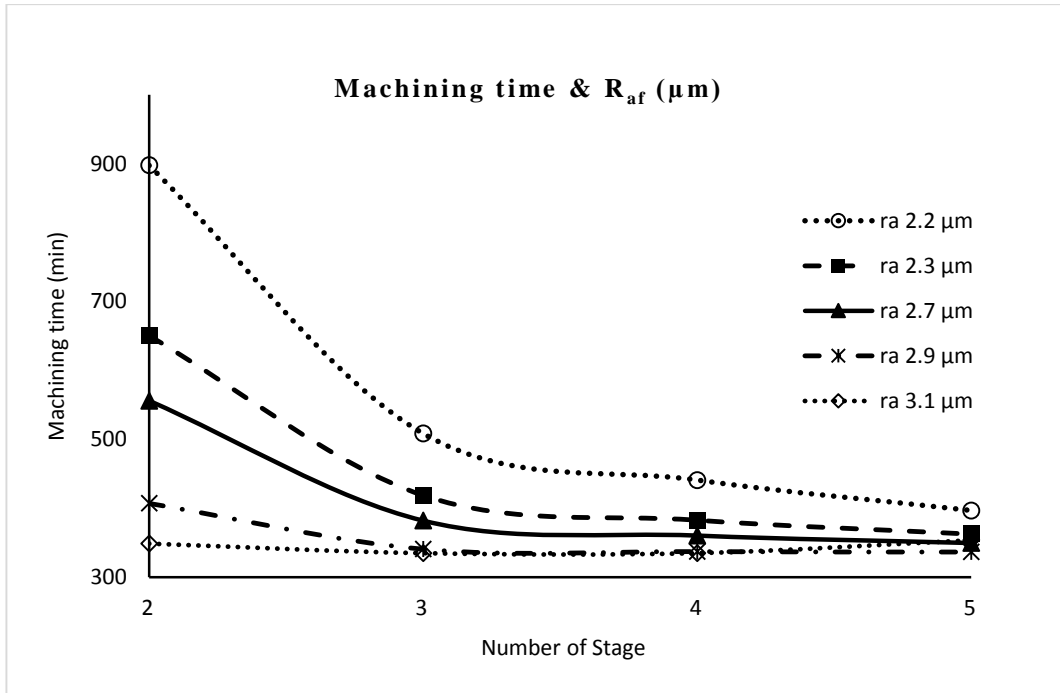


**Figure 6.18** Relation between the machining time and  $R_{af}$

### 6.6.2 Case Study 2

In the case study 2, a cylindrical shape was chosen. The input data given in Table 6.18 was used to show the effect of diameter (i.e., surface area) of the machining stock. For cylindrical shape, the machining stock geometry of each stage is given in Figure 6.19 and the corresponding equations are;

$$SA = \frac{\pi(d)^2}{4} \quad 6.19$$

$$SA_i = \frac{\pi(d_i)^2}{4} \quad 6.20$$

$$d_n = d - 2 \times \sum_i^n C_{ti} \quad 6.21$$

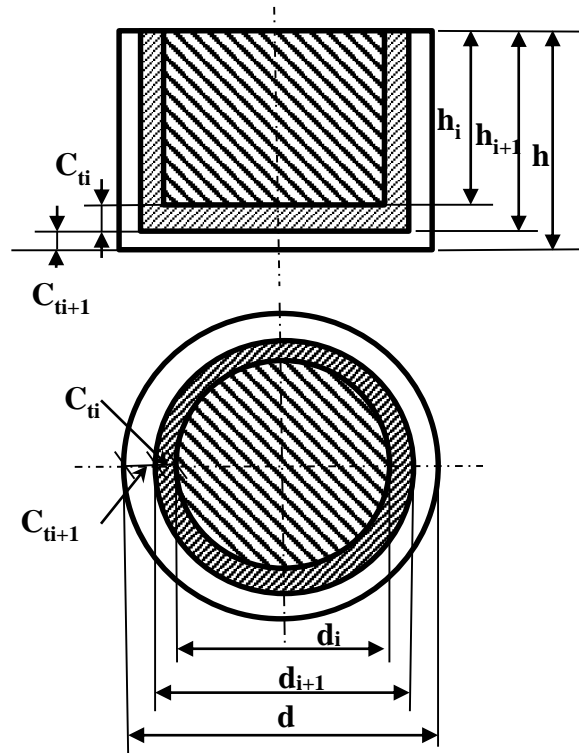


**Figure 6.19** View of three-stage machining for cylindrical shape

**Table 6.18** Surface area and machining stage

$\phi$ (mm)	Height (mm)	$k$	$R_{af}$ ( $\mu\text{m}$ )	SA ( $\text{mm}^2$ )	Total machining time (min) for each stage				
					1 stage	2 stage	3 stage	4 stage	5 stage
5.5	30	2.5	2.3	24	83	10			
8	30	2.5	2.3	50	175	17	16		
11	30	2.5	2.3	95	332	29	28		
16	30	2.5	2.3	201	701	45	34	35	35
19.5	30	2.5	2.3	299	1042	64	49	49	50
22	30	2.5	2.3	380	1326	79	61	61	62
27.6	30	2.5	2.3	598	2087	120	78	72	66
32	30	2.5	2.3	804	2806	158	104	95	87
39	30	2.5	2.3	1195	4167	230	151	137	127
40.7	30	2.5	2.3	1301	4538	249	164	149	138
42.2	30	2.5	2.3	1399	4879	267	176	159	148
45	30	2.5	2.3	1590	5548	301	199	180	167
50.5	30	2.5	2.3	2003	6987	375	247	223	208
55	30	2.5	2.3	2376	8288	442	290	262	246
61.8	30	2.5	2.3	3000	10464	553	361	327	308
65	30	2.5	2.3	3318	11575	610	397	361	339
71.4	30	2.5	2.3	4004	13967	731	474	432	407
79.8	30	2.5	2.3	5001	17447	907	585	534	505
85	30	2.5	2.3	5675	19795	1025	660	604	572
94.4	30	2.5	2.3	6999	24415	1258	808	739	702
100	30	2.5	2.3	7854	27398	1408	902	826	786
112.8	30	2.5	2.3	9993	34860	1782	1138	1044	995
133.5	30	2.5	2.3	13998	48829	2480	1578	1450	1386
150	30	2.5	3.3	17671	61645	3119	1979	1821	1744

The machining surface area influences vitally the machining stages (see Table 6.18). If the set-up time is taken as 10 minutes for each stage, the total time changes as seen in Table 6.19 and Figure 6.20. From these results, the number of machining stages may be related to the surface area as:

- SA < 400 mm<sup>2</sup> : 2-stage machining  
 400 ≤ SA < 2400 mm<sup>2</sup> : 3-stage machining  
 2400 ≤ SA < 4000 mm<sup>2</sup> : 4-stage machining  
 SA > 4000 mm<sup>2</sup> : 5-stage machining

**Table 6.19** Surface area and machining stages (with setup time)

ø (mm)	Height (mm)	k	R <sub>af</sub>	SA	Total machining time (min) for each stages				
			(μm)		1 stage	2 stage	3 stage	4 stage	5 stage
5.5	30	2.5	2.3	24	83	20			
8	30	2.5	2.3	50	175	27	36		
11	30	2.5	2.3	95	332	39	48		
16	30	2.5	2.3	201	701	55	54	65	75
19.5	30	2.5	2.3	299	1042	74	69	79	90
22	30	2.5	2.3	380	1326	89	81	91	102
27.6	30	2.5	2.3	598	2087	130	98	102	106
32	30	2.5	2.3	804	2806	168	124	125	127
39	30	2.5	2.3	1195	4167	240	171	167	167
40.7	30	2.5	2.3	1301	4538	259	184	179	178
42.2	30	2.5	2.3	1399	4879	277	196	189	188
45	30	2.5	2.3	1590	5548	311	219	210	207
50.5	30	2.5	2.3	2003	6987	385	267	253	248
55	30	2.5	2.3	2376	8288	452	310	292	286
61.8	30	2.5	2.3	3000	10464	563	381	357	348
65	30	2.5	2.3	3318	11575	620	417	391	379
71.4	30	2.5	2.3	4004	13967	741	494	462	447
79.8	30	2.5	2.3	5001	17447	917	605	564	545
85	30	2.5	2.3	5675	19795	1035	680	634	612
94.4	30	2.5	2.3	6999	24415	1268	828	769	742
100	30	2.5	2.3	7854	27398	1418	922	856	826
112.8	30	2.5	2.3	9993	34860	1792	1158	1074	1035
133.5	30	2.5	2.3	13998	48829	2490	1598	1480	1426
150	30	2.5	3.3	17671	61645	3129	1999	1851	1784

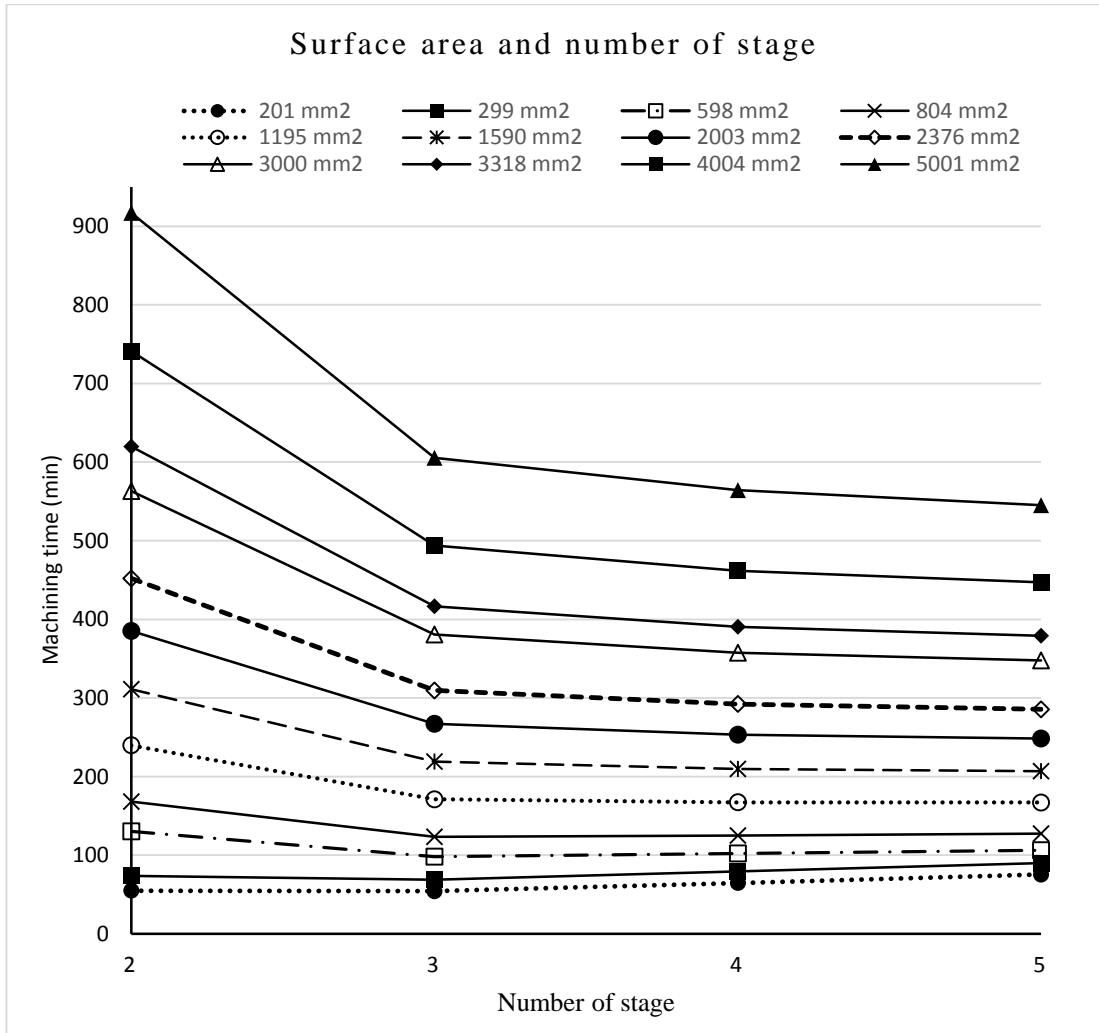


**Figure 6.20** The effects of surface area on the machining stages

### 6.6.3 Case Study 3

A spherical surface having 20 mm in diameter was selected for this study. The solid model of the hemi-spherical material stock is shown in Figure 6.21. For this 3D shape (neither rectangular nor cylindrical), “other” option on the input menu of the computer program must be used and the frontal surface area was given as input.

The volume and frontal surface area of the part were;

$$V = \frac{2}{3} \times \pi \times r^3 = \frac{2}{3} \times \pi \times 20^3 = 16755.16 \text{ mm}^3$$

$$A = 2 \times \pi \times r^2 = 2 \times \pi \times 20^2 = 2513.27 \text{ mm}^2, \text{ respectively}$$

Desired average surface roughness was 2.4  $\mu\text{m}$  and cutting thickness coefficient (k) was 3.

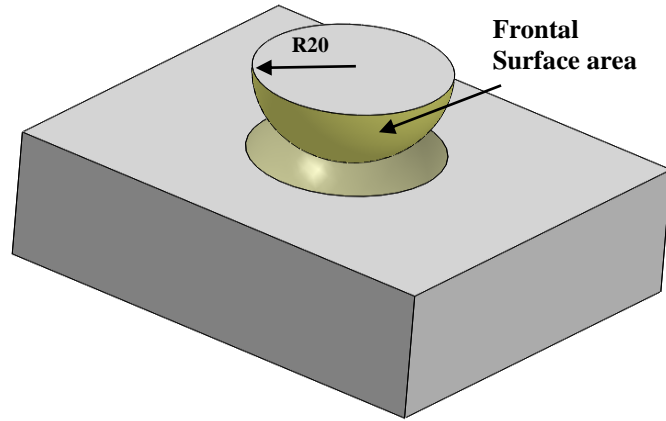


**Figure 6.21** The solid model of spherical surface

**Table 6.20** The multi-stage program outputs for the spherical example

No of stages	<i>I</i> (amp)	<i>T<sub>on</sub></i> ( $\mu$ s)	<i>T<sub>off</sub></i> ( $\mu$ s)	MRR (mm <sup>3</sup> /min)	<i>R<sub>a</sub></i> ( $\mu$ m)	EWR (%)	AWLT ( $\mu$ m)	Time (min)	Total Mach-time (min)
5	44	100	12	375.2	8.7	13.3	19.7	43.2	53.7
	37	50	12	300.1	5.2	7.5	20.7	6.8	
	31	50	200	243.4	3.2	0.5	24.8	1.2	
	25	12	50	209.2	3.1	8.6	9.4	0.9	
	3	100	50	52.2	2.4	2.4	20.1	1.6	
4	44	100	12	375.2	8.7	13.3	19.7	43.5	54.6
	37	50	12	300.1	5.2	7.5	20.7	6.8	
	12	100	100	195.9	3.4	1.6	18.6	1.5	
	3	100	50	52.2	2.4	2.4	20.1	2.8	
3	44	100	12	375.2	8.7	13.3	19.7	44.0	55.9
	31	50	50	244.2	6.1	5.3	10.7	8.5	
	3	100	50	52.2	2.4	2.4	20.1	3.4	
2	25	100	200	241.5	5.7	1.3	25.1	68.6	75.8
	3	100	50	52.2	2.4	2.4	20.1	7.2	
1	3	100	50	52.2	2.4	2.4	20.1	321.0	321.0

It can be seen from the results (Table 6.20), 3-stage machining is enough. The program calculates the volume of machining stock for each stage by considering the depth of cut according to cutting thickness coefficient.

$$V_T = 16755.16 \text{ mm}^3$$

$$SA = 2513.27 \text{ mm}^2$$

$$C_{t1} = AWLT_1 \times k = 19.7 \mu\text{m} \times \frac{0.001 \text{ mm}}{1 \mu\text{m}} \times 3 = 0.0591 \text{ mm}$$

$$C_{t2} = AWLT_2 \times k = 10.7 \mu\text{m} \times \frac{0.001 \text{ mm}}{1 \mu\text{m}} \times 3 = 0.0321 \text{ mm}$$

$$h = \frac{V_T}{SA} = \frac{16755.16}{2513.27} = 6.667 \text{ mm}$$

$$h_1 = h - (C_{t1} + C_{t2}) = 6.5754 \text{ mm}$$

$$h_2 = h - (C_{t2}) = 6.6345 \text{ mm}$$

$$V_1 = SA \times h_1 = 16526.99 \text{ mm}^3$$

$$V_2 = SA \times h_2 - V_1 = 147.624 \text{ mm}^3$$

$$V_3 = V_T - (SA \times h_2) = 80.54 \text{ mm}^3$$

$$t_1 = \frac{V_1}{MRR_1} = \frac{16526.99}{375.2} = 44.048 \text{ min}$$

$$RV_1 = \frac{13.3 \times 375.2 \left(\frac{\text{mm}^3}{\text{min}}\right)}{100} \times \frac{7.8}{8.9} \times 44.048 = 1926.42 \text{ mm}^3$$

$$V'_2 = V_2 + RV_1 = 147.624 + 1926.26 = 2074.04 \text{ mm}^3$$

$$t_2 = \frac{V'_2}{MRR_2} = \frac{2073.884}{244.2} = 8.493 \text{ min}$$

$$RV_2 = \frac{5.3 \times 244.2 \left(\frac{\text{mm}^3}{\text{min}}\right)}{100} \times \frac{7.8}{8.9} \times t_2 = 96.33 \text{ mm}^3$$

$$V'_3 = V_3 + RV_2 = 80.676 + 96.41 = 177.01 \text{ mm}^3$$

$$t_3 = \frac{V'_3}{MRR_3} = \frac{177.01}{52.2} = 3.39 \text{ min}$$

$$t_T = t_1 + t_2 + t_3 = 44.05 + 8.5 + 3.39 = 55.9 \text{ min}$$

#### 6.6.4 Case Study 4

The multi-stage EDM of a butt mould is taken as an example. Due to the 3D complex shape of the butt mould, “*other*” option on the input menu of the computer program was used. The frontal surface area and the volume were calculated by using 3D (SolidWorks) model of the butt mould (Figure 6.22). According to the calculation, input data of the example are given in Table 6.21. The program results are given in Table 6.22 and the solid model of the machining stock is shown in Figure 6.23 for 3-stage machining.

**Table 6.21** Input data of a butt mould for case study 4

Material	1.2344 tool steel
Electrode	Copper
Frontal surface area	7135.77 mm <sup>2</sup>
Output (volume of workpiece)	45457.67 mm <sup>3</sup>
Desired surface quality $R_{af}$	2.2 μm
Cutting thickness coefficient $k$	3

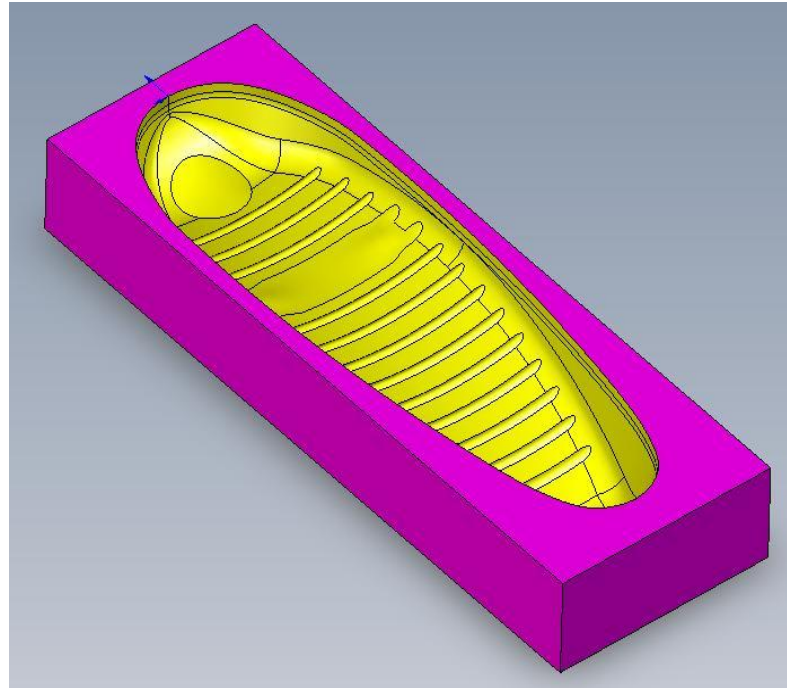


**Figure 6.22** Solid model of the butt mould

**Table 6.22** Outputs of the program for the butt mould.

No of stages	$I$ (amp)	$T_{on}$ (μs)	$T_{off}$ (μs)	MRR (mm <sup>3</sup> /min)	$R_a$ (μm)	EWR (%)	AWLT (μm)	Time (min)	Total Mach-time (min)
5	44	100	12	375.2	8.7	13.3	19.7	116.9	203.1
	37	50	12	300.1	5.2	7.5	20.7	18.4	
	31	50	200	243.4	3.2	0.5	24.8	3.3	
	25	12	50	209.2	3.1	8.6	9.4	2.6	
	3	6	3	3.9	2.2	3.9	6	61.9	
4	37	50	12	300.1	5.2	7.5	20.7	147.6	226.1
	31	50	200	243.4	3.2	0.5	24.8	13.8	
	25	12	50	209.2	3.1	8.6	9.4	2.6	
	3	6	3	3.9	2.2	3.9	6	62.1	
3	44	100	12	375.2	8.7	13.3	19.7	119.4	268.5
	31	50	50	244.2	6.1	5.3	10.7	23.1	
	3	6	3	3.9	2.2	3.9	6	126.0	
2	25	100	200	241.5	5.7	1.3	25.1	186.0	455.0
	3	6	3	3.9	2.2	3.9	6	269.0	
1	3	6	3	3.9	2.2	3.9	6	11656.0	11656.0

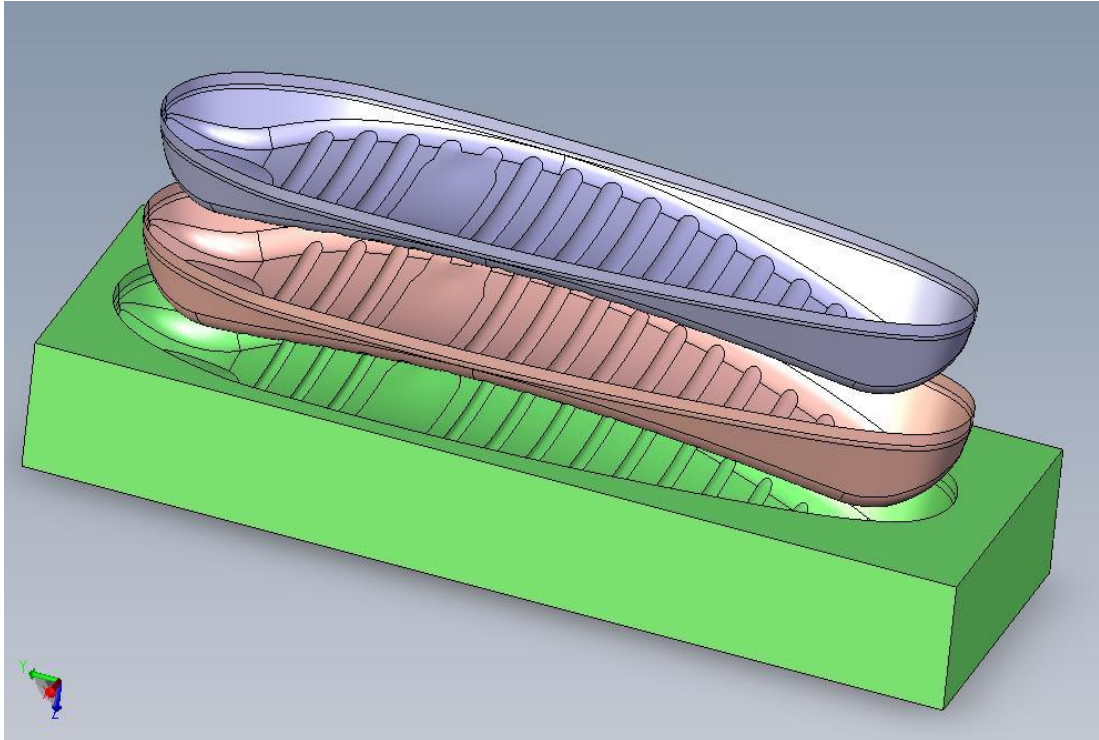


**Figure 6.23** The solid model of the machining stock for 3-stage.

The computer program calculates the volume of machining stock for each stage by considering the depth of cut according to AWLT and (k) as;

$$V_T = 45457.67 \text{ mm}^3$$

$$SA = 7135.77 \text{ mm}^2$$

$$h = \frac{V_T}{SA} = \frac{45457.77}{7135.77} = 6.37 \text{ mm}$$

$$C_{t1} = AWLT_1 \times k = 19.7 \mu\text{m} \times \frac{0.001 \text{ mm}}{1 \mu\text{m}} \times 3 = 0.0591 \text{ mm}$$

$$C_{t2} = AWLT_2 \times k = 10.7 \mu\text{m} \times \frac{0.001 \text{ mm}}{1 \mu\text{m}} \times 3 = 0.0321 \text{ mm}$$

$$h_1 = h - (C_{t1} + C_{t2}) = 6.279 \text{ mm}$$

$$h_2 = h - (C_{t2}) = 6.338 \text{ mm}$$

$$V_1 = SA \times h_1 = 7135.7 \times 6.279 = 44806.9 \text{ mm}^3$$

$$V_2 = (SA \times h_2) - V_1 = 421.7 \text{ mm}^3$$

$$V_3 = V_T - (SA \times h_2) = 229.1 \text{ mm}^3$$

$$t_1 = \frac{V_1}{MRR_1} = \frac{44807}{375.2} = 119.42 \text{ min}$$



$$RV_1 = \frac{13.3 \times 375.2 \left(\frac{\text{mm}^3}{\text{min}}\right)}{100} \times \frac{7.8}{8.9} \times 119.42 = 5223 \text{ mm}^3$$

$$V'_2 = V_2 + RV_1 = 421.7 + 5223.15 = 5644.5 \text{ mm}^3$$

$$t_2 = \frac{V'_2}{MRR_2} = \frac{5644.5}{244.2} = 23.1 \text{ min}$$

$$RV_2 = \frac{5.33 \times 244.2 \left(\frac{\text{mm}^3}{\text{min}}\right)}{100} \times \frac{7.8}{8.9} \times t_2 = 262.18 \text{ mm}^3$$

$$V'_3 = V_3 + RV_2 = 229.1 + 262.2 = 491.2 \text{ mm}^3$$

$$t_3 = \frac{V'_3}{MRR_3} = \frac{491.2}{3.9} = 126 \text{ min}$$

$$t_T = t_1 + t_2 + t_3 = 119.42 + 23.1 + 126 = 268.5 \text{ min}$$

## 6.7 Verification Study

An experimental work was carried out to verify the results of the developed computer program. For simplicity, a cylindrical shape was chosen. The input and the output data of the study are given in Tables 6.23 and 6.24, respectively. However, discharge current levels of the EDM machine which was used for this verification study were 50, 25, 18, 12, 9, 6 and 3 amperes. From the alternatives which were generated by the computer program, suitable parameter sets chosen according to discharge current levels of the existing EDM machine (see Table 6.25).

**Table 6.23** Input data of the verification example

Material	1.2344 tool steel
Electrode	Copper
Diameter of the part	50 mm
Height of the part	10 mm
Cutting coefficient factor (k)	4
Desired surface quality $R_{af}$	2.8 $\mu\text{m}$ .

**Table 6.24** The multi-stage program outputs

No of trials	<i>I</i> (amp)	<i>T<sub>on</sub></i> (μs)	<i>T<sub>off</sub></i> (μs)	MRR (mm <sup>3</sup> /min)	<i>R<sub>a</sub></i> (μm)	EWR (%)	AWLT (μm)	Time (min)	Mach-time (min)
35	44	100	12	375.2	8.7	13.3	19.7	49.566	69.4
	37	50	12	300.1	5.2	7.5	20.7	8.1258	
	31	50	200	243.4	3.2	0.5	24.8	1.8381	
	25	12	50	209.2	3.1	8.6	9.4	1.6697	
	6	12	3	19.5	2.8	6.3	10	8.1513	
2	50	200	25	390	10.9	25.9	62.4	47.048	73.8
	44	100	12	375.2	8.7	13.3	19.7	13.391	
	31	50	50	244.2	6.1	5.3	10.7	3.5286	
	6	12	3	19.5	2.8	6.3	10	9.7922	
9	44	100	12	375.2	8.7	13.3	19.7	51.194	75.2
	31	50	50	244.2	6.1	5.3	10.7	10.299	
	6	12	3	19.5	2.8	6.3	10	13.73	
5	25	100	200	241.5	5.7	1.3	25.1	79.843	109.2
	6	12	3	19.5	2.8	6.3	10	29.366	
1	6	12	3	19.5	2.8	6.3	10	1006.90	1006.9

**Table 6.25** Set of suitable parameters for the existing EDMachine

No of trials	<i>I</i> (amp)	<i>T<sub>on</sub></i> (μs)	<i>T<sub>off</sub></i> (μs)	MRR (mm <sup>3</sup> /min)	<i>R<sub>a</sub></i> (μm)	EWR (%)	AWLT (μm)	Time (min)	Mach-time (min)
31	50	200	25	390	10.9	25.9	62.4	46.017	83.6
	25	100	200	241.5	5.7	1.3	25.1	20.38	
	18	50	50	175.4	3.5	5.2	16.5	2.3018	
	12	100	100	195.9	3.4	1.6	18.6	1.271	
	6	12	3	19.5	2.8	6.3	10	13.61	
16	50	200	25	390	10.9	25.9	62.4	46.659	82.5
	25	100	200	241.5	5.7	1.3	25.1	20.644	
	18	50	50	175.4	3.5	5.2	16.5	2.3219	
	6	12	3	19.5	2.8	6.3	10	12.872	
4	50	200	25	390	10.9	25.9	62.4	47.233	89.2
	25	100	200	241.5	5.7	1.3	25.1	20.88	
	6	12	3	19.5	2.8	6.3	10	21.046	
5	25	100	200	241.5	5.7	1.3	25.1	79.843	109.2
	6	12	3	19.5	2.8	6.3	10	29.366	
1	6	12	3	19.5	2.8	6.3	10	1006.90	1006.9

3-stage machine was selected for the experimental study. The machining parameter sets for the rough stage was ( $I=50$  amp,  $T_{on}=200\mu s$  and  $T_{off}=50\mu s$ ), for middle stage was ( $I=25$  amp,  $T_{on}=100\mu s$  and  $T_{off}=200\mu s$ ), and for finish stage was ( $I=6$  amp,  $T_{on}=12\mu s$  and  $T_{off}=3\mu s$ ).

The initial and final weights of the workpiece and the electrodes ( $W_i$ ,  $W_f$ ,  $E_i$  and  $E_f$ ) were measured and were given in Table 6.25. Photos of the white layers and experimental results of the  $R_a$  and AWLT and the machining times for each stage are given in Figure 6.24 and in Table 6.25.

**Table 6.26** The verification experiment results

<i>I</i> <b>A</b>	<i>Ton</i> <b>μs</b>	<i>Toff</i> <b>μs</b>	<i>Wi</i> <b>g</b>	<i>Wf</i> <b>g</b>	<i>Ei</i> <b>g</b>	<i>Ef</i> <b>g</b>	<i>Time</i> <b>min</b>	<b>MRR</b> <b>g/min</b>	<b>TWR</b> <b>g/min</b>	<b>MRR</b> <b>mm<sup>3</sup>/min</b>	<b>Ra</b> <b>μm</b>	<b>EWR</b> <b>%</b>	<b>AWLT</b> <b>μm</b>
50	200	25	748.7	609.5	513.4	477.1	48	2.901	0.757	371.9	11	26.1	60
25	100	200	598.0	558.0	517.0	516.5	22	1.817	0.024	233.0	5.7	1.3	25
6	12	3	596.5	592.9	518.1	517.9	24	0.149	0.006	19.2	2.8	3.8	10

The machining times from rough to finish stages for the verification results were obtained as 48, 22 and 24 minutes, respectively (Table 6.25). It can be seen that from the Tables 6.24 and 6.25, the difference in the total machining times between the developed program and the experimental one is  $94-89.2=4.8$  minutes (about 5.4 %). The desired surface quality for the verifying example was achieved as  $R_a=2.8\ \mu\text{m}$ . So that the developed program for multi-stage EDM machining is suitable for practical applications.

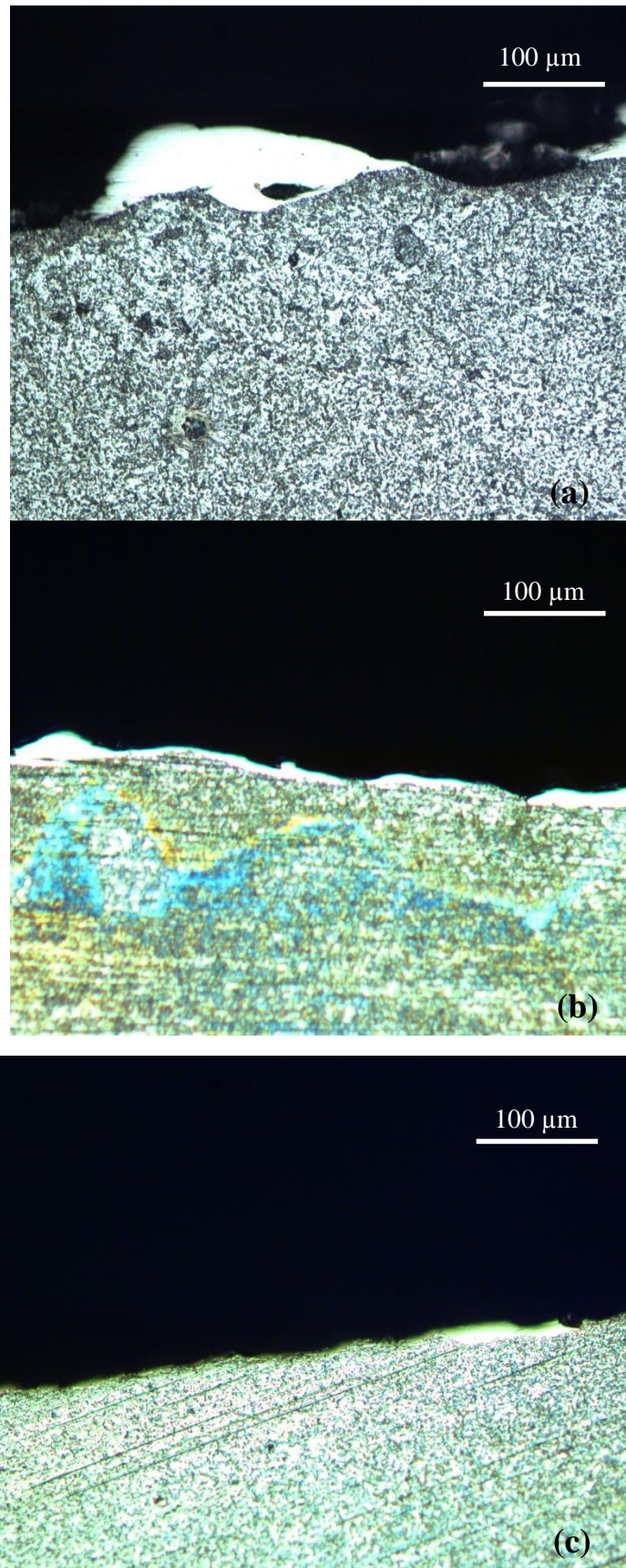


**Figure 6.24** Photos of the white layers of the verification example (a ) rough , (b) middle and (c) finish stage

## 6.8 Summary of the Results of the Case Studies

In this chapter, the developed multi-stage EDM strategy and the computer program were explained. This program gives the number of EDM stages from rough to finish and EDM parameter sets for each stage according to the minimum machining time. The case studies were performed to explain the program and the strategy. Their results of them show that;

- Multi-stage EDM machining is necessary in order to achieve the required surface quality with minimum machining time.
- The determination of number of stages and the corresponding parameter sets are difficult tasks and far beyond the manual calculation. The developed computer program generates all alternatives and the user can easily decide the suitable one considering the limitations in time and/or cost of the operation.
- The machining surface area influences vitally the machining stages. If the surface area is smaller than  $400 \text{ mm}^2$ , 2-stage machining is enough. If the surface area is between  $400$  and  $2400 \text{ mm}^2$ , 3-stage machining is suitable. If the surface area is in between  $2400$  and  $4000 \text{ mm}^2$ , 4-stage machining is the solution. For the surface area bigger than  $4000 \text{ mm}^2$ , 5-stage machining can be chosen.
- Increasing the cutting thickness coefficient ( $k$ ) increases machining time proportionally.
- The verification study shows that the multi-stage machining strategy and the developed computer program can be used successfully.

## CHAPTER 7

### CONCLUSIONS AND FUTURE WORKS

#### 7.1 Conclusions

In this thesis, a parameter selection model for ram type EDM process by using multi-stage strategy was developed. Three main tasks were realized namely; the experimental study, the modelling study and the development of multi-stage strategy.

In the experimental study, the most effective electrical parameters i.e., discharge currents ( $I$ ), pulse on-time ( $T_{on}$ ), pulse off-time ( $T_{off}$ ) were taken as inputs and main performance parameters (MRR, EWR,  $R_a$  and AWLT) were measured as outputs. The followings have been concluded from the experimental results;

- The increase in pulse on-time leads to an increase in the material removal rate, surface roughness and the white layer thickness.
- The increase in pulse current leads to a sharp increase in the material removal rate and the surface roughness.
- Electrode wear ratio decreases by the increase of pulse on-time, and increases by the increase in the pulse current.
- A slight decrease could be observed in the white layer thickness by an increase in the pulse current.
- High discharge current and  $T_{on}$  provide low surface finish quality but this combination would increase material removal rate and reduce machining cost.
- Better surface quality was obtained when applying smaller discharge current and pulse on-time are applied.
- EDM is a highly nonlinear process and its performance is influenced by various machine parameters.

- It is very difficult to attain high MRR and excellent surface feature in the same breath in one-stage machining. Therefore, multi-stage machining process is necessary.
- The experimental studies show that white layer in roughing stage was mainly discontinuous and non-uniform and much more than that in the finishing stage. However, in the finishing stage, the thickness of the white layer was very small for all EDMed surfaces

The aim of the modelling study is to develop suitable models to predict accurately EDM outputs by correlating the input parameters. Because, alternative machining parameters sets were necessary to develop the multi-stage strategy. Alternative mathematical models (by using ANN, GEP and ANFIS) were developed to predict EDM performances using the results which were obtained from EDM experiments. The most appropriate model amongst all the models was proposed. At the end of the modelling study, sets of EDM parameters were constructed. Based on the modelling studies, the following conclusions have been made:

- All of the models (ANN, GEP and ANFIS) were successful for prediction of EDM performances by learning complex relationship between the input and output parameters in terms of statistical parameters.
- GEP model was less successful among others; however, it has a simple and explicit mathematical formulation.
- The results produced by both ANN and ANFIS models also presented relatively good level of accuracy. However, the ANFIS model was more successful than the ANN model.

During the development of the multi-stage strategy a backward-chain method was developed to define the stages of EDM. The alternatives of machining stages were determined according to the current range between the discharge current of rough and finish stage. To determine the depth of cut for each stage, as a strategy, the AWLT of the previous machining stage was taken as a criterion. The machining depth of any subsequent stage was chosen as 2-3 times larger than the previous AWLT to eliminate the negative effects of the white layer and HAZ.

Then, a multi-stage EDM selection program was developed by using MATLAB package program. The developed program computes the number of stages required to complete the operation, their sequence from rough to finish and sets of the machining parameters for each stage according to minimum machining time.

Some Case studies and a verification experiment for each one were performed to explain the developed multi-stage strategy and the computer program. These case studies showed that;

- Multi-stage EDM machining is necessary in order to achieve the required surface quality with minimum machining time,
- The determination of number of stages and the corresponding parameter sets are a difficult task and far beyond the manual calculation. The developed computer program generates all alternatives and the user can easily decide the suitable one considering the limitations in time and/or cost of the operation,
- The machining surface area influences vitally the machining stages. If the surface area is smaller than  $400 \text{ mm}^2$ , 2-stage machining is enough. If the surface area is between 400 and  $2400 \text{ mm}^2$ , 3-stage machining is suitable. If the surface area is between 2400 and  $4000 \text{ mm}^2$ , 4-stage machining is suitable. For the surface area bigger than  $4000 \text{ mm}^2$ , 5-stage machining can be chosen,
- Increasing of cutting thickness coefficient (k) increases machining time proportionally,
- The verification study shows that the multi-stage machining strategy and the developed computer program can be used successfully.

## **7.2 Future Works**

The following subjects may be recommended for the future researches:

- In this thesis, the workpiece material was DIN 1.2344 and the electrode was copper, the machining characteristic of other workpiece and electrode materials may also be investigated.
- Further experiments can be performed for various parameter settings in terms of the voltage, the polarity, the flushing pressure and the gap distance which were kept constant in the thesis.



- The developed strategy can be integrated into a CAD/CAM program. Then, the electrode design for any machining stage can be done for 3D complex shapes.
- Cost analysis of multi-stage machining by using the developed strategy may also be investigated.
- The strategy can be applied for wire EDM.

## REFERENCES

- Amorim, F.L., Weingaertner, W.L. (2007). The behaviour of graphite and copper electrodes on the finish die-sinking electrical discharge machining (EDM) of AISI P20 tool steel. *Journal of the Brazilian Society of Mechanical Sciences*. **29**:366-371
- Amorim, F.L., Weingaertner, W.L., Bassani, I.A. (2010). Aspects on the optimization of die-sinking EDM of Tungsten Carbide-Cobalt. *Journal of the Brazilian Society of Mechanical Sciences*. **32**: 496-502
- Armstrong, N.A. (2006). Pharmaceutical experimental design and interpretation. Taylor & Francis group. New York.
- Assarzadeh, S., Ghoreishi, M. (2008). Neural-network-based modeling and optimization of the electro-discharge machining process. *International Journal Advanced Manufacturing Technology*. **39**:488–500 DOI 10.1007/s00170-007-1235-1
- Cevik, A. (2007). Genetic programming based formulation of rotation capacity of wide flange beams. *Journal of Constructional Steel Research*. **63**: 884-893.
- Cevik, A., Guzelbey, I.H. (2007). A soft computing based approach for the prediction of ultimate strength of metal plates in compression. *Engineering Structures*. **29**: 383-394.
- Cobine, J.D., Burger, E.E. (1955). Analysis of electrode phenomena in the high-current arc. *Journal of Applied Physics*. **26(7)**: 895–900.
- Crookall, J.R., Heuvelman, C.J. (1971). Electro-discharge machining-the state of the art. *Annual of the CIRP*. **20**:113-120.
- Ekmekci, B. (2009). White layer composition, heat treatment, and crack formation in electric discharge machining process. *Metallurgical and Materials Transactions B*. **40**:70–81.
- El-Hofy, H. (2005). Advanced machining processes: Non-traditional and hybrid machining processes. McGraw-Hill Companies. Mechanical Engineering Series. DOI: 10.1036/0071466940

- Elman, C.J. (2001). *Electrical Discharge Machining*. Society of Manufacturing Engineers Dearborn, Michigan. ISBN 087263521X
- Ferreira, C. (2001). Gene expression programming: a new adaptive algorithm for solving problems. *Complex Systems*. **13(2)**: 87-129.
- Garg, R.K., Singh, K.K., Sachdeva, A., Sharma, V.S., Ojha, K., Singh, S. (2010). Review of research work in sinking EDM and WEDM on metal matrix composite materials. *International Journal Advanced Manufacturing Technology*. **50**:611–624. DOI 10.1007/s00170-010-2534-5
- Germer, L.H., Haworth, F.E. (1949). Erosion of electrical contacts on make. *Journal of Applied physics*. **20(11)**: 085– 1109.
- Griffiths, B.J. (2001). *Manufacturing surface technology: Surface integrity & functional performance*. London: Penton Press
- Guo, L.E., Xing, X.F. (2000). The technology of multi-cutting on machine tool of WEDM-HS. *Electromachining & Mould*. **5**: 5-9
- Haron, C.H., Ghani, J.A., Burhanuddin, Y., Seong, Y.K., Swee, C.Y. (2008). Copper and graphite electrodes performance in electrical-discharge machining of XW42 tool steel. *Journal of Materials Processing Technology*. **201**:570–573
- Hasçalık, A., Çaydaş, U. (2007). Electrical discharge machining of titanium alloy. *Applied Surface Science*. **253(22)**: 9007–9016
- Haykin, S. (2009). *Neural Networks and Learning Machines*. Prentice Hall, 3rd Edition. New Jersey
- Huang, J.T., Liao, Y.S., Hsue, W.J. (1999). Determination of finish-cutting operation number and machining-parameters setting in wire electrical discharge machining. *Journal of Materials Processing Technology*. **87**: 69–81
- Imanaga, S., Araya, T., Haneda, M., Kishi, M., Ishii, T. (1989). Advanced precision process of electro discharge machining. *International Symposium on Electro Machining (ISEM)*. **9**: 61–63.

- Jang, J.S.R. (1993). Anfis: Adaptive-network-based fuzzy inference systems. *IEEE Transactions on Systems, Man and Cybernetics*. **23(3)**: 665-685.
- Jang, J.S.R., Sun, T.C., Mizutani, E. (1997). Neuro-fuzzy and soft computing: a computational approach to learning and machine intelligence. Prentice Hall
- Joshi, S.N., Pande, S.S. (2011). Intelligent process modelling and optimization of die-sinking electric discharge machining. *Applied Soft Computing*. **11**: 2743–2755
- Kansal H K, Singh, S., Kumar, P. (2005). Parametric optimization of powder mixed EDM by response surface methodology. *Journal of Materials Processing Technology*. **169(3)**: 427–436
- Kim J., Kasabov, N. (1999). ANFIS: Adaptive Neuro-fuzzy inference systems and their application to nonlinear dynamical systems. *Neural Networks*. **12**: 1301-1319.
- Kishi, M., Suzuki, S., Araya, S. (1989). Optimisation of multi-stage planetary machining parameters in NC die sinking EDM. *International Symposium on Electro Machining (ISEM)*. **9**: 34–37.
- Kok, M., Kanca, E., Eyercioglu, O. (2011). Prediction of surface roughness in abrasive Waterjet machining of particle reinforced MMCs using genetic expression programming. *International Journal of Advanced Manufacturing Technology*. DOI 10.1007/s00170-010-3122-4
- Koza, JR. (1992). Genetic programming: on the programming of computers by means of natural selection. MIT Press, Cambridge (MA)
- Kumar, S., Singh, R., Singh, T.P., Sethi, B.L. (2008). Surface modification by electrical discharge machining: A review. *Journal of Materials Processing Technology*. **209**: 3675-3587.
- Lazarenko, BR. (1943). About the inversion of metal erosion and methods to fight ravage of electric contacts. WEI-Institute. Moscow in Russian.
- Ledvon, G., (2004). Manufacturing engineering handbook, The McGraw-Hill Companies.

- Lee, H.T., Hsu, F.C., Tai, T.Y. (2004). Study of surface integrity using the small area EDM process with a copper-tungsten electrode. *Materials Science and Engineering*. **364**:346–356
- Lee, H.T., Tai, T.Y. (2003). Relationship between EDM parameters and surface crack formation. *Journal of Materials Processing Technology*. **142**:676–683
- Lee, L.C., Lim, L.C., Narayanan, V., Venkatesh, V.C. (1988). Quantification of surface damage of tool steels after EDM. *International Journal of Machine Tools & Manufacture*. **28(44)**:359–372
- Lee, S.H., Li, X.P. (2001). Study of the effect of machining parameters on the machining characteristics in electrical discharge machining of tungsten carbide. *Journal of Material Processing Technology*. **115(3)**, 344-358
- Li, M.Q., Li, M.H., Zhang, J.R. (2003). The technical study and application of multi-cutting on machine tool of WEDM-HS. *Electromachining & Mould*. **4**:45-47
- Liao, Y.S., Chen, Y.Y. (2001). A computer-aided process planning system for the finishing operations of EDM. *International Symposium on Electro Machining (ISEM)* **13**: 171–185.
- Liao, Y.S., Huang, J.T., Chen, Y.H. (2004). A study to achieve a fine surface finish in Wire-EDM. *Journal of Materials Processing Technology*. **149**:165–171.
- Loose, J.P., Zhou, S., Ceglarek, D. (2007). Kinematic analysis of dimensional variation propagation for multistage machining processes with general fixture layouts. *IEEE Transactions on Automation Science and Engineering*. **4(2)**: 41
- Maji, K., Pratihar, D.K. (2010). Forward and reverse mappings of electrical discharge machining process using adaptive network-based fuzzy inference system. *Expert Systems with Applications*. **37**: 8566–8574.
- Mandal, D., Pal, S.K., Saha, P. (2007). Modelling of electrical discharge machining process using back propagation neural network and multi-objective optimizations using non-dominating sorting genetic algorithm-II. *Journal of Materials Processing Technology*. **186**: 154-162

Metals Handbook (1989). Vol. 16. Machining, Materials Park, OH: ASM International

Niwa, S., Furuya, M. (1995). A study on optimum machining conditions in EDM process for making mould and dies. *International Symposium on Electro Machining (ISEM)*. **11**: 325–332.

Ong, C.S, Huang, J.J., Tzeng, G.H. (2005). Building credit scoring models using genetic programming. *Expert Systems with Applications*. **29(1)**: 41–47.

Ozgedik, A., Cogun, C. (2006). An experimental investigation of tool wear in electric discharge machining. *International Journal of Advanced Manufacturing Technology*. **27**: 488-496.

Pandey, A., Singh, S. (2010). Current research trends in variants of Electrical Discharge Machining: A review. *International Journal of Engineering Science and Technology*. **2(6)**: 2172-2191

Pradhan, M.K. (2013). Estimating the effect of process parameters on surface integrity of EDMed AISI D2 tool steel by response surface methodology coupled with grey relational analysis. *International Journal Advanced Manufacturing Technology*. **67**:2051–2062.

Ramasawmy, H., Blunt, L., Rajurkar, K. (2005). Investigation of the relationship between the white layer thickness and 3D surface texture parameters in the die sinking EDM process. *Precis Eng*. **29(4)**:479–490

Rao, G.K.M., Satyanarayana, S., Praveen, M. (2008). Influence of machining parameters on electric discharge machining of maraging steels-an experimental investigation. *Proceeding of the world congress on Eng*. **2**:1536-1541

Roy, R.K. (2001). Design of experiments using the Taguchi approach. John Willey & Sons, Inc. New York.

Sanchez, J.A., Lacalle, L.N., Lamikiz, A., Bravo, U. (2002). Dimensional accuracy optimisation of multi-stage planetary EDM. *International Journal of Machine Tools & Manufacture*. **42**: 1643–1648

- Sanchez, J.A., Lopez de Lacalle, L.N., Lamikiz, A., Bravo, A. (2002). Dimensional accuracy optimisation of multi-stage planetary EDM. *International Journal of Machine Tools & Manufacture*. **42**:1643–1648
- Sanchez, J.A., Lopez de Lacalle, L.N., Lamikiz, A., Bravo, U. (2006). Study on gap variation in multi-stage planetary EDM. *International Journal of Machine Tools & Manufacture*. **46**:1598-1603
- Sarkar, S., Sekh, M., Mitra, S., Bhattacharyya, B. (2008). Modelling and optimization of wire electrical discharge machining of  $\gamma$ -TiAl in trim cutting operation. *Journal of materials processing technology*. **205**: 376–387
- Scott, D., Boyina, S., Rajurkar, K.P. (1991). Analysis and optimization of parameter combination in wire electrical discharge machining. *International Journal of Production Research*. **29(11)**: 2189–2207.
- Singh, U.P., Miller, P.P., and Urquhart, W. (1985). The influence of electro discharge machining parameters on machining characteristics. *Proceedings of the 21th International Machine Tool Design and Research Conference*. **25**: 337-345.
- Sommer, C., Sommer, S. (2005). Complete EDM Handbook. [www.reliableedm.com](http://www.reliableedm.com).
- Su, J. C., Kao, J. Y., Tarng, Y. S. (2004). Optimisation of the electrical discharge machining process using a GA-based neural network. *International Journal Advanced Manufacturing Technology*. **24**: 81–90
- Sugeno, M., Kang, G.T. (1988). Structure identification of fuzzy model. *Fuzzy Sets and Systems*. **26**:15–33.
- Taguchi, G., Chowdhury, S., Taguchi, S. (2000). Robust engineering. McGraw Hill;
- Tai, T., Lu, S. (2009) Improving the fatigue life of electro-discharge machined SDK11 tool steel via the suppression of surface cracks. *International Journal of Fatigue*. **31(3)**: 433–438
- Tzeng, Y.F., Chen, F.C. (2003). A simple approach for robust design of high speed electrical discharge machining technology. *International Journal of Machine Tools & Manufacture*. **43**: 217-227.

Wang, C.C., Yan, B.H. (2000). Blind hole drilling of Al<sub>2</sub>O<sub>3</sub>/6061 Al composite using rotary electro discharge machining. *Journal of Materials Processing Technology*. **102**: 90-102.

Wong, Y.S.; Lim, L.C.; Lee, L.C. (1995) Effect of flushing on electro discharge machined surface. *Journal of Materials Processing Technology*. **48**: 299-305.

Yilmaz, O., Eyercioglu, O., Gindy, N.Z. (2006). A user friendly fuzzy based system for the selection of electro discharge machining process parameters. *Journal of Materials Processing Technology*. **172**: 363–371.

Youssef, H.A., El-Hofy, H. (2008). Machining technology: machine tools and operations. CRC Press, Taylor & Francis Group. ISBN 978-1-4200-4339-6

Zingerman, A.S. (1956). The effect of thermal conductivity upon the electrical erosion of metals. *Souvenir of Physics Technology*. **1**:11945–1958.



## **APPENDICES**

## APPENDIX A. RESULTS OF EXPERIMENTAL STUDIES

**Table A. 1** Experimental data for the first group L<sub>25</sub>

Sno	I	Ton	Toff	Wi	Wf	Ei	Ef	Time	MRR	EWR	MRR	EWR	Ra	AWLT	Rt
	Amp	μs	μs	g	g	g	g	min	g/min	g/min	mm <sup>3</sup> /min	%	μm	μm	μm
1	6	50	50	81.197	72.380	35.855	35.723	12.26	0.719	0.011	92.2	1.5	3.2	21.2	56.0
2	25	100	25	80.274	75.987	33.417	32.731	3.25	1.319	0.211	169.1	16.0	9.0	35.2	42.2
3	12	25	50	80.219	71.175	36.012	35.876	8.02	1.128	0.017	144.6	1.5	3.9	8.7	38.2
4	25	50	12	80.308	76.230	37.864	37.203	3.27	1.247	0.202	159.9	16.2	5.1	32.2	38.9
5	6	25	25	81.032	79.492	34.657	34.634	4.59	0.336	0.005	43.0	1.5	3.7	12.8	27.8
6	12	50	3	79.709	76.345	36.206	35.500	7.42	0.453	0.095	58.1	21.0	6.9	22.3	50.0
7	12	100	6	79.149	77.914	36.320	36.080	3.24	0.381	0.074	48.9	19.4	8.1	17.4	58.0
8	12	12	25	80.718	78.132	34.518	34.479	3.49	0.741	0.011	95.0	1.5	5.0	11.6	29.7
9	25	12	3	80.277	72.061	36.564	35.397	9.03	0.910	0.129	116.6	14.2	4.8	13.6	39.2
10	6	100	3	81.433	80.322	35.553	35.421	6.46	0.172	0.020	22.1	11.9	5.6	14.5	46.1
11	3	12	6	81.082	80.127	35.764	35.724	19.56	0.049	0.002	6.3	4.2	2.4	7.8	13.7
12	6	12	12	79.328	77.615	36.300	36.274	10	0.171	0.003	22.0	1.5	3.7	8.8	19.3
13	6	6	3	79.745	79.309	37.130	37.108	4.5	0.097	0.005	12.4	5.0	2.5	6.5	25.7
14	12	3	12	80.438	79.177	37.275	37.256	3.3	0.382	0.006	49.0	1.5	5.6	11.4	30.4
15	25	25	6	80.229	74.948	34.411	33.577	4.51	1.171	0.185	150.1	15.8	5.2	13.8	39.2
16	3	100	50	79.654	75.058	34.667	34.400	11.36	0.405	0.023	51.9	5.8	2.5	20.6	16.0
17	18	100	12	81.253	78.891	30.535	30.032	3	0.787	0.168	100.9	21.3	7.7	36.6	57.2
18	18	50	6	79.512	76.177	34.816	34.209	4.13	0.808	0.147	103.5	18.2	6.9	17.1	51.4
19	3	50	25	79.950	78.068	35.739	35.622	15.27	0.123	0.008	15.8	6.2	3.2	6.6	14.3
20	3	25	12	80.436	79.580	36.166	36.119	15.55	0.055	0.003	7.1	5.5	2.8	7.5	11.6
21	18	3	25	80.270	69.011	35.668	35.499	11.21	1.004	0.015	128.8	1.5	3.3	17.1	26.9
22	18	12	50	78.623	59.930	35.710	35.430	13.43	1.392	0.021	178.4	1.5	3.6	11.7	27.5
23	25	3	50	80.448	51.450	36.276	35.841	18.56	1.562	0.023	200.3	1.5	2.9	8.2	23.3
24	3	6	3	80.784	80.134	36.089	36.063	21.49	0.030	0.001	3.9	4.0	2.2	6.0	14.9
25	18	25	3	80.002	76.793	36.860	36.314	4.1	0.783	0.133	100.4	17.0	6.5	17.9	48.4

**Table A. 2** Experimental data for the second group L25

Sno	I	Ton	Toff	Wi	Wf	Ei	Ef	Time	MRR	EWR	MRR	EWR	Ra	AWLT	Rt
	Amp	$\mu$ s	$\mu$ s	g	g	g	g	min	g/min	g/min	mm <sup>3</sup> /min	%	$\mu$ m	$\mu$ m	$\mu$ m
26	9	400	200	79.434	66.605	35.179	34.987	7.43	1.727	0.026	221.4	1.5	6.7	33.4	38.8
27	25	800	100	79.356	77.582	35.504	34.798	1.46	1.215	0.484	155.8	39.8	5.5	62.7	30.9
28	12	200	200	79.946	73.643	34.992	34.897	3.53	1.786	0.027	228.9	1.5	7.6	28.6	62.3
29	25	400	50	79.216	77.628	36.410	36.021	1.33	1.194	0.293	153.1	24.5	6.3	46.5	50.7
30	9	200	100	78.512	71.476	35.006	34.788	5.3	1.328	0.041	170.2	3.1	5.1	16.5	35.5
31	12	400	12	87.358	78.366	35.491	35.465	4.2	2.141	0.006	274.5	6.9	0.3	25.4	37.4
32	12	800	25	87.358	79.930	36.662	35.466	15.44	0.481	0.077	61.7	6.8	16.1	25.6	40.7
33	12	100	100	77.848	72.671	35.544	35.466	3.41	1.518	0.023	194.6	1.5	7.9	18.6	46.1
34	25	100	12	80.702	79.335	34.167	33.854	1.16	1.179	0.270	151.1	22.9	6.7	33.9	52.2
35	9	800	12	85.635	79.503	35.049	34.043	12.5	0.491	0.080	62.9	3.8	16.4	22.4	8.8
36	6	100	25	78.985	77.541	34.995	34.809	7.22	0.200	0.026	25.6	12.9	4.8	22.5	40.4
37	9	100	50	78.147	74.777	33.460	33.261	4.13	0.816	0.048	104.6	5.9	3.0	24.2	49.2
38	9	50	25	81.024	79.394	33.881	33.762	3.35	0.487	0.036	62.4	7.3	5.1	20.2	35.5
39	12	50	50	79.654	77.445	34.702	34.669	2.03	1.088	0.016	139.5	1.5	3.9	20.6	40.1
40	25	200	25	78.550	77.175	33.592	33.321	1.16	1.185	0.233	151.9	19.7	8.1	52.2	75.6
41	6	800	200	85.630	79.615	34.749	34.376	5.8	1.037	0.064	133.0	2.3	6.2	79.5	9.1
42	18	800	50	78.743	78.491	35.162	35.159	0.58	0.434	0.005	55.7	5.4	1.2	37.0	38.5
43	18	400	25	78.698	78.114	34.682	34.464	1.55	0.377	0.140	48.3	37.3	7.3	27.0	49.1
44	6	400	100	80.697	55.483	31.303	27.370	29.55	0.853	0.133	109.4	15.6	3.3	24.3	22.2
45	6	200	50	79.101	74.668	35.440	34.771	11.15	0.398	0.060	51.0	15.1	6.2	19.5	39.2
46	18	50	100	84.451	82.015	33.981	33.821	2.49	0.978	0.064	125.4	7.4	6.6	12.8	47.1
47	18	100	200	79.206	74.814	36.616	36.550	2.42	1.815	0.027	232.7	1.5	7.9	27.1	50.8
48	25	50	200	79.201	74.391	29.209	29.137	2.63	1.829	0.027	234.5	1.5	4.4	22.4	30.7
49	6	50	12	77.602	76.848	35.531	35.464	6.24	0.121	0.011	15.5	4.2	8.9	15.0	29.3
50	18	200	12	79.633	78.793	35.548	35.330	1.4	0.600	0.155	76.9	25.9	6.4	46.3	64.5

**Table A. 3** Experimental data for randomly input parameters

Sno	I	Ton	Toff	Wi	Wf	Ei	Ef	Time	MRR	EWR	MRR	EWR	Ra	AWLT	Rt
	Amp	$\mu$ s	$\mu$ s	g	g	g	g	min	g/min	g/min	mm <sup>3</sup> /min	%	$\mu$ m	$\mu$ m	$\mu$ m
51	3	3	3	81.348	81.140	36.118	36.113	38.37	0.005	0.000	0.7	2.6	2.2	6.7	14.2
52	6	3	6	80.555	79.894	35.787	35.777	9.27	0.071	0.001	9.1	1.5	3.4	2.0	22.4
53	12	50	6	80.725	78.933	36.900	36.629	4	0.448	0.068	57.4	15.1	6.8	14.3	47.2
54	25	3	25	81.791	58.863	36.902	36.558	18.41	1.245	0.019	159.7	1.5	2.2	9.4	19.7
55	6	50	12	79.552	77.678	35.817	35.624	12.21	0.153	0.016	19.7	10.3	4.6	11.0	28.1
56	25	12	12	80.251	74.051	35.616	35.523	5.45	1.138	0.017	145.9	1.5	3.9	11.5	29.4
57	6	12	3	80.749	76.764	35.750	35.455	26.37	0.151	0.011	19.4	7.4	2.8	10.0	27.1
58	25	50	3	79.820	70.554	35.743	33.241	8.03	1.154	0.312	147.9	27.0	6.5	21.8	48.7
59	12	25	3	80.343	77.847	35.050	34.698	5.45	0.458	0.065	58.7	14.1	6.3	12.2	44.1
60	3	12	3	80.783	79.317	36.086	36.001	22	0.067	0.004	8.5	5.8	2.4	2.8	16.3
61	3	25	6	79.651	78.626	35.780	35.709	15.38	0.067	0.005	8.5	6.9	2.7	17.7	16.7
62	3	50	12	80.817	80.290	34.847	34.805	14.47	0.036	0.003	4.7	8.0	3.4	25.4	17.4
63	3	100	25	78.672	77.659	36.557	36.449	18.15	0.056	0.006	7.2	10.7	3.9	11.9	22.3
64	6	3	3	79.339	78.962	27.792	27.780	6.08	0.062	0.002	7.9	3.2	3.4	3.6	25.0
65	6	25	6	77.649	76.909	36.139	36.073	4.32	0.171	0.015	22.0	8.9	3.9	14.3	27.5
66	6	50	6	80.994	80.667	36.750	36.719	2.05	0.160	0.015	20.5	9.5	4.5	24.8	33.3
67	6	100	12	79.405	79.099	35.932	35.897	3.13	0.098	0.011	12.5	11.3	5.7	20.8	38.4
68	12	3	3	79.549	78.483	35.960	35.912	5.15	0.207	0.009	26.5	4.5	5.7	14.8	38.8
69	9	100	12	79.102	78.365	35.211	35.104	3.16	0.233	0.034	29.9	14.5	6.9	31.6	46.6
70	9	400	50	78.434	76.962	35.997	35.804	7.48	0.197	0.026	25.2	13.1	5.7	25.0	40.5
71	12	400	25	79.065	78.922	35.032	34.988	2.33	0.061	0.019	7.8	30.9	7.2	35.7	37.6
72	18	100	50	78.366	76.525	35.764	35.652	1.42	1.297	0.079	166.2	6.1	5.7	23.4	37.0
73	18	200	25	78.343	77.220	35.590	35.389	1.43	0.785	0.141	100.7	17.9	7.7	33.5	56.2
74	18	400	12	78.491	77.996	35.455	35.252	1.58	0.313	0.129	40.1	41.1	5.6	30.8	46.8
75	25	200	12	110.194	101.689	140.900	138.195	8.32	1.022	0.325	131.1	31.8	11.0	58.1	88.0

**Table A. 3 Continues**

76	50	200	25	112.016	87.150	143.552	136.374	8.17	3.044	0.879	390.2	28.9	8.8	62.4	79.3
77	50	100	12	110.735	89.211	138.742	132.435	7.47	2.881	0.844	369.4	29.3	9.0	50.7	74.0
78	50	25	6	110.117	99.537	134.728	132.728	4.36	2.427	0.459	311.1	18.9	5.4	24.8	40.3
79	50	50	6	111.772	89.458	140.424	134.823	8.25	2.705	0.679	346.8	25.1	6.5	33.7	51.8
80	50	100	50	111.198	89.396	125.418	124.023	12.29	1.774	0.114	227.4	6.4	7.1	41.1	52.3
81	50	200	200	110.848	84.766	142.427	142.036	14.17	1.841	0.028	236.0	1.5	9.4	52.7	131.3
82	50	1600	200	111.022	96.938	145.700	139.785	11.48	1.227	0.515	157.3	42.0	14.7	119.4	138.6
83	50	800	100	110.682	88.400	140.994	129.395	9.08	2.454	1.277	314.6	52.1	15.2	158.1	124.9
84	50	400	100	110.224	95.357	143.277	140.913	8.24	1.804	0.287	231.3	15.9	10.9	111.1	101.6
85	50	200	50	111.630	96.578	144.084	141.585	8.35	1.803	0.299	231.1	16.6	13.2	104.8	70.5
86	12	200	12	79.519	78.930	34.610	34.515	2.46	0.239	0.039	30.7	8.5	16.1	35.6	57.5
87	50	400	800	131.013	99.309	145.309	144.348	17.46	1.816	0.055	232.8	15.9	3.0	156.8	4.5

## APPENDIX B. TABLES OF CASE STUDY 1

**Table B. 1** Alternatives of two-stages machining for Case Study 1

<i>No</i>	<i>I</i> (amp)	<i>T<sub>on</sub></i> ( $\mu$ s)	<i>T<sub>off</sub></i> ( $\mu$ s)	MRR (mm <sup>3</sup> /min)	<i>R<sub>a</sub></i> ( $\mu$ m)	EWR (%)	AWLT ( $\mu$ m)	Time (min)	Mach-time (min)
1	50	200	25	390	10.9	25.9	62.4	273.5	1880.6
	3	50	25	15.9	2.7	5.6	6.6	1607.1	
2	44	100	12	375.2	8.7	13.3	19.7	286.7	1102.1
	3	50	25	15.9	2.7	5.6	6.6	815.4	
3	37	50	12	300.1	5.2	7.5	20.7	358.4	831.1
	3	50	25	15.9	2.7	5.6	6.6	472.7	
4	31	50	50	244.2	6.1	5.3	10.7	441.3	770.7
	3	50	25	15.9	2.7	5.6	6.6	329.4	
5	25	100	200	241.5	5.7	1.3	25.1	445.0	556.0
	3	50	25	15.9	2.7	5.6	6.6	111.0	
6	18	100	200	234.2	7.9	1.5	27.1	458.6	584.2
	3	50	25	15.9	2.7	5.6	6.6	125.6	
7	12	200	200	230.4	7.6	1.5	28.6	466.1	593.6
	3	50	25	15.9	2.7	5.6	6.6	127.6	
8	9	12	50	132	4.4	0.7	18.9	815.1	882.2
	3	50	25	15.9	2.7	5.6	6.6	67.2	
9	6	12	50	107.7	2.9	1.4	19.3	998.9	1108.1
	3	50	25	15.9	2.7	5.6	6.6	109.2	

**Table B. 2** Alternatives of three-stages machining for Case Study 1

<i>No</i>	<i>I</i> (amp)	<i>T<sub>on</sub></i> ( $\mu$ s)	<i>T<sub>off</sub></i> ( $\mu$ s)	MRR (mm <sup>3</sup> /min)	<i>R<sub>a</sub></i> ( $\mu$ m)	EWR (%)	AWLT ( $\mu$ m)	Time (min)	Mach-time (min)
1	50	200	25	390	10.9	25.9	62.4	272.40	553.6
	44	100	12	375.2	8.7	13.3	19.7	67.84	
	3	50	25	15.9	2.7	5.6	6.6	213.32	
2	50	200	25	390	10.9	25.9	62.4	272.35	490.4
	37	50	12	300.1	5.2	7.5	20.7	84.80	
	3	50	25	15.9	2.7	5.6	6.6	133.28	
3	50	200	25	390	10.9	25.9	62.4	272.89	466.3
	31	50	50	244.2	6.1	5.3	10.7	104.42	
	3	50	25	15.9	2.7	5.6	6.6	89.02	
4	50	200	25	390	10.9	25.9	62.4	272.11	429.6
	25	100	200	241.5	5.7	1.3	25.1	105.28	
	3	50	25	15.9	2.7	5.6	6.6	52.26	
5	50	200	25	390	10.9	25.9	62.4	272.00	438.3
	18	100	200	234.2	7.9	1.5	27.1	108.52	
	3	50	25	15.9	2.7	5.6	6.6	57.76	
6	50	200	25	390	10.9	25.9	62.4	271.91	442.0
	12	200	200	230.4	7.6	1.5	28.6	110.28	
	3	50	25	15.9	2.7	5.6	6.6	59.79	
7	50	200	25	390	10.9	25.9	62.4	272.44	500.8
	9	12	50	132	4.4	0.7	18.9	192.86	
	3	50	25	15.9	2.7	5.6	6.6	35.47	

**Table B. 2** Continues

8	50	200	25	390	10.9	25.9	62.4	272.42	554.6
	6	12	50	107.7	2.9	1.4	19.3	236.35	
	3	50	25	15.9	2.7	5.6	6.6	45.83	
9	44	100	12	375.2	8.7	13.3	19.7	285.53	410.0
	37	50	12	300.1	5.2	7.5	20.7	43.02	
	3	50	25	15.9	2.7	5.6	6.6	81.46	
10	44	100	12	375.2	8.7	13.3	19.7	286.10	391.4
	31	50	50	244.2	6.1	5.3	10.7	52.98	
	3	50	25	15.9	2.7	5.6	6.6	52.32	
11	44	100	12	375.2	8.7	13.3	19.7	285.28	382.0
	25	100	200	241.5	5.7	1.3	25.1	53.42	
	3	50	25	15.9	2.7	5.6	6.6	43.28	
12	44	100	12	375.2	8.7	13.3	19.7	285.16	387.6
	18	100	200	234.2	7.9	1.5	27.1	55.06	
	3	50	25	15.9	2.7	5.6	6.6	47.41	
13	44	100	12	375.2	8.7	13.3	19.7	285.07	390.5
	12	200	200	230.4	7.6	1.5	28.6	55.95	
	3	50	25	15.9	2.7	5.6	6.6	49.44	
14	44	100	12	375.2	8.7	13.3	19.7	285.63	414.1
	9	12	50	132	4.4	0.7	18.9	97.85	
	3	50	25	15.9	2.7	5.6	6.6	30.63	
15	44	100	12	375.2	8.7	13.3	19.7	285.61	441.7
	6	12	50	107.7	2.9	1.4	19.3	119.91	
	3	50	25	15.9	2.7	5.6	6.6	36.15	
16	37	50	12	300.1	5.2	7.5	20.7	356.62	423.0
	31	50	200	243.4	3.2	0.5	24.8	30.73	
	3	50	25	15.9	2.7	5.6	6.6	35.70	
17	37	50	12	300.1	5.2	7.5	20.7	356.79	419.3
	25	50	200	236	4.3	0.1	22.4	31.71	
	3	50	25	15.9	2.7	5.6	6.6	30.80	
18	37	50	12	300.1	5.2	7.5	20.7	357.21	443.8
	18	50	50	175.4	3.5	5.2	16.5	42.71	
	3	50	25	15.9	2.7	5.6	6.6	43.86	
19	37	50	12	300.1	5.2	7.5	20.7	357.06	427.1
	12	100	100	195.9	3.4	1.6	18.6	38.23	
	3	50	25	15.9	2.7	5.6	6.6	31.84	
20	37	50	12	300.1	5.2	7.5	20.7	357.04	442.3
	9	12	50	132	4.4	0.7	18.9	56.73	
	3	50	25	15.9	2.7	5.6	6.6	28.53	
21	37	50	12	300.1	5.2	7.5	20.7	357.01	458.5
	6	12	50	107.7	2.9	1.4	19.3	69.52	
	3	50	25	15.9	2.7	5.6	6.6	31.96	
22	31	50	50	244.2	6.1	5.3	10.7	439.10	498.5
	25	100	200	241.5	5.7	1.3	25.1	21.58	
	3	50	25	15.9	2.7	5.6	6.6	37.78	
23	31	50	50	244.2	6.1	5.3	10.7	439.86	507.0
	18	50	50	175.4	3.5	5.2	16.5	29.76	
	3	50	25	15.9	2.7	5.6	6.6	37.35	
24	31	50	50	244.2	6.1	5.3	10.7	439.67	496.1
	12	100	100	195.9	3.4	1.6	18.6	26.63	
	3	50	25	15.9	2.7	5.6	6.6	29.84	

**Table B. 2** Continues

25	31	50	50	244.2	6.1	5.3	10.7	439.65	506.8
	9	12	50	132	4.4	0.7	18.9	39.52	
	3	50	25	15.9	2.7	5.6	6.6	27.66	
26	31	50	50	244.2	6.1	5.3	10.7	439.61	518.3
	6	12	50	107.7	2.9	1.4	19.3	48.44	
	3	50	25	15.9	2.7	5.6	6.6	30.21	
27	25	100	200	241.5	5.7	1.3	25.1	443.49	481.0
	18	50	50	175.4	3.5	5.2	16.5	10.04	
	3	50	25	15.9	2.7	5.6	6.6	27.44	
28	25	100	200	241.5	5.7	1.3	25.1	443.31	479.1
	12	100	100	195.9	3.4	1.6	18.6	8.98	
	3	50	25	15.9	2.7	5.6	6.6	26.79	
29	25	100	200	241.5	5.7	1.3	25.1	443.28	482.9
	9	12	50	132	4.4	0.7	18.9	13.33	
	3	50	25	15.9	2.7	5.6	6.6	26.32	
30	25	100	200	241.5	5.7	1.3	25.1	443.25	487.1
	6	12	50	107.7	2.9	1.4	19.3	16.34	
	3	50	25	15.9	2.7	5.6	6.6	27.54	
31	18	100	200	234.2	7.9	1.5	27.1	456.03	505.1
	12	200	200	230.4	7.6	1.5	28.6	8.62	
	3	50	25	15.9	2.7	5.6	6.6	40.42	
32	18	100	200	234.2	7.9	1.5	27.1	456.91	498.4
	9	12	50	132	4.4	0.7	18.9	15.07	
	3	50	25	15.9	2.7	5.6	6.6	26.41	
33	18	100	200	234.2	7.9	1.5	27.1	456.88	503.1
	6	12	50	107.7	2.9	1.4	19.3	18.47	
	3	50	25	15.9	2.7	5.6	6.6	27.72	
34	12	200	200	230.4	7.6	1.5	28.6	464.31	506.0
	9	12	50	132	4.4	0.7	18.9	15.31	
	3	50	25	15.9	2.7	5.6	6.6	26.42	
35	12	200	200	230.4	7.6	1.5	28.6	464.27	510.8
	6	12	50	107.7	2.9	1.4	19.3	18.77	
	3	50	25	15.9	2.7	5.6	6.6	27.74	
36	9	12	50	132	4.4	0.7	18.9	811.95	848.8
	6	12	50	107.7	2.9	1.4	19.3	9.88	
	3	50	25	15.9	2.7	5.6	6.6	27.01	

**Table B. 3** Alternatives of four-stages machining for Case Study 1

<i>No</i>	<i>I</i> (amp)	<i>T<sub>on</sub></i> ( $\mu$ s)	<i>T<sub>off</sub></i> ( $\mu$ s)	<b>MRR</b> (mm <sup>3</sup> /min)	<i>R<sub>a</sub></i> ( $\mu$ m)	<b>EWR</b> (%)	<b>AWLT</b> ( $\mu$ m)	<b>Time</b> (min)	<b>Mach-time</b> (min)
1	50	200	25	390	10.9	25.9	62.4	271.3	392.1
	44	100	12	375.2	8.7	13.3	19.7	67.6	
	37	50	12	300.1	5.2	7.5	20.7	11.3	
	3	50	25	15.9	2.7	5.6	6.6	42.0	
2	50	200	25	390	10.9	25.9	62.4	271.8	377.8
	44	100	12	375.2	8.7	13.3	19.7	67.7	
	31	50	50	244.2	6.1	5.3	10.7	13.9	
	3	50	25	15.9	2.7	5.6	6.6	24.4	



**Table B. 3** Continues

3	50	200	25	390	10.9	25.9	62.4	271.0	389.0
	44	100	12	375.2	8.7	13.3	19.7	67.5	
	25	100	200	241.5	5.7	1.3	25.1	14.0	
	3	50	25	15.9	2.7	5.6	6.6	36.5	
4	50	200	25	390	10.9	25.9	62.4	270.9	392.3
	44	100	12	375.2	8.7	13.3	19.7	67.5	
	18	100	200	234.2	7.9	1.5	27.1	14.4	
	3	50	25	15.9	2.7	5.6	6.6	39.5	
5	50	200	25	390	10.9	25.9	62.4	270.8	394.5
	44	100	12	375.2	8.7	13.3	19.7	67.5	
	12	200	200	230.4	7.6	1.5	28.6	14.6	
	3	50	25	15.9	2.7	5.6	6.6	41.6	
6	50	200	25	390	10.9	25.9	62.4	271.4	391.5
	44	100	12	375.2	8.7	13.3	19.7	67.6	
	9	12	50	132	4.4	0.7	18.9	25.6	
	3	50	25	15.9	2.7	5.6	6.6	26.9	
7	50	200	25	390	10.9	25.9	62.4	271.3	399.1
	44	100	12	375.2	8.7	13.3	19.7	67.6	
	6	12	50	107.7	2.9	1.4	19.3	31.4	
	3	50	25	15.9	2.7	5.6	6.6	28.8	
8	50	200	25	390	10.9	25.9	62.4	271.0	398.3
	37	50	12	300.1	5.2	7.5	20.7	84.4	
	31	50	200	243.4	3.2	0.5	24.8	8.7	
	3	50	25	15.9	2.7	5.6	6.6	34.2	
9	50	200	25	390	10.9	25.9	62.4	271.1	395.0
	37	50	12	300.1	5.2	7.5	20.7	84.4	
	25	50	200	236	4.3	0.1	22.4	8.9	
	3	50	25	15.9	2.7	5.6	6.6	30.5	
10	50	200	25	390	10.9	25.9	62.4	271.4	396.5
	37	50	12	300.1	5.2	7.5	20.7	84.5	
	18	50	50	175.4	3.5	5.2	16.5	12.0	
	3	50	25	15.9	2.7	5.6	6.6	28.4	
11	50	200	25	390	10.9	25.9	62.4	271.3	393.7
	37	50	12	300.1	5.2	7.5	20.7	84.5	
	12	100	100	195.9	3.4	1.6	18.6	10.8	
	3	50	25	15.9	2.7	5.6	6.6	27.1	
12	50	200	25	390	10.9	25.9	62.4	271.3	398.3
	37	50	12	300.1	5.2	7.5	20.7	84.5	
	9	12	50	132	4.4	0.7	18.9	16.0	
	3	50	25	15.9	2.7	5.6	6.6	26.5	
13	50	200	25	390	10.9	25.9	62.4	271.3	403.2
	37	50	12	300.1	5.2	7.5	20.7	84.5	
	6	12	50	107.7	2.9	1.4	19.3	19.6	
	3	50	25	15.9	2.7	5.6	6.6	27.8	
14	50	200	25	390	10.9	25.9	62.4	271.5	416.3
	31	50	50	244.2	6.1	5.3	10.7	103.9	
	25	100	200	241.5	5.7	1.3	25.1	5.8	
	3	50	25	15.9	2.7	5.6	6.6	35.1	

**Table B. 3 Continues**

15	50	200	25	390	10.9	25.9	62.4	272.0	410.5
	31	50	50	244.2	6.1	5.3	10.7	104.1	
	18	50	50	175.4	3.5	5.2	16.5	8.0	
	3	50	25	15.9	2.7	5.6	6.6	26.4	
16	50	200	25	390	10.9	25.9	62.4	271.9	409.6
	31	50	50	244.2	6.1	5.3	10.7	104.0	
	12	100	100	195.9	3.4	1.6	18.6	7.2	
	3	50	25	15.9	2.7	5.6	6.6	26.5	
17	50	200	25	390	10.9	25.9	62.4	271.9	412.8
	31	50	50	244.2	6.1	5.3	10.7	104.0	
	9	12	50	132	4.4	0.7	18.9	10.7	
	3	50	25	15.9	2.7	5.6	6.6	26.2	
18	50	200	25	390	10.9	25.9	62.4	271.8	416.2
	31	50	50	244.2	6.1	5.3	10.7	104.0	
	6	12	50	107.7	2.9	1.4	19.3	13.1	
	3	50	25	15.9	2.7	5.6	6.6	27.3	
19	50	200	25	390	10.9	25.9	62.4	271.2	405.6
	25	100	200	241.5	5.7	1.3	25.1	104.9	
	18	50	50	175.4	3.5	5.2	16.5	4.7	
	3	50	25	15.9	2.7	5.6	6.6	24.8	
20	50	200	25	390	10.9	25.9	62.4	271.1	406.2
	25	100	200	241.5	5.7	1.3	25.1	104.9	
	12	100	100	195.9	3.4	1.6	18.6	4.2	
	3	50	25	15.9	2.7	5.6	6.6	26.0	
21	50	200	25	390	10.9	25.9	62.4	271.1	408.2
	25	100	200	241.5	5.7	1.3	25.1	104.9	
	9	12	50	132	4.4	0.7	18.9	6.3	
	3	50	25	15.9	2.7	5.6	6.6	26.0	
22	50	200	25	390	10.9	25.9	62.4	271.1	410.4
	25	100	200	241.5	5.7	1.3	25.1	104.9	
	6	12	50	107.7	2.9	1.4	19.3	7.7	
	3	50	25	15.9	2.7	5.6	6.6	26.8	
23	50	200	25	390	10.9	25.9	62.4	270.4	421.8
	18	100	200	234.2	7.9	1.5	27.1	107.9	
	12	200	200	230.4	7.6	1.5	28.6	4.0	
	3	50	25	15.9	2.7	5.6	6.6	39.5	
24	50	200	25	390	10.9	25.9	62.4	271.0	412.0
	18	100	200	234.2	7.9	1.5	27.1	108.1	
	9	12	50	132	4.4	0.7	18.9	6.9	
	3	50	25	15.9	2.7	5.6	6.6	26.0	
25	50	200	25	390	10.9	25.9	62.4	270.9	414.4
	18	100	200	234.2	7.9	1.5	27.1	108.1	
	6	12	50	107.7	2.9	1.4	19.3	8.5	
	3	50	25	15.9	2.7	5.6	6.6	26.9	
26	50	200	25	390	10.9	25.9	62.4	270.9	413.9
	12	200	200	230.4	7.6	1.5	28.6	109.9	
	9	12	50	132	4.4	0.7	18.9	7.2	
	3	50	25	15.9	2.7	5.6	6.6	26.0	

**Table B. 3 Continues**

27	50	200	25	390	10.9	25.9	62.4	270.9	416.4
	12	200	200	230.4	7.6	1.5	28.6	109.9	
	6	12	50	107.7	2.9	1.4	19.3	8.8	
	3	50	25	15.9	2.7	5.6	6.6	26.9	
28	50	200	25	390	10.9	25.9	62.4	271.4	495.4
	9	12	50	132	4.4	0.7	18.9	192.1	
	6	12	50	107.7	2.9	1.4	19.3	5.2	
	3	50	25	15.9	2.7	5.6	6.6	26.6	
29	44	100	12	375.2	8.7	13.3	19.7	284.1	366.2
	37	50	12	300.1	5.2	7.5	20.7	42.8	
	31	50	200	243.4	3.2	0.5	24.8	5.3	
	3	50	25	15.9	2.7	5.6	6.6	34.0	
30	44	100	12	375.2	8.7	13.3	19.7	284.2	363.0
	37	50	12	300.1	5.2	7.5	20.7	42.8	
	25	50	200	236	4.3	0.1	22.4	5.5	
	3	50	25	15.9	2.7	5.6	6.6	30.5	
31	44	100	12	375.2	8.7	13.3	19.7	284.6	360.9
	37	50	12	300.1	5.2	7.5	20.7	42.9	
	18	50	50	175.4	3.5	5.2	16.5	7.4	
	3	50	25	15.9	2.7	5.6	6.6	26.1	
32	44	100	12	375.2	8.7	13.3	19.7	284.5	360.3
	37	50	12	300.1	5.2	7.5	20.7	42.9	
	12	100	100	195.9	3.4	1.6	18.6	6.6	
	3	50	25	15.9	2.7	5.6	6.6	26.4	
33	44	100	12	375.2	8.7	13.3	19.7	284.4	363.2
	37	50	12	300.1	5.2	7.5	20.7	42.9	
	9	12	50	132	4.4	0.7	18.9	9.8	
	3	50	25	15.9	2.7	5.6	6.6	26.1	
34	44	100	12	375.2	8.7	13.3	19.7	284.4	366.4
	37	50	12	300.1	5.2	7.5	20.7	42.9	
	6	12	50	107.7	2.9	1.4	19.3	12.0	
	3	50	25	15.9	2.7	5.6	6.6	27.2	
35	44	100	12	375.2	8.7	13.3	19.7	284.7	375.4
	31	50	50	244.2	6.1	5.3	10.7	52.7	
	25	100	200	241.5	5.7	1.3	25.1	3.4	
	3	50	25	15.9	2.7	5.6	6.6	34.6	
36	44	100	12	375.2	8.7	13.3	19.7	285.2	367.5
	31	50	50	244.2	6.1	5.3	10.7	52.8	
	18	50	50	175.4	3.5	5.2	16.5	4.7	
	3	50	25	15.9	2.7	5.6	6.6	24.8	
37	44	100	12	375.2	8.7	13.3	19.7	285.0	368.0
	31	50	50	244.2	6.1	5.3	10.7	52.8	
	12	100	100	195.9	3.4	1.6	18.6	4.2	
	3	50	25	15.9	2.7	5.6	6.6	26.0	
38	44	100	12	375.2	8.7	13.3	19.7	285.0	370.0
	31	50	50	244.2	6.1	5.3	10.7	52.8	
	9	12	50	132	4.4	0.7	18.9	6.3	
	3	50	25	15.9	2.7	5.6	6.6	26.0	

**Table B. 3 Continues**

39	44	100	12	375.2	8.7	13.3	19.7	285.0	372.3
	31	50	50	244.2	6.1	5.3	10.7	52.8	
	6	12	50	107.7	2.9	1.4	19.3	7.7	
	3	50	25	15.9	2.7	5.6	6.6	26.8	
40	44	100	12	375.2	8.7	13.3	19.7	284.3	365.8
	25	100	200	241.5	5.7	1.3	25.1	53.2	
	18	50	50	175.4	3.5	5.2	16.5	3.9	
	3	50	25	15.9	2.7	5.6	6.6	24.4	
41	44	100	12	375.2	8.7	13.3	19.7	284.2	366.8
	25	100	200	241.5	5.7	1.3	25.1	53.2	
	12	100	100	195.9	3.4	1.6	18.6	3.5	
	3	50	25	15.9	2.7	5.6	6.6	25.8	
42	44	100	12	375.2	8.7	13.3	19.7	284.2	368.5
	25	100	200	241.5	5.7	1.3	25.1	53.2	
	9	12	50	132	4.4	0.7	18.9	5.2	
	3	50	25	15.9	2.7	5.6	6.6	25.9	
43	44	100	12	375.2	8.7	13.3	19.7	284.2	370.5
	25	100	200	241.5	5.7	1.3	25.1	53.2	
	6	12	50	107.7	2.9	1.4	19.3	6.4	
	3	50	25	15.9	2.7	5.6	6.6	26.7	
44	44	100	12	375.2	8.7	13.3	19.7	283.5	380.9
	18	100	200	234.2	7.9	1.5	27.1	54.7	
	12	200	200	230.4	7.6	1.5	28.6	3.3	
	3	50	25	15.9	2.7	5.6	6.6	39.4	
45	44	100	12	375.2	8.7	13.3	19.7	284.1	370.6
	18	100	200	234.2	7.9	1.5	27.1	54.9	
	9	12	50	132	4.4	0.7	18.9	5.7	
	3	50	25	15.9	2.7	5.6	6.6	25.9	
46	44	100	12	375.2	8.7	13.3	19.7	284.1	372.6
	18	100	200	234.2	7.9	1.5	27.1	54.8	
	6	12	50	107.7	2.9	1.4	19.3	7.0	
	3	50	25	15.9	2.7	5.6	6.6	26.8	
47	44	100	12	375.2	8.7	13.3	19.7	284.0	371.6
	12	200	200	230.4	7.6	1.5	28.6	55.7	
	9	12	50	132	4.4	0.7	18.9	5.9	
	3	50	25	15.9	2.7	5.6	6.6	25.9	
48	44	100	12	375.2	8.7	13.3	19.7	284.0	373.8
	12	200	200	230.4	7.6	1.5	28.6	55.7	
	6	12	50	107.7	2.9	1.4	19.3	7.3	
	3	50	25	15.9	2.7	5.6	6.6	26.8	
49	44	100	12	375.2	8.7	13.3	19.7	284.5	413.1
	9	12	50	132	4.4	0.7	18.9	97.5	
	6	12	50	107.7	2.9	1.4	19.3	4.5	
	3	50	25	15.9	2.7	5.6	6.6	26.6	
50	37	50	12	300.1	5.2	7.5	20.7	355.9	404.8
	31	50	200	243.4	3.2	0.5	24.8	30.7	
	25	12	50	209.2	3.1	8.6	9.4	2.7	
	3	50	25	15.9	2.7	5.6	6.6	15.4	

**Table B. 3 Continues**

51	37	50	12	300.1	5.2	7.5	20.7	354.7	434.4
	31	50	200	243.4	3.2	0.5	24.8	30.6	
	18	800	200	67.9	3	12.7	27.2	8.3	
	3	50	25	15.9	2.7	5.6	6.6	40.8	
52	37	50	12	300.1	5.2	7.5	20.7	354.9	425.4
	31	50	200	243.4	3.2	0.5	24.8	30.6	
	9	100	50	105.3	3	5.7	24.2	5.4	
	3	50	25	15.9	2.7	5.6	6.6	34.6	
53	37	50	12	300.1	5.2	7.5	20.7	355.2	417.7
	31	50	200	243.4	3.2	0.5	24.8	30.6	
	6	12	50	107.7	2.9	1.4	19.3	5.3	
	3	50	25	15.9	2.7	5.6	6.6	26.6	
54	37	50	12	300.1	5.2	7.5	20.7	355.6	413.8
	25	50	200	236	4.3	0.1	22.4	31.6	
	18	50	50	175.4	3.5	5.2	16.5	2.8	
	3	50	25	15.9	2.7	5.6	6.6	23.8	
55	37	50	12	300.1	5.2	7.5	20.7	355.5	415.2
	25	50	200	236	4.3	0.1	22.4	31.6	
	12	100	100	195.9	3.4	1.6	18.6	2.5	
	3	50	25	15.9	2.7	5.6	6.6	25.7	
56	37	50	12	300.1	5.2	7.5	20.7	355.4	418.2
	25	50	200	236	4.3	0.1	22.4	31.6	
	9	25	50	125.8	4.3	0.4	20.1	3.9	
	3	50	25	15.9	2.7	5.6	6.6	27.4	
57	37	50	12	300.1	5.2	7.5	20.7	355.4	418.1
	25	50	200	236	4.3	0.1	22.4	31.6	
	6	12	50	107.7	2.9	1.4	19.3	4.5	
	3	50	25	15.9	2.7	5.6	6.6	26.6	
58	37	50	12	300.1	5.2	7.5	20.7	355.9	427.8
	18	50	50	175.4	3.5	5.2	16.5	42.6	
	12	100	100	195.9	3.4	1.6	18.6	3.5	
	3	50	25	15.9	2.7	5.6	6.6	25.8	
59	37	50	12	300.1	5.2	7.5	20.7	355.5	439.6
	18	50	50	175.4	3.5	5.2	16.5	42.5	
	9	100	50	105.3	3	5.7	24.2	6.6	
	3	50	25	15.9	2.7	5.6	6.6	35.0	
60	37	50	12	300.1	5.2	7.5	20.7	355.8	431.6
	18	50	50	175.4	3.5	5.2	16.5	42.6	
	6	12	50	107.7	2.9	1.4	19.3	6.5	
	3	50	25	15.9	2.7	5.6	6.6	26.7	
61	37	50	12	300.1	5.2	7.5	20.7	355.3	432.6
	12	100	100	195.9	3.4	1.6	18.6	38.0	
	9	100	50	105.3	3	5.7	24.2	4.8	
	3	50	25	15.9	2.7	5.6	6.6	34.4	
62	37	50	12	300.1	5.2	7.5	20.7	355.7	425.0
	12	100	100	195.9	3.4	1.6	18.6	38.1	
	6	12	50	107.7	2.9	1.4	19.3	4.7	
	3	50	25	15.9	2.7	5.6	6.6	26.6	

**Table B. 3 Continues**

63	37	50	12	300.1	5.2	7.5	20.7	355.7	442.9
	9	12	50	132	4.4	0.7	18.9	56.5	
	6	12	50	107.7	2.9	1.4	19.3	4.2	
	3	50	25	15.9	2.7	5.6	6.6	26.5	
64	31	50	50	244.2	6.1	5.3	10.7	437.7	486.7
	25	100	200	241.5	5.7	1.3	25.1	21.5	
	18	50	50	175.4	3.5	5.2	16.5	3.4	
	3	50	25	15.9	2.7	5.6	6.6	24.1	
65	31	50	50	244.2	6.1	5.3	10.7	437.5	487.8
	25	100	200	241.5	5.7	1.3	25.1	21.5	
	12	100	100	195.9	3.4	1.6	18.6	3.1	
	3	50	25	15.9	2.7	5.6	6.6	25.8	
66	31	50	50	244.2	6.1	5.3	10.7	437.4	489.3
	25	100	200	241.5	5.7	1.3	25.1	21.5	
	9	12	50	132	4.4	0.7	18.9	4.5	
	3	50	25	15.9	2.7	5.6	6.6	25.9	
67	31	50	50	244.2	6.1	5.3	10.7	437.4	491.1
	25	100	200	241.5	5.7	1.3	25.1	21.5	
	6	12	50	107.7	2.9	1.4	19.3	5.6	
	3	50	25	15.9	2.7	5.6	6.6	26.6	
68	31	50	50	244.2	6.1	5.3	10.7	438.2	496.7
	18	50	50	175.4	3.5	5.2	16.5	29.7	
	12	100	100	195.9	3.4	1.6	18.6	3.0	
	3	50	25	15.9	2.7	5.6	6.6	25.8	
69	31	50	50	244.2	6.1	5.3	10.7	437.7	507.6
	18	50	50	175.4	3.5	5.2	16.5	29.6	
	9	100	50	105.3	3	5.7	24.2	5.6	
	3	50	25	15.9	2.7	5.6	6.6	34.7	
70	31	50	50	244.2	6.1	5.3	10.7	438.2	499.9
	18	50	50	175.4	3.5	5.2	16.5	29.6	
	6	12	50	107.7	2.9	1.4	19.3	5.5	
	3	50	25	15.9	2.7	5.6	6.6	26.6	
71	31	50	50	244.2	6.1	5.3	10.7	437.5	502.8
	12	100	100	195.9	3.4	1.6	18.6	26.5	
	9	100	50	105.3	3	5.7	24.2	4.5	
	3	50	25	15.9	2.7	5.6	6.6	34.3	
72	31	50	50	244.2	6.1	5.3	10.7	438.0	495.5
	12	100	100	195.9	3.4	1.6	18.6	26.5	
	6	12	50	107.7	2.9	1.4	19.3	4.4	
	3	50	25	15.9	2.7	5.6	6.6	26.6	
73	31	50	50	244.2	6.1	5.3	10.7	437.9	507.9
	9	12	50	132	4.4	0.7	18.9	39.4	
	6	12	50	107.7	2.9	1.4	19.3	4.1	
	3	50	25	15.9	2.7	5.6	6.6	26.5	
74	25	100	200	241.5	5.7	1.3	25.1	441.8	479.7
	18	50	50	175.4	3.5	5.2	16.5	10.0	
	12	100	100	195.9	3.4	1.6	18.6	2.2	
	3	50	25	15.9	2.7	5.6	6.6	25.6	

**Table B. 3** Continues

75	25	100	200	241.5	5.7	1.3	25.1	441.3	489.7
	18	50	50	175.4	3.5	5.2	16.5	10.0	
	9	100	50	105.3	3	5.7	24.2	4.1	
	3	50	25	15.9	2.7	5.6	6.6	34.2	
76	25	100	200	241.5	5.7	1.3	25.1	441.8	482.3
	18	50	50	175.4	3.5	5.2	16.5	10.0	
	6	12	50	107.7	2.9	1.4	19.3	4.0	
	3	50	25	15.9	2.7	5.6	6.6	26.5	
77	25	100	200	241.5	5.7	1.3	25.1	441.2	488.3
	12	100	100	195.9	3.4	1.6	18.6	8.9	
	9	100	50	105.3	3	5.7	24.2	4.0	
	3	50	25	15.9	2.7	5.6	6.6	34.2	
78	25	100	200	241.5	5.7	1.3	25.1	441.6	481.0
	12	100	100	195.9	3.4	1.6	18.6	9.0	
	6	12	50	107.7	2.9	1.4	19.3	3.9	
	3	50	25	15.9	2.7	5.6	6.6	26.5	
79	25	100	200	241.5	5.7	1.3	25.1	441.6	485.2
	9	12	50	132	4.4	0.7	18.9	13.3	
	6	12	50	107.7	2.9	1.4	19.3	3.9	
	3	50	25	15.9	2.7	5.6	6.6	26.5	
80	18	100	200	234.2	7.9	1.5	27.1	454.3	493.6
	12	200	200	230.4	7.6	1.5	28.6	8.6	
	9	12	50	132	4.4	0.7	18.9	4.9	
	3	50	25	15.9	2.7	5.6	6.6	25.9	
81	18	100	200	234.2	7.9	1.5	27.1	454.3	495.5
	12	200	200	230.4	7.6	1.5	28.6	8.6	
	6	12	50	107.7	2.9	1.4	19.3	6.0	
	3	50	25	15.9	2.7	5.6	6.6	26.7	
82	18	100	200	234.2	7.9	1.5	27.1	455.1	500.6
	9	12	50	132	4.4	0.7	18.9	15.0	
	6	12	50	107.7	2.9	1.4	19.3	3.9	
	3	50	25	15.9	2.7	5.6	6.6	26.5	
83	12	200	200	230.4	7.6	1.5	28.6	462.5	508.2
	9	12	50	132	4.4	0.7	18.9	15.3	
	6	12	50	107.7	2.9	1.4	19.3	3.9	
	3	50	25	15.9	2.7	5.6	6.6	26.5	

**Table B. 4** Alternatives of five-stages machining for Case Study 1

<i>No</i>	<i>I</i> (amp)	<i>T<sub>on</sub></i> ( $\mu$ s)	<i>T<sub>off</sub></i> ( $\mu$ s)	<b>MRR</b> (mm <sup>3</sup> /min)	<i>R<sub>a</sub></i> ( $\mu$ m)	<b>EWR</b> (%)	<b>AWLT</b> ( $\mu$ m)	<b>Time</b> (min)	<b>Mach-time</b> (min)
1	50	200	25	390	10.9	25.9	62.4	269.9	384.9
	44	100	12	375.2	8.7	13.3	19.7	67.2	
	37	50	12	300.1	5.2	7.5	20.7	11.2	
	31	50	200	243.4	3.2	0.5	24.8	2.7	
	3	50	25	15.9	2.7	5.6	6.6	33.8	
2	50	200	25	390	10.9	25.9	62.4	270.0	381.8
	44	100	12	375.2	8.7	13.3	19.7	67.3	
	37	50	12	300.1	5.2	7.5	20.7	11.2	
	25	50	200	236	4.3	0.1	22.4	2.8	
	3	50	25	15.9	2.7	5.6	6.6	30.4	
3	50	200	25	390	10.9	25.9	62.4	270.4	377.0
	44	100	12	375.2	8.7	13.3	19.7	67.3	
	37	50	12	300.1	5.2	7.5	20.7	11.2	
	18	50	50	175.4	3.5	5.2	16.5	3.8	
	3	50	25	15.9	2.7	5.6	6.6	24.3	
4	50	200	25	390	10.9	25.9	62.4	270.3	378.0
	44	100	12	375.2	8.7	13.3	19.7	67.3	
	37	50	12	300.1	5.2	7.5	20.7	11.2	
	12	100	100	195.9	3.4	1.6	18.6	3.4	
	3	50	25	15.9	2.7	5.6	6.6	25.8	
5	50	200	25	390	10.9	25.9	62.4	270.2	379.7
	44	100	12	375.2	8.7	13.3	19.7	67.3	
	37	50	12	300.1	5.2	7.5	20.7	11.2	
	9	12	50	132	4.4	0.7	18.9	5.1	
	3	50	25	15.9	2.7	5.6	6.6	25.9	
6	50	200	25	390	10.9	25.9	62.4	270.2	381.6
	44	100	12	375.2	8.7	13.3	19.7	67.3	
	37	50	12	300.1	5.2	7.5	20.7	11.2	
	6	12	50	107.7	2.9	1.4	19.3	6.2	
	3	50	25	15.9	2.7	5.6	6.6	26.7	
7	50	200	25	390	10.9	25.9	62.4	270.4	387.5
	44	100	12	375.2	8.7	13.3	19.7	67.4	
	31	50	50	244.2	6.1	5.3	10.7	13.8	
	25	100	200	241.5	5.7	1.3	25.1	1.6	
	3	50	25	15.9	2.7	5.6	6.6	34.3	
8	50	200	25	390	10.9	25.9	62.4	270.9	377.9
	44	100	12	375.2	8.7	13.3	19.7	67.5	
	31	50	50	244.2	6.1	5.3	10.7	13.8	
	18	50	50	175.4	3.5	5.2	16.5	2.2	
	3	50	25	15.9	2.7	5.6	6.6	23.5	
9	50	200	25	390	10.9	25.9	62.4	270.8	379.6
	44	100	12	375.2	8.7	13.3	19.7	67.4	
	31	50	50	244.2	6.1	5.3	10.7	13.8	
	12	100	100	195.9	3.4	1.6	18.6	2.0	
	3	50	25	15.9	2.7	5.6	6.6	25.6	



**Table B. 4 Continues**

10	50	200	25	390	10.9	25.9	62.4	270.8	380.8
	44	100	12	375.2	8.7	13.3	19.7	67.4	
	31	50	50	244.2	6.1	5.3	10.7	13.8	
	9	12	50	132	4.4	0.7	18.9	2.9	
	3	50	25	15.9	2.7	5.6	6.6	25.8	
11	50	200	25	390	10.9	25.9	62.4	270.8	382.1
	44	100	12	375.2	8.7	13.3	19.7	67.4	
	31	50	50	244.2	6.1	5.3	10.7	13.8	
	6	12	50	107.7	2.9	1.4	19.3	3.6	
	3	50	25	15.9	2.7	5.6	6.6	26.5	
12	50	200	25	390	10.9	25.9	62.4	270.1	378.7
	44	100	12	375.2	8.7	13.3	19.7	67.3	
	25	100	200	241.5	5.7	1.3	25.1	13.9	
	18	50	50	175.4	3.5	5.2	16.5	3.3	
	3	50	25	15.9	2.7	5.6	6.6	24.0	
13	50	200	25	390	10.9	25.9	62.4	270.0	379.9
	44	100	12	375.2	8.7	13.3	19.7	67.3	
	25	100	200	241.5	5.7	1.3	25.1	13.9	
	12	100	100	195.9	3.4	1.6	18.6	3.0	
	3	50	25	15.9	2.7	5.6	6.6	25.7	
14	50	200	25	390	10.9	25.9	62.4	270.0	381.4
	44	100	12	375.2	8.7	13.3	19.7	67.3	
	25	100	200	241.5	5.7	1.3	25.1	13.9	
	9	12	50	132	4.4	0.7	18.9	4.4	
	3	50	25	15.9	2.7	5.6	6.6	25.9	
15	50	200	25	390	10.9	25.9	62.4	270.0	383.1
	44	100	12	375.2	8.7	13.3	19.7	67.2	
	25	100	200	241.5	5.7	1.3	25.1	13.9	
	6	12	50	107.7	2.9	1.4	19.3	5.4	
	3	50	25	15.9	2.7	5.6	6.6	26.6	
16	50	200	25	390	10.9	25.9	62.4	269.4	392.8
	44	100	12	375.2	8.7	13.3	19.7	67.1	
	18	100	200	234.2	7.9	1.5	27.1	14.3	
	12	200	200	230.4	7.6	1.5	28.6	2.7	
	3	50	25	15.9	2.7	5.6	6.6	39.3	
17	50	200	25	390	10.9	25.9	62.4	269.9	382.1
	44	100	12	375.2	8.7	13.3	19.7	67.2	
	18	100	200	234.2	7.9	1.5	27.1	14.4	
	9	12	50	132	4.4	0.7	18.9	4.8	
	3	50	25	15.9	2.7	5.6	6.6	25.9	
18	50	200	25	390	10.9	25.9	62.4	269.9	383.9
	44	100	12	375.2	8.7	13.3	19.7	67.2	
	18	100	200	234.2	7.9	1.5	27.1	14.4	
	6	12	50	107.7	2.9	1.4	19.3	5.8	
	3	50	25	15.9	2.7	5.6	6.6	26.7	
19	50	200	25	390	10.9	25.9	62.4	269.8	382.5
	44	100	12	375.2	8.7	13.3	19.7	67.2	
	12	200	200	230.4	7.6	1.5	28.6	14.6	
	9	12	50	132	4.4	0.7	18.9	5.0	
	3	50	25	15.9	2.7	5.6	6.6	25.9	

**Table B. 4 Continues**

20	50	200	25	390	10.9	25.9	62.4	269.8	384.4
	44	100	12	375.2	8.7	13.3	19.7	67.2	
	12	200	200	230.4	7.6	1.5	28.6	14.6	
	6	12	50	107.7	2.9	1.4	19.3	6.1	
	3	50	25	15.9	2.7	5.6	6.6	26.7	
21	50	200	25	390	10.9	25.9	62.4	270.3	393.6
	44	100	12	375.2	8.7	13.3	19.7	67.3	
	9	12	50	132	4.4	0.7	18.9	25.5	
	6	12	50	107.7	2.9	1.4	19.3	4.0	
	3	50	25	15.9	2.7	5.6	6.6	26.5	
22	50	200	25	390	10.9	25.9	62.4	270.5	381.3
	37	50	12	300.1	5.2	7.5	20.7	84.2	
	31	50	200	243.4	3.2	0.5	24.8	8.7	
	25	12	50	209.2	3.1	8.6	9.4	2.6	
	3	50	25	15.9	2.7	5.6	6.6	15.3	
23	50	200	25	390	10.9	25.9	62.4	269.5	410.7
	37	50	12	300.1	5.2	7.5	20.7	83.9	
	31	50	200	243.4	3.2	0.5	24.8	8.6	
	18	800	200	67.9	3	12.7	27.2	8.0	
	3	50	25	15.9	2.7	5.6	6.6	40.7	
24	50	200	25	390	10.9	25.9	62.4	269.7	402.0
	37	50	12	300.1	5.2	7.5	20.7	84.0	
	31	50	200	243.4	3.2	0.5	24.8	8.6	
	9	100	50	105.3	3	5.7	24.2	5.1	
	3	50	25	15.9	2.7	5.6	6.6	34.5	
25	50	200	25	390	10.9	25.9	62.4	269.9	394.3
	37	50	12	300.1	5.2	7.5	20.7	84.1	
	31	50	200	243.4	3.2	0.5	24.8	8.6	
	6	12	50	107.7	2.9	1.4	19.3	5.0	
	3	50	25	15.9	2.7	5.6	6.6	26.6	
26	50	200	25	390	10.9	25.9	62.4	270.2	389.8
	37	50	12	300.1	5.2	7.5	20.7	84.1	
	25	50	200	236	4.3	0.1	22.4	8.9	
	18	50	50	175.4	3.5	5.2	16.5	2.8	
	3	50	25	15.9	2.7	5.6	6.6	23.8	
27	50	200	25	390	10.9	25.9	62.4	270.1	391.3
	37	50	12	300.1	5.2	7.5	20.7	84.1	
	25	50	200	236	4.3	0.1	22.4	8.9	
	12	100	100	195.9	3.4	1.6	18.6	2.5	
	3	50	25	15.9	2.7	5.6	6.6	25.7	
28	50	200	25	390	10.9	25.9	62.4	270.0	394.2
	37	50	12	300.1	5.2	7.5	20.7	84.1	
	25	50	200	236	4.3	0.1	22.4	8.9	
	9	25	50	125.8	4.3	0.4	20.1	3.8	
	3	50	25	15.9	2.7	5.6	6.6	27.4	
29	50	200	25	390	10.9	25.9	62.4	270.1	394.1
	37	50	12	300.1	5.2	7.5	20.7	84.1	
	25	50	200	236	4.3	0.1	22.4	8.9	
	6	12	50	107.7	2.9	1.4	19.3	4.5	
	3	50	25	15.9	2.7	5.6	6.6	26.6	

**Table B. 4 Continues**

30	50	200	25	390	10.9	25.9	62.4	270.4	394.6
	37	50	12	300.1	5.2	7.5	20.7	84.2	
	18	50	50	175.4	3.5	5.2	16.5	12.0	
	12	100	100	195.9	3.4	1.6	18.6	2.3	
	3	50	25	15.9	2.7	5.6	6.6	25.6	
31	50	200	25	390	10.9	25.9	62.4	270.1	404.8
	37	50	12	300.1	5.2	7.5	20.7	84.1	
	18	50	50	175.4	3.5	5.2	16.5	12.0	
	9	100	50	105.3	3	5.7	24.2	4.3	
	3	50	25	15.9	2.7	5.6	6.6	34.2	
32	50	200	25	390	10.9	25.9	62.4	270.4	397.3
	37	50	12	300.1	5.2	7.5	20.7	84.2	
	18	50	50	175.4	3.5	5.2	16.5	12.0	
	6	12	50	107.7	2.9	1.4	19.3	4.2	
	3	50	25	15.9	2.7	5.6	6.6	26.5	
33	50	200	25	390	10.9	25.9	62.4	270.0	403.1
	37	50	12	300.1	5.2	7.5	20.7	84.1	
	12	100	100	195.9	3.4	1.6	18.6	10.7	
	9	100	50	105.3	3	5.7	24.2	4.1	
	3	50	25	15.9	2.7	5.6	6.6	34.2	
34	50	200	25	390	10.9	25.9	62.4	270.3	395.7
	37	50	12	300.1	5.2	7.5	20.7	84.2	
	12	100	100	195.9	3.4	1.6	18.6	10.7	
	6	12	50	107.7	2.9	1.4	19.3	4.0	
	3	50	25	15.9	2.7	5.6	6.6	26.5	
35	50	200	25	390	10.9	25.9	62.4	270.3	400.8
	37	50	12	300.1	5.2	7.5	20.7	84.2	
	9	12	50	132	4.4	0.7	18.9	15.9	
	6	12	50	107.7	2.9	1.4	19.3	3.9	
	3	50	25	15.9	2.7	5.6	6.6	26.5	
36	50	200	25	390	10.9	25.9	62.4	270.6	407.1
	31	50	50	244.2	6.1	5.3	10.7	103.6	
	25	100	200	241.5	5.7	1.3	25.1	5.8	
	18	50	50	175.4	3.5	5.2	16.5	3.2	
	3	50	25	15.9	2.7	5.6	6.6	24.0	
37	50	200	25	390	10.9	25.9	62.4	270.5	408.4
	31	50	50	244.2	6.1	5.3	10.7	103.5	
	25	100	200	241.5	5.7	1.3	25.1	5.8	
	12	100	100	195.9	3.4	1.6	18.6	2.8	
	3	50	25	15.9	2.7	5.6	6.6	25.7	
38	50	200	25	390	10.9	25.9	62.4	270.5	409.9
	31	50	50	244.2	6.1	5.3	10.7	103.5	
	25	100	200	241.5	5.7	1.3	25.1	5.8	
	9	12	50	132	4.4	0.7	18.9	4.2	
	3	50	25	15.9	2.7	5.6	6.6	25.9	
39	50	200	25	390	10.9	25.9	62.4	270.5	411.6
	31	50	50	244.2	6.1	5.3	10.7	103.5	
	25	100	200	241.5	5.7	1.3	25.1	5.8	
	6	12	50	107.7	2.9	1.4	19.3	5.2	
	3	50	25	15.9	2.7	5.6	6.6	26.6	

**Table B. 4 Continues**

40	50	200	25	390	10.9	25.9	62.4	271.0	410.4
	31	50	50	244.2	6.1	5.3	10.7	103.7	
	18	50	50	175.4	3.5	5.2	16.5	8.0	
	12	100	100	195.9	3.4	1.6	18.6	2.1	
	3	50	25	15.9	2.7	5.6	6.6	25.6	
41	50	200	25	390	10.9	25.9	62.4	270.7	420.4
	31	50	50	244.2	6.1	5.3	10.7	103.6	
	18	50	50	175.4	3.5	5.2	16.5	8.0	
	9	100	50	105.3	3	5.7	24.2	4.0	
	3	50	25	15.9	2.7	5.6	6.6	34.1	
42	50	200	25	390	10.9	25.9	62.4	270.9	413.0
	31	50	50	244.2	6.1	5.3	10.7	103.7	
	18	50	50	175.4	3.5	5.2	16.5	8.0	
	6	12	50	107.7	2.9	1.4	19.3	3.9	
	3	50	25	15.9	2.7	5.6	6.6	26.5	
43	50	200	25	390	10.9	25.9	62.4	270.6	419.4
	31	50	50	244.2	6.1	5.3	10.7	103.5	
	12	100	100	195.9	3.4	1.6	18.6	7.2	
	9	100	50	105.3	3	5.7	24.2	4.0	
	3	50	25	15.9	2.7	5.6	6.6	34.1	
44	50	200	25	390	10.9	25.9	62.4	270.8	412.0
	31	50	50	244.2	6.1	5.3	10.7	103.6	
	12	100	100	195.9	3.4	1.6	18.6	7.2	
	6	12	50	107.7	2.9	1.4	19.3	3.9	
	3	50	25	15.9	2.7	5.6	6.6	26.5	
45	50	200	25	390	10.9	25.9	62.4	270.8	415.4
	31	50	50	244.2	6.1	5.3	10.7	103.6	
	9	12	50	132	4.4	0.7	18.9	10.6	
	6	12	50	107.7	2.9	1.4	19.3	3.9	
	3	50	25	15.9	2.7	5.6	6.6	26.5	
46	50	200	25	390	10.9	25.9	62.4	270.2	407.0
	25	100	200	241.5	5.7	1.3	25.1	104.6	
	18	50	50	175.4	3.5	5.2	16.5	4.7	
	12	100	100	195.9	3.4	1.6	18.6	2.0	
	3	50	25	15.9	2.7	5.6	6.6	25.6	
47	50	200	25	390	10.9	25.9	62.4	269.9	416.8
	25	100	200	241.5	5.7	1.3	25.1	104.4	
	18	50	50	175.4	3.5	5.2	16.5	4.7	
	9	100	50	105.3	3	5.7	24.2	3.7	
	3	50	25	15.9	2.7	5.6	6.6	34.1	
48	50	200	25	390	10.9	25.9	62.4	270.2	409.5
	25	100	200	241.5	5.7	1.3	25.1	104.5	
	18	50	50	175.4	3.5	5.2	16.5	4.7	
	6	12	50	107.7	2.9	1.4	19.3	3.6	
	3	50	25	15.9	2.7	5.6	6.6	26.5	
49	50	200	25	390	10.9	25.9	62.4	269.8	416.4
	25	100	200	241.5	5.7	1.3	25.1	104.4	
	12	100	100	195.9	3.4	1.6	18.6	4.2	
	9	100	50	105.3	3	5.7	24.2	3.9	
	3	50	25	15.9	2.7	5.6	6.6	34.1	

**Table B. 4 Continues**

50	50	200	25	390	10.9	25.9	62.4	270.0	409.1
	25	100	200	241.5	5.7	1.3	25.1	104.5	
	12	100	100	195.9	3.4	1.6	18.6	4.2	
	6	12	50	107.7	2.9	1.4	19.3	3.8	
	3	50	25	15.9	2.7	5.6	6.6	26.5	
51	50	200	25	390	10.9	25.9	62.4	270.0	411.1
	25	100	200	241.5	5.7	1.3	25.1	104.5	
	9	12	50	132	4.4	0.7	18.9	6.3	
	6	12	50	107.7	2.9	1.4	19.3	3.8	
	3	50	25	15.9	2.7	5.6	6.6	26.5	
52	50	200	25	390	10.9	25.9	62.4	269.4	411.5
	18	100	200	234.2	7.9	1.5	27.1	107.5	
	12	200	200	230.4	7.6	1.5	28.6	4.0	
	9	12	50	132	4.4	0.7	18.9	4.8	
	3	50	25	15.9	2.7	5.6	6.6	25.9	
53	50	200	25	390	10.9	25.9	62.4	269.4	413.3
	18	100	200	234.2	7.9	1.5	27.1	107.5	
	12	200	200	230.4	7.6	1.5	28.6	4.0	
	6	12	50	107.7	2.9	1.4	19.3	5.8	
	3	50	25	15.9	2.7	5.6	6.6	26.7	
54	50	200	25	390	10.9	25.9	62.4	269.9	414.9
	18	100	200	234.2	7.9	1.5	27.1	107.7	
	9	12	50	132	4.4	0.7	18.9	6.9	
	6	12	50	107.7	2.9	1.4	19.3	3.8	
	3	50	25	15.9	2.7	5.6	6.6	26.5	
55	50	200	25	390	10.9	25.9	62.4	269.8	416.8
	12	200	200	230.4	7.6	1.5	28.6	109.4	
	9	12	50	132	4.4	0.7	18.9	7.2	
	6	12	50	107.7	2.9	1.4	19.3	3.8	
	3	50	25	15.9	2.7	5.6	6.6	26.5	
56	44	100	12	375.2	8.7	13.3	19.7	283.6	349.5
	37	50	12	300.1	5.2	7.5	20.7	42.7	
	31	50	200	243.4	3.2	0.5	24.8	5.3	
	25	12	50	209.2	3.1	8.6	9.4	2.6	
	3	50	25	15.9	2.7	5.6	6.6	15.3	
57	44	100	12	375.2	8.7	13.3	19.7	282.6	379.0
	37	50	12	300.1	5.2	7.5	20.7	42.6	
	31	50	200	243.4	3.2	0.5	24.8	5.3	
	18	800	200	67.9	3	12.7	27.2	7.9	
	3	50	25	15.9	2.7	5.6	6.6	40.7	
58	44	100	12	375.2	8.7	13.3	19.7	282.7	370.2
	37	50	12	300.1	5.2	7.5	20.7	42.6	
	31	50	200	243.4	3.2	0.5	24.8	5.3	
	9	100	50	105.3	3	5.7	24.2	5.1	
	3	50	25	15.9	2.7	5.6	6.6	34.5	
59	44	100	12	375.2	8.7	13.3	19.7	283.0	362.5
	37	50	12	300.1	5.2	7.5	20.7	42.6	
	31	50	200	243.4	3.2	0.5	24.8	5.3	
	6	12	50	107.7	2.9	1.4	19.3	5.0	
	3	50	25	15.9	2.7	5.6	6.6	26.6	

**Table B. 4 Continues**

60	44	100	12	375.2	8.7	13.3	19.7	283.3	358.0
	37	50	12	300.1	5.2	7.5	20.7	42.7	
	25	50	200	236	4.3	0.1	22.4	5.5	
	18	50	50	175.4	3.5	5.2	16.5	2.8	
	3	50	25	15.9	2.7	5.6	6.6	23.8	
61	44	100	12	375.2	8.7	13.3	19.7	283.2	359.4
	37	50	12	300.1	5.2	7.5	20.7	42.7	
	25	50	200	236	4.3	0.1	22.4	5.4	
	12	100	100	195.9	3.4	1.6	18.6	2.5	
	3	50	25	15.9	2.7	5.6	6.6	25.7	
62	44	100	12	375.2	8.7	13.3	19.7	283.1	362.4
	37	50	12	300.1	5.2	7.5	20.7	42.7	
	25	50	200	236	4.3	0.1	22.4	5.4	
	9	25	50	125.8	4.3	0.4	20.1	3.8	
	3	50	25	15.9	2.7	5.6	6.6	27.4	
63	44	100	12	375.2	8.7	13.3	19.7	283.1	362.3
	37	50	12	300.1	5.2	7.5	20.7	42.7	
	25	50	200	236	4.3	0.1	22.4	5.4	
	6	12	50	107.7	2.9	1.4	19.3	4.5	
	3	50	25	15.9	2.7	5.6	6.6	26.6	
64	44	100	12	375.2	8.7	13.3	19.7	283.5	361.3
	37	50	12	300.1	5.2	7.5	20.7	42.7	
	18	50	50	175.4	3.5	5.2	16.5	7.3	
	12	100	100	195.9	3.4	1.6	18.6	2.1	
	3	50	25	15.9	2.7	5.6	6.6	25.6	
65	44	100	12	375.2	8.7	13.3	19.7	283.2	371.3
	37	50	12	300.1	5.2	7.5	20.7	42.7	
	18	50	50	175.4	3.5	5.2	16.5	7.3	
	9	100	50	105.3	3	5.7	24.2	3.9	
	3	50	25	15.9	2.7	5.6	6.6	34.1	
66	44	100	12	375.2	8.7	13.3	19.7	283.5	363.9
	37	50	12	300.1	5.2	7.5	20.7	42.7	
	18	50	50	175.4	3.5	5.2	16.5	7.3	
	6	12	50	107.7	2.9	1.4	19.3	3.8	
	3	50	25	15.9	2.7	5.6	6.6	26.5	
67	44	100	12	375.2	8.7	13.3	19.7	283.1	370.4
	37	50	12	300.1	5.2	7.5	20.7	42.7	
	12	100	100	195.9	3.4	1.6	18.6	6.6	
	9	100	50	105.3	3	5.7	24.2	4.0	
	3	50	25	15.9	2.7	5.6	6.6	34.1	
68	44	100	12	375.2	8.7	13.3	19.7	283.4	363.0
	37	50	12	300.1	5.2	7.5	20.7	42.7	
	12	100	100	195.9	3.4	1.6	18.6	6.6	
	6	12	50	107.7	2.9	1.4	19.3	3.9	
	3	50	25	15.9	2.7	5.6	6.6	26.5	
69	44	100	12	375.2	8.7	13.3	19.7	283.3	366.1
	37	50	12	300.1	5.2	7.5	20.7	42.7	
	9	12	50	132	4.4	0.7	18.9	9.7	
	6	12	50	107.7	2.9	1.4	19.3	3.8	
	3	50	25	15.9	2.7	5.6	6.6	26.5	

**Table B. 4 Continues**

70	44	100	12	375.2	8.7	13.3	19.7	283.7	366.8
	31	50	50	244.2	6.1	5.3	10.7	52.5	
	25	100	200	241.5	5.7	1.3	25.1	3.4	
	18	50	50	175.4	3.5	5.2	16.5	3.1	
	3	50	25	15.9	2.7	5.6	6.6	24.0	
71	44	100	12	375.2	8.7	13.3	19.7	283.6	368.1
	31	50	50	244.2	6.1	5.3	10.7	52.5	
	25	100	200	241.5	5.7	1.3	25.1	3.4	
	12	100	100	195.9	3.4	1.6	18.6	2.8	
	3	50	25	15.9	2.7	5.6	6.6	25.7	
72	44	100	12	375.2	8.7	13.3	19.7	283.6	369.5
	31	50	50	244.2	6.1	5.3	10.7	52.5	
	25	100	200	241.5	5.7	1.3	25.1	3.4	
	9	12	50	132	4.4	0.7	18.9	4.2	
	3	50	25	15.9	2.7	5.6	6.6	25.9	
73	44	100	12	375.2	8.7	13.3	19.7	283.6	371.2
	31	50	50	244.2	6.1	5.3	10.7	52.5	
	25	100	200	241.5	5.7	1.3	25.1	3.4	
	6	12	50	107.7	2.9	1.4	19.3	5.1	
	3	50	25	15.9	2.7	5.6	6.6	26.6	
74	44	100	12	375.2	8.7	13.3	19.7	284.1	369.0
	31	50	50	244.2	6.1	5.3	10.7	52.6	
	18	50	50	175.4	3.5	5.2	16.5	4.7	
	12	100	100	195.9	3.4	1.6	18.6	2.0	
	3	50	25	15.9	2.7	5.6	6.6	25.6	
75	44	100	12	375.2	8.7	13.3	19.7	283.8	378.8
	31	50	50	244.2	6.1	5.3	10.7	52.5	
	18	50	50	175.4	3.5	5.2	16.5	4.7	
	9	100	50	105.3	3	5.7	24.2	3.7	
	3	50	25	15.9	2.7	5.6	6.6	34.1	
76	44	100	12	375.2	8.7	13.3	19.7	284.1	371.5
	31	50	50	244.2	6.1	5.3	10.7	52.6	
	18	50	50	175.4	3.5	5.2	16.5	4.7	
	6	12	50	107.7	2.9	1.4	19.3	3.6	
	3	50	25	15.9	2.7	5.6	6.6	26.5	
77	44	100	12	375.2	8.7	13.3	19.7	283.7	378.4
	31	50	50	244.2	6.1	5.3	10.7	52.5	
	12	100	100	195.9	3.4	1.6	18.6	4.2	
	9	100	50	105.3	3	5.7	24.2	3.9	
	3	50	25	15.9	2.7	5.6	6.6	34.1	
78	44	100	12	375.2	8.7	13.3	19.7	283.9	371.1
	31	50	50	244.2	6.1	5.3	10.7	52.6	
	12	100	100	195.9	3.4	1.6	18.6	4.2	
	6	12	50	107.7	2.9	1.4	19.3	3.8	
	3	50	25	15.9	2.7	5.6	6.6	26.5	
79	44	100	12	375.2	8.7	13.3	19.7	283.9	373.1
	31	50	50	244.2	6.1	5.3	10.7	52.6	
	9	12	50	132	4.4	0.7	18.9	6.3	
	6	12	50	107.7	2.9	1.4	19.3	3.8	
	3	50	25	15.9	2.7	5.6	6.6	26.5	

**Table B. 4 Continues**

70	44	100	12	375.2	8.7	13.3	19.7	283.7	366.8
	31	50	50	244.2	6.1	5.3	10.7	52.5	
	25	100	200	241.5	5.7	1.3	25.1	3.4	
	18	50	50	175.4	3.5	5.2	16.5	3.1	
	3	50	25	15.9	2.7	5.6	6.6	24.0	
71	44	100	12	375.2	8.7	13.3	19.7	283.6	368.1
	31	50	50	244.2	6.1	5.3	10.7	52.5	
	25	100	200	241.5	5.7	1.3	25.1	3.4	
	12	100	100	195.9	3.4	1.6	18.6	2.8	
	3	50	25	15.9	2.7	5.6	6.6	25.7	
72	44	100	12	375.2	8.7	13.3	19.7	283.6	369.5
	31	50	50	244.2	6.1	5.3	10.7	52.5	
	25	100	200	241.5	5.7	1.3	25.1	3.4	
	9	12	50	132	4.4	0.7	18.9	4.2	
	3	50	25	15.9	2.7	5.6	6.6	25.9	
73	44	100	12	375.2	8.7	13.3	19.7	283.6	371.2
	31	50	50	244.2	6.1	5.3	10.7	52.5	
	25	100	200	241.5	5.7	1.3	25.1	3.4	
	6	12	50	107.7	2.9	1.4	19.3	5.1	
	3	50	25	15.9	2.7	5.6	6.6	26.6	
74	44	100	12	375.2	8.7	13.3	19.7	284.1	369.0
	31	50	50	244.2	6.1	5.3	10.7	52.6	
	18	50	50	175.4	3.5	5.2	16.5	4.7	
	12	100	100	195.9	3.4	1.6	18.6	2.0	
	3	50	25	15.9	2.7	5.6	6.6	25.6	
75	44	100	12	375.2	8.7	13.3	19.7	283.8	378.8
	31	50	50	244.2	6.1	5.3	10.7	52.5	
	18	50	50	175.4	3.5	5.2	16.5	4.7	
	9	100	50	105.3	3	5.7	24.2	3.7	
	3	50	25	15.9	2.7	5.6	6.6	34.1	
76	44	100	12	375.2	8.7	13.3	19.7	284.1	371.5
	31	50	50	244.2	6.1	5.3	10.7	52.6	
	18	50	50	175.4	3.5	5.2	16.5	4.7	
	6	12	50	107.7	2.9	1.4	19.3	3.6	
	3	50	25	15.9	2.7	5.6	6.6	26.5	
77	44	100	12	375.2	8.7	13.3	19.7	283.7	378.4
	31	50	50	244.2	6.1	5.3	10.7	52.5	
	12	100	100	195.9	3.4	1.6	18.6	4.2	
	9	100	50	105.3	3	5.7	24.2	3.9	
	3	50	25	15.9	2.7	5.6	6.6	34.1	
78	44	100	12	375.2	8.7	13.3	19.7	283.9	371.1
	31	50	50	244.2	6.1	5.3	10.7	52.6	
	12	100	100	195.9	3.4	1.6	18.6	4.2	
	6	12	50	107.7	2.9	1.4	19.3	3.8	
	3	50	25	15.9	2.7	5.6	6.6	26.5	
79	44	100	12	375.2	8.7	13.3	19.7	283.9	373.1
	31	50	50	244.2	6.1	5.3	10.7	52.6	
	9	12	50	132	4.4	0.7	18.9	6.3	
	6	12	50	107.7	2.9	1.4	19.3	3.8	
	3	50	25	15.9	2.7	5.6	6.6	26.5	



**Table B. 4 Continues**

90	37	50	12	300.1	5.2	7.5	20.7	354.0	429.4
	31	50	200	243.4	3.2	0.5	24.8	30.5	
	25	12	50	209.2	3.1	8.6	9.4	2.7	
	18	800	200	67.9	3	12.7	27.2	3.6	
	3	50	25	15.9	2.7	5.6	6.6	38.6	
91	37	50	12	300.1	5.2	7.5	20.7	354.2	423.4
	31	50	200	243.4	3.2	0.5	24.8	30.5	
	25	12	50	209.2	3.1	8.6	9.4	2.7	
	9	100	50	105.3	3	5.7	24.2	2.3	
	3	50	25	15.9	2.7	5.6	6.6	33.6	
92	37	50	12	300.1	5.2	7.5	20.7	354.6	416.5
	31	50	200	243.4	3.2	0.5	24.8	30.6	
	25	12	50	209.2	3.1	8.6	9.4	2.7	
	6	12	50	107.7	2.9	1.4	19.3	2.3	
	3	50	25	15.9	2.7	5.6	6.6	26.4	
93	37	50	12	300.1	5.2	7.5	20.7	353.0	432.7
	31	50	200	243.4	3.2	0.5	24.8	30.4	
	18	800	200	67.9	3	12.7	27.2	8.3	
	9	100	50	105.3	3	5.7	24.2	6.1	
	3	50	25	15.9	2.7	5.6	6.6	34.9	
94	37	50	12	300.1	5.2	7.5	20.7	353.3	424.8
	31	50	200	243.4	3.2	0.5	24.8	30.4	
	18	800	200	67.9	3	12.7	27.2	8.3	
	6	12	50	107.7	2.9	1.4	19.3	6.0	
	3	50	25	15.9	2.7	5.6	6.6	26.7	
95	37	50	12	300.1	5.2	7.5	20.7	353.5	421.0
	31	50	200	243.4	3.2	0.5	24.8	30.5	
	9	100	50	105.3	3	5.7	24.2	5.4	
	6	12	50	107.7	2.9	1.4	19.3	5.1	
	3	50	25	15.9	2.7	5.6	6.6	26.6	
96	37	50	12	300.1	5.2	7.5	20.7	354.3	416.0
	25	50	200	236	4.3	0.1	22.4	31.5	
	18	50	50	175.4	3.5	5.2	16.5	2.8	
	12	100	100	195.9	3.4	1.6	18.6	1.9	
	3	50	25	15.9	2.7	5.6	6.6	25.6	
97	37	50	12	300.1	5.2	7.5	20.7	353.9	425.7
	25	50	200	236	4.3	0.1	22.4	31.5	
	18	50	50	175.4	3.5	5.2	16.5	2.8	
	9	100	50	105.3	3	5.7	24.2	3.6	
	3	50	25	15.9	2.7	5.6	6.6	34.0	
98	37	50	12	300.1	5.2	7.5	20.7	354.2	418.5
	25	50	200	236	4.3	0.1	22.4	31.5	
	18	50	50	175.4	3.5	5.2	16.5	2.8	
	6	12	50	107.7	2.9	1.4	19.3	3.5	
	3	50	25	15.9	2.7	5.6	6.6	26.5	
99	37	50	12	300.1	5.2	7.5	20.7	353.7	425.6
	25	50	200	236	4.3	0.1	22.4	31.4	
	12	100	100	195.9	3.4	1.6	18.6	2.5	
	9	100	50	105.3	3	5.7	24.2	3.9	
	3	50	25	15.9	2.7	5.6	6.6	34.1	

**Table B. 4 Continues**

100	37	50	12	300.1	5.2	7.5	20.7	354.1	418.3
	25	50	200	236	4.3	0.1	22.4	31.5	
	12	100	100	195.9	3.4	1.6	18.6	2.5	
	6	12	50	107.7	2.9	1.4	19.3	3.8	
	3	50	25	15.9	2.7	5.6	6.6	26.5	
101	37	50	12	300.1	5.2	7.5	20.7	354.0	419.9
	25	50	200	236	4.3	0.1	22.4	31.5	
	9	25	50	125.8	4.3	0.4	20.1	3.9	
	6	12	50	107.7	2.9	1.4	19.3	4.0	
	3	50	25	15.9	2.7	5.6	6.6	26.5	
102	37	50	12	300.1	5.2	7.5	20.7	354.2	438.0
	18	50	50	175.4	3.5	5.2	16.5	42.4	
	12	100	100	195.9	3.4	1.6	18.6	3.5	
	9	100	50	105.3	3	5.7	24.2	3.9	
	3	50	25	15.9	2.7	5.6	6.6	34.1	
103	37	50	12	300.1	5.2	7.5	20.7	354.5	430.7
	18	50	50	175.4	3.5	5.2	16.5	42.4	
	12	100	100	195.9	3.4	1.6	18.6	3.5	
	6	12	50	107.7	2.9	1.4	19.3	3.8	
	3	50	25	15.9	2.7	5.6	6.6	26.5	
104	37	50	12	300.1	5.2	7.5	20.7	354.1	434.8
	18	50	50	175.4	3.5	5.2	16.5	42.3	
	9	100	50	105.3	3	5.7	24.2	6.6	
	6	12	50	107.7	2.9	1.4	19.3	5.2	
	3	50	25	15.9	2.7	5.6	6.6	26.6	
105	37	50	12	300.1	5.2	7.5	20.7	354.0	428.3
	12	100	100	195.9	3.4	1.6	18.6	37.9	
	9	100	50	105.3	3	5.7	24.2	4.8	
	6	12	50	107.7	2.9	1.4	19.3	5.1	
	3	50	25	15.9	2.7	5.6	6.6	26.6	
106	31	50	50	244.2	6.1	5.3	10.7	436.0	488.4
	25	100	200	241.5	5.7	1.3	25.1	21.4	
	18	50	50	175.4	3.5	5.2	16.5	3.4	
	12	100	100	195.9	3.4	1.6	18.6	2.0	
	3	50	25	15.9	2.7	5.6	6.6	25.6	
107	31	50	50	244.2	6.1	5.3	10.7	435.5	498.0
	25	100	200	241.5	5.7	1.3	25.1	21.4	
	18	50	50	175.4	3.5	5.2	16.5	3.4	
	9	100	50	105.3	3	5.7	24.2	3.6	
	3	50	25	15.9	2.7	5.6	6.6	34.0	
108	31	50	50	244.2	6.1	5.3	10.7	436.0	490.8
	25	100	200	241.5	5.7	1.3	25.1	21.4	
	18	50	50	175.4	3.5	5.2	16.5	3.4	
	6	12	50	107.7	2.9	1.4	19.3	3.5	
	3	50	25	15.9	2.7	5.6	6.6	26.5	
109	31	50	50	244.2	6.1	5.3	10.7	435.3	497.8
	25	100	200	241.5	5.7	1.3	25.1	21.4	
	12	100	100	195.9	3.4	1.6	18.6	3.0	
	9	100	50	105.3	3	5.7	24.2	3.9	
	3	50	25	15.9	2.7	5.6	6.6	34.1	

**Table B. 4 Continues**

110	31	50	50	244.2	6.1	5.3	10.7	435.8	490.5
	25	100	200	241.5	5.7	1.3	25.1	21.4	
	12	100	100	195.9	3.4	1.6	18.6	3.0	
	6	12	50	107.7	2.9	1.4	19.3	3.8	
	3	50	25	15.9	2.7	5.6	6.6	26.5	
111	31	50	50	244.2	6.1	5.3	10.7	435.7	492.0
	25	100	200	241.5	5.7	1.3	25.1	21.4	
	9	12	50	132	4.4	0.7	18.9	4.5	
	6	12	50	107.7	2.9	1.4	19.3	3.8	
	3	50	25	15.9	2.7	5.6	6.6	26.5	
112	31	50	50	244.2	6.1	5.3	10.7	436.1	506.6
	18	50	50	175.4	3.5	5.2	16.5	29.5	
	12	100	100	195.9	3.4	1.6	18.6	3.0	
	9	100	50	105.3	3	5.7	24.2	3.9	
	3	50	25	15.9	2.7	5.6	6.6	34.1	
113	31	50	50	244.2	6.1	5.3	10.7	436.5	499.4
	18	50	50	175.4	3.5	5.2	16.5	29.5	
	12	100	100	195.9	3.4	1.6	18.6	3.0	
	6	12	50	107.7	2.9	1.4	19.3	3.8	
	3	50	25	15.9	2.7	5.6	6.6	26.5	
114	31	50	50	244.2	6.1	5.3	10.7	436.0	502.9
	18	50	50	175.4	3.5	5.2	16.5	29.5	
	9	100	50	105.3	3	5.7	24.2	5.6	
	6	12	50	107.7	2.9	1.4	19.3	5.1	
	3	50	25	15.9	2.7	5.6	6.6	26.6	
115	31	50	50	244.2	6.1	5.3	10.7	435.9	498.4
	12	100	100	195.9	3.4	1.6	18.6	26.4	
	9	100	50	105.3	3	5.7	24.2	4.5	
	6	12	50	107.7	2.9	1.4	19.3	5.1	
	3	50	25	15.9	2.7	5.6	6.6	26.6	
116	25	100	200	241.5	5.7	1.3	25.1	439.7	489.8
	18	50	50	175.4	3.5	5.2	16.5	10.0	
	12	100	100	195.9	3.4	1.6	18.6	2.2	
	9	100	50	105.3	3	5.7	24.2	3.9	
	3	50	25	15.9	2.7	5.6	6.6	34.1	
117	25	100	200	241.5	5.7	1.3	25.1	440.1	482.6
	18	50	50	175.4	3.5	5.2	16.5	10.0	
	12	100	100	195.9	3.4	1.6	18.6	2.2	
	6	12	50	107.7	2.9	1.4	19.3	3.8	
	3	50	25	15.9	2.7	5.6	6.6	26.5	
118	25	100	200	241.5	5.7	1.3	25.1	439.6	485.3
	18	50	50	175.4	3.5	5.2	16.5	10.0	
	9	100	50	105.3	3	5.7	24.2	4.1	
	6	12	50	107.7	2.9	1.4	19.3	5.0	
	3	50	25	15.9	2.7	5.6	6.6	26.6	
119	25	100	200	241.5	5.7	1.3	25.1	439.5	484.0
	12	100	100	195.9	3.4	1.6	18.6	8.9	
	9	100	50	105.3	3	5.7	24.2	4.0	
	6	12	50	107.7	2.9	1.4	19.3	5.0	
	3	50	25	15.9	2.7	5.6	6.6	26.6	
120	18	100	200	234.2	7.9	1.5	27.1	452.5	496.3
	12	200	200	230.4	7.6	1.5	28.6	8.6	
	9	12	50	132	4.4	0.7	18.9	4.8	
	6	12	50	107.7	2.9	1.4	19.3	3.8	
	3	50	25	15.9	2.7	5.6	6.6	26.5	

## **Curriculum Vitae**

M. Veysel akır was born in Besni on January 15, 1974. He received his BSc degree and MSc Degree in Mechanical Engineering from the University of Gaziantep in July 1996 and December 2003, respectively. He has worked as a lecturer in the department of Mechanical in Vocational School of Kilis since 1997. His main areas of interest are non-traditional machining process, electro discharge machining, computer aided design, and machine design.